Università degli Studi di Messina

Dipartimento di Scienze Chimiche, Biologiche, Farmaceutiche ed Ambientali

Dottorato di Ricerca in "Scienze Chimiche"

Doctor of Philosophy in "Chemical Sciences"

ADVANCED CHROMATOGRAPHY AND MASS SPECTROMETRY TECHNIQUES FOR THE ANALYSIS OF BIOACTIVE CONSTITUENTS IN FOOD AND CLINICAL FIELDS

Ph.D. Thesis of: **Marianna Oteri**

Supervisor: Prof. **Paola Donato**

Coordinator:

Prof. Sebastiano Campagna

SSD CHIM/10

XXXI Ciclo 2015-2018

… al mio Papà….

TABLE OF CONTENTS

CHAPTER I

General Introduction 1

1.1. Introduction 1

1.2. General trends 3

REFERENCES 4

CHAPTER II

Liquid Chromatography coupled to Mass Spectrometry and Statistical Analyisis 7

2.1. *Reuse of dairy product: evaluation of the lipid profile evolution during and after their shelf-life* 7

2.1.1. Introduction 7

2.1.2. Materials and Method 9

2.1.2.1. Chemicals and Materials. 9

2.1.2.2. Samples 9

2.1.2.3. Sample Preparation 10

2.1.2.4. Analytical Determination 10

2.1.2.5. Statistical Analysis 13

2.1.3. Results and Discussion 13

2.1.4. FAMEs Analysis Optimization 14

2.1.5. TAGs Analysis 18

2.1.6. FAMEs and TAGs Profile Evolution 23

2.1.7. Conclusions 27

REFERENCES 28

2.2. *Chemical characterisation of old cabbage (Brassica oleracea L. var. acephala) seed oil by liquid chromatography and different spectroscopic detection systems* 32
2.2.1. Introduction..... 32
2.2.2. Materials and methods..... 33
2.2.2.1. Chemicals and reagents. 33
2.2.2.2. Seed material 34
2.2.3. Results and Discussion..... 35
2.2.3.1. FAMEs composition by GC-FID and GC-MS. 35
2.2.3.2. Triacylglycerol analysis by NARP-HPLC-APCI-MS. 37
2.2.3.3. Tocopherol analysis by NP-HPLC-RF.. 38
2.2.3.4. Carotenoid analysis by RP-HPLC-PDA/APCI-MS and UV–vis Spectrophotometry..... 40
2.2.3.5. Polyphenol analysis by RP-HPLC-PDA/ESI-MS.. 41
2.2.4. Conclusions..... 43
REFERENCES 43

2.3. *Analysis of lipid profile in lipid storage myopathy*..... 47
2.3.1. Introduction..... 47
2.3.2. Materials and methods..... 49
2.3.2.1. Patient selection. 49
2.3.2.2. FAMEs characterization 51
2.3.2.3. TGs characterization..... 53
2.3.3. Results and discussion..... 54
2.3.3.1. FAMEs profile 55
2.3.3.2. IMTGs profile 57
2.3.3.3. Statistical analysis..... 64
2.3.4. Conclusions..... 66

REFERENCES 66

2.4. *Determination of amines and phenolic acids in wine with benzoylchloride derivatization and liquid chromatography–mass spectrometry* 71
2.4.1. Introduction 71
2.4.2. Experimental 75
2.4.2.1. Chemicals and reagents. 75
2.4.2.2. Sample preparation and derivatization 75
2.4.2.3. Metabolite analysis by LC–MS/MS 76
2.4.2.4. Method evaluation 76
2.4.2.5. Statistical analysis 77
2.4.3. Results and Discussion 77
2.4.3.1. Metabolite selection 77
2.4.3.2. Figures of merit 78
2.4.3.3. Wine analysis 82
2.4.3.4. Comparison to current methods 88
2.4.4. Conclusions 89
REFERENCES 90

CHAPTER III

Building of a Linear Retention Index System in Liquid Chromatography 97

3.1. *Proposal of a linear retention index system for improving identification reliability of triacylglycerol profiles in lipid samples by liquid chromatography methods* 97
3.1.1. Introduction 97
3.1.2. Experimental 101
3.1.2.1. Reagents and Materials 101

3.1.2.2. Samples and sample preparation 101
3.1.2.3. UHPLC-ELSD instrumentation and analytical conditions 102
3.1.2.4. HPLC-ESI-MS instrumentation and analytical conditions 103
3.1.2.5. LRI calculation and data analysis 104
3.1.3. Results and Discussion 104
3.1.3.1. Chromatographic method development 105
3.1.3.2. LRI database 108
3.1.3.3. LRI repeatability 113
3.1.3.4. HPLC-ESI-MS analyses 115
3.1.4. Conclusions 118
REFERENCES 119

CHAPTER IV

Multidimensional Liquid Chromatography 123
4.1. *Comprehensive lipid profiling in the Mediterranean mussel (Mytilus galloprovincialis) using hyphenated and multidimensional chromatography techniques coupled to mass spectrometry detection* 123
4.1.1. Introduction 123
4.1.2. Materials and Methods 126
4.1.2.1. Solvents and Chemicals 126
4.1.2.2. Samples and sample preparation 127
4.1.2.3. Instrumentation and software 129
4.1.2.4. Analytical conditions 130
4.1.3. Results and Discussion 133
4.1.3.1. Online HILIC×RP-MS 133
4.1.3.2. MS and MS/MS analyses 141
4.1.3.3. Offline HILIC-RP-LC 162
4.1.3.4. GC-MS analyses 162

4.1.4. Conclusions 164
REFERENCES 165

CHAPTER V
Carbon-dioxide based techniques for the analysis of lipids and lipid-like compounds 171
5.1. *Supercritical fluid chromatography×ultrahigh pressure liquid chromatography for red chilli pepper fingerprinting by photodiode array, quadrupole-time-of-flight and ion mobility mass spectrometry (SFC×RP-UHPLC-PDA-QToF MS-IMS)* 171
5.1.1. Introduction 171
5.1.2. Materials and methods 175
5.1.2.1. Chemicals 175
5.1.2.2. Sample and sample preparation 175
5.1.2.3. SFC×RP-UHPLC-QToF MS-IMS instrument 175
5.1.2.4. Columns 176
5.1.2.5. SFC×RP-UHPLC-PDA-QToF MS-IMS analyses 176
5.1.3. Results and Discussion 178
5.1.4. Conclusions 193
REFERENCES 194

5.2. *Triacylglycerol Fingerprinting in Edible Oils by Subcritical Solvent Chromatography* 199
5.2.1. Introduction 199
5.2.2. Materials and Method 205
5.2.2.1. Chemicals and materials 205
5.2.2.2. Samples and sample preparation 206
5.2.2.3. Instruments 206

5.2.2.4. Analytical conditions 206
5.2.3. Results and Discussion 207
5.2.3.1. Optimization of chromatographic conditions 207
5.2.3.2. Chromatographic separation and identification of triacylglycerols 209
5.2.3.3. IMS separation of triacylglycerols 216
5.2.4. Conclusions 217
REFERENCES 218

CHAPTER VI
Application of matrix assisted laser desorption/ionization time-of-flight mass spectrometry in lipid research 223
6.1. *Structural analysis of triacylglycerols in vegetable oil by using high-resolution MALDI-ToF/ToF mass spectrometry* 223
6.1.1. Introduction 223
6.1.2. Experimental 227
6.1.2.1. Samples and sample preparation 227
6.1.2.2. MALDI-ToF MS analyses 228
6.1.3. Results and Discussion 229
REFERENCES 245

APPENDIX I
Supplementary materials 247
Chapter II 247
2.1. *Reuse of dairy product: evaluation of the lipid profile evolution during and after their shelf-life* 247
2.2. *Chemical characterisation of old cabbage (Brassica oleracea L. var. acephala) seed oil by liquid chromatography and different spectroscopic detection systems* 263

2.3. *Analysis of lipid profile in lipid storage myopathy* 271
2.4. *Determination of amines and phenolic acids in wine with benzoylchloride derivatization and liquid chromatography–massspectrometry*..... 275
Chapter III..... 284
3.1. *Proposal of a linear retention index system for improving identification reliability of triacylglycerol profiles in lipid samples by liquid chromatography methods*..... 284
Chapter IV 296
4.1. *Comprehensive lipid profiling in the Mediterranean mussel (Mytilus galloprovincialis) using hyphenated and multidimensional chromatography techniques coupled to mass spectrometry detection* 296

APPENDIX II
List of publications..... 305

ACKNOWLEDGMENTS.....307

CHAPTER I
General Introduction

1.1. Introduction

The complete set of lipids in an organism or a cell along with its interactions with other molecules, such as other lipids, proteins, and metabolites constitutes the lipidome. Lipidomics is the comprehensive and quantitative study of the lipidome. It involves identification and quantitation of thousands of biological pathways involving lipids and their interactions.

Lipids are the essential metabolites in human body; their main biological functions are the energy storage, endocrine actions, morphogenesis, building blocks of cellular and subcellular membranes and signaling molecules [1].

The dysregulation of lipids is related to various serious human diseases, such as cancer, Alzheimer, cardiovascular diseases, and lysosomal disorders [2].

Using lipidomics approaches, it has become easier to study the lipids species in an organism.

Lipidomics is an emerging field in the name of the 'omics' for system-level analysis of lipids and their interacting partners within a cell. Lipidomics aims to define and quantitate all of the molecular lipid species present in a cell [3]. The lipid molecular species can be described by the eight known categories of lipids, numerous classes, and subclasses, such us fatty acids, glycerolipids, sphingolipids, prenols, sterols, glycerophospholipids, poliketides and saccharolipides.

Current studies related to lipid identification and determination, or lipidomics in biological samples, are one of the most important issues in modern bioanalytical chemistry. There are many articles dedicated to specific analytical strategies and to the actual analytical methodologies used in lipidomics in various kinds of biological samples. The most important methods used to

characterize the lipidomics in modern bioanalysis are: *chromatography/separation* methods (thin layer chromatography (TLC), (ultra) high-pressure liquid chromatography ((U)HPLC), gas chromatography (GC), (ultra-performance) supercritical fluid chromatography ((UHP)SFC), and capillary electrophoresis (CE)); *spectroscopic* methods (Raman spectroscopy (RS), Fourier transform infrared spectroscopy (FT-IR) and nuclear magnetic resonance (NMR)); *mass spectrometry* and also *hyphenated* methods (*matrix-assisted laser desorption/ionization* (MALDI), hyphenated methods, which include liquid chromatography–mass spectrometry (LC-MS), gas chromatography–mass spectrometry (GC-MS) and also multidimensional techniques). These are being used to identify and quantify all the lipid species in order to understand their function in biological systems [4].

MS technology has been proved to be highly efficient in the characterization and quantification of lipid molecular species in lipid extracts. One of the reasons behind this could be the ability of MS to characterize and separate each ionized particle according to their mass-to-charge *(m/z*) ratio. MS can also provide structural information by fragmenting the lipid ions which can be achieved by using tandem MS, or MS/MS.

Basically, there are two different approaches for lipidomics analysis:

- to apply some extraction protocols optimized for each lipid category, and then subject to LC to separate the present lipids molecular species optimally [5-10], then the LC eluate is coupled directly to the mass spectrometer for further analysis such as molecular fragmentation (MS/MS), ion scanning, etc.
- another approach, also known as "shotgun lipidomics", involves the offline extraction of lipids followed by MS analysis without LC separation [11].

Several tools are available for lipidomics and some are emerging concerning the combination of genomics and lipidomics to identify clinically relevant biomarkers. For example, SimLipid is a high-throughput characterization tool

for lipids [12]. It analyzes lipid mass spectrometric data to profile them using LC coupled with MALDI-MS, MS/MS data, and also remove the overlapping isotopic peaks from multiple spectra in batch mode [13].

"Lipidomics" applies to studying lipid metabolism on a broad scale and it may elucidate the biochemical mechanism(s) underlying specific changes in lipid metabolism.

Advances in mass spectrometry have greatly accelerated the lipidomics field. Chemical derivatization has shown its broad use in improving analytical sensitivity and specificity in lipidomics.

Lipidomics aims to quantitatively define lipid classes, including their molecular species, in biological systems and it has experienced rapid progress, mainly because of continuous technical advances in instrumentation that are now enabling quantitative lipid analyses with an unprecedented level of sensitivity and precision. The still-growing category of lipids includes a broad diversity of chemical structures with a wide range of physicochemical properties. Reflecting this diversity, different methods and strategies are being applied to the quantification of lipids.

1.2. General trends

Since its advent, LC is being exploited by separation scientists and applied to a wider and wider range of sample matrices for the separation, identification and quantification of ever more compounds, particularly in lipidomic analysis. The unceasing progresses in column and stationary phases production, and the enormous developments in detection techniques have contributed to the outstanding success of chromatography, as an invaluable tool in analytical chemistry in many different fields including nutraceutical, food, environmental, clinical, forensic, and pharmaceutical applications. The great advantages to be gained by the use of LC are especially increased with the hyphenation to MS

(LC-MS). Recent trends in the area of LC-MS and related techniques involve: (*a*) the shift from conventional HPLC-MS to ultra high pressure liquid chromatography (UHPLC)-MS or other fast LC-MS techniques (core-shell particles, high-temperature LC and monolithic columns) requiring fast MS analyzers (typically time-of-flight (TOF)-based systems); (*b*) the use of supercritical fluid chromatography (SFC) for fast and "green" separations, with reduction in solvents consumption; (c) the use of multidimensional liquid chromatography techniques (MDLC) for complex samples, and other dimension also in MS, such as ion mobility spectrometry (IMS)-MS, the coupling of two or more mass analyzer (tandem MS); (d) the shift from low-resolution to (ultra)high-resolution MS to allow accurate mass measurements. Each of these techniques will be described in detail in the following chapters, illustrating selected applications developed for the analysis of lipid and lipid-like molecules, as well as other bioactive compounds.

REFERENCES

[1] van Meer, G.; de Kroon, A. I. J. Cell Sci. 2011, 124, 5−8.

[2] Yang, K.; Han, X. Trends Biochem. Sci. 2016, 41, 954−969.

[3] Dennis, E. A. Lipidomics joins the omics evolution. Proceedings of the National Academy of Sciences, 2009, 106, 2089-2090.

[4] Holcapek M., Liebisch G., Ekroos K. Lipidomic Analysis. Anal. Chem. 2018, 90, 4249−4257.

[5] Krank, J., Murphy, R. C., Barkley, R. M., Duchoslav, E., & McAnoy, A. Qualitative analysis and quantitative assessment of changes in neutral glycerol lipid molecular species within cells. Methods in enzymology, 2007, 432, 1-20.

[6] Ivanova, P. T., Milne, S. B., Byrne, M. O., Xiang, Y., & Brown, H. A. Glycerophospholipid identification and quantitation by electrospray ionization mass spectrometry. Methods in enzymology, 2007, 432, 21-57.

[7] Deems, R., Buczynski, M. W., Bowers-Gentry, R., Harkewicz, R., & Dennis, E. A. Detection and quantitation of eicosanoids via high performance liquid chromatography-electrospray ionization-mass spectrometry. Methods in enzymology, 2007, 432, 59-82.

[8] Sullards, M. C., Allegood, J. C., Kelly, S., Wang, E., Haynes, C. A., Park, H., … & Merrill, A. H. Structure-Specific, Quantitative Methods for Analysis of Sphingolipids by Liquid Chromatography–Tandem Mass Spectrometry:"Inside-Out" Sphingolipidomics. Methods in enzymology, 2007, 432, 83-115.

[9] Garrett, T. A., Guan, Z., & Raetz, C. R. Analysis of Ubiquinones, Dolichols, and Dolichol Diphosphate-Oligosaccharides by Liquid Chromatography-Electrospray Ionization-Mass Spectrometry. Methods in enzymology, 2007, 432, 117-143.

[10] McDonald, J. G., Thompson, B. M., McCrum, E. C., & Russell, D. W. Extraction and analysis of sterols in biological matrices by high performance liquid chromatography electrospray ionization mass spectrometry. Methods in enzymology, 2007, 432, 145-170.

[11] Ejsing, C. S., Sampaio, J. L., Surendranath, V., Duchoslav, E., Ekroos, K., Klemm, R. W., … & Shevchenko, A. Global analysis of the yeast lipidome by quantitative shotgun mass spectrometry. Proceedings of the National Academy of Sciences, 2009, 106, 2136-2141.

[12] Wenk, M. R. Lipidomics: new tools and applications. Cell, 2010, 143, 888-895.

[13] Isaac, G., McDonald, S., & Astarita, G. (2011). Automated Lipid Identification Using UPLC/HDMSE in Combination with SimLipid. Waters Application Note 720004169en.

CHAPTER II
Liquid Chromatography coupled to Mass Spectrometry and Statistical Analysis

2.1. Reuse of dairy product: evaluation of the lipid profile evolution during and after their shelf-life

2.1.1. Introduction

Food waste has long been known as one of the main issue to be faced to combat hunger, reduce the environmental impact, and increase income. Food losses or waste are generally used alternatively, but a slight difference can be addressed between the two terms. “Food losses” refer to the decrease in edible food mass occurring during the food supply chain steps (e.g., production, harvesting, post-harvesting, handling, processing, distribution, and consumption), while “Food waste” generally refers to the final steps of the food chain, related to suppliers and consumers [1-3]. Nevertheless, a third term, “food by-product” is taking place to consider the potentiality of some food losses to be reused inside the food or feed chain. An exact estimation of food loss in the world is not possible due to a lack of data related to a rather complex worldwide scenario. In 2011, the Food and Agriculture Organization (FAO) published a report with the attempt of a rough estimation of this phenomenon. It concluded that about one-third of the edible parts of food produced for human consumption gets lost or wasted (which means about 1.3 billion ton per year). It was also pinpointed that in the industrialized countries (i.e., Europe, North America, and industrialized Asia) more than 40 % of food losses occur at retailers and consumers level [1].

Among the seven commodity groups considered, the most wasted ones, at least in Europe, were roots and tubers crops (>50 %) followed by fruits and vegetables (>40 %), cereals and fish, and seafoods (>30 %), while less spoilage

occurs for oilseed and meat (about 20 %) and milk and dairy products (about 10 %). In the latter commodity most of the loss (40–65 %) occurs, for all the industrialized countries, at the consumption level. Considering such concerning numbers many efforts have been carried out in the last decade to transform "food wastes" into "by-products". Special attention has been paid to the possibility to recover and reuse bioactive compounds (e.g., phenols, carotenoids, phytosterols) to be added as additives (e.g., to extend shelf-life) or as an ingredient in functional foods. Concerning dairy products, lactose and proteins have been the main compounds recovered from food by-products [4,5], while little attention has been paid to the functional components, especially in the lipidic fraction, present in such nutrient food commodities. The milk fat fraction has been demonized for years due to the presence of a relatively high amount of cholesterol and saturated fatty acids, portrayed as the major risk factor for heart disease. More recently, such a fraction has been rehabilitated since many studies have proven the positive health effects of trans fatty acids of animal origin, mainly conjugated linoleic acid (CLA). The latter is a group of naturally occurring fatty acids synthesized from linoleic acid by bacteria present in alimentary tract of ruminant animals or as a result of endogenous conversion of trans-vaccenic acid by Δ9-desaturase in tissues, especially the mammary glands [6-9].

The aim of the present work is to evaluate the change occurring in the profile of the lipidic fraction of different dairy products during and after their natural shelf-life, to evaluate if worthy considering their reuse in the animal feed chain [10]. Both the total fatty acid profile, as methyl derivatives (FAMEs), and triacylglycerols (TAGs) have been considered. A preliminary work has been made to optimize faster analytical methods. Furthermore, three kinds of soft cheese were chosen as representative of perishable dairy products to investigate the effect of different formulation on the lipid profile.

2.1.2. Materials and Method

2.1.2.1. Chemicals and Materials

Ethanol, diethyl ether, sodium sulfate, acetone, sodium methoxylate, hydrochloric acid, and ammonium hydroxide solution were supplied by Sigma-Aldrich (Milan, Italy). Hexane, n-pentane, and acetonitrile (ACN) were purchased from PanReac AppliChem (Barcelona, Spain). Isopropyl alcohol (IPA) LC-grade was from Fluka (Buchs, Switzerland). Boron trifluoride in methanol was purchased from Merck (Milan, Italy).

2.1.2.2. Samples

Three different types of a typical Italian soft cheese (stracchino) of the same brand but with different formulation, namely a stracchino classic (SC), a stracchino added with yogurt (SY) and a stracchino added with probiotic (SP), were freshly collected in a local retailer. Seven food packs for each type, belonging to the same production batch, were purchased to follow the evolution of the lipidic profile every 7 days for 7 times. The sampling design is summarized in Table 1(II-2.1.).

Table 1(II-2.1.). Sampling plan.

SAMPLES		Frequency of extraction	Number of extraction	Extraction method
Commercial denomination	**Code**			
Soft cheese				
Stracchino classic	SC	every 7 days	7	SBR-mini
Stracchino with yogurt	SY	every 7 days	7	SBR-mini
Stracchino with probiotic	SP	every 7 days	7	SBR-mini

2.1.2.3. Sample Preparation

Extraction

All the samples were extracted using a miniaturized Schmid–Bondzynski–Ratzlaff (SBR) procedure [11]. Previously, the miniaturized method (called SBR-mini) was compared with the original one (SBR) by analyzing a sample of SC three times.

SBR. Briefly, about 10 g of the sample accurately weighed and dissolved in 20 mL of hydrochloric acid and 20 mL of ethyl alcohol. The preparation was done in a volumetric flask inserted in a boiling-water bath and kept gently moved (for 30 min at 50 °C) with constant magnetic stirring until complete dissolution. Then, the flask was cooled down in running water and a mixture of 200 mL of n-hexane and ethyl ether (1:2, v/v) was added and the mixture was shaken for additional 15 min. The suspension was left to stand for 10 min to allow phase separation. The extraction protocol was repeated three times. The organic extracts were pooled, dried over anhydrous sodium sulfate, filtered, and then brought to dryness under vacuum; the final dry residue was stored at −18 °C until use.

SBR-mini. The aforementioned method was miniaturized as follow: about 1 g of the sample was dissolved in 2 mL of hydrochloric acid and 2 mL of ethyl alcohol. Then lipids were extracted with 20 mL mixture of n-hexane and ethyl ether (1:2, v/v) following the same procedure described for the original method.

2.1.2.4. Analytical Determination

After extraction, all the samples were divided to be analyzed by high performance liquid chromatography (HPLC) coupled to mass spectrometry (MS), for TAGs analysis; and by gas chromatography (GC)–MS and GC–flame ionization detector (FID) for FAMEs profile determination.

LC–MS Analysis

About 75 mg of each sample extract were diluted in 5 mL of acetone and then filtered through a 0.45 μm Acrodisc nylon membrane filter (Pall Life Sciences, Ann Arbor, MI, USA) prior to LC–MS analyses.

Non-aqueous reversed-phase (NARP)-HPLC with atmospheric pressure chemical ionization (APCI)-MS analyses were performed on a Shimadzu Prominence LC-20A System (Shimadzu, Milan, Italy), consisting of a CBM-20A controller, two LC-20 AD dual-plunger parallel-flow pumps, and a DGU-20A5 degasser. The LC system was coupled to an LCMS-2010 mass spectrometer through an APCI source operated in the positive ionization mode. Chromatographic separation was achieved on Ascentis Express Fused-core C18 columns, 150 mm× 4.6 mm ID, 2.7 μm *d.p.*, kindly provided by Supelco/Sigma-Aldrich (Bellefonte, PA, USA). Mobile phases consisted of (A) ACN, and (B) IPA, under the following gradient: 0 min, 0 % B; 50 min, 70 % B (hold for 4 min); 54 min, 0 % B. The mobile phase flow rate was 1 mL/min.

Injection volume: 15 μL. MS parameters were as follows: *m/z* range: 250–1100; scan speed: 4000 amu/s; nebulizing gas (N_2) flow rate: 2.5 L/min; event time: 0.2 s; detector voltage: 1.6 kV; interface voltage: 4.5 kV; interface temperature: 470 °C; CDL temperature: 300 °C; heat block temperature: 300 °C. The LCMSsolution software (version 3.50 SP2 Shimadzu, Milan, Italy) was used for data collection and handling.

GC–FID and GC–MS Analysis

Fatty acid methyl esters were obtained according to a previously applied procedure in milk samples [12]. Conventional GC–MS analyses of FAME samples were carried out on a GCMS-QP2010 (Shimadzu, Milan, Italy) equipped with a split/splitless injector, an AOC-20i autosampler, and a quadrupole MS detector.

Oven programmed temperature, 50–280 °C at 3 °C/min; helium was used as

carrier gas at constant linear velocity, 30 cm/s. A 30 m× 0.25-mm ID, 0.25 μm d_f Supelcowax-10 column (Sigma-Aldrich/Supelco, Bellefonte, USA) was used for the separation; injection volume and mode: 0.5 μL, split ratio: 1:250. MS parameters were as follows: mass range 40–400 amu; acquisition frequency 5 Hz. Ion source temperature, 200 °C and interface temperature, 250 °C.

Fast GC–MS analyses were carried out using a Supelcowax-10 column, 10 m× 0.10 mm ID × 0.10 μm d_f.

Oven temperature program: 50–280 °C (hold 2 min) at 40 and 80 °C/min. Helium was used as carrier gas at constant linear velocity, 70 cm/s. Injection volume and mode: 0.5 μL, split ratio: 1:250. MS parameters were as follows: mass range 40–400 amu; acquisition frequency 10 Hz. Ion source temperature, 200 °C and interface temperature, 250 °C.

The GCMSsolution software (version 2.71 Shimadzu, Milan, Italy) was used for data collection and handling. Identification was carried out through library search into the FAMEs: Mass Spectral Database (Wiley), with the simultaneous use of linear retention indices (LRIs) [13].

Conventional GC–FID analyses were performed on a Shimadzu GC-2010 instrument equipped with a split/splitless injector and a Shimadzu autosampler AOC-20is (Shimadzu, Milan, Italy). Data acquisition was performed using Shimadzu's GCSolution Software. Column: Supelcowax-10, 30 m× 0.25 mm ID× 0.25 μm d_f. Inlet pressure: 100 KPa.

Carrier gas: He, u: 30.1 cm/s. Injection volume: 1.0 μL. Split ratio: 1:100. Detector: FID; Temperature: 280 °C. H2: 40.0 mL/ min, air flow: 400.0 mL/min. Temperature program: 50–280 °C (hold for 5 min) at 3 °C/min, with a total run time of about 80 min.

Fast GC–FID analyses were performed on the same Shimadzu instrument. Column: Supelcowax-10, 10 m× 0.10 mm ID× 0.10 μm d_f. Carrier gas: H_2, carrier gas at constant linear velocity, 70 cm/s. Injection volume: 0.2 μL.

Split ratio: 1:50. Detector: FID H2: 50.0 mL/min, air: 400.0 mL/min. Oven temperature program: 50–280 °C (hold for 2 min) at 40 and 80 °C/min. The chromatographic runs lasted about 8 and 5 min, respectively.

Individual fatty acid methyl esters (FAMEs) are reported as the percentage of total FAMEs. Area correction was performed to correct the FID response for the short-chain fatty acids by means of theoretical relative response factors (TRF) [14]. Reliability of TRF was previously checked by means of standard mixtures analysis.

2.1.2.5. Statistical Analysis

A principal component analysis (PCA) was performed as an unsupervised method to ascertain the degree of differentiation between samples considering the FAMEs and TAGs identified as variables. PCA and three-way PCA were performed by using an R-based chemometric software (http://gruppochemiometria.it 2014).

PCA is a well-exploited technique to extract and visualize significant information from a data set. An orthogonal rotation is performed to transform the *v*-dimensional space of the *v* original variables into a *c*-dimensional space (with $c < v$) of uncorrelated variables (new axes). The coefficients of the original variables defining each Principal Component are called "loadings" and the projections of the objects on the new axes are called "scores". The three-way PCA takes in account the three-dimensional structure of the data set and simplify the interpretation of possible correlations.

2.1.3. Results and Discussion

The aim of the present investigation was the optimization of rapid and reliable analytical methods for dairy products characterization and the investigation of the variation of the FAMEs and TAGs profile during storage of fresh-cheese

products and after their best-by-date. This is the preliminary part of a project that has, as the final objective, the characterization of the lipidic profile of best-by-date dairy products to evaluate their nutritional value for possible reintroduction in the food or feed chain after their isolation.

Considering the relatively large number of samples that has been analyzed in the entire project, the first step of the research work was to speed up the entire analytical procedure, along with the reduction of the solvent volumes involved in the extraction step. Furthermore, a limited number of samples were chosen to investigate how the lipid profile changes over time. Three kinds of cheese (all with a fat content of 26.5% reported on the label) were selected, namely a SC, SY, and SP.

The extraction method was simply scaled-down by ten-fold, starting from the classical SBR method. The extraction yields of the conventional and reduced SBR method were compared. The same sample was extracted three times and the two average yields were compared using a *t* test. No significant difference ($p>0.05$) was observed, with a lipid extraction yield of about 25 %.

The fresh sample of SC was extracted three times and each extraction was evaluated both in term of FAMEs and TAGs profile by injecting three times the same extract to evaluate the overall variability of the methods. The quantitative variability (expressed as CV%) for the three injections, was in average of about 4 % for all FAMEs (with maximum values of about 10 %) and of about 6.5%for all TAGs (with maximum values of about 15 %); while the overall variability (considering the three extractions and the three injections for each extraction, n =9) was about 10 % for both FAMEs and TAGs (with maximum values of about 20 %).

2.1.4. FAMEs Analysis Optimization

Conventional GC–MS analysis was carried out for identification purposes.

Different filtering criteria were used, namely mass spectrum similarity match above 80 %, linear retention indices (LRI) in a ±10 range compared with the indices reported in the FAMEs Library (calculated based on a FAMEs mixture). Comparison with data reported in the literature for similar samples was carried out for further confirmation [12].

The FAMEs samples obtained from the extraction of the three different stracchino samples (e.g., SC, SY, and SP) were injected into a GC–FID, using conventional conditions, and two fast conditions. The conventional run, performed using a 30m× 0.25mm ID column lasted about 80 min, while using a 10 m×0.1 mm ID column, at 40 and 80 °C/min, a total run time of about 8 and 5 min was obtained, respectively. The GC–FID analyses were performed in triplicate for quantitative comparison purposes. Figure 1 (II-2.1.) shows a comparison of the three chromatograms obtained in the conventional (Figure 1a (II-2.1.), 80 min), and fast (Figure 1b (II-2.1.) and Figure 1c (II-2.1.); 8 and 5 min, respectively) conditions for the SC sample (the others comparisons, SY and SP, are reported in Supplementary Figures 1S (II-2.1.) and 2S (II-2.1.). In the boxes are reported expansions of the C18 part of each chromatogram.

Such a drastic reduction in the GC run time cannot be attained without a cost, in terms of peak resolution, different degrees of partial coelution, as can be observed in the conventional and very fast chromatogram expansions, reported in Figure 1 (II-2.1.). Of the 62 identified peaks, only four compounds (three different C18:1 isomers and C18:2n6) in the 8 min run and seven (C17:1, three different C18:1 isomers, two different C18:2, and C20:1n9) in the 5 min run were coeluted.

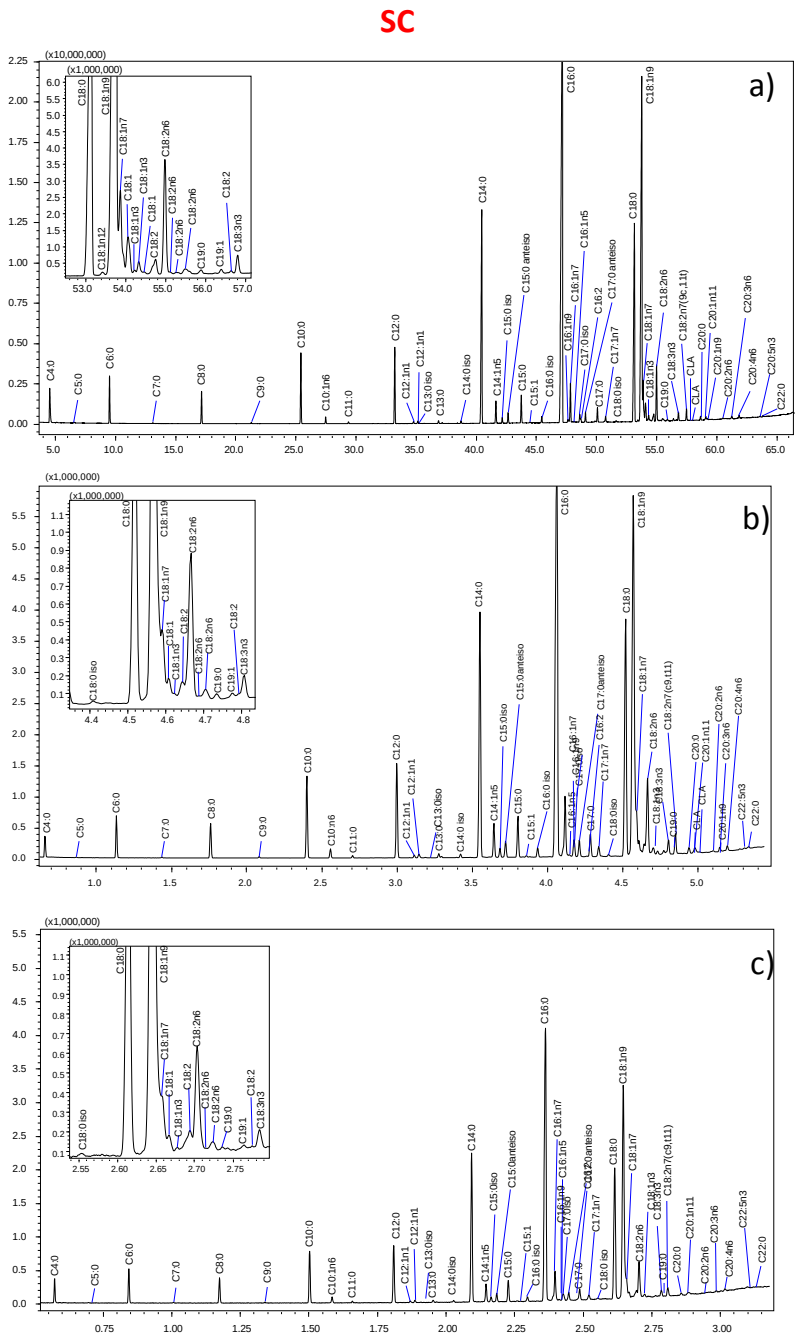

Figure 1 (II-2.1.). GC–FID FAMEs profile of SC sample, obtained using different chromatographic conditions. **a)** conventional run (80 min); **b)** fast run (8 min); and **c)** faster run (5 min).

The quantitative comparison is graphically shown in Figure 2 (II-2.1.). for the SC sample (all the quantitative data of SC, SY, and SP are reported in Supplementary Table 1S (II-2.1.).

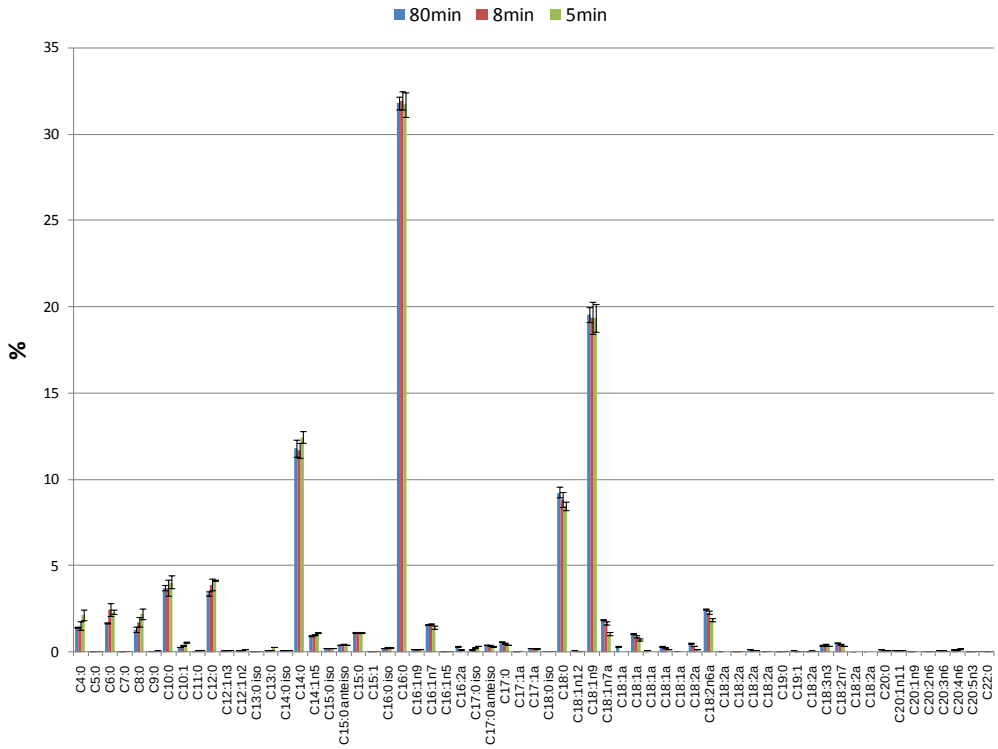

Figure 2 (II-2.1.). Quantitative comparison of FAMEs for the SC sample obtained applying the three different GC–FID conditions.

GC peak area repeatability (CV%) was determined for all the conditions tested, CV% values are reported in Supplementary Table 1S (II-2.1.) and are in average as follow: 4.6, 5.1, and 4.4 % for conventional conditions; 7.1, 8.6, and 5.6 % for fast conditions lasting about 8 min; and 6.4, 5.0, and 3.9 % for fast conditions lasting about 5 min, for SC, SP, and SY, respectively.

Considering the extremely high advantage in terms of throughput, a little resolution loss was considered more than acceptable; thus, the fast chromatographic conditions (8 min run time) were chosen for all the following

analysis.

2.1.5. TAGs Analysis

TAGs profile of milk and dairy products is highly complex since TAGs are synthesized from a large number of fatty acids [15-17]. Consequently, the identification and quantification of individual TAGs have proved an extremely difficult and frustrating exercise with only a few species being identified. The retention of TAGs is governed by the partition number (PN), which is defined as PN=CN (carbon number)− 2 ×DB (double bond). The separation of most TAGs within one PN group is feasible under optimized chromatographic conditions [18,19] and the retention of TAGs within the same PN group increases with decreasing DB in the acyl chains. In the case of TAGs, still with the same PN but also with equal CNs and DB number, retention depends also on the combination of single FAs onto the glycerol backbone [19,20,21]. The separation of *cis*-/*trans*-isomers [22,23], DB positional isomers [24,25] or partially separated regioisomers [26] has also been reported in NARP-HPLC. The HPLC–APCI-MS method used in this work was previously used to elucidate the TAGs profile in milk and dairy samples [18]. TAGs were identified according to their HPLC–APCI-MS mass spectra considering m/z values of pseudo molecular $[M+H]^+$ and "diacylglycerol" fragment $[M+H–RCOOH]^+$ ions. However, GC–FID/MS data were of fundamental support during the identification process of TAGs.

The APCI interface is considered the most suitable detector for TAGs analysis since it is characterized by a good linearity range and a relatively low difference in response factors among different TAGs compositions [19,27]. Furthermore, when a single quadrupole MS is employed, APCI has the added benefit of unambiguous structural identification due to a more extensive fragmentation compared to ESI. In fact, the MS spectra generated by ESI is characterized by a

sets of a protonated ions $[M+X]^+$ (X=H; Na; NH4, etc.), but less or no fragmentation is formed. These $[M+X]^+$ ions may correspond to a certain number of different TAGs protonated molecules, thus causing an overestimation of the real number of TAGs occurred in the investigated samples (false positives) [27]. Using APCI a more characteristic fragments are obtained, with a relative abundance (%) of the protonated $[M+H]^+$ ions varying according to the degree of unsaturation (e.g., C18:1-C18:1-C18:1 > C18:1-C18:1-C16:0>C18:1-C16:0-C16:0>C16:0-C16:0-C16:0) [18,28], and informative fragments,

such as $[M+H-2(RiCOOH)]^+$ corresponding to monoacylglycerol (MAG) fragments, which can support a most reliable assignment of isobaric compounds. Additionally, APCI-MS has the added benefit of information on regioisomers. Neutral loss of RCOOH from the equivalent side positions sn-1

and *sn*-3 is preferred over cleavage from the position *sn*-2 [19,27]. The positions *sn*-1 and *sn*-3 are considered equivalent because they cannot be distinguished by NARP-HPLC, thus, FA in *sn*-1 and sn-3 positions are ordered, conventionally, by decreasing molecular weight, i.e.,

C18:0-C18:1-C16:0 (not C16:0-C18:1-C18:0). For the identification of trace peaks, the extracted ion current chromatograms of selected *m/z* values were used to confirm the presence or absence of compounds. Figure 3 (II-2.1.) shows the total ion current (TIC) chromatogram (two expansions), with the peaks identity corresponding to the TAGs identification reported in Table 2 (II-2.1.); while the TAGs profiles of SY and SP are reported in Supplementary Figures 3S (II-2.1.) and 4S (II-2.1.), respectively. A good separation of detected TAGs was obtained, even if a large number of coelutions were observed. Table 2 (II-2.1.) reports the number of peaks separated and the TAGs identified within each peak, for the three kinds of samples analyzed.

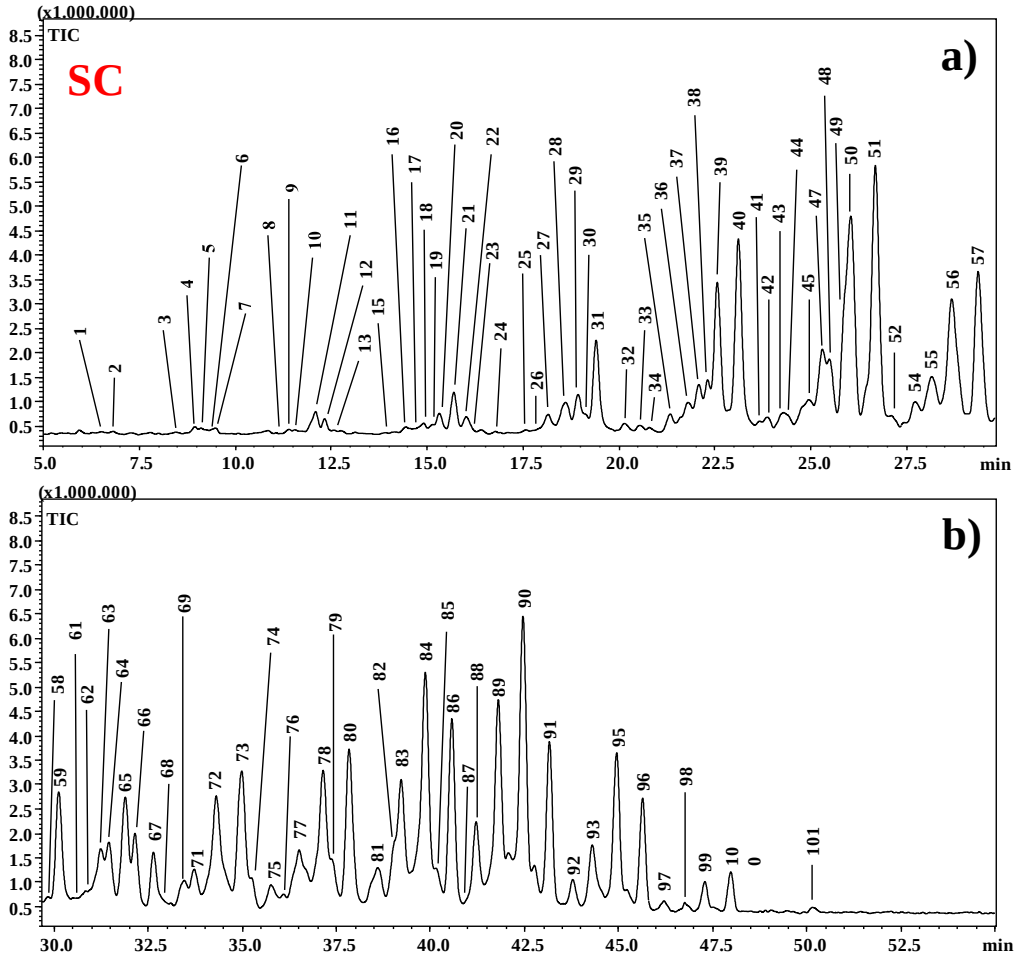

Figure 3 (II-2.1.) Enlargement of TIC chromatogram of SC sample by NARP-HPLC–APCI-MS. a) min 5.0–29.5; b) min 29.5–55.0.

Table 2 (II-2.1.). Peak identity with TAG identification in SC, SY, and SP samples.

Peak n.	TAGs	SC	SY	SP	Peak n.	TAGs	SC	SY	SP
1	C8:0-C8:0-C8:0	x	x	x	**30**	C18:1-C18:3-C4:0	x	x	x
	C10:0-C6:0-C6:0	x	x	x		C18:2-C14:0-C4:0	x	x	x
2	C10:0-C8:0-C6:0	x	x	x		C16:1-C14:0-C4:0	x	x	x
	C10:0-C10:0-C4:0	x	x	x		C16:0-C14:1-C4:0	x	x	x
	C12:0-C8:0-C4:0	x	x	x	**31**	C14:0-C14:0-C4:0	x	x	x
3	C10:0-C8:0-C8:0	x	x	x		C16:0-C12:0-C4:0	x	x	x
	C10:0-C10:0-C6:0	x	x	x	**32**	***C15:0-C15:0-C4:0***	x	x	x
	C12:0-C8:0-C6:0	x	x	x	**33**	C15:0-C14:0-C4.0	x	x	x
4	***C12:0-C10:0-C4:0***	x		x		C15:0-C12:0-C6:0	x	x	x
5	***C8:0-C14:0-C4:0***	x	x	x	**34**	***C16:1-C15:0-C4:0***	x	x	x
6	C18:1-C6:0-C4:0	x	x	x	**35**	C15:0-C14:0-C4:0	x	x	x
7	C16:0-C6:0-C4:0	x	x	x		C18:1-C10:0-C8:0	x	x	x
8	***C10:0-C10:0-C8:0***	x	x	x		C18:2-C10:0-C10:0	x	x	x
9	***C12:0-C10:0-C6:0***	x	x	x	**36**	C14:0-C10:0-C10:0	x	x	x
10	***C14:0-C8:0-C6:0***	x	x	x		C16:0-C10:0-C8:0	x	x	x
11	C18:1-C8:0-C4:0	x	x	x		C12:0-C12:0-C10:0	x	x	x
	C16:0-C6:0-C6:0	x	x	x		C14:0-C12:0-C8:0	x	x	x
	C14:0-C10:0-C4:0	x	x	x	**37**	C18:1-C18:2-C4:0	x	x	x
12	***C8:0-C16:0-C4:0***	x	x	x		C18:1-C16:1-C4:0	x	x	x
13	***C10:1-C16:0-C4:0***	x	x	x	**38**	C14:0-C14:0-C6:0	x	x	x
14	C18:0-C6:0-C4:0		x	x		C16:0-C12:0-C6:0	x	x	x
15	***C15:0-C10:0-C4:0***	x	x	x	**39**	C18:2-C16:0-C4:0	x	x	x
16	C12:0-C10-0-C8:0	x	x	x		C16:0-C16:1-C4:0	x	x	x
	C10:0-C10:0-C10:0	x	x	x		C18:1-C14:0-C4:0	x	x	x
17	C14:0-C8:0-C8:0	x	x	x	**40**	C16:0-C14:0-C4:0	x	x	x
	C18:0-C8:0-C6:0	x	x	x		C18:0-C12:0-C4:0	x	x	x
18	***C14:0-C10:0-C6:0***	x	x	x	**41**	C18:1-C15:0-C4:0	x	x	x
19	***C16:0-C8:0-C6:0***	x	x	x		C15:0-C10:0-C10:0	x	x	x
20	***C18:1-C10:0-C4:0***	x	x	x	**42**	C16:0-C16:0-C2:0	x	x	x
21	C16:0-C10:0-C4:0	x	x	x	**43**	C16:0-C15:0-C4:0[a]	x	x	x
	C14:0-C12:0-C4:0	x	x	x		C17:0-C14:0-C4:0[b]	x	x	x
22	***C18:3-C14:0-C4:0***	x	x	x	**44**	C18:0-C15:0-C4:0	x	x	x
23	***C12:1-C16:0-C4:0***	x		x		C17:1-C16:0-C4:0[c]	x	x	x
24	C15:0-C12:0-C4:0	x	x	x	**45**	C18:1-C10:0-C10:0	x	x	x
	C15:0-C10:0-C6:0	x	x	x		C18:1-C18:2-C6:0	x	x	x
25	***C12:0-C15:0-C4:0***	x	x	x		C18:1-C12:0-C8:0	x	x	x
26	***C12:0-C10:0-C10:0***	x				C18:1-C16:1-C6:0		x	x
27	C14:0-C10:0-C8:0	x	x	x		C18:1-C14:1-C8:0		x	x
	C16:0-C8:0-C8:0	x	x	x	**46**	C16:0-C15:0-C4:0[a]		x	
	C18:1-C10:0-C6:0	x	x	x		C17:0-C14:0-C4:0[b]		x	
	C16:1-C12:0-C6:0	x	x	x		C17:1-C16:0-C4:0[c]		x	
28	C14:0-C12:0-C6:0	x	x	x	**47**	C16:0-C10:0-C10:0	x	x	x
	C18:0-C8:0-C6:0	x	x	x		C14:0-C14:0-C8:0	x	x	x
	C16:0-C10:0-C6:0	x	x	x		C14:0-C12:0-C10:0	x	x	x
29	C18:1-C12:0-C4:0	x	x	x		C12:0-C12:0-C12:0	x	x	x
	C18:2-C18:2-C4:0	x	x	x		C18:0-C10:0-C8:0		x	x
	C16:1-C16:1-C4:0	x	x	x					

Peak n.	TAGs	SC	SY	SP	Peak n.	TAGs	SC	SY	SP
48	C18:1-C18:1-C4:0	x	x	x	**66**	C16:0-C16:0-C8:0	x	x	x
	C18:1-C14:10-C6:0	x	x	x		C18:0-C14:0-C8:0	x	x	x
49	***C14:0-C16:0-C6:0***	x	x	x	**67**	***C18:0-C16:0-C6:0***	x	x	x
50	***C18:1-C16:0-C4:0***	x	x	x	**68**	C18:1-C15:0-C10:0	x	x	x
51	C16:0-C16:0-C4:0	x	x	x		C17:0-C14:0-C10:0	x	x	x
	C18:0-C14:0-C4:0	x	x	x		C17:0-C16:0-C8:0	x	x	x
52	C18:1-C15:0-C6:0	x	x	x	**69**	C18:0-C18:0-C4:0	x	x	x
	C18:1-C17:0-C4:0	x	x	x		C16:0-C15:0-C10:0	x	x	x
53	***C17:0-C17:0-C4:0***		x	x	**70**	***C18:1-C12:0-C18:2***		x	
54	C16:0-C15:0-C6:0	x	x	x	**71**	C18:1-C18:1-C10:0	x	x	x
	C18:0-C15:0-C4:0	x	x	x		C18:1-C16:1-C12:0	x	x	x
	C17:0-C16:0-C4:0	x	x	x	**72**	C16:1-C16:1-C14:0	x	x	x
55	C18:1-C18:1-C6:0	x	x	x		C18:2-C16:0-C12:0	x	x	x
	C18:1-C18:2-C8:0	x	x	x		C18:1-C16:0-C10:0	x	x	x
	C18:1-C12:0-C10:0	x	x	x		C16:0-C16:1-C12:0	x	x	x
	C16:1-C16:1-C10:0	x	x	x		C18:1-C14:0-C12:0	x	x	x
	C18:1-C14:0-C8:0	x	x	x		C18:0-C18:1-C8:0	x	x	x
56	C14:0-C12:0-C12:0	x	x	x		C18:0-C16:1-C10:0	x	x	x
	C14:0-C14:0-C10:0	x	x	x	**73**	C16:0-C14:0-C12:0	x	x	x
	C16:0-C12:0-C10	x	x	x		C16:0-C16:0-C10:0	x	x	x
	C16:0-C14:0-C8:0	x	x	x		C14:0-C14:0-C14:0	x	x	x
	C18:1-C16:0-C6:0	x	x	x		C18:0-C14:0-C10:0	x	x	x
	C20:1-C14:0-C6:0		x	x		C18:0-C12:0-C12:0	x	x	x
57	C16:0-C16:0-C6:0	x	x	x	**74**	***C18:0-C16:0-C8:0***	x	x	x
	C18:0-C14:0-C6:0	x	x	x	**75**	C18:0-C18:0-C6:0	x	x	x
58	C18:0-C18:1-C4:0	x	x	x		C18:0-C15:0-C10:0	x	x	x
	C15:0-C14:0-C10:0		x	x		C17:0-C16:0-C10:0	x	x	x
59	***C18:0-C16:0-C4:0***	x	x	x		C18:1-C15:0-C12:0	x	x	x
60	C17:0-C16:0-C6:0		x	x	**76**	C18:1-C18:2-C18:2	x	x	x
	C18:0-C15:0-C6:0		x	x		C18:1-C18:2-C16:1	x	x	x
	C15:0-C12:0-C12:0		x	x	**77**	C18:1-C18:2-C14:0	x	x	x
	C16:0-C13:0-C10:0		x	x		C18:1-C16:1-C16:1	x	x	x
	C20:1-C15:0-C6:0		x	x		C18:1-C18:3-C16:0	x	x	x
61	C18:1-C18:2-C10:0	x	x	x		C18:1-C18:1-C12:0	x	x	x
	C16:0-C15:0-C8:0	x	x	x		C16:0-C16:1-C16:1	x	x	x
62	***C18:1-C18:1-C8:0***	x	x	x		C18:1-C16:1-C14:0	x	x	x
63	C18:2-C16:0-C10:0	x	x	x	**78**	C18:2-C16:0-C14:0	x	x	x
	C18:2-C14:0-C12:0	x	x	x		C18:1-C16:0-C12:0	x	x	x
	C18:1-C14:0-C10:0	x	x	x		C18:0-C18:1-C10-0	x	x	x
	C16:0-C16:1-C10:0	x	x	x		C18:1-C14:0-C14:0	x	x	x
	C18:1-C12:0-C12:0	x	x	x	**79**	C16:0-C16:1-C14:0	x	x	x
64	C18:1-C16:0-C8:0	x	x	x		C16:0-C16:0-C14:1	x	x	x
	C18:1-C14:1-C12:1	x	x	x		C18:0-C14:0-C14:1	x	x	x
	C14:0-C14:0-C14:1	x	x	x	**80**	C18:0-C16:0-C10:0	x	x	x
65	C18:0-C18:1-C6:0	x	x	x		C16:0-C16:0-C12:0	x	x	x
	C14:0-C14:0-C12:0	x	x	x		C18:0-C14:0-C12:0	x	x	x
	C16:0-C12:0-C12:0	x	x	x		C16:0-C14:0-C14:0	x	x	x
	C16:0-C14:0-C10:0	x	x	x					
	C18:0-C12:0-C10:0	x	x	x					

Peak n.	TAGs	SC	SY	SP	Peak n.	TAGs	SC	SY	SP
81	C18:0-C18:0-C8:0	x	x	x	**91**	C18:1-C18:1-C17:0	x	x	x
	C16:0-C15:0-C14:0	x	x	x		C16:0-C16:0-C16:0	x	x	x
	C17:0-C16:0-C12:0	x	x	x		C18:0-C16:0-C14:0	x	x	x
	C18:1-C18:1-C18:2	x	x	x	**92**	C18:1-C17:0-C16:0	x	x	x
82	C18:1-C18:1-C16:1	x	x	x		C18:0-C16:0-C15:0[d]	x	x	x
	C18:1-C18:2-C16:0	x	x	x		C17:0-C16:0-C16:0[e]	x	x	x
	C18:0-C18:2-C16:1			x		C20:1-C18:1-C18:1	x	x	x
83	C18:1-C18:1-C14:0	x	x	x	**93**	***C18:0-C18:1-C18:1***	x	x	x
	C18:0-C16:1-C16:1	x	x	x	**94**	C18:0-C18:0-C18:2		x	
84	C18:1-C16:0-C16:1	x	x	x		C18:0-C18:1-C15:0		x	
	C16:0-C16:0-C16:1	x	x	x		C18:0-C16:0-C15:0[d]		x	
	C18:2-C16:0-C16:0	x	x	x		C17:0-C16:0-C16:0[e]		x	
	C18:0-C18:2-C14:0	x	x	x		C20:1-C18:1-C16:1		x	
85	C18:1-C16:0-C14:0	x	x	x	**95**	***C18:0-C16:0-C18:1***	x	x	x
	C18:0-C18:1-C12:1	x	x	x	**96**	C18:0-C16:0-C16:0[f]	x	x	x
86	C18:0-C14:0-C14:0	x	x	x		C18:0-C18:0-C14:0[g]	x	x	x
	C16:0-C16:0-C14:0	x	x	x	**97**	C18:0-C18:1-C17:0[h]	x	x	x
	C18:0-C16:0-C12:0	x	x	x		C18:0-C17:0-C16:0[i]	x	x	x
87	C18:1-C16:0-C15:0	x	x	x		C18:0-C18:0-C15:0[l]	x	x	x
	C18:1-C18:1-C15:0	x	x	x	**98**	C18:0-C16:0-C16:0[f]	x	x	x
88	C18:1-C18:1-C18:1	x	x	x		C18:0-C18:0-C14:0[g]	x	x	x
	C17:0-C16:0-C14:0	x	x	x		C18:0-C18:1-C17:0[h]	x	x	x
	C16:0-C16:0-C15:0	x	x	x		C18:0-C17:0-C16:0[i]	x	x	x
	C18:0-C18:2-C15:0	x	x	x		C18:0-C18:0-C15:0[l]	x	x	x
89	C18:0-C18:0-C16:0	x	x	x	**99**	***C18:0-C18:1-C18:0***	x	x	x
	C18:0-C18:2-C16:0	x	x	x	**100**	***C18:0-C16:0-C18:0***	x	x	x
90	C18:1-C16:0-C16:0	x	x	x	**101**	C18:0-C18:0-C18:0	x	x	x
	C18:0-C18:1-C14:0	x	x	x		C20:0-C16:0-C16:0	x	x	x

TAGs in ***italic***: most abundant regioisomer; TAG x : same x indicates pair of TAGs with the same APCI mass spectrum, but different chromatographic retention on RP column.

2.1.6. FAMEs and TAGs Profile Evolution

The simple evaluation of the percentage profile of the three kinds of stracchino samples over time did not highlight any significant changed. Therefore, more powerful unsupervised data handling for discriminate among samples was applied. The data obtained from both the FAMEs and TAGs profiles of SC, SY, and SP was evaluated all together performing both a three-way PCA (applying the Tuker3 model and j-scaling the variables) and a traditional PCA to evaluate a general trend. The three-way PCA allows a much easier interpretation of the

information present in the data set since it directly takes into account its three-way structure. A matrix, containing 101 TAGs peaks and 62 FAMEs, was built. The data used for such an elaboration are reported in Supplementary Table 2S (II-2.1.). Figure 4 (II-2.1.) reports the plot of object (Figure 4a (II-2.1.) and the plot of conditions (Figure 4b (II-2.1.) obtained from the three-way PCA elaboration while the plot of variables is reported in the Supplementary information (Supplementary Figure 5S (II-2.1.). As evident from the plot of objects, it was possible to clearly discriminate among the three different product types, namely SC (1), SY (2), and SP (3). Furthermore, a general trend was observed following the age of the products (plot of conditions). The products were analyzed at seven different sampling times, namely the fresh product (condition 1), at the expiring date (condition 2), and later every week for a total of five more sampling time (condition 3-7). The first sampling time (1, fresh product) was located rather far from the other conditions, except for the condition 3, which seemed to be an outlier. Performing the three-way PCA separately on the matrices obtained by the analysis of FAMEs and TAGs, it was observed that the general trend was mainly affected by the behavior of TAGs over time. While, in the elaboration of the FAMEs matrix only the sampling time 1 (t0, fresh product) was located quite far from the other conditions (data not shown). Such a general behavior can be explained by hydrolysis of the lipid components, while the occurrence of other deterioration processes on such a fraction (e.g., oxidation) during the experiment timeframe can be considered not significant.

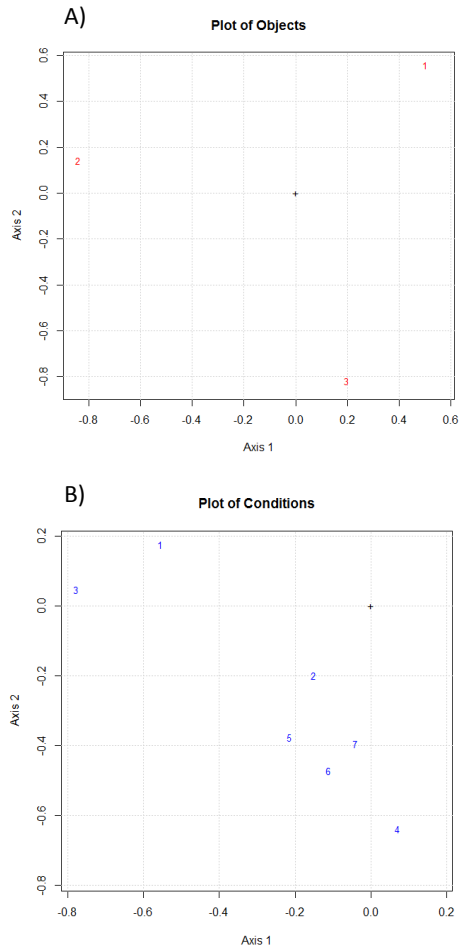

Figure 4 (II-2.1.). a Plot of Object and b Plot of Condition obtained by performing the three-way PCA on the entire data set of FAMEs and TAGs.

A traditional PCA was also performed on the entire matrix of data. The score plot of component 1 *vs* component 3 is shown in Figure 5 (II-2.1.) (57.2 % of total variance), while the loading plot is reported in Supplementary Figure 6S (II-2.1.) The results highlighted that the variability between SC and SY over storage time was far lower than the variability observed for SP after the expiring date. This behavior is probably due to the hydrolysis, along with the

enzymatic activity, which mainly occurred in the SP sample, due to the presence of active microorganisms.

Differently from other lipidic products, such as vegetable oils, which undergo mainly to oxidation process of unsaturated FAMEs, in dairy products TAGs are the main fraction affected by over-storage. Such a behavior was more evident in the SP samples, probably due to the presence of particularly acid resistant Lactobacilli strains, namely *L. acidophilus* and *L. casei* (as reported in the label), which most probably remain active longer, despite the increasing acidity deriving from lactose fermentation, and caused a different product evolution compared to SC and SY. It is interesting to highlight that the sample of fresh SP (SP, t0) was not significantly different from SC and SY, while the evolution of the lipid profile of the SP samples (SP exp and SP exp 1–5) resulted very different from SC and SY. The main change on the lipid profile occurred during the shelf-life of the product, between t0 and t exp, then the overall profile remained almost the same. Many studies have reported the effect of probiotic intake in the human lipid profile, while little information has been found on the product modification related to the microbiological activity [29,30].

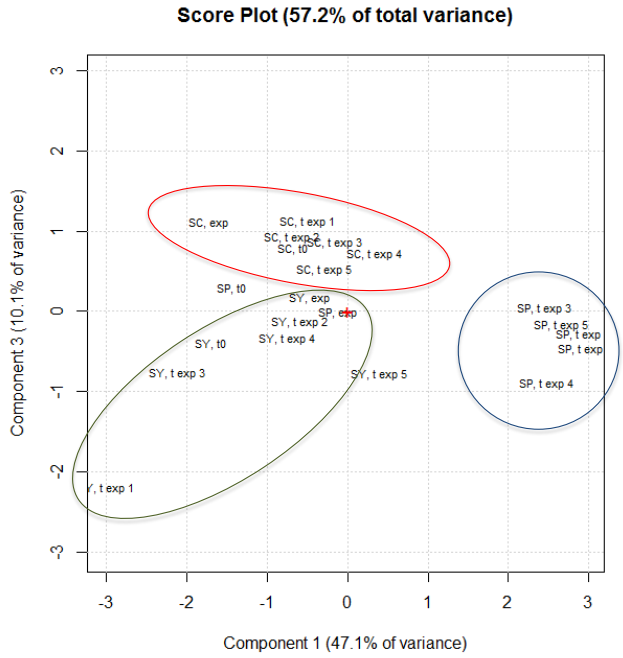

Figure 5 (II-2.1.). Score plot on PC1 and PC3 of FAMEs and TAGs of the SC, SY, and SP samples analyzed during the project.

2.1.7. Conclusions

In this study, the reliability of fast GC approaches for the evaluation of FAMEs profile in dairy products was proven by a qualitative and quantitative comparison. Such a rapid method for FAMEs analysis, along with a previous optimized LC–MS method for TAGs evaluation were applied to characterize the lipid profile of dairy products starting from the fresh product and following the lipid evolution after their best-by-date. Unsupervised data handling, namely PCA and three-way PCA, was applied to highlight the main differences among the three different kinds of samples analyzed and how they changed over time. Not significant differences were highlighted for SC and SY, while far more peculiar was the evolution of the lipid profile of SP, even if not further

significantly difference were highlighted after the expiring date. Such a behavior can be an interesting topic for future research. This work was the preliminary step of a larger project, devoted to the characterization of a large number of different expired dairy products to evaluate their nutritional value for possible re-introduction in the food or feed chain. The not significant change in the lipid fraction, except for particular products such as SP, will allow us to analyze the expired dairy products once delivered in our lab and consider their profile stable over a reasonable timeframe.

REFERENCES

[1] Food and Agriculture Organization of the United Nations (2011). Available at http://www.fao.org/docrep/014/mb060e/mb060e.pdf.

[2] Galanakis CM (2012) Recovery of high added-value components from food wastes: conventional, emerging technologies and commercialized applications. Trends Food Sci Technol 26:68–87.

[3] Parfitt J, Barthe M, MacNaughton S (2010) Food waste within food supply chains: quantification and potential for change to 2050. Phil Trans R Soc B 365:3065–3081.

[4] Bund RK, Pandit AB (2007) Rapid lactose recovery from paneer whey using sonocrystallization: a process optimization. Chem Eng Process 46:846–850.

[5] El-Sayed MMH, Chase HA (2011) Trends in whey protein fractionation. Biotechnol Lett 33:1501–1511.

[6] Agatha G, Voigt A, Kauf E, Zintl F (2004) Conjugated linoleic acid modulation of cell membrane in leukemia cells. Cancer Lett 209:87–103.

[7] Kritchevsky D, Tepper SA, Wright S, Tso P, Czarnecki SK (2000) Influence of conjugated linoleic acid (CLA) on establishment and progression of atherosclerosis in rabbits. J Am Coll Nutr 19: 472S–477S.

[8] Lee KW, Lee HJ, Cho HY, Kim YJ (2005) Role of the conjugated linoleic acid in the prevention of cancer. Crit Rev Food Sci Nutr 45:135–144.

[9] Parodi PW (2004) Milk fat in human nutrition. Aust J Dairy Technol 59:3–29.

[10] Shantha NC, Ram LN, O'Leary J, Hicks CL, Decker EA (1995) Conjugated linoleic acid concentrations in dairy products as affected by processing and storage. J Food Sci 60:695–697

[11] IDF (1986) Cheese and processed cheese products. Determination of fat content, international standard 5B. International Dairy Federation, Brussels, Belgium.

[12] Russo M, Cichello F, Ragonese C, Donato P, Cacciola F, Dugo P, Mondello L (2013) Profiling and quantifying polar lipids in milk by hydrophilic interaction liquid chromatography coupled with evaporative light-scattering and mass spectrometry detection. Anal Bioanal Chem 405:4617–4626.

[13] Van Den Dool H, Kratz PD (1963) A generalization of the retention index system including linear temperature programmed gas–liquid partition chromatography. J Chromatogr A 11:463–471.

[14] Ackman RG (2007) In: Chow CK (ed) Fatty acids in foods and their health implications, 3rd edn., Taylor & Francis, Boca Raton.

[15] Jensen RG (2002) The composition of bovine milk lipids: January 1995 to December 2000. J Dairy Sci 85:295–350.

[16] Jensen RG, Newberg DS (1995) Milk lipids B. Bovine milk lipids. In: Jensen RG (ed) Handbook of milk composition. Academic Press, San Diego, CA, pp 543–575.

[17] Patton S, Jensen RG (1975) Lipid metabolism and membrane functions of the mammary gland. Prog Chem of Fats and other Lipids 14.

[18] Beccaria M, Sullini G, Cacciola F, Donato P, Dugo P, Mondello L (2014) High performance characterization of triacylglycerols in milk and milk-related

samples by liquid chromatography and mass spectrometry. J Chromatogr A 1360:172–187.

[19] Holčapek M, Lísa M, Jandera P, Kabátová N (2005) Quantitation of triacylglycerols in plant oils using HPLC with APCI-MS, evaporative light-scattering, and UV detection. J Sep Sci 28:1315–1333.

[20] Beccaria M, Costa R, Sullini G, Grasso E, Cacciola F, Dugo P, Mondello L (2015) Determination of the triacylglycerol fraction in fish oil by comprehensive liquid chromatography techniques with the support of gas chromatography and mass spectrometry data. Anal Bioanal Chem 407:5211–5225.

[21] Lísa M, Holčapek M (2008) Triacylglycerols profiling in plant oils important in food industry, dietetics and cosmetics using highperformance liquid chromatography-atmospheric pressure chemical ionization mass spectrometry. J Chromatogr A 1198–1199:115–130.

[22] Lin JT, Woodruff CL, McKeon TA (1997) Non-aqueous reversed-phase high-performance liquid chromatography of synthetic triacylglycerols and diacylglycerols. J Chromatogr A 782:41–48.

[23] Mottram HR, Crossman ZM, Evershed RP (2001) Regiospecific characterisation of the triacylglycerols in animal fats using high performance liquid chromatography-atmospheric pressure chemical ionisation mass spectrometry. Analyst 126:1018–1024.

[24] Laakso P (1997) Characterization of α- and γ-linolenic acid oils by reversed-phase high-performance liquid chromatographyatmospheric pressure chemical ionization mass spectrometry. J Am Oil Chem Soc 74:1291–1300.

[25] Lísa M, Holčapek M, Řezanka T, Kabátová N (2007) High-performance liquid chromatography-atmospheric pressure chemical ionization mass spectrometry and gas chromatography-flame ionization detection characterization of Δ5-polyenoic fatty acids in triacylglycerols from conifer

seed oils. J Chromatogr A 1146:67–77.

[26] Momchilova S, Tsuji K, Itabashi Y, Nikolova-Damyanova B, Kuskis A (2004) Resolution of triacylglycerol positional isomers by reversed-phase high-performance liquid chromatography. J Sep Sci 27:1033–1036.

[27] Byrdwell WC (2001) Atmospheric pressure chemical ionization mass spectrometry for analysis of lipids. Lipids 36:327–346.

[28] Holčapek M, Jandera P, Zderadička P, Hrubá L (2003) Characterization of triacylglycerol and diacylglycerol composition of plant oils using high-performance liquid chromatography-atmospheric pressure chemical ionization mass spectrometry. J Chromatogr A 1010:195–215.

[29] Marth EH, Steele JL (2001) Applied dairy microbiology, 2nd ed.,Marcel Dekker, Inc.

[30] Ogué-Bon E, Khoo C, Hoyles L,McCartney AL, Gibson GR, Rastall RA (2011) FEMS Microbiol Ecol 75:365–376.

2.2. Chemical characterisation of old cabbage (*Brassica oleracea L. var. acephala*) seed oil by liquid chromatography and different spectroscopic detection systems

2.2.1. Introduction

Recently, there has been a worldwide interest in the characterisation of yet underexploited high-quality oils. The remarkably high content of these oils in nutritionally, medicinally or industrially desirable fatty acids (FAs) make them highly valuable for various purposes [1-6].

Despite the wide range of vegetable oils sources, the world consumption is dominated by palm, soybean, rapeseed and sunflower oils. Vegetable oils with a high relative amount of minor lipid components are of great importance for human health [7] and their composition is important from the nutritional point of view. In particular, ω-3 FAs play a fundamental role in physiology, especially during foetal and infant growth and they are also important for the prevention of cardiovascular diseases as they are antithrombotic, anti-inflammatory, antiarrythmic and promote plaque stabilisation [8].

Cabbage (*Brassica oleracea* L.) is one of the most consumed fresh vegetables all over the world. Cabbage belongs to the Cruciferae family, which includes cauliflower, kale, broccoli and brussels sprouts. It originates from Western Europe and its different varieties are characterised by variable sizes, shapes and colours of both leaves and heads [9]. Cabbage was and is still currently used in the treatment of different diseases such as headaches, gout, diarrhoea and peptic ulcers. Several epidemiological studies indicated an inverse association between consumption of vegetables from *B. oleracea* and a reduced risk of cancer and cardiovascular diseases.

The biological action is assumed to be provided by its content in compounds

such as carotenes, tocopherols and glucosinolates [10,11]. It was also demonstrated that the most bioactive compounds in cabbage are phenolic compounds such as flavonoids, isoflavone, flavones, anthocyanin and catechins [12].

A particular variety of cabbage, cultivated in the Sicilian village of Rosolini (Italy), is known as 'old cabbage', a particular variety named after its long life span up to 7 years mainly due to the fact that it is cultivated on the border of the stocking place of organic manure (Supplementary Figure 1S (II-2.2.).

The old cabbage belongs to the 'acephala' variety and is able to survive also in dry soils. It is cultivated starting from self-production seeds and can cover up to one square metre of surface. To date, a detailed chemical characterisation of the oil extracted from the seeds of *B. oleracea* var. *acephala* grown in Rosolini is not available. In this study, we evaluate the triacylglycerol (TAG), carotenoid, tocopherol and polyphenol contents of this oil. FAs were analysed as methyl ester derivatives (FAMEs) by gas chromatography (GC) combined with flame ionisation detection (FID) and mass spectrometry (MS). TAGs were analysed by non-aqueous reversed-phase high-performance liquid chromatography (NARP-HPLC) combined with atmospheric pressure chemical ionisation mass spectrometry (APCI-MS).

Tocopherols were separated by normal-phase liquid chromatography (NP-HPLC) coupled to a fluorescence detection (RF). Finally, the polyphenolic fingerprint of the major polyphenols was achieved by RP-HPLC with photodiode array (PDA) and electrospray (ESI) MS detection.

2.2.2. Materials and methods

2.2.2.1. Chemicals and reagents

Reagent grade N,N-dimethyl-formamide (DMF), *n*-hexane (Hex), acetone, ethyl acetate, ethyl ether and LC-MS grade methanol (MeOH), water (H2O),

ethanol (EtOH), methyl tert-butyl ether (MTBE), acetonitrile (ACN), isopropanol (IPA) were all obtained from Sigma-Aldrich/Supelco (Milan, Italy).

α-tocopherol, *γ*-tocopherol and *δ*-tocopherol were provided by Sigma-Aldrich/Supelco (Milan, Italy). Carotenoid standards for HPLC analysis (lutein, *β*-carotene) were purchased from extrasynthese (Genay, France).

2.2.2.2. Seed material

Mature pods of *B. oleracea* L. var. *acephala* species were collected in January 2015 from Rosolini located in the South-eastern part of the Sicilian region. The seeds were collected and then hand-picked to eliminate damaged ones. The selected seeds were sun-dried for three days, carefully cleaned, weighed (5 g) and ground to powder. Press-extraction was carried out using screwless cold presses; the oil thus obtained (450 mg) was subsequently treated according to the class of analytes to investigate.

Analysis of the fatty acid content

The seed oil was dissolved in 1 mL of Hex and 1 mL of a 2 N solution of NaOH in MeOH was added, shaken for 15 s and left to stratify (about 5 min). The supernatant representing the hexane layer was then analysed by GC-MS and GC-FID system. (See supplementary materials).

Analysis of the triacylglycerol content

11.4 mg of the seed oil was weighed and dissolved in 1 mL of acetone; afterwards the sample was filtered through a 0.45-μm Acrodisc nylon membrane filter (Pall Life Sciences, Ann Arbor, MI, USA) prior to LC-MS analyses. (See supplementary materials).

Analysis of the tocopherol content

10 mg of the seed oil sample was carefully weighed and dissolved in 1 mL of Hex. (See supplementary materials).

Analysis of the carotenoid content

See supplementary materials

Analysis of the polyphenolic content

See supplementary materials

2.2.3. Results and Discussion

2.2.3.1. FAMEs composition by GC-FID and GC-MS

The fatty acid profile of the old cabbage oil was determined by GC-FID and C-MS analysis after preparation of FAMEs as previously described [3,13-15].

FAMEs were identified by comparing their mass spectra and their retention indices with those listed in a dedicated database [16]. Individual FA quantities were determined by GC-FID analysis of FAMEs using theoretical relative response factors (TRF) and expressed as mass fraction of the total FAME content (%) applying the formula:

$$FA_{x(TRF)}/FA_{TOT(TRF)} \times 100$$

where $FA_{x(TRF)}$ refers to the peak area of the FAME considered and $FA_{TOT(TRF)}$ refers to the total peak area of the FAMEs contained in the sample, both corrected by using TRF. Figure 1 (II-2.2.) shows the GC-FID chromatogram of the FAMEs identified whose names along with the relative percentage and standard deviation are reported in Supplementary Table 1S (II-2.2.).

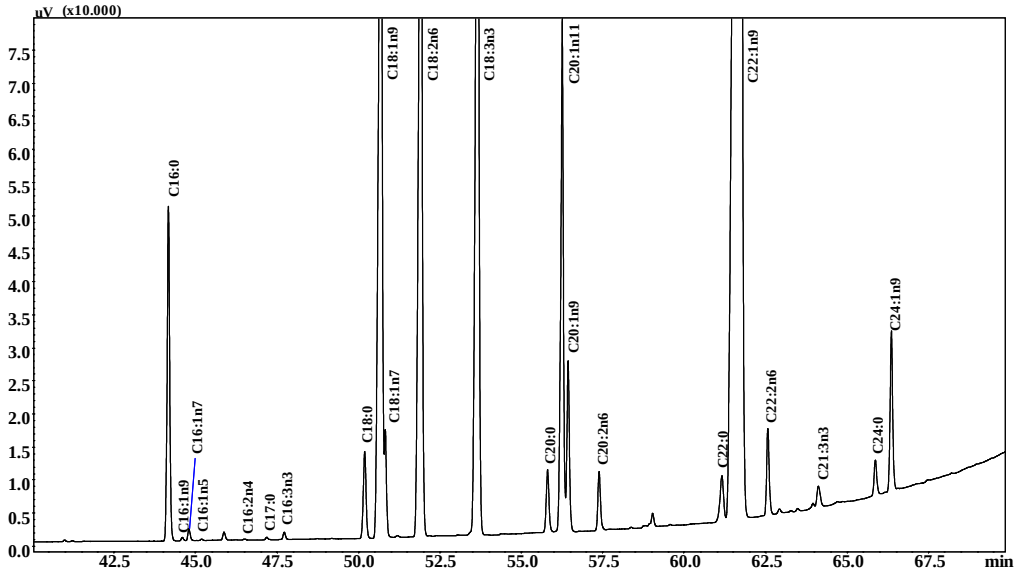

Figure 1 (II-2.2.). 40–70 min enlargement of the GC-FID chromatogram of the FAMEs identified. The experimental conditions are reported in the supplementary material.

where $FA_{x(TRF)}$ refers to the peak area of the FAME considered and $FA_{TOT(TRF)}$ refers to the total peak area of the FAMEs contained in the sample, both corrected by using TRF. Figure 1 (II-2.2.) shows the GC-FID chromatogram of the FAMEs identified whose names along with the relative percentage and standard deviation are reported in Supplementary Table 1S (II-2.2.). These results show that approximately 94.4% of total FAs consisted of unsaturated FAs (UFA), approximately three quarters of which were monounsaturated (MUFA), while the rest was represented by polyunsaturated FAs (PUFA). The PUFA fraction consisted primarily of two essential FAs, linoleic (L) and linolenic (Ln) acid, accounting for 11.4% and 10.2% of total FA contents. Among MUFAs, erucic acid (Er) accounted for being the about 50% of the whole FA content, and this finding is in agreement with previous reports [17,18].

2.2.3.2. Triacylglycerol analysis by NARP-HPLC-APCI-MS

TAGs were identified by positive-ion APCI-MS: protonated molecular ions $[M+H]^+$ were used for molecular weight assignments and fragment ions $[M+H-RiCOOH]^+$ for the identification of the FAs on the glycerol chain [3,19-21]. The NARP-HPLC-APCI-MS total ion current (TIC) chromatogram of the oil is shown in Figure 2 (II-2.2.), whereas Supplementary Table 2S (II-2.2.) reports the retention times, corrected average Area %, SD and CV% (three replicates) of the identified TAGs. Since NARP-HPLC is not capable of resolving TAGs according to the regioisomeric position, the conventional notation of TAGs used refers to the initial of FA trivial names arranged according to their decreasing molecular weights [20,21]. Figure 2 (II-2.2.) and Supplementary Table 2S (II-2.2.) show that some TAGs partially or completely co-eluted the incomplete separation of (e.g. PN = 46, GPLn + OLn; PN = 52, ErGL + NrGLn). These results may be explained considering that TAG retention times in NARP-HPLC increase with increasing partition number (PN) defined as the total carbon number (CN) of all acyl chains minus two times the number of double bonds (DBs), PN = CN−2DB. As a consequence, TAGs with the same PN are, usually, very difficult to resolve.

In addition, the retention behaviour of TAGs with the same CN is strongly influenced by the FA composition of the individual TAG, mainly by the unsaturation degree and acyl chain length. The triacylglycerol profile of the old cabbage oil sample determined by NARP-HPLC is well-correlated with the FA composition measured by GC-FID and GC-MS. NARP-HPLC identified TAGs containing 12 different FAs (P: Palmitic acid (C16:0); S: Stearic acid (C18:0); O: Oleic acid (C18:1); L: Linoleic acid (C18:2); Ln: Linolenic acid (C18:3); A: Arachidic acid (C20:0); G: Gadoleic acid (C20:1); B: Behenic acid (C22:0); Es: Eicosadienoic acid (C20:2); Er: Erucic acid (C22:1); Li: Lignoceric acid (C24:0); Nr: Nervonic acid (C24:1)). The predominant components accounting

for >40% of total composition were erucyl–gadoleil linolein (ErGL), dierucyl linolein (ErErL) and dierucyl olein (ErErO). Most of the TAGs in the old cabbage oil (about 50%) contained at least one residue of erucic acid. Such a high content in erucic acid raises serious concerns on the use of this variety to produce edible oil. TAG % contents were calculated as the ratio of the TIC area of the TAG and the sum of TIC areas of all identified TAGs, multiplied by 100. The NARP-HPLC-APCI-MS TAG areas were corrected by applying the relative response factors published by Holcapek and co-workers [19].

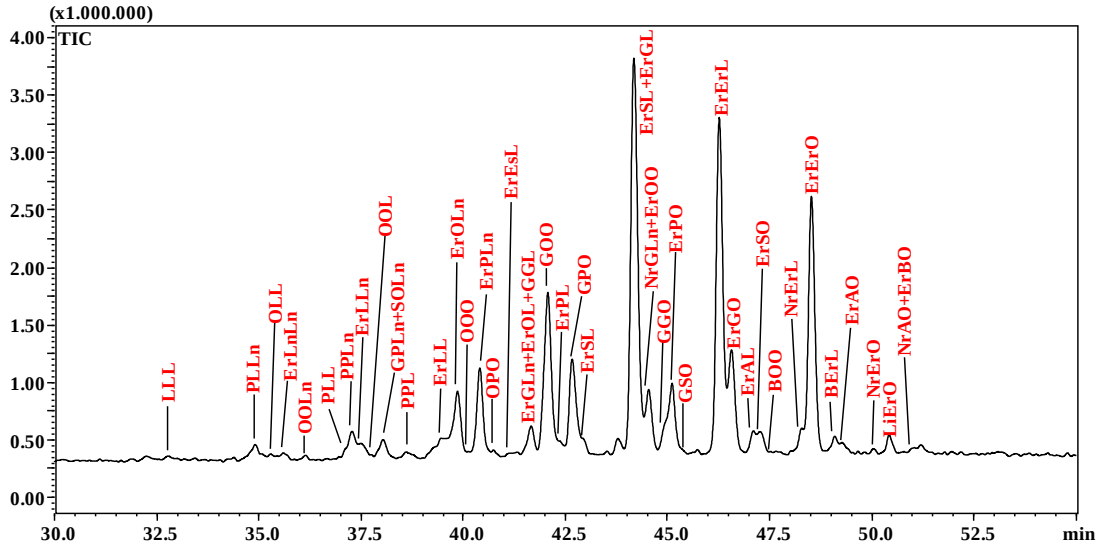

Figure 2 (II-2.2.) 30–55 min enlargement of the TIC chromatogram of NARP-HPLC-APCI-MS analysis of TAGs. The experimental conditions are reported in the supplementary material.

2.2.3.3. Tocopherol analysis by NP-HPLC-RF

Tocopherols are a class of lipid-soluble compounds known as vitamin E which are essential to human health, are also strong antioxidants that protect oils from oxidation. Among the four homologues of tocopherols, α-tocopherol is

considered the strongest antioxidant whereas γ-tocopherol is the strongest inflammatory agent [22,23]. α-tocopherol is the most abundant tocopherol in olive oil, whereas γ- and δ-tocopherols are found mainly in seed oils like soybean and sunflower oil [3]. In this contribution, the tocopherol content of the old cabbage sample was determined by NP-LC coupled to fluorimetric detection. Tocopherols were identified by comparing their retention times with the ones of reference materials. LOD and LOQ values were as follows: α-tocopherol, 0.8 and 1.4 mg/kg; γ-tocopherol, 0.1 mg/kg both; δ-tocopherol, 0.4 and 0.6 mg/kg. γ-tocopherol accounted for more than 66% of the entire tocopherol content in the extracted oil, followed by α-tocopherol (roughly 30%) and δ-tocopherol (Table 1 (II-2.2.)). The total and individual tocopherol contents differed from those previously reported for common vegetable seed oils, e.g. soybean and sunflower characterised by 79% of δ-tocopherol and 84% of α-tocopherol, respectively [24]. The variability in the concentrations of α and γ-tocopherol in vegetable oils can be related to the conditions of cultivation, storage and processing of the seeds or grains which must be properly and constantly evaluated and monitored for the preservation of the organoleptic and nutritional quality of the final product.

Table 1 (II-2.2.). Composition (mg/kg) of tocopherols by NP-HPLC-RF analysis.

Compound	**mg/Kg**	**LOD**	**LOQ**	**t_R(min)±%RSD**
α-tocopherol	31.91	0.80	1.40	5.01±0.02
γ-tocopherol	70.94	0.10	0.10	6.95±0.03
δ-tocopherol	4.13	0.40	0.60	9.83±0.08
Tot	106.98			

2.2.3.4. Carotenoid analysis by RP-HPLC-PDA/APCI-MS and UV–vis Spectrophotometry

The present report describes for the first time the carotenoid composition of old cabbage seed oil. In total, 13 different carotenoids were differentiated by utilising their retention time values, UV–vis and MS spectral data, and comparison with available reference materials. The UV–vis and APCI-MS identification parameters, along with quantitative data of the carotenoid content in the extracted oil, are reported in **Table 2 (II-2.2.)**. The total content in carotenoids was 10.9 ppm and all-*E*-lutein was the main component (7.7 ppm). Various *cis* isomers of lutein were also detected. Taking into consideration the reference values suggested by Britton and Khachik [25], that classified the quantity of a carotenoid as very high when above 20 μg g−1 and high when between 5 and 20 μg g−1, the all-*E*-lutein content measured in this work can be defined as relatively high. Interestingly, neither chlorophylls/chlorophyll derivatives nor xanthophyll esters were detected in the studied samples. An apo-carotenoid probably formed from an oxidative degradation of lutein was detected as a minor component, and due do its low concentration all spectra recorded were not clear, thus it was not fully characterised. The provitamin A, all-*E*-β-carotene and its 9-*Z*-isomer were detected and quantified by both HPLC and direct UV–vis spectrophotometry, although they were present in very low amounts (10.6 ppb and 4.2 ppb, respectively). Moreover, the values of the total carotenoids content determined by HPLC and by the photometric determination were comparable.

Table 2 (II-2.2.). Composition (μg/kg) of carotenoids by RP-HPLC-PDA/APCI-MS.

N°	Compound	UV/VIS spectrum	[M + H]+ APCI (+)	Fragments APCI (+)	μg/kg
1	Violaxanthin	417, 439, 470	601	583, 565	351.5 ± 2.6
2	Apocarotenoid of lutein	421	n.d.	n.d.	70.8 ± 0.3
3	8-R-neochrome	400, 422, 449	601	583, 565	72.3 ± 0.5
4	Lutein-5,6-epoxide	416, 438, 469	585	567, 549	215.2 ± 0.9
5	Mutatoxanthin	405, 429, 454	585	567, 549	116.5 ± 1.1
6	15-Z-lutein	332, 416, 440, 466	569	551, 533, 476	742.8 ± 2.3
7	13/13'Z-lutein	332, 417, 439, 466	569	551, 533, 476	637.6 ± 3.9
8	E-lutein	420, 445, 473	569	551, 533, 476	7743 ± 62
9	Zeaxanthin	426, 451, 476	569	551, 533, 476	98.7 ± 0.8
10	9/9'-Z-lutein	330, 416, 440, 468	569	551, 533, 476	526.9 ± 3.4
11	9/9'-Z-lutein	331, 417, 441, 468	569	551, 533, 476	346.0 ± 2.8

Notes:
n.d.: not detected.
All compounds expressed quantitatively as All-E-lutein.

2.2.3.5. Polyphenol analysis by RP-HPLC-PDA/ESI-MS

The polyphenol compounds were characterised by RP-HPLC-PDA/ESI-MS and their separation is shown in Figure 3 (II-2.2.). The partially porous C18 column, operated under gradient conditions, allowed baseline separation for all identified compounds within a total run time of roughly 40 min. A total of 11 different polyphenol compounds, 6 hydroxycinnamic acids and 5 flavonoids, were identified by combining information from retention times, PDA and MS data (**Table 3 (II-2.2.)**). In particular, the early eluting compounds were represented by chlorogenic acid and hydrocinnamic acid derivatives, followed by acylated derivatives of kaempferol and quercetin glycosides whereas the last eluted ones were represented by hydrocinnamic acids glycosides. These results are consistent with a recent study on the polyphenol contents of the leaves of B. oleracea L. Convar. acephala [26]. Since in previous works only the leaves

samples were taken under consideration, this is the first report on the polyphenol composition of old cabbage seed oil.

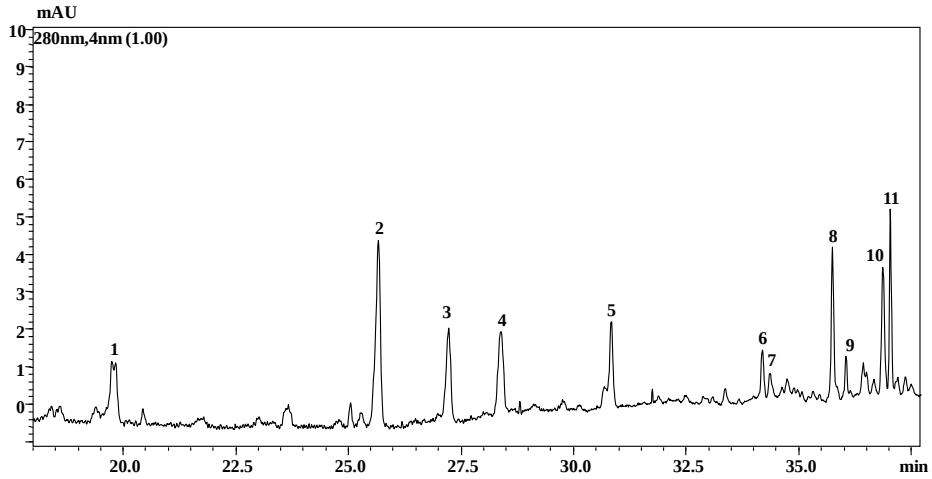

Figure 3 (II-2.2.). 18–37.5 min enlargement of the RP-PLC-PDA chromatogram extracted at 280 nm) of the polyphenolic content. The experimental conditions are reported in the supplementary material.

Table 3 (II-2.2.). Characterisation of polyphenolic compounds by RP-HPLC-PDA/ESI-MS.

Peak No	t_R	λ_{max} UV/vis (nm)	*m/z* [M-H]-	Compound
1	19.8	220, 330	353	Chlorogenic acid
2	25.6	220, 330	793	Hydroxycinnamic acid derivative
3	27.1	220, 270, 300	963	Kaempferol-3-hydroxyferuloyl-diglucoside-7-glucoside
4	28.2	248, 340	1155	Quercetin-3-sinapoyl-diglucoside-7-glucoside
5	30.2	240, 330	1139	Kaempferol-3-sinapoyl-diglucoside-7-glucoside
6	34.1	240, 330	672*	Kaempferol-3-disinapoyl-triglucoside-7-diglucoside
7	34.2	240, 330	753*	Kaempferol-3-disinapoyl-triglucoside-7-glucoside
8	35.7	240, 330	723	Sinapoyl-feruloyl-triglucoside
9	36.1	240, 330	753	Disinapoyl-diglucoside
10	36.8	240, 330	959	Trisinapoyl-diglucoside
11	37.1	240, 330	929	Disinapoyl-feruloyl-diglucoside

* detected as "**$[M-2H]^{2-}$**

2.2.4. Conclusions

This study investigates in great details the composition of the oil extracted from the seeds of B. oleracea, variety acephala (old cabbage). The contents in FAs, triacylglycerols, tocopherols, carotenoids and polyphenols were determined by GC-FID, GC-MS, HPLC-MS and HPLC-FL. The fatty acid profile showed that erucic acid is the most abundant component of this oil accounting for more than 50% of its composition, followed by the essential FAs, linoleic and linolenic acid. γ-tocopherol was the most abundant tocopherol (>50% of total tocopherol composition). The carotenoid and polyphenol analysis led to the identification of 13 carotenoids and 15 polyphenol. This study shows that the old cabbage seed oil contains more than 30% in health promoting unsaturated FAs, although the high percentage of erucic acid could raise serious concern on human health; therefore, the utilisation for human consumption of this oil rich in many healthy phytochemicals should be discouraged unless its erucic acid content is removed or reduced. Alternatively, this oil characterised by high content in erucic acid could be a valuable and renewable raw material for the manufacturing of a wide array of industrial products.

REFERENCES

[1] Tranchida PQ, Donato P, Dugo G, Mondello L, Dugo P. 2007. Comprehensive chromatographic methods for the analysis of lipids. TrAC Trends Anal Chem. 26:191–205.

[2] Dugo G, Cicero N, Furci P, Cavallaro N, Lo Turco V. 2011. Sensory analysis and fatty acids in fishes of the strait of Messina. Riv Ital Sostanze Gr. LXXXVIII: 32–37.

[3] Fanali C, Dugo L, Cacciola F, Beccaria M, Grasso S, Dacha M, Dugo P, Mondello L. 2011. Chemical characterization of Sacha Inchi (*Plukenetia volubilis* L.) oil. J Agric Food Chem. 59:13043–13049.

[4] Mondello L, Beccaria M, Donato P, Cacciola F, Dugo G, Dugo P. 2011. Comprehensive two dimensional liquid chromatography with evaporative light-scattering detection for the analysis of triacylglycerols in *Borago officinalis*. J Sep Sci. 34:688–692.

[5] Ragonese C, Tedone L, Beccaria M, Torre G, Cacciola F, Dugo P, Mondello L. 2014. Characterisation of lipid fraction of marine macroalgae by means of chromatography techniques coupled to mass spectrometry. Food Chem. 145:932–940.

[6] Dugo G, Rotondo A, Mallamace D, Cicero N, Salvo A, Rotondo E, Corsaro C. 2015. Enhanced detection of aldehydes in extra-virgin olive oil by means of band selective NMR spectroscopy. Phys A. 420:258–264.

[7] Nasri N, Elfalleh W, Tlili N, Hannachi H, Triki S, Khaldi A. 2012. Minor lipid components of some *Acacia* species: potential dietary health benefits of the unexploited seeds. Lipids Health Dis. 11: 11–49.

[8] Galli C, Marangoni F. 2006. N-3 fatty acids in the Mediterranean diet. Prostaglandins Leukot Essent Fatty Acids. 75:129–133.

[9] Nieuwhof M. 1969. Cole crops: botany, cultivation and utilization. World crops series. London: Leonard Hill.

[10] Brooks JD, Paton VG, Vidanes G. 2001. Potent induction of phase 2 enzymes in human prostate cells by sulforaphane. Cancer Epidemiol Biomarkers Prev. 10:949–954.

[11] Liang H, Yuan Q, Liu M. 2013. Simultaneous determination of glucoraphanin and sulforaphane in *Brassica oleracea* seeds by high-performance liquid chromatography with evaporative light scattering detector. Nat Prod Res. 27:194–197.

[12] McDougall GJ, Fyffe S, Dobson P, Stewart D. 2007. Anthocyanins from red cabbage stability to simulated gastrointestinal digestion. Phytochem. 68:1285–1294.

[13] Ragonese C, Tranchida PQ, Dugo P, Dugo G, Sidisky LM, Robillard MV, Mondello L. 2009. Evaluation of use of a dicationic liquid stationary phase in the fast and conventional gas chromatographic analysis of health-hazardous C-18 *cis*/*trans* fatty acids. Anal Chem. 81:5561–5568.

[14] Ragonese C, Tranchida PQ, Sciarrone D, Mondello L. 2009. Conventional and fast gas chromatography analysis of biodiesel blends using an ionic liquid stationary phase. J Chromatogr A. 1216:8992–8997.

[15] Tuttolomondo T, Dugo G, Leto C, Cicero N, Tropea A, Virga G, Leone R, Licata M, La Bella S. 2015. Agronomical and chemical characterization of *Thymbra capitata* (L.) Cav. biotypes from Sicily, Italy. Nat Prod Res. 29: 1928–1934. doi:10.1080/14786419.2014.997726.

[16] Mondello L. 2011. FAMEs fatty acid methyl esters: mass spectral database. Hoboken, NJ: Wiley.

[17] Mahler KA, Auld DL. 1989. Fatty acid composition of 2100 accessions of *Brassica*. Miscellaneous series bulletin no 125. Moscow: Agricultural Experiment Station, University of Idaho; p. 112. ID 83843.

[18] Mackenzie SL, Giblin EM, Barton DL, McFerson JR, Tenaschuk D, Taylor DC. 1997. Erucic acid distribution in *Brassica oleracea* seed oil triglycerides. In: Williams JP, Khan MU, Lem NW, editors. Physiology, biochemistry and molecular biology of plant lipids. Dordrecht: Academic Publishers; p. 319–321.

[19] Holcapek M, Lisa M, Jandera P, Kabatova N. 2005. Quantitation of triacylglycerols in plant oils using HPLC with APCI-MS, evaporative light-scattering, and UV detection. J Sep Sci. 28:1315–1333.

[20] Dugo P, Beccaria M, Fawzy N, Donato P, Cacciola F, Mondello L. 2012. Mass spectrometric elucidation of triacylglycerol content of *Brevoortia tyrannus* (menhaden) oil using non-aqueous reversed-phase liquid

chromatography under ultra high pressure conditions. J Chromatogr A. 1259:227–236.

[21] Beccaria M, Sullini G, Cacciola F, Donato P, Dugo P, Mondello L. 2014. High performance characterization of triacylglycerols in milk and milk-related samples by liquid chromatography and mass spectrometry. J Chromatogr A. 1360:172–187.

[22] Sen CK, Khanna S, Roy S. 2007. Tocotrienols in health and disease: the other half of the natural vitamin E family. Mol Aspects Med. 28:692–728.

[23] Zingg JM. 2007. Modulation of signal transduction by vitamin E. Mol Aspects Med. 28:400–422.

[24] Grilo EC, Costa PN, Gurgel CSS, de Lima Beserra AF, de Souza Almeida FN, Dimenstein R. 2014. Alphatocopherol and gamma-tocopherol concentration in vegetable oils. Food Sci Technol (Campinas). 34:379–385.

[25] Britton G, Khachik F. 2009. Carotenoids in food. In: Britton G, Liaaen-Jensen S, Pfander H., editors. *Carotenoids vol. 5: nutrition and health*. Basel: Birkhauser; p. 45–66.

[26] Olsen H, Aaby K, Borge GIA. 2009. Characterization and quantification of flavonoids and hydroxycinnamic acids in Curly Kale (*Brassica oleracea* L. Convar. *acephala* Var. *sabellica*) by HPLC-DAD-ESI-MS *n*. J Agric Food Chem. 57:2816–2825.

2.3. Analysis of lipid profile in lipid storage myopathy

2.3.1. Introduction

Lipid dysmetabolism can often cause different extent of lipid accumulation in skeletal muscle, fibers and in other organs causing a series of myopathies. Such dysfunctions usually involve intra-muscolar triglycerides (IMTG) catabolism, the transport of long-chain fatty acids and carnitine uptake, or β-oxidation. According to the specific pathway affected by some extent of dysfunction, the myopathies can be classified into two main classes: lipid storage myopathy (LSM) and intramitochondrial lipid storage. The former, among which primary carnitine deficiency (PCD), multiple acyl-coenzyme A dehydrogenase deficiency (MADD) and neutral lipid storage disease with ichthyosis (NLSDI) or myopathy (NLSDM) are included, determines an increase of extra mitochondrial lipid accumulation at different extent. On the other side the intramitochondrial lipid storage dysfunction, among which deficiencies of carnitinepalmitoyltransferase II (CPTII) enzyme [1], mitochondrial trifunctional protein (MTP) [2] and very-long-chain acyl-CoA dehydrogenase (VLCAD) are included, causes often a mild or even absent intramitochondrial lipid storage [3-4].

The clinical manifestation, especially in late onset patients, of these diseases can be generally classified into two categories corresponding to the above myopathy classes. LSM patients often shown a constant or progressive muscle weakness associated with or without metabolic crisis; while recurrent rhabdomyolysis triggered by infections, fasting or vigorous exercise usually occur in the patients with disorders affecting intramitochondrial fatty acid transport and β-oxidation. The interpretations of the clinical manifestations in infantile onset patients is more challenging since they are somehow similar among all types of lipid disorders, including hypotonia, hepatomegaly,

hypoketotichypoglycemic encephalopathy, and cardiomyopathy [5].

To perform a reliable diagnosis different laboratory evaluations are required. A urinary organic acid profiles, plasma carnitine, and acylcarnitines are usually required for CPT and MADD diagnosis. In fact, C5 to C10 dicarboxylicaciduria and acylglycine derivatives are usually present in urines; mainly medium- and long-chain blood acylcarnitines are usually present at high concentration in blood; while plasma free carnitine level can decrease but in some cases retains normal. Moreover, mitochondrial enzymes (such as flavin-dependent and respiratory chain enzymes) can shown a reduced biochemical activityin MADD [6-8]. A reliable CPTII diagnosis requires an enzymatic assay in leukocyte, cultured fibroblast or biopsied muscle, and then confirm the diagnosis, through molecular analysis of CPTII gene.

Among the LSM, NLSDM is probably the most severe although rare disorder, still not fully clarified [4]. In fact, this genetic disorder is caused by a defect in the enzyme that catalyzes the breakdown of triglycerides (TGs) in many tissues, namely the adipose triglyceride lipase (ATGL). Dysfunction of ATGL protein can result in a reduction in the hydrolysis of fatty acids (FAs) from the skeleton of glycerol, causing an accumulation of lipids in many tissues, including skin, bone marrow, heart, liver, and muscles [4,9-10].

Usually, the diagnosis of disease of lipid accumulation and its characterization go through dosage of Acyl CoA in plasma accompanied with evidence of droplets of lipids intra-fibrils of the patient muscle biopsy, but often it is not enough. Also, the literature to date, does not report protocols for the study of intramyofibrillare lipid deposits; although it would be very useful to understand the pathophysiological mechanisms of LS diseases, and to identify the nature of lipids deposited in muscle fiber.

In the last decades, the attention on the lipid profile related to several diseases has significantly increased. In particular, the application of innovative

methodological approacheshave been widely investigated for quality and quantity characterization of lipids[11-14]. The first fundamental step for a reliable charcaterization of lipidsis the extraction from the biological tissue [15]. The most applied method was first proposed by Folch et al. in 1957 [16], and later modified by Bligh and Dyer in 1959 [17]. The lipid extract obtained can be directly analyzed to determine the intact lipid profile by liquid chromatography (LC) or derivatized, following different procedures, to investigate the fatty acid methyl esters (FAMEs) profile by gas chromatography (GC) [12,18]. Few studies overpassed the extraction step for FAMEs determination, performing direct derivatization on the biological tissue obtaining comparable results [19-20].

The aim of this study was to characterize the lipid profile, as FAMEs and intact TGs, present in muscle biopsies of patients already diagnosed for lipid accumulation diseases, namely CPTII, MADD, and NLSDM, to evaluate the feasibility of this approach for biomarkers identification.

2.3.2. Materials and methods

2.3.2.1. Patient selection

A total of 11 muscle specimens of pharmacologically untreated patients were available for this study. Nine out of eleven patients investigated, were diagnosed as afflicted with LSM and were recruited from the Neuromuscular Center of the Department of Neurosciences of the University of Messina (Italy). The muscle biopsies were stored in the Bank of DNA, Nerve and Muscle Tissues, of the Department of Neurological Sciences. The Institutional Review Board (IRB) of the Department of Neurosciences of the University of Messina, Italy, discussed and approved this project two years ago, with the aim of a retrospective research for biomarkers on biological materials of patients with specific muscle disorders that were contained in the Department Biobank.

Written informed consent was obtained from all subjects or their caregivers at the moment of diagnostic procedures, even for research purpose, according to the Declaration of Helsinki [21].

LSM was diagnosed based on characteristic pathological attributes, including accumulations of small clear vacuoles in hematoxylin and eosin-stained samples that were positive for fat according to oil red O and Sudan black stains on muscle biopsy of each patient. Accordingly, nine unrelated patients with LSMs (4 CPTII, 3 MADD, 2 NLSDM) were recruited and two normal people, who were all subjected to muscle biopsy. Figure 1 (II-2.3) represents different biopsies sections of vastus Lateralis muscle from patients affected with Lipid Storage Myopathies. Clinical information of patients is summarized in Table 1 (II-2.3.).

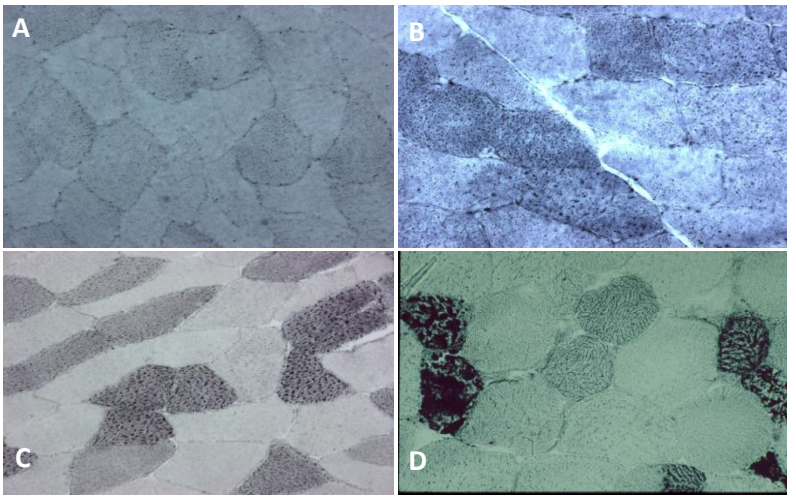

Figure 1 (II-2.3.). Representatives biopsies sections of vastus Lateralis muscle from patients affected with Lipid Storage Myopathies: Sudan Black Stain, original magnification 280 X.A: Lipid distribution in normal skeletal muscle biopsy; B: Slight increased distribution of droplet lipid in CPTII deficiency; C: Moderate increased neutral lipid in MADD; D:Markedly increased lipid in NLSDM.

Table 1(II-2.3.). Clinical information of patients.

PatientsCohort	Age at onset	Sex	*CK max (nv<250U/I)	MuscleBiopsyLipid Distribution
CPT II -1	14	M	35000	Moderate Lipid Storage (+)
CPT II-2	25	F	5000	Moderate Lipid Storage (+)
CPT II-3	7	F	1000	Moderate Lipid Storage (+)
CPT II-4	20	F	20000	Moderate Lipid Storage (+)
MADD-1	23	M	2000	Lipid Storage (+++)
MADD-2	52	M	6500	Lipid Storage (+++)
MADD-3	38	M	700	Lipid Storage (++)
NLSDM-1	20	M	10000	Lipid Storage (+++)
NLSDM-2	38	M	9200	Lipid Storage (+++)
Control-1	22	M	200	Normal Distribution
Control-2	38	F	190	Normal Distribution

*CK: Creatinin Kinase

2.3.2.2. FAMEs characterization

Simultaneous extraction and derivatization from muscle tissues

All chemicals were purchased from Sigma–Aldrich (St. Louis, MO, USA). Methyl heptanoate (Me. C7:0) and methyl nonanoate (Me. C9:0) have been used as internal standards for quantification of FAMEs in the real samples. Muscle tissue samples were analysed after a previous transesterification step carried out as follow: about 7-9 mg of sample, collected in an Eppendorf tube, were added with 10 μL of the Me. C9:0 solution (1 mg/mL) and with 100 μL of methanolictrimethylsulfonium hydroxide solution (TMSH) 0.25 M (Fluka). The mixture was sonicated for 15 min. Then 10 μL of the Me. C7:0 solution (1 mg/mL) and 100 μL of *n*-hexane were added, the mixture was centrifuged for 15 min. The supernatant was collected and stored in a capped vial at 4 °C prior GC analysis, both in GC- flame ionization detector (FID) and GC-mass spectrometer (MS), for quantitative and qualitative purpose, respectively.

Analytical determination

GC-MS: The FAMEs profile identification of all samples was carried out on a GCMS-QP2010 (Shimadzu, Milan, Italy) equipped with a split-splitless injector and an AOC-20i autosampler. The chromatographic column was a Supelcowax-10 (30 m × 0.25 mm id, 0.25 μm film thickness) column (Supelco-Sigma Aldrich, USA). The programmed oven temperature was: 50 °C (hold 1 min) to 280°C at 3.0 °C/min. Injection volume: 2.0 μL; injection mode: splitless (hold 1 min); Helium was used as the carrier gas at 35 cm/s linear velocity.

MS parameters were as follows: mass range 40–400 amu, scan speed: 2000 amu/s. Ion source temperature: 200 °C, interface temperature: 250 °C. The GCMSsolution software (version 2.71 Shimadzu, Milan, Italy) was used for data collection and handling.

A Fatty Acid Ethyl Esters (FAEEs) standard solution has been used for Linear Retention Indices (LRIs) calculation to support identification of analytes. In fact, peaks assignment was carried out based on a double filter, namely the MS similarity spectra (over 80 %) and a LRIs ±10 range compared to the value reported in the commercial database used [FAMEs Mass Spectral Library (Shimadzu, Japan)].

GC-FID: FAMEs quantification was carried out on a GC-2010 (Shimadzu, Milan, Italy) equipped with a split-splitless injector (280°C), an AOC-20i autosampler, and a FID detector. A Supelcowax-10 (30 m × 0.25 mm id, 0.25 μm film thickness) column (Supelco) was operated under programmed temperature: 40 °C to 280°C at 3.0 °C/min. Injection volume: 2.0 μL; split ratio: 1:10. Helium was used as the carrier gas (30 cm/s). Final results were expressed as relative percentage of fatty acids in tissue. All analyses were performed in triplicates (n=3).

2.3.2.3. TGs characterization

TGs extraction

About 10 mg of muscle sample were added with 1 mL of *n*-hexane (>95 % purity) and sonicated for 2 hours. Then, the mixture was centrifuged at 15000 rpm for 15 min. The extraction was performed in triplicate. The supernatants were collected and dried under a gentle stream of nitrogen and stored at −18 °C until analysis. The extracted residue was re-dissolved in 200 µL of acetone prior to the following analysis.

NARP-HPLC-APCI-MS of IMTG

Non-aqueous reversed phase high performance liquid chromatography (NARP-HPLC) coupled to MS was used to perform IMTGs analysis. The NARP-HPLC-MS analyses were performed on a Shimadzu Prominence LC-20A System (Shimadzu, Milan, Italy), consisting of a CBM-20A controller, two LC-20AD dual-plunger parallel-flow pumps, a DGU-20A_5 degasser. The LC system was coupled to a quadrupole LCMS-2010 through an APCI (atmospheric pressure chemical ionization) source operated in positive ionization mode. Chromatographic separation was achieved on a 150 × 4.6 mm i.d., 2.7 µm *d.p.* (Fused-core) Ascentis Express C18 column (Sigma-Aldrich/Supelco, Bellefonte, PA, USA). A linear gradient of increasing IPA (B) percentages in ACN (A) was run, at a mobile phase flow rate of 1 mL/min: 0 min, 0% B; 50 min, 70% B (hold for 5 min); 56 min, 0% B. MS parameters were as follows: *m/z* range, 300-1100; scan speed: 4000 amu/s; nebulizing gas (N_2) flow rate, 2.5 L/min; event time: 0.2 s; detector voltage, 1.6 kV; interface voltage, 4.5 kV; interface temperature, 400 °C; CDL temperature, 250 °C; heat block temperature, 250 °C. The *LCMSSolution* software (version 3.50 SP2 Shimadzu, Milan, Italy) was used for data collection and handling. Injection volume: 20 µL.

2.3.3. Results and discussion

The differential diagnosis of myopathy lipid storage in our patients has been rushed along the clinical algorithm of neuromuscular diseases, clinical neurophysiological bioptical and laboratory studies [22]. The first clinically significant value, taken into account to make a diagnosis is creatine kinase (CK). High CK values (> 250) indicate systemic muscular suffering [4].

The highest CK value was found in CPTII-1 and CPTII-4, followed by both NLSDM patients; however it is worthy to underline that there is no correlation between the CK values and the severity of the disease. While, it is closely correlate with the rate of lipid accumulation.

The analysis of muscle biopsy of three categories of disease (CPTII; MADD, and NLSDM) showed a heterogeneous distribution of lipids intra-fibrillare. In fact, in these metabolic diseases, not all of the patient's muscles are affected in the same manner [23]. Patients with CPTII deficiency shown a moderate accumulation of lipids, whereas in patients afflicted with MADD and NLSDM the distribution of lipid was from moderate to markedly increased (Figure 1 (II-2.3)). However, there is a close correlation between the rate of lipid storage and the pathology itself, while other factors, such as age of onset, type of muscle, etc, can modulate the degree of intracellular lipid distribution [4].

The muscle biopsy samples were divided in two parts; one part was directly processed to obtain FAMEs by TMSH derivatization and then analysed by GC-MS and FID, while the other half was solvent extracted for IMTGs analysis. The extraction procedure was based on a previous work [24], where three different procedures for lipid extraction from marine organisms were compared, namely Folch, Bligh & Dyer and ultrasound sonication with *n*-hexane. No significant differences were observed comparing the TGs profile of the extracts obtained with the different procedures. Therefore, the sonication extraction was herein applied after slight modification to adapt the procedure to the low

quantity of sample available (about 10 mg).

2.3.3.1. FAMEs profile

The muscle tissue was directly derivatized by TMSH and injected in GC. Conventional GC-MS analysis was carried out for identification purposes. Different filtering criteria were used, namely mass spectrum similarity match above 80% and LRIs in a ± 10 range compared with the indices reported in the FAMEs Library (calculated based on a FAEEs mixture). Quantification was performed using the GC-FID data. The amount of FAMEs is expressed as relative percentage (Table 2 (II-2.3)). The FAMEs profile was almost the same in the two control samples, while it was significantly different within and among the different diseases. The most representative FAMEs in all samples were: C16:0 in the 13-24 % range, C18:1n9 in the 20-52% range, and C18:2n6 in the 10-25% range. Followed by C18:0 in the 1-15% range, C18:1n7 and C16:1n7 in the 1-5% range. Arachidonic acid (C20:4n6), considered a marker of inflammatory status since it is a precursor of eicosanoids [25], varied significantly among all the samples and it was rather high (6.5 and 7.5%) in the two control samples. The samples presenting the highest values of arachidonic acid were the samples named CPTII-3 and CPTII-4, 10.1 % and 9.2 %, respectively; while all the other samples presented lower values in the 1-4.5% range. In Figure 2 (II-2.3) is reported the GC-MS chromatogram of the sample named CPTII-3. This result was consistent with the CPTII muscle deficiency. In fact, there was a prevalence of accumulation of medium chain fatty acids, due to the alteration of the flow cytosolic/mitochondrial matrix controlled by the CPTII enzyme.

Table 2 (II-2.3.). Relative percentage (Area%) of FAMEs calculated from the GC-FID data.

FAME	CPT II-1	CPT II-2	CPT II-3	CPT II-4	MADD-1	MADD-2	MADD-3	NLSDM-1	NLSDM-2	Control-1	Control-2
	Area %	Area %	Area %	Area %	Area %	Area %	Area %	Area %	Area %	Area %	Area %
Me. C12:0	0.22	0.11	0.00	0.02	0.67	0.32	0.22	0.16	0.11	0.02	0.03
Me. C13:0	0.00	0.00	0.27	0.22	0.04	0.00	0.00	0.01	1.78	0.22	0.32
Me. C14:0	1.56	1.47	1.03	1.27	3.79	2.16	1.17	1.49	4.30	1.59	1.64
Me. C14:1n5	0.11	0.19	0.06	0.05	0.16	0.15	0.07	0.28	1.41	0.29	0.28
Me. C15:0 iso	0.01	0.02	0.00	0.09	0.00	0.00	0.00	0.01	0.41	0.00	0.00
Me. C15:0 anteiso	0.03	0.04	0.06	0.05	0.00	0.00	0.00	0.01	0.06	0.04	0.04
Me. C15:0	0.12	0.11	0.21	0.18	0.17	0.11	0.14	0.10	0.21	0.20	0.21
Me. C16:0 iso	0.02	0.03	0.00	0.03	0.04	0.00	0.03	0.04	0.05	0.03	0.04
Me. C16:0	23.71	20.79	20.17	18.88	14.64	13.21	19.63	17.95	18.70	20.46	19.79
Me. C16:1n9	0.35	0.43	0.29	0.29	7.04	5.70	0.58	2.24	3.56	0.48	0.50
Me. C16:1n7	2.28	4.87	1.48	1.10	1.78	2.02	1.82	7.09	1.74	4.75	4.45
Me. C16:1n5	0.02	0.04	0.00	0.00	0.00	0.04	0.07	0.06	0.00	0.09	0.08
Me. C16:2	0.00	0.00	0.00	0.00	0.56	0.49	0.00	0.12	0.66	0.10	0.00
Me. C17:0 iso	0.04	0.08	0.08	0.11	0.00	0.00	0.05	0.00	0.00	0.07	0.09
Me. C17:0 anteiso	0.06	0.08	0.00	0.00	0.08	0.07	0.06	0.09	0.00	0.00	0.00
Me. C17:0	0.22	0.17	0.27	0.25	0.22	0.14	0.21	0.09	0.29	0.21	0.21
Me. C17:1n7	0.17	0.20	0.00	0.07	0.13	0.12	0.10	0.23	0.11	0.21	0.21
Me. C18:0 iso	0.00	0.02	0.00	0.00	0.04	0.00	0.00	0.01	0.00	0.00	0.00
Me. C18:0	6.00	6.86	15.22	14.41	9.31	8.11	4.92	1.40	10.63	9.03	9.80
Me. C18:1n9	47.20	38.24	20.33	19.28	35.73	40.35	48.94	51.86	30.19	25.92	24.88
Me. C18:1n7	2.62	3.65	2.35	2.48	2.67	3.18	4.56	3.56	2.33	2.97	2.31
Me. C18:2n6	10.61	14.53	23.18	27.61	14.58	18.39	13.52	9.90	15.16	19.31	24.48
Me. C18:3n6	0.06	0.00	0.00	0.00	0.00	0.00	0.00	0.05	0.00	0.15	0.14
Me. C18:3n3	0.27	0.27	0.13	0.19	0.26	0.24	0.43	0.16	0.35	0.37	0.36
Me. C18:2n7	0.09	0.21	0.00	0.10	0.13	0.09	0.09	0.09	0.10	0.16	0.15
Me. C20:0	0.04	0.00	0.21	0.11	0.10	0.17	0.14	0.03	0.10	0.00	0.00
Me. C20:1n9	0.43	0.37	0.26	0.29	0.30	0.37	0.58	0.39	0.36	0.27	0.19
Me. C20:2n6	0.28	0.40	0.22	0.20	0.34	0.28	0.37	0.29	0.24	0.19	0.20
Me. C20:3n6	0.42	0.42	1.18	0.97	0.75	0.31	0.30	0.32	0.65	1.32	1.11
Me. C20:4n6	1.93	4.26	10.12	9.15	4.23	2.69	1.09	1.01	3.71	7.54	6.54
Me. C20:5n3	0.05	0.13	0.00	0.24	0.11	0.11	0.04	0.02	0.42	0.72	0.24
Me. C22:4n6	0.21	0.60	1.04	0.68	0.78	0.45	0.40	0.42	0.57	0.56	0.67
Me. C22:5n7	0.16	0.34	0.42	0.23	0.32	0.00	0.00	0.13	0.18	0.24	0.27
Me. C22:5n3	0.18	0.47	0.58	0.63	0.56	0.36	0.30	0.19	0.46	0.39	0.00
Me. C22:6n3	0.53	0.62	0.83	0.81	0.46	0.38	0.18	0.21	1.17	2.10	0.77

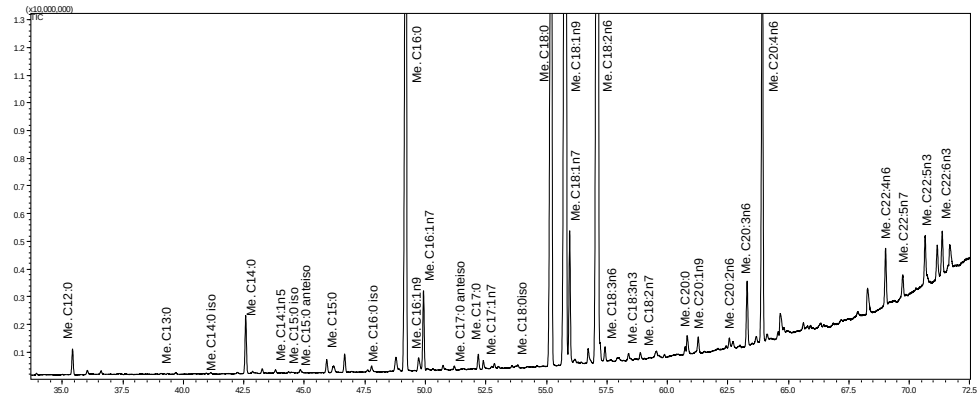

Figure 2 (II-2.3). GC–MS chromatogram of CPTII-3 sample.

2.3.3.2. IMTGs profile

In the analyzed samples, IMTGs have been identified using positive-ion mode APCI-MS based on both protonated molecules $[M+H]^+$, used for the molecular weight assignment, and fragment ions $[M+H-R_iCOOH]^+$, used for the identification of individual FAs. For the unambiguous identification of trace peaks, the extracted ion current chromatograms of selected *m/z* values were used to clearly confirm the presence or absence of compounds. TAGs fragmentation pathway by APCI($^+$) has been already reported and discussed in details elsewhere; therefore readers are directed to literature for further explanation [27-28]. Additionally, the predicted elution order, under NARP conditions, was used to support TGs identification [26]. The retention of TGs in NARP-HPLC systems increases with increasing the partition number (PN), reflecting the relation between carbon numbers (CNs) and double bonds (DBs) in all acyl chains (PN = CNs – 2*DBs). In general, the retention of TGs within the same PN group increases with decreasing double bond number (DBN) in the acyl chains (*e.g.,* PN42: C18:2C18:2C18:2< C16:1C16:1C16:1; PN44: C18:1C18:2C18:2 < C18:1C18:2C16:1); while TGs within the same PN and equal CNs and DBNs are eluted according to the combination of FAs onto the

glycerol backbone (*e.g.* PN 42, DBN 6: C18:2C18:2C18:2 < C18:1C18:2C18:3) [26-32]. The standard notation of TGs, using CN:DB, was used. FAs bonded to glycerol backbone were reportedin order of decreasing molecular weight (e.g. C18:0C18:1C16:0, but not C16:0C18:1C18:0),as suggested elsewhere [32-34].

The TGs of the analyzed samples eluted within a 50 min gradient, according to their increasing hydrophobicity, with a calculated PN ranging from 36 to 52 and DBN from 0 to 9. As can be seen in Figure 3 (II-2.3), several co-elution occurred. A total of 107 TGs were tentatively identified from the 67 peaks separated. TGs are usually reported as relative abundance derived from the total ion current (TIC) area corrected with the response factors (RFs) referred to triolein (C18:1C18:1C18:1) [28-29,31]. However, due to the several co-elution issue, a relative quantification was performed based on the TIC area of the 67 peaks separated, in order to perform the statistical analysis without introducing bias deriving from the assumption of an equal contribution of each TG co-eluted in a peak (Table 3 (II-2.3)).

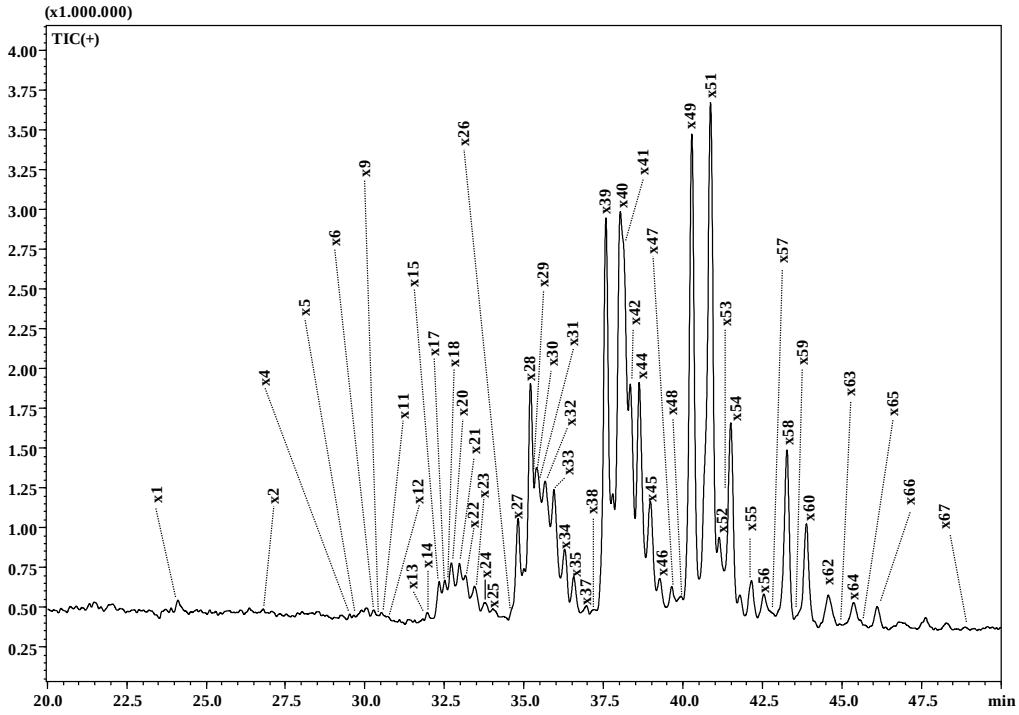

Figure 3 (II-2.3). NARP-HPLC-APCI-MS chromatogram of MADD-2 sample.

Table 3 (II-2.3). TG composition espressed as Area%.

			1	3	A	B	C	D	E	2	G	4	5
N. Peak	**TG**	**PN**	**CPT II-1**	**CPT II-2**	**CPT II-3**	**CPT II-4**	**MADD-1**	**MADD-2**	**MADD-3**	**NLSDM-1**	**NLSDM-2**	**Control-1**	**Control-2**
			AREA %	AREA %	AREA %	AREA %	AREA %	AREA %	AREA %	AREA %	AREA %	AREA %	AREA %
X1	C18:3C18:3C18:3	36			0.12	1.71	2.65	0.27	0.77		0.55		
X2	C18:3C18:2C18:3	38			0.09	1.53	1.59	0.10	0.48		0.34		
X3	C18:2C12:0C12:0	38								0.27			
X4	C18:2C18:2C18:3	40			0.09	0.65	0.88	0.16	0.44		0.15		
X5	C18:3C18:1C18:3	40			0.08	0.50	0.59	0.11	0.29	0.75	0.26		
	C18:2C18:2C12:0	40											
X6	C18:3C18:3C16:0	40			0.08	0.63	1.23	0.24	0.35		0.45		
X7	C20:2C12:0C12:0	40								0.16			
	C20:4C16:1C16:1	40											
X8	C16:1C16:1C12:0	40								0.65			
	C16:1C18:2C12:0	40											
X9	C18:1C12:0C12:0	40			0.10	0.49	0.68	0.19		0.57	0.16		
X10	C14:0C14:0C14:1	40								0.73			
	C16:1C14:0C12:0	40											
X11	C16:0C14:1C12:0	40			0.08	0.25	0.69	0.17		0.61	0.15		
X12	C14:0C14:0C12:0	40			0.05	0.18	0.50	0.11		0.16	0.11		
	C16:0C12:0C12:0	40											
X13	C22:6C18:3C16:0	40			0.04	0.14	0.11	0.10	0.03	0.40	0.04		
	C20:4C18:2C18:2	40											
X14	C18:2C18:2C18:2	42	0.41	0.44	0.07	0.19	0.26	0.12	0.19	0.02	0.09	0.77	0.27
X15	C18:2C18:2C16:1	42	0.66	0.42	0.05	0.53	0.60	0.68	0.11	0.19	0.11	0.15	0.23
X16	C14:1C16:1C18:1	42	0.20	0.37									
X17	C18:1C18:2C18:3	42	0.64	0.69	0.14	0.74	0.78	0.74	0.32	0.34	0.43	0.18	0.67
	C18:2C16:1C16:1	42											
X18	C18:2C18:2C14:0	42		0.18	0.10	0.48	0.89	0.36	0.19	0.17	0.53	0.17	0.57
X19	C18:2C16:0C14:1	42	0.17	0.19									0.40
X20	C18:3C18:2C16:0	42	0.27	0.24	0.36	0.75	2.70	0.72	0.24	1.06	0.54	0.59	0.46
	C18:1C18:2C12:0	42											
	C16:1C16:1C14:0	42											

X21	C18:1C18:2C14:1 C18:1C16:1C12:0	42 42			0.26	0.87	1.60	1.25	0.25	2.08	0.71		
X22	C14:0C14:0C18:2 C16:0C18:2C12:0	42 42	0.29	0.35	0.32	0.29	1.86	0.80	0.20	0.38	0.64	1.14	0.32
X23	C18:1C14:0C12:0 C16:0C16:1C12:0	42 42	0.61	0.63	0.20	0.26	0.84	0.88	0.16	2.09	0.47	0.45	0.50
X24	C20:4C18:1C16:1	42			0.18	0.37	0.37	0.34	0.13		0.32		
X25	C22:6C18:1C18:1 C16:0C14:0C12:0 C14:0C14:0C14:0 C18:0C12:0C12:0	42 42 42 42	0.13	0.22	0.10	0.22	0.47	0.22	0.16	0.77	0.19	0.84	0.21
X26	C22:6C18:1C16:0	42	0.24	0.15	0.21	0.43	0.09	0.10	0.16	0.42	0.18	0.53	0.33
X27	C18:1C18:2C18:2	44	1.90	2.14	0.59	0.97	0.72	1.78	1.43	0.75	0.94	0.92	1.89
X28	C18:1C18:2C16:1	44	1.23	0.82	0.49	1.80	2.75	4.84	0.45	1.27	1.60	1.71	2.23
X29	C18:1C18:1C18:3 C18:1C16:1C16:1	44 44	0.80	0.41	0.53	1.44	1.66	1.03	0.67	1.64	2.07	1.47	1.27
X30	C18:2C18:2C16:0	44	2.64	2.06	1.63	1.55	0.92	1.06	1.47	1.09	2.28	1.80	3.05
X31	C18:1C18:2C14:0 C16:0C18:2C16:1	44 44	1.85	1.11	1.49	2.42	1.74	1.38	0.91	0.98	2.22	2.73	3.34
X32	C18:1C18:1C12:0 C18:1C16:1C14:0 C18:318:1C16:0	44 44 44	1.25	0.98	1.60	1.74	1.96	3.49	0.87	2.16	1.86	1.99	1.63
X33	C18:1C16:0C14:1 C16:0C16:1C16:1 C22:5C18:1C16:0	44 44 44	0.36	0.65	0.54	0.79	3.81	2.93	0.42	1.74	1.08	1.54	1.00
X34	C16:0C18:2C14:0 C20:4C18:1C18:1	44 44	0.79	0.62	0.72	0.29	2.28	1.48	0.24	1.74	0.82	0.32	0.50
X35	C18:1C14:0C14:0 C18:1C16:0C12:0 C14:0C16:0C16:1 C18:1C16:0C14:1	44 44 44 44	0.85	1.03	1.22	0.82	1.84	0.86	0.60	2.54	0.94	1.22	0.88
X36	C20:4C18:1C16:0	44	0.49	0.62	0.47	0.58			0.24	1.90	0.86	0.81	0.64

X37	C16:0C16:0C12:0 C18:0C14:0C12:0 C16:0C14:0C14:0 C22:6C18:0C18:1 C18:1C18:2C15:0	44 44 44 44 45	0.42	0.20	0.27	0.23	0.72	0.25	0.25	0.60	0.24	0.27	0.19
X38	C17:1C16:0C14:0 C20:1C18:2C18:2	45 46	0.13	0.51	0.07	0.22	0.40	0.16	0.16	0.33	0.11	0.26	0.21
X39	C18:1C18:1C18:2	46	8.13	7.30	4.00	5.42	3.77	7.53	7.42	4.17	5.65	4.58	7.03
X40	C18:1C18:1C16:1	46	2.95	1.52	1.74	4.48	6.47	8.80	1.21	0.97	4.26	4.40	3.88
X41	C18:1C18:2C16:0	46	13.58	11.67	12.86	10.18	3.01	5.74	10.93	12.12	11.36	12.29	14.27
X42	C18:1C18:1C14:0	46	5.67	2.99	6.39	7.78	4.75	4.01	2.69	4.29	9.05	9.15	7.22
X43	C18:1C16:0C16:1	46	0.33	0.35						1.64		0.75	0.65
X44	C18:2C16:0C16:0	46	2.39	2.06	2.18	1.45	4.59	4.94	1.40	2.13	2.36	1.85	1.84
X45	C18:1C16:0C14:0	46	2.83	3.17	3.70	2.47	3.75	2.68	1.66	4.48	3.42	3.72	3.18
X46	C16:0C16:0C16:1	46	0.29	0.05	1.02	0.65	1.15	0.80	0.33	0.49	0.63	0.07	0.17
X47	C16:0C16:0C14:0 C18:0C14:0C14:0 C18:1C15:0C15:0 C18:1C18:1C15:0 C18:1C16:0C15:0	46 46 47 47 47	0.82	1.02	1.29	1.19	1.28	0.64	0.54	1.29	0.79	1.01	0.82
X48	C20:1C18:1C18:2 C18:1C18:1C20:2	48 48	0.15	0.22	0.19	0.33	0.56	0.45	0.41	0.13	0.23	0.07	0.05
X49	C18:1C18:1C18:1	48	8.81	8.18	8.25	8.37	6.74	9.50	14.03	5.76	8.81	8.33	7.39
X50	C18:0C18:1C18:2	48	2.11	4.27						2.33		1.17	0.24
X51	C18:1C18:1C16:0	48	17.88	17.21	25.43	20.08	10.06	12.52	23.59	15.03	20.88	20.54	19.85
X52	C18:0C18:1C16:1	48					1.61	1.55					
X53	C18:0C18:2C16:0	48	1.04	1.61	1.28	1.29	0.94	0.97	1.22	1.36	0.86	1.27	0.80
X54	C16:0C18:1C16:0	48	5.75	9.08	8.47	5.25	3.29	3.24	5.11	7.07	5.23	5.58	5.40
X55	C16:0C16:0C16:0 C18:0C16:0C14:0 C18:1C18:1C17:0	48 48 49	1.25	1.89	1.36	0.83	1.31	0.91	0.97	1.27	0.71	0.91	0.81
X56	C20:1C18:1C18:1	50	0.32	0.21	0.28	0.28	0.60	0.57	0.65	0.09	0.17	0.15	0.13
X57	C20:1C18:1C16:0	50	0.29	0.28	0.19	0.24	0.37	0.29	0.21	0.18	0.22	0.12	0.12
X58	C18:0C18:1C18:1	50	2.66	3.45	4.02	2.20	2.89	3.46	5.82	2.67	2.08	1.84	2.01

X59	C18:0C18:2C18:0 C20:1C18:0C14:0	50 50			0.29	0.11	0.26	0.27	0.20		0.06		
X60	C18:0C18:1C16:0	50	3.02	4.71	3.60	2.08	2.20	2.00	4.45	2.59	1.30	1.45	1.76
X61	C18:0C18:0C16:1	50				0.05	0.22						
X62	C18:0C16:0C16:0	50	1.24	1.37	0.47	0.60	0.80	0.86	2.47	0.52	0.21	0.41	0.58
X63	C17:0C18:0C18:1	51			0.05	0.10	0.21	0.08	0.25		0.03		
X64	C20:1C18:1C18:0	52			0.10	0.18	0.22	0.61	0.95		0.12		
X65	C20:0C18:1C18:1	52	0.77	0.93	0.03	0.08	0.16	0.18	0.24	0.28	0.06	0.14	0.38
X66	C18:0C18:1C18:0 C20:0C18:1C16:0	52 52	0.71	0.75	0.43	0.27	0.51	0.48	0.81	0.38	0.18	0.20	0.39
X67	C18:0C18:0C16:0 C20:0C16:0C16:0	52 52	0.68	0.68	0.16	0.13	0.25	0.15	0.39	0.20	0.06	0.14	0.24

2.3.3.3. Statistical analysis

The simple evaluation of the percentage profile of the samples was not much informative. Therefore, more powerful unsupervised data handling for discriminate among samples was applied. The Principal Component Analysis (PCA) on the percentage of FAMEs and IMTGs profile were first performed separately. More than 50% of variance was explained in both cases with the first two components; however, no significant clustering was observed considering the Score Plot obtained from the IMTGs data; while a slight degree of discrimination was observed in the Score Plot obtained from the FAMEs data (data not shown). However, to increase the level of information considered in the PCA analysis, both data obtained from FAMEs and IMTGs profiles of the 3 MADD, 4 CPT, 2 LS1, and 2 control biopsies were evaluated all together performing a PCA. A matrix, containing 67 TGs peaks and 35 FAMEs, was built. The data used for such an elaboration are reported in Supplementary Table 1S (II-2.3). Figure 4 (II-2.3) reports the Score Plot (Figure 4a (II-2.3)) and the Loading Plot (Figure 4b (II-2.3)) obtained from the PCA elaboration. Using the entire set of information, a clear clustering was observed and each disease was well-discriminated from both the control samples and the other diseases considered (43.3% of total variance).

The PCA results obtained were very promising, suggesting the feasibility to investigate the lipidome of muscle biopsies to extrapolate biomarkers for supporting a reliable diagnosis of LSM diseases.

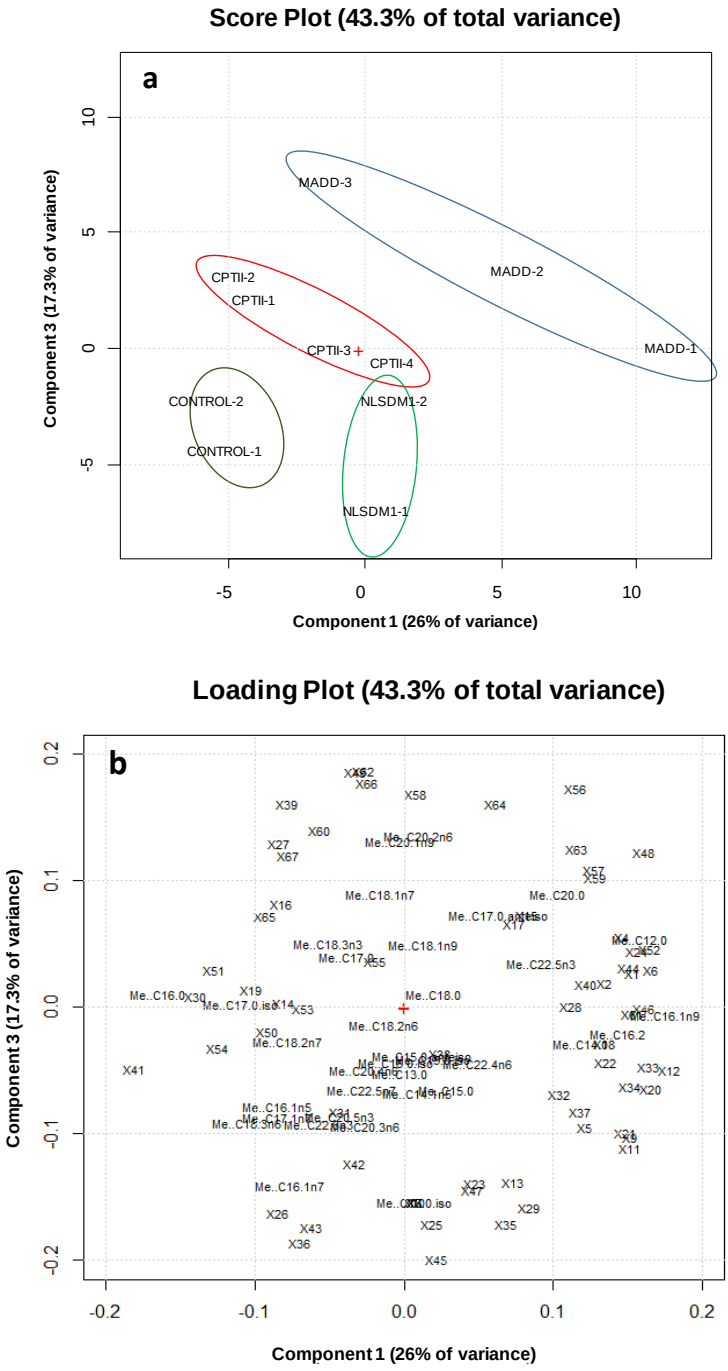

Figure 4 (II-2.3). Score Plot (A) and Loading Plot (B) obtained from the PCA elaboration by using the entire set of information (FAMEs and TGs).

2.3.4. Conclusions

The lipid profile of rare myopathies, of which the diagnosis can be challenging, was investigated for the first time. The FAMEs and TGs profiles were reliably identified and a relative quantification was carried out. The entire dataset of information obtained were statistically elaborated, performing a PCA. The three pathologies investigated, along with the controls were well discriminated. Considering the rarity of these diseases and the difficulties in their diagnosis, the number of samples is unavoidably limited. However, the discrimination obtained in the PCA seems very promising to extrapolate diagnostic information, which can support or replace the present approaches used for define the specific disease. Further studies will be necessary to understand if the lipid profile can provide useful information on the selection of a suitable treatment and on the monitoring of the response to therapy of patients.

REFERENCES

[1] S. Di Mauro, P.M. Di Mauro, Muscle carnitine palmitoyl transferase deficiency and myoglobinuria, Science 182 (1973) 929–931.

[2] S.E. Olpin, S. Clark, B.S. Andresen, C. Bischoff, R.K. Olsen, N. Gregersen, A.Chakrapani, M. Downing, N.J. Manning, M. Sharrard, J.R. Bonham, F. Muntoni, D.N. Turnbull, M. Pourfarzam, Biochemical, clinical and molecular findings in LCHAD and general mitochondrial trifunctional protein deficiency, J. Inherit. Metab. Dis. 28 (2005) 533–544.

[3] C. Bruno, S. Di Mauro, Lipid storage myopathies, Curr. Opin. Neurol. 21 (2008)601–606.

[4] W.C. Liang, I. Nishino, State of the art in muscle lipid diseases, Acta Myol. 29(2010) 351–356.

[5] B.S. Andresen, S. Olpin, B.J.H.M. Poorthuis, H.R. Scholte, C. Vianey-Saban, R.Wanders, L. Ijlst, A. Morris, M. Pourfarzam, K. Bartlett, E.R.

Baumgartner, J.B.de Klerk, L.D. Schroeder, T.J. Corydon, H. Lund, V. Winter, P. Bross, L. Bolund, N. Gregersen, Clear correlation of genotype with disease phenotype in very-long-chain acyl-CoA dehydrogenase deficiency, Am. J. Hum. Genet. 64(1999) 478–494.

[6] R.K.J. Olsen, S.E. Olpin, B.S. Andresen, Z.H. Miedzybrodzka, M. Pourfarzam, B. Merinero, F.E. Frerman, M.W. Beresford, J.C.S. Dean, N. Cornelius, O. Andersen, A. Oldfors, E. Holme, N. Gregersen, D.M. Turnbull, A.A.M. Morris, ETFDH mutations as a major cause of riboflavin-responsive multiple acyl-CoA dehydrogenation deficiency, Brain 130 (2007) 2045–2054.

[7] K. Gempel, H. Topaloglu, B. Talim, P. Schneiderat, B.G. Schoser, V.H. Hans, B.Pálmafy, G. Kale, A. Tokatli, C. Quinzii, M. Hirano, A. Naini, S. Di Mauro, H. Prokisch, H. Lochmüller, R. Horvath, The myopathic form of coenzyme Q10deficiency is caused by mutations in the electron transferring-flavoprotein dehydrogenase (ETFDH) gene, Brain 130 (2007) 2037–2044.

[8] W.C. Liang, A. Ohkuma, Y.K. Hayashi, L.C. López, M. Hirano, I. Nonaka, S. Noguchi, L.H. Chen, Y.J. Jong, I. Nishino, ETFDH mutations CoQ10 levels, and respiratory chain activities in patients with riboflavin- responsive multiple acyl-CoA dehydrogenase deficiency, Neuromuscul. Disord. 19 (2009)212–216.

[9] J. Fischer, C. Lefevre, E. Morava, J.M. Mussini, P. Laforêt, A. Negre-Salvayre, M. Lathrop, R. Salvayre, The gene encoding adipose triglyceride lipase (PNPLA2)is mutated in neutral lipid storage disease with myopathy, Nat. Genet. 39(2007) 28–30.

[10] M. Schweiger, G. Schoiswohl, A. Lass, F.P.W. Radner, G. Haemmerle, R. Malli, W. Graier, I. Cornaciu, M. Oberer, R. Salvayre, J. Fischer, R. Zechner, R. Zimmermann, The C-terminal region of human adipose triglyceride lipase affects enzyme activity and lipid droplet binding, J. Biol. Chem. 283 (2008)17211–17220.

[11] T. Seppänen-Laakso, I. Laakso, R. Hiltunen, Analysis of fatty acids by

gaschromatography, and its relevance to research on health and nutrition, Anal.Chim. Acta 465 (2002) 39–62.

[12] A. Ruiz-Rodriguez, G. Reglero, E. Ibá˜nez, Recent trands in the advanced analysis of bioactive fatty acids. A review, J. Pharm. Biomed. Anal. 51 (2010)305–326.

[13] M. Lísa, E. Cífková, M. Holˇcapek, Lipidomic profiling of biological tissues using off-line two-dimensional high-performance liquid chromatography-mass spectrometry, J. Chromatogr. A 1218 (2011) 5146–5156.

[14] E. Cífková, M. Holˇcapek, M. Lísa, D. Vrána, B. Melichar, V.ˇStudent, Lipidomic differentiation between human kidney tumors and surrounding normal tissues using HILIC-HPLC/ESI–MS and multivariate data analysis, J. Chromatogr. B 1000 (2015) 14–21.

[15] C.C. Teo, W.P.K. Chong, E. Tan, N.B. Basri, Z.-J. Low, Y.S. Ho, Advances in sample preparation and analytical techniques for lipidomics study of clinical samples, TrAC—Trends Anal. Chem. 66 (2015) 1–18.

[16] J. Folch, M. Lees, G.H.S. Stanley, A simple method for the isolation and purification of total lipides from animal tissues, J. Biol. Chem. 226 (1957)497–509.

[17] E.G. Bligh, W.J. Dyer, A rapid method of total lipid extraction and purification, Can. J. Biochem. Physiol. 37 (1959) 911–917.

[18] A. Ostermann, M. Müller, I. Willenberg, N.H. Schebb, Determining the fatty acid composition in plasma and tissues as fatty acid methyl esters by gaschromatography—a comparison of different derivatization and extraction procedures, Prostaglandins Leukot. Essent. Fatty Acid 91 (2014) 235–241.

[19] G. Lepage, C.C. Roy, Direct transesterification of all classes of lipids in a one-step reaction, J. Lipid Res. 27 (1986) 114–120.

[20] X. Kang, J. Wang, A simplified method for analysis of polyunsaturated fatty acids, BMC Biochem. 6 (2005) 5–9.

[21] World Medical Association, Declaration of Helsinki: ethical principles for medical research involving human subjects, JAMA 310 (20) (2013)2191–2194, http://dx.doi.org/10.1001/jama.2013.281053 (PMID 24141714.Retrieved July 24, 2015).

[22] A. Berardo, S. Di Mauro, M. Hirano, A diagnostic algorithm for metabolic myopathies, Curr. Neurol. Neurosci. Rep. 2 (2010) 118–126.

[23] S. Di Donato, A. Castiglione, M. Rimoldi, F. Cornelio, F. Vendemia, G. Cardace,B. Bertagnolio, Heterogeneity of carnitine-palmitoyl transferase deficiency, J. Neurol. Sci. 50 (1981) 207–215.

[24] R. Costa, M. Beccaria, E. Grasso, A. Albergamo, M. Oteri, P. Dugo, S. Fasulo, L. Mondello, Sample preparation techniques coupled to advanced chromatographic methods for marine organisms investigation, Anal. Chim. Acta 875 (2015) 41–53.

[25] C.D. Funk, Prostaglandins and leukotrienes: advances in eicosanoid biology, Science 294 (2001) 1871–1875.

[26] J.T. Lin, L.R. Snyder, T.A. McKeon, Prediction of relative retention times of triacylglycerols in non-aqueous reversed-phase high-performance liquid chromatography, J. Chromatogr. A 808 (1998) 43–49.

[27] M. Holˇcapek, P. Jandera, P. Zderadicka, L. Hrubá, Characterization of triacylglycerol and diacylglycerol composition of plant oils using high-performance liquid chromatography-atmospheric pressure chemical ionization mass spectrometry, J. Chromatogr. A 1010 (2003) 195–215.

[28] C. Baiocchi, C. Medana, F. Dal Bello, V. Giancotti, R. Aigotti, D. Gastaldi, Analysis of regioisomers of polyunsaturated triacylglycerols in marine matrices by HPLC/HRMS, Food Chem. 166 (2015) 551–560.

[29] M. Beccaria, E. Moret, G. Purcaro, L. Piazzale, A. Cotroneo, P. Dugo, L. Mondello, L. Conte, Reliability of the ΔECN42 limit and global method for extra virgin olive oil purity assessment using different analytical approaches,

Food Chem. 190 (2016) 216–225.

[30] M. Beccaria, R. Costa, G. Sullini, E. Grasso, F. Cacciola, P. Dugo, L. Mondello, Determination of the triacylglycerol fraction in fish oil by comprehensive liquid chromatography techniques with the support of gas chromatography and mass spectrometry data, Anal. Bioanal. Chem 407 (2015) 5211–5225.

[31] M. Holˇcapek, M. Lísa, P. Jandera, N. Kabátová, Quantitation of triacylglycerols in plant oils using HPLC with APCI-MS evaporative light-scattering, and UVdetection, J. Sep. Sci. 28 (2005) 1315–1333.

[32] M. Beccaria, G. Sullini, F. Cacciola, P. Donato, P. Dugo, L. Mondello, Highperformance characterization of triacylglycerols in milk and milk-related samples by liquid chromatography and mass spectrometry, J. Chromatogr. A1360 (2014) 172–187.

[33] M. Lísa, M. Holˇcapek, Triacylglycerols profiling in plant oils important in food industry, dietetics and cosmetics using high-performance liquid chromatography atmospheric pressure chemical ionization mass spectrometry, J. Chromatogr. A 1198–1199 (2008) 115–130.

[34] S. Salivo, M. Beccaria, G. Sullini, P. Tranchida, P. Dugo, L. Mondello, Analysis of human plasma lipids by using comprehensive two-dimensional gaschromatography with dual detection and with the support of high-resolution time-of-flight mass spectrometry for structural elucidation, J. Sep. Sci. 38(2015) 267–275.

2.4. Determination of amines and phenolic acids in wine with benzoylchloride derivatization and liquid chromatography–mass spectrometry

This research activity has been carried out at University of Michigan (Ann Arbor, MI, USA) under the supervision of Professor Robert Kennedy within the "Research & Mobility Project".

2.4.1. Introduction

Consumers, regulators, and producers are increasingly interested in obtaining information on the characteristics and the quality of food products [1]. This interest has spawned development of a wide variety of methods for analyzing consumable goods (e.g., wine, honey, tea, olive oil and juices) [2]. With respect to wine, various national organizations require strict control over factors such as geographical origin and grape varieties to maintain consistency and quality [3]. Thus, characterization methods are required to assess authenticity and detect wine fraud. Separation techniques such as LC and GC have been widely used for wine characterization and classification. Two important families of LC-amenable wine components are phenols and biogenic amines. Compositional profiles of phenolic and/or amino species have been correlated with significant factors such as organoleptic properties, wine-making practices, and grape varieties [4,5]. In this work, we describe a new approach to assay of phenols and amines in wine using derivatization followed by LC–MS/MS for separation and quantification.

Phenols are a family of bioactive compounds found in wine that have drawn significant attention over the last few years. These aromatic secondary metabolites are ubiquitous in the plant kingdom. They comprise a complex

family of more than 8000 substances with highly diverse structures and sizes from <100 Da to >30,000 Da for highly polymerized polyphenolic species. The main reasons for the interest in phenols are their antioxidant properties, great abundance in our diet, probable role in the prevention of various diseases, and contribution to sensorial properties [6–8]. Wine is an excellent natural source of various phenols that range from phenolic acids like benzoic- or cinnamic-like derivatives to different classes of polyphenolic flavonoids such as flavones, flavan-3-ols, flavonols and anthocyanins [9]. For this reason, analytical methods such as comprehensive LC techniques have been exploited over the last few years especially to quantify phenols in wine [10–12].

In addition to phenols, biogenic amines have also been the subject of some studies [13–18]. Some of the biogenic amines usually found in wines are agmatine, spermine, spermidine, putrescine, cadaverine, histamine, and tyramine. These compounds are all produced by microorganisms during fermentation via decarboxylation of free amino acids. The consumption of some of them, e.g., histamine and tyramine, can lead to headaches, nausea, hot flushes, skin rashes, sweating, respiratory distress, and cardiac/intestinal problems [19]. Because these components may be responsible for the biological responses to wine consumption, their measurement in different wine varieties of various origins has great importance. LC with UV detection has been widely used for the determination of amines and phenolic compounds in wine and other beverages. Phenols can be detected in their native state [11,20–22], while amines require derivatization to be compatible with UV detection [23–26]. Although these methods are adequate for measuring a few metabolites, the limited selectivity makes it difficult to characterize a large (e.g., 20+) panel of metabolites, especially in complex mixtures. Mass spectrometry (MS) detection offers away to overcome these limitations. MS has much better selectivity than UV detection, making it possible to distinguish many more metabolites, even

co-eluting compounds, in complex mixtures. Using tandem mass spectrometry (MS/MS) allows for greater confidence in peak identification from unique fragmentation pat-terns. Additionally, MS/MS is more sensitive than UV, allowing for the measurement of trace metabolites which may not be detected with UV. Mass spectrometry does suffer from instrument drift and matrix effects, but this problem can be corrected through the use of internal standards labeled with stable isotopes. Some work has been done for the analysis of native amines and phenolic compounds in wine with LC–MS [12,27–29]. However, there are still challenges which much be addressed. Polar amines are poorly retained with reversed phase chromatography, and sensitivity for some trace metabolites may still be limiting. Some of the same derivatization techniques used in UV detection of amines can be beneficial to mass spectrometry and help overcome these challenges. Tagging metabolites with a hydrophobic moiety increases retention of polar metabolites, while also increasing ESI ionization efficiency up to 10,000-fold [30,31]. Additionally, derivatization makes it easy to generate internal standards for each targeted metabolite through the use of stable isotope labeled derivatizing reagents. Labeling improves quantification by accounting for instrument drift and matrix effects, and can aid in peak selection in the presence of background peaks and retention time drift. Several reagents have been reported that have use for amines and phenols by LC–MS. Derivatization with 1,2-naphthoquinone-4-sulfonate has been used with LC–MS for wine analysis previously[17]. Dansyl chloride derivatization has been used in wine for LC-UV analysis [24]. This same reagent has recently been promoted for the determination of phenols and amine metabolites with LC–MS in a variety of samples including urine, cerebrospinal fluid, and plasma [31–34]. Benzoyl chloride (BzCl) has also been used for LC-UV [35–38] as well as LC–MS [30,39]. Like dansyl chloride, this reagent reacts with amines, phenols, and some hydroxyls. BzCl may have

advantages, though, over other reagents for food analysis. The reaction is near instantaneous at room temperature and produces photostable derivatives [30,39]. Furthermore,13C labeled reagent is readily available at a reasonable cost enabling routine creation of internal standards for all analytes. Here, we demonstrate the application of BzCl derivatization with LC–MS/MS for determination of 56 amine and phenol metabolites in wine. To our knowledge, this method is unique in its capability to measure both amines and phenols in wine in a single, quick assay. Furthermore, the method assays a much larger panel of compounds than other methods, is shown to provide accurate quantitative data, and may enable distinguishing of varietals and location of production for wine.

Compound abbreviations

ACh: Acetylcholine; Ado: Adenosine; Agm: Agmatine; Ala: Alanine; Arg: Arginine; Asn: Asparagine; Asp: Aspartic acid; βAla: β-Alanine; Cad: Cadaverine; Caf : Caffeic acid; Ch: Choline; Cit: Citrulline; Cou: *p*-Coumaric aicd; Cys: Cysteine; DA: Dopamine; DOMA: 3,4-Dihydroxymandelic acid; DOPA: 3,4-Dihydroxyphenylalanine; DOPAC: 3,4-Dihydroxyphenylacetic acid; DOPEG: 3,4-Dihydroxyphenylglycol; ETA: Ethanolamine; Fer: Ferulic acid; GABA: γ-Aminobutyric acid; Gal: Gallic acid; Glc: Glucose; Gln: Glutamine; Glu: Glutamic acid; Gly: Glycine; His: Histidine; Hist: Histamine; HVA: Homovanillic acid; Lys: Lysine; Met: Methionine; MOPEG: 3-Methoxy-4-hydroxyphenylglycol; NAP: N-Acetylputrescine; Orn: Ornithine; PCA: Protocatechuic acid; Phe: Phenylalanine; PhEt: Phenethylamine; Pro: Proline; Put: Putrescine; Ser: Serine; Sin: Sinapic acid; Spd: Spermidine; Spm: Spermine; Tau: Taurine; Thr: Threonine; TOH: Tyrosol; Trp: Tryptophan; TrpA: Tryptamine; Tyr: Tyrosine; TyrA: Tyramine; VA: Vanillic acid; Val: Valine; VMA: Vanillylmandelic acid; VN: Vanillin; Xle: Leucine/Isoleucine.

2.4.2. Experimental

2.4.2.1. Chemicals and reagents

All chemicals were purchased from Sigma-Aldrich (St. Louis, MO) unless otherwise noted. Water and acetonitrile were Burdick &Jackson HPLC grade purchased from VWR (Radnor, PA). Stock solutions of 2 M Glc; 1 M Ch; 50 mM Pro; 10 mM ACh, Ala, Arg, Asn, Asp, _Ala, Cad, Cit, Cys, DA, DOMA, DOPA, DOPAC (Acros Organics, Geel, Belgium), DOPEG, ETA, GABA, Gln, Glu, Gly, His, Hist, HVA (Tocris, Bristol, UK), Leu, Lys, Met, MOPEG, NAP, Orn (Acros Organics, Geel, Belgium), Phe, PhEt (MP Biomedicals, Santa Ana, CA), Put, Ser, Spd, Spm, Tau, Thr, TyrA Val, VMA; 5 mM Ado, Trp; 2 mM Tyr; 250 _M TrpA, and 20 nM d4-ACh and d4-Ch (C/D/N Isotopes, Pointe-Claire, Canada) were prepared in water and stored at −80◦C. Stock solutions of 10 mM Caf, Cou (TCI Chemicals, Philadelphia, PA), Fer, Gal(Acros Organics, Geel, Belgium), PCA, Sin, TOH, VA, and VN were prepared in ethanol and stored at −20◦C. Wine was purchased from a local retailer. The varietals selected were Cabernet Sauvignon and Merlot, each from California and Australia. A standard mixture was prepared in water for use in calibration standards. Preparation of calibration standards and internal standards has previously been described; exact procedures for this work are given in Supplemental 1. Single-use aliquots of calibration standards and internal standards were prepared and stored at−80◦C. On the day of use, an internal standard aliquot was thawed, diluted 100-fold in 20% (v/v) acetonitrile containing 1% (v/v) sulfuric acid, and spiked with deuterated acetylcholine and Choline toa final concentration of 20 nM. A fresh BzCl solution was prepared daily.

2.4.2.2. Sample preparation and derivatization

Three aliquots of 500 _L from each wine sample were filtered through Amicon

Ultra spin filters (30k MWCO, Millipore Sigma, Billerica, MA) by centrifugation for 5 min at 12,100g. The filtered wine was diluted 10-fold in water. Filtered, diluted wine was derivatized by sequential addition of 10 _L 100 mM sodium carbonate, 10 _L2% (v/v) BzCl in acetonitrile, and 10 _L internal standard solution. Calibration standards were prepared in water and derivatized in the same manner.

2.4.2.3. Metabolite analysis by LC–MS/MS

Analysis was performed using a Waters (Milford, MA) nanoAcquity UPLC. An Acquity HSS T3 C18 column (1 mm x 100 mm,1.8 _m, 100 Å pore size) was used. The autosampler was kept at ambient temperature, and the column was kept at 27◦C. The injection size was 5 _L using partial loop injection mode. Mobile phase A was 10 mM ammonium formate with 0.15% formic acid. Mobile phase B was acetonitrile. The flow rate was 100 _L/min, and the gradient used was: initial, 0% B; 0.01 min, 15% B; 0.5 min, 17% B; 14 min,55% B; 14.5 min, 70% B; 18 min, 100% B; 19 min, 100% B; 19.1 min,0% B; 20 min, 0% B. A 10 min re-equilibration period followed each injection. Detection was performed on an Agilent (Santa Clara, CA) 6410 B triple quadrupole mass spectrometer in dynamic multiple reaction monitoring (dMRM) mode. Electrospray ionization was used in positive mode at 4 kV. The gas temperature was 350◦C, gas flow was 11 L/min, and the nebulizer was at 15 psi. MRM conditions are listed in Supplemental 2. Peak integration was performed using Agilent Mass Hunter Quantitative Analysis for QQQ, version B.05.00.All peaks were visually inspected to ensure proper integration.

2.4.2.4. Method evaluation

Limits of detection (LOD) were calculated as three standard deviations of the blank, using a six point calibration with three replicates. Limits of

quantification (LOQ) were calculated as ten standard deviations of the blank. Calibration ranges are listed in Supplemental 1. The same calibration was used to determine linearity for each metabolite. Repeatability was defined as the RSD for triplicate analysis of an aqueous standard at relevant metabolite concentrations. Recovery was determined by spiking three aliquots each of 200 μL wine with 40 μL of either water or 5X concentrated standards (refer to Supplemental 1 for individual concentrations). The spiked wine was prepared and analyzed as described in Section ***2.4.2.2.*** The expected concentration was determined by adding the known, spiked concentration to the measured concentration of the sample spiked with water. Recovery was calculated by comparing the concentration of the standard spiked wine to the expected concentration.

2.4.2.5. Statistical analysis

Single factor ANOVA and unpaired, two-tailed student's t-tests were performed. Differences were deemed significant if $P \leq 0.05$ following Holm-Bonferroni correction

2.4.3. Results and discussion

2.4.3.1. Metabolite selection

We have previously described BzCl derivatization of 70 amine and phenol metabolites in biological samples [39]. We used that previous work as a basis for developing a method for analysis of wine to test the utility of this approach for food analysis. Of the70 compounds previously assayed, 46 were selected as potentially relevant in wine. An additional 10 metabolites were chosen to add to the method: hydroxybenzoic acids gallic acid, protocatechuic acid, and vanillic acid; hydroxycinnamic acids caffeic acid, ferulic acid, *p*-coumaric acid, and sinapic acid; phenolic aldehyde vanillin; phenylethanoid tyrosol; and polyamine

cadaverine. These metabolites were selected based on their relevance in wine and availability. In principle, BzCl derivatization could be used for the assay of additional phenolic acids as well. Attempts to extend the method to some other polyphenols revealed some limitations. Due to the excess of reagent in the reaction mixture, the BzCl reaction typically goes to completion. In the case of sinapic acid, a low yield of underivatized product was observed, which we believe is due to steric hindrance of the4-phenol. Linear calibrations were still achieved, so this did not appear to limit quantification. Additionally, flavonols did not appear to label efficiently with BzCl. Quercetin, for example, has five potential labeling sites. Unlabeled, singly labeled, and doubly labeled quercetin were the primary species detected. This finding is in contrast with metabolites like dopamine, which has three labeling sites, and only triply labeled dopamine is detected. We believe the poor reaction efficiency is due to resonance stabilization and hydrogen bonding between the phenols. While the conditions used here are not compatible with flavonol detection, these metabolites can be detected directly using LC–MS [12], or with dansyl chloride [33], where the harsher reaction conditions allow for derivatization of flavonols.

2.4.3.2. Figures of merit

After pilot experiments revealed that the 56 target compounds could be labeled with BzCl, we developed a LC–MS/MS method that utilized gradient elution and multiple reaction monitoring with optimized MS/MS for each compound. Figure 1 (II-2.4.) shows that reasonable separation was achieved using a 20 min gradient. No differences in peak shape were observed between aqueous standards and wine. LODs, repeatability, recovery, and linearity for each metabolite are listed in Table 1 (II-2.4.). LODs for all but 12 of the studied metabolites were below 10 nM, and all were below 1 μM. Every metabolite studied was above the limit of detection in the wines. Thus, the sensitivity of

the method is appropriate for wine analysis, and could even be applied to wine subject to greater dilution. RSDs were below10% for all metabolites except vanillin, vanillic acid, agmatine, and vanillylmandelic acid. RSDs for these metabolites were below 15%. All metabolites produced linear calibrations (R2> 0.99), allowing for reliable quantification. All quantification was based on comparison to internal standards consisting of13C-BzCl labeled standards added to the samples. The significance of using internal standards was assessed by comparing concentrations calculated based on analyte peak area alone to analyte peak area normalized to internal standard peak area. Without internal standards, calculated concentrations ranged from 27% to 136% of the value determined through use of internal standards (Figure 4 (II-2.4.)). This result demonstrates the necessity of including internal standards for each metabolite for accurate quantification in complex samples. Individual internal standards are easily prepared for this method through the use of ^{13}C-BzCl.To assess accuracy and recovery of the method, wine was spiked with a known concentration of standards, and the calculated concentration was compared to the expected concentration. If the internal standards were not sufficiently accounting for matrix effects, we would expect low accuracy from this experiment. How-ever, calculated recovery ranged from 80% to 150%, and average recovery was 101%. Of the 56 metabolites, 46 had recoveries within the range of 90% to 110%. Gallic acid had the lowest recovery of80%, and adenosine, protocatechuic acid, and sinapic acid had the three highest recoveries, all at or above 130%. Inspection of the data revealed that each of these metabolites had a single deviant point contributing to the inaccuracy. Accuracy was greatly improved if this point is removed, so we expect that these problems were sample preparation errors and that a greater number of replicates would further improve these calculations. In general, recoveries were repeatable, further demonstrating that the method allows for accurate and

reliable quantification.

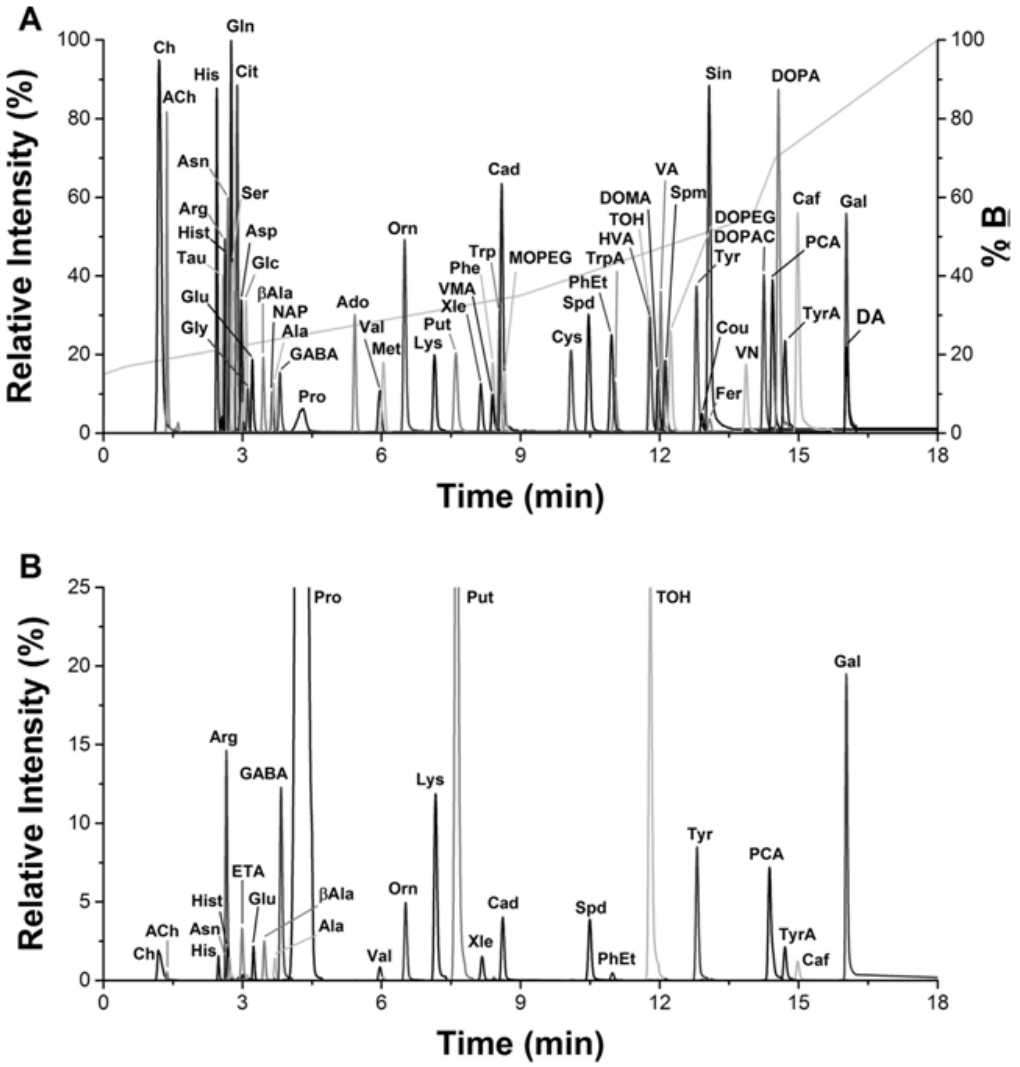

Figure 1 (II-2.4.). Extracted ion chromatogram of 56 amine and phenolic metabolites. A. Standards in aqueous solution. Gradient is overlaid as % B. B. Example chromatogram from filtered, diluted wine. No significant differences in peak shape or retention times were observed between standards and wine samples.

Table 1 (II-2.4.). Summary of limit of detection (LOD), limit of quantification (LOQ), repeatability (RSD), and linearity for a six point calibration using aqueous standards (n = 3).

Compound	LOD (nM)	LOQ (nM)	RSD (%)	Recovery (%)	Linearity (R^2)
Ch	40	60	0.5	98.6 ± 2.56	0.9995
ACh	0.5	1	1.5	88.0 ± 12.0	0.9998
His	1	2	1.2	102±4.71	0.9927
Tau	2	5	2.5	101±10.7	0.9996
Arg	2	4	1.5	98.3±2.61	0.9993
Hist	1	3	1.8	88.1±3.21	0.9994
Asn	1	3	0.4	99.0±2.03	0.9958
Gln	0.4	0.8	1.5	115±12.3	0.9921
Ser	60	200	2.5	106±3.59	0.9998
Cit	0.5	1	1.9	99.0±3.30	0.9999
Agm	0.2	0.6	12	109±14.5	0.9939
ETA	4	8	5.6	100±5.93	0.9995
Asp	4	7	4.1	98.1±1.74	0.999
Glc	300	900	2.5	104±6.81	0.9999
Gly	8	20	2.9	99.3±4.28	0.9942
Glu	5	9	0.5	94.3±0.56	0.999
BAla	1	3	0.5	97.6±1.23	0.9999
NAP	0.2	0.4	4.6	99.3±6.10	0.9995
Ala	8	20	0.6	101±3.06	0.9999
GABA	3	6	6.3	104±3.85	0.9995
Pro	200	400	4.2	94.8±0.35	0.9972
Ado	0.3	0.7	0.7	139±28.6	0.9959
Val	3	6	2.4	97.8±0.56	0.9973
Met	1	2	2.0	98.6±2.14	0.9988
Orn	2	4	3.3	101±0.55	0.9997
Lys	6	10	3.9	92.8±1.13	0.9947
Put	3	5	6.3	92.4±3.36	0.9973
Xle	7	10	4.4	90.8±1.90	0.9996
Phe	2	3	0.7	99.3±3.61	0.9997
Thr	2	3	4.3	103±4.30	0.9994
VMA	1	2	13	120±13.6	0.9958
Trp	4	5	1.8	103±5.53	0.995
Cad	0.4	0.8	0.4	84.9±2.81	0.9996
MOPEG	0.3	0.6	1.3	105±1.66	0.9993
Cys	0.2	0.5	6.6	108±10.9	0.9996
Spd	0.3	0.6	6.0	95.7±3.65	0.9958
PhEt	0.9	2	1.7	87.7±1.17	0.9986
TrpA	0.03	0.04	0.8	106±4.06	0.995
TOH	40	60	2.6	97.2±12.1	0.9973
HVA	0.7	2	3.5	91.4±8.36	0.9992
DOMA	0.3	0.8	5.5	102.6±10.2	0.9989
VA	20	40	11	112±8.96	0.9905
Spm	0.2	0.6	4.4	98.7±1.07	0.9903
DOPEG	0.1	0.2	1.8	90.1±6.25	0.9953
Tyr	10	20	3.0	105±2.11	0.9997
Cou	30	70	1.8	107±6.83	0.9961
Fer	90	100	8.0	89.5±8.44	0.9993
Sin	3	8	5.1	130±12.9	0.9971
VN	4	8	11	105±11.1	0.994
DOPAC	0.1	0.2	4.4	96.5±4.34	0.9999
PCA	20	40	8.6	155±13.7	0.9999
DOPA	0.5	1	6.5	105±18.0	0.9932
TyrA	20	30	1.5	87.6±8.20	0.998
Caf	70	100	0.1	102±4.39	0.9915
Gal	700	1000	5.2	80.4±8.17	0.9999
DA	0.7	1	5.2	97.1±15.4	0.9994

2.4.3.3. Wine analysis

To demonstrate the suitability of the method for wine, we com-pared four: a Californian Merlot, a Californian Cabernet Sauvignon, an Australian Merlot, and an Australian Cabernet Sauvignon. These choices allowed us to determine if the method could distinguish between region of production or varietal based on the metabolites included. The wine was filtered prior to analysis to remove any particulate matter. No difference was observed in calculated concentrations after filtration with spin columns or syringe filters, so spin columns were chosen for the ability to prepare multiple samples simultaneously. Filtered wine was then diluted 10 or 100fold in water prior to derivatization. We found that low abundance metabolites such as tryptamine and vanillylmandelic acid were undetectable after 100 fold dilution, so 10 fold dilution was selected for analysis. Calculated concentrations for each of the tested wines are listed in Table 2 (II-2.4.). When compared by region of production, 24 of the 56 metabolites were found to be different ($P < 0.05$) between Australian and Californian wines (Figure 3 (II-2.4.)). These distinguishing compounds were polyamines spermidine and spermine; phenolic acids caffeic acid, gallic acid, homovanillic acid, protocatechuic acid, and vanillic acid; amino acids asparagine, aspartate, histidine, leucine/isoleucine, lysine, phenylalanine, serine, threonine, tyrosine, and valine; and biogenic amines choline, DOPA, DOPEG, histamine, phenethylamine, tryptamine, and tyramine. All of these were found to be higher in Australian wines except homovanillic acid, spermine, and caffeic acid. Differences in amines and phenols based on geographic origin have been observed previously using LC with spectrophotometric detection [15,40], and may result from differences in climate, soil conditions, or fertilizers. Larger sample sizes would be required to determine if these differences are generalizable among the different regions. Further study would also be required to deter-mine the exact relationship

between these metabolites and the location of production. Of the 56 metabolites assayed, five were found to differ significantly ($P \leq 0.05$) based on varietal following Holm-Bonferroni correction (Figure 2 (II-2.4.)). These included polyamines cadaverine, putrescine, and N-acetyl putrescine; ferulic acid, and glutamic acid. The polyamines were higher in Cabernets, while ferulic acid and glutamate were higher in the Merlots. It is important to note that wines can be labeled as a particular varietal as long as that varietal makes up 75% of the composition in the United States, or 85%in Australia. Without knowing what the remaining composition is, we cannot draw conclusions of the relationship between these metabolites and the specific varietals. Larger sample sizes would be required to determine if these differences are generalizable among the different varietals; however, these results show the feasibility of distinguishing the different types of wine used here by the 56 compounds measured.

Table 2 (II-2.4.). Concentrations of amine and phenolic metabolites in wine. Concentrations are not corrected for dilution. Data is average ± standard deviation (RSD), n = 3.

Compound	Units	Australia Cabernet		Australia Merlot		California Cabernet		California Merlot	
ACh	nM	544 ± 34.6	(6.35)	467 ± 124	(26.6)	353 ± 8.87	(2.51)	356 ± 19.7	(5.53)
Ado	nM	52.3 ± 3.48	(6.56)	25.9 ± 2.65	(10.2)	15.8 ± 1.76	(11.1)	19.7 ± 2.12	(10.7)
Agm	nM	58.9 ± 2.96	(5.02)	35.9 ± 7.53	(21.0)	27.9 ± 3.15	(11.3)	16.0 ± 5.97	(37.3)
Ala	µM	35.0 ± 2.96	(8.48)	37.7 ± 2.23	(5.92)	21.7 ± 0.74	(3.42)	36.5 ± 2.79	(7.64)
Arg	µM	20.2 ± 2.02	(9.99)	18.7 ± 1.15	(6.16)	17.4 ± 0.38	(2.15)	15.4 ± 0.58	(3.74)
Asn	µM	10.5 ± 1.47	(14.0)	10.4 ± 0.74	(7.16)	7.29 ± 0.20	(2.70)	7.94 ± 0.75	(9.42)
Asp	µM	7.81 ± 0.93	(11.9)	6.82 ± 0.42	(6.16)	4.46 ± 0.11	(2.38)	5.24 ± 0.30	(5.74)
BAla	µM	17.9 ± 1.64	(9.20)	14.0 ± 1.20	(8.53)	15.7 ± 0.81	(5.15)	15.0 ± 0.93	(6.19)
Cad	nM	407 ± 40.9	(10.0)	53.8 ± 4.00	(7.44)	456 ± 4.11	(0.90)	45.3 ± 2.77	(6.11)
Caf	µM	1.42 ± 0.14	(9.53)	1.7 ± 0.14	(8.25)	3.75 ± 0.19	(5.11)	3.77 ± 0.34	(9.13)
Ch	µM	233 ± 18.7	(8.02)	202 ± 6.72	(3.33)	149 ± 0.91	(0.61)	139 ± 8.19	(5.90)
Cit	nM	392 ± 45.5	(11.6)	268 ± 27.0	(10.1)	428 ± 32.01	(7.47)	523 ± 14.6	(2.80)
Cou	µM	1.83 ± 0.20	(11.03)	1.37 ± 0.14	(10.3)	2.08 ± 0.03	(1.42)	1.82 ± 0.22	(11.9)
Cys	nM	252 ± 30.4	(12.1)	547 ± 44.9	(8.21)	518 ± 34.2	(6.61)	1250 ± 75.5	(6.06)
DA	nM	4.24 ± 0.77	(18.1)	4.56 ± 0.89	(19.4)	6.31 ± 1.53	(24.2)	4.35 ± 0.81	(18.5)
DOMA	nM	19.1 ± 2.78	(14.6)	17.2 ± 0.41	(2.36)	18.1 ± 1.04	(5.78)	14.7 ± 1.60	(10.9)
DOPA	nM	11.7 ± 0.71	(6.05)	12.3 ± 2.24	(18.1)	6.36 ± 0.80	(12.5)	5.33 ± 1.26	(23.7)
DOPAC	nM	9.95 ± 1.37	(13.8)	12.9 ± 0.67	(5.20)	11.1 ± 0.91	(8.20)	6.31 ± 0.45	(7.20)
DOPEG	nM	4.69 ± 0.54	(11.5)	5.51 ± 0.47	(8.45)	3.23 ± 0.06	(1.76)	2.60 ± 0.28	(10.7)
ETA	µM	23.1 ± 2.68	(11.6)	26.6 ± 3.21	(12.1)	26.8 ± 1.65	(6.17)	26.7 ± 2.34	(8.77)
Fer	µM	14.5 ± 1.90	(13.1)	27.8 ± 3.85	(13.9)	13.9 ± 1.60	(11.5)	22.9 ± 1.49	(6.50)
GABA	µM	29.7 ± 4.44	(14.9)	18.9 ± 1.20	(6.37)	12.0 ± 0.28	(2.29)	14.4 ± 1.14	(7.97)
Gal	µM	12.8 ± 1.91	(14.9)	15.7 ± 1.21	(7.71)	8.47 ± 0.55	(6.47)	7.83 ± 1.08	(13.8)
Glc	mM	1.54 ± 0.13	(8.54)	1.55 ± 0.06	(3.85)	1.15 ± 0.06	(5.63)	1.58 ± 0.10	(6.61)
Gln	nM	485 ± 37.3	(7.69)	417 ± 49.1	(11.8)	357 ± 10.5	(2.95)	512 ± 58.6	(11.5)
Glu	µM	12.8 ± 1.06	(8.28)	15.5 ± 0.58	(3.71)	11.7 ± 0.27	(2.34)	17.6 ± 1.43	(8.10)
Gly	µM	18.9 ± 1.68	(8.90)	20.8 ± 1.71	(8.22)	13.01 ± 1.03	(7.90)	20.2 ± 3.35	(16.6)
His	µM	16.4 ± 1.80	(11.0)	14.1 ± 0.88	(6.23)	10.07 ± 0.09	(0.90)	12.1 ± 0.69	(5.70)
Hist	µM	1.49 ± 0.24	(15.8)	1.16 ± 0.11	(9.57)	0.35 ± 0.003	(0.94)	0.36 ± 0.02	(4.33)
HVA	nM	50.2 ± 3.22	(6.41)	52.7 ± 2.62	(4.98)	64.6 ± 3.13	(4.85)	66.7 ± 6.51	(9.76)
Lys	µM	8.03±0.57	(7.09)	8.92±0.96	(10.8)	4.50±0.06	(1.34)	5.49±0.33	(5.94)

Compound	Units	Australia Cabernet		Australia Merlot		California Cabernet		California Merlot	
Met	nM	946±99.6	(10.5)	981±54.6	(5.57)	799±12.9	(1.61)	911±67.5	(7.40)
MOPEG	nM	9.84±1.15	(11.7)	15.0±2.35	(15.7)	13.6±1.42	(10.5)	13.2±2.64	(20.1)
NAP	nM	406±32.3	(7.96)	171±26.2	(15.3)	402±5.57	(1.39)	170±7.09	(4.18)
Orn	µM	4.01±0.42	(10.4)	4.04±0.32	(7.90)	5.13±0.05	(0.93)	7.76±0.53	(6.89)
PCA	µM	10.8±1.14	(10.6)	15.2±1.89	(12.4)	7.20±0.51	(7.06)	6.36±0.45	(7.03)
Phe	µM	4.89±0.47	(9.66)	5.20±0.20	(3.87)	2.55±0.07	(2.88)	3.11±0.29	(9.38)
PhEt	nM	79.9±10.5	(13.1)	49.7±4.79	(9.64)	34.3±1.38	(4.03)	9.89±0.86	(8.74)
Pro	mM	2.57±0.20	(7.66)	2.52±0.17	(6.58)	3.16±0.19	(5.92)	2.51±0.12	(4.76)
Put	µM	8.23±1.01	(12.2)	4.30±0.55	(12.7)	11.5±0.24	(2.08)	4.50±0.46	(10.1)
Ser	µM	8.61±0.27	(3.14)	10.1±0.79	(7.87)	5.62±0.23	(4.08)	7.09±0.77	(10.8)
Sin	nM	38.3±16.9	(44.2)	35.6±11.7	(32.9)	46.4±8.10	(17.5)	35.9±0.84	(2.34)
Spd	nM	690±82.6	(12.0)	605±51.3	(8.48)	434±10.4	(2.39)	450±22.5	(5.00)
Spm	nM	61.0±8.37	(13.7)	75.3±6.27	(8.33)	119±7.44	(6.24)	141±14.6	(10.4)
Tau	nM	167±20.9	(12.6)	174±16.5	(9.50)	239±37.3	(15.6)	165±19.2	(11.7)
Thr	µM	2.18±0.37	(17.0)	2.53±0.23	(8.89)	1.24±0.01	(0.73)	1.49±0.18	(12.0)
TOH	µM	34.6±5.53	(16.0)	29.4±0.32	(1.08)	28.2±1.90	(6.75)	19.0±1.93	(10.2)
Trp	nM	467±57.6	(12.4)	717±17.3	(2.42)	286±23.7	(8.28)	508±35.5	(6.98)
TrpA	nM	1.17±0.21	(17.6)	1.44±0.04	(3.04)	0.52±0.05	(9.81)	0.44±0.03	(6.55)
Tyr	nM	2.71±0.26	(9.45)	3.01±0.16	(5.22)	1.87±0.01	(0.57)	2.28±0.16	(6.85)
TyrA	nM	640±108	(16.9)	591±58.2	(9.85)	163±17.0	(10.4)	244±20.2	(8.29)
VA	µM	3.10±0.26	(8.41)	3.31±0.22	(6.75)	1.50±0.08	(5.36)	2.45±0.60	(24.5)
Val	µM	4.14±0.46	(11.2)	4.37±0.34	(7.75)	2.40±0.09	(3.78)	2.86±0.17	(6.09)
VMA	nM	53.3±9.79	(18.4)	49.4±8.24	(16.7)	36.3±7.32	(20.2)	55.6±0.77	(1.39)
VN	nM	128±22.9	(17.9)	235±23.4	(9.93)	101±1.81	(1.79)	120±7.86	(6.53)
Xle	µM	5.59±0.10	(1.79)	5.16±0.29	(5.71)	2.79±0.08	(2.84)	3.10±0.27	(8.71)

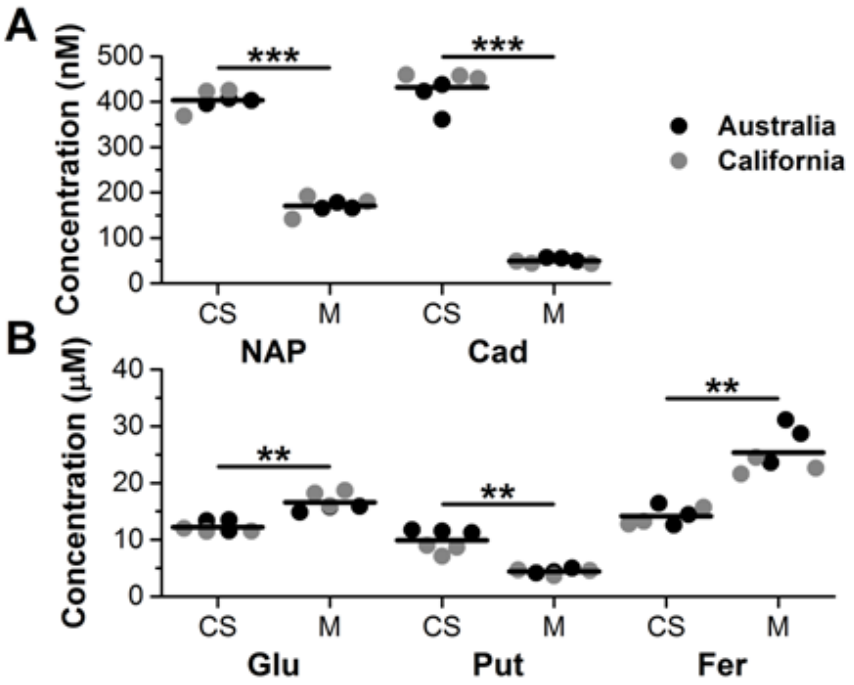

Figure 2 (II-2.4.). Metabolites showing significant differences between wine varietals. A. Metabolites at nanomolar concentrations. B. Metabolites at micromolar concentrations. Unpaired, two-tailed Student's t-tests were performed and the Holm-Bonferroni correction was used. Each point is a single sample, and the horizontal bar is the mean. Data shown is uncorrected for dilution. * $p \leq 0.05$; ** $p \leq 0.01$;*** $p \leq 0.001$. CS: Cabernet Sauvignon; M: Merlot; NAP: N-acetyl putrescine; Cad: cadaverine; Glu: glutamic acid; Put: putrescine; Fer: ferulic acid.

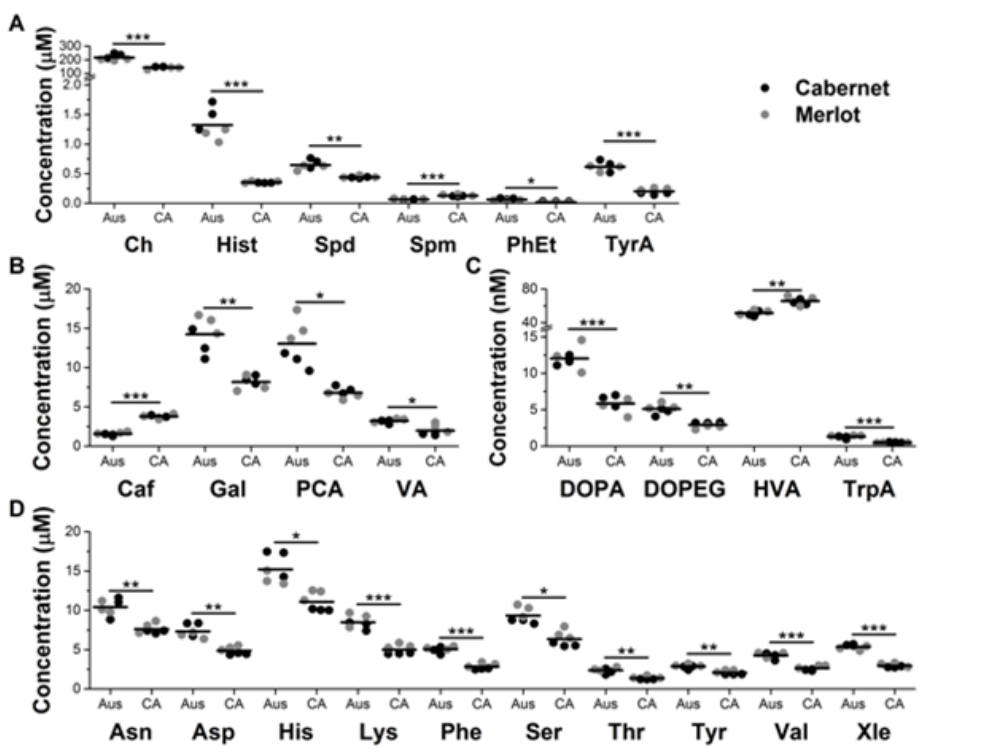

Figure 3 (II-2.4.). Metabolites showing significant differences between locations of production. A. Biogenic amines. B. Phenolic acids. C. Trace metabolites. D. Amino acids. Unpaired, two-tailed Student's t-tests were performed and the Holm-Bonferroni correction was used. Data shown is uncorrected for dilution. * $p \leq 0.05$; ** $p \leq 0.01$; *** $p \leq 0.001$. Aus: Australia; CA: California; Ch: Choline; Hist: histamine; Spd: spermidine; Spm: spermine; PhEt: phenethylamine; TyrA: tyramine; Caf: caffeic acid; Gal: gallic acid; PCA: protocatechuic acid; VA: vanillic acid; DOPA: 3,4-dihydroxyphenylalanine; DOPEG: 3,4-dihydroxyphenylglycol; HVA: homovanillic acid; TrpA: tryptamine; Asn: asparagine; Asp: aspartic acid; His: histidine; Lys: lysine; Phe: phenylalanine; Ser: serine; Thr: threonine; Tyr: tyrosine; Val: valine; Xle: leucine/isoleucine.

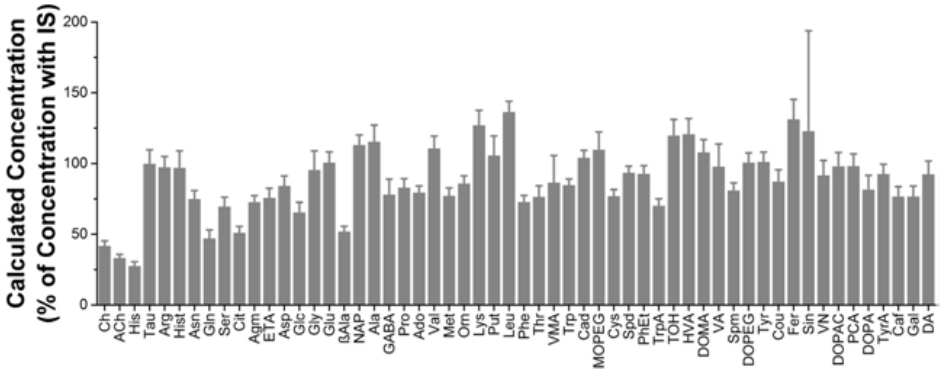

Figure 4 (II-2.4.). Accuracy of concentrations without internal standards relative to concentrations calculated with internal standards. Without internal standards, concentrations ranged from 27% to 136% of the concentrations normalized to internal standards. Data shown is average ± standard deviation (n = 3).

2.4.3.4. Comparison to current methods

Comparison of the BzCl-LC–MS/MS method to other methods used for measurement of phenols and amines in wine reveals that it has substantial advantages for quantitative, multiplexed assays that can provide significant information on the wine. LC-UV is a commonly used technique for the analysis of amines and phenols in wine. It is particularly well suited to phenols, which are naturally UV active. Methods for up to 20 phenols have been established[22]. 2D-LC can increase selectivity, at the cost of analysis time and complexity of the fluidics [11]. Amines can be detected by UV after derivatization, and methods for up to 33 amines have been established [23]. UV detection is simple and inexpensive, but LC–MS/MS offers greater flexibility, because both amines and phenols can be detected. Additionally, while trace amines such as tryptamine, phenethylamine, and agmatine are not consistently detected with UV, these metabolites were above our LODs in all samples tested. Studies on using LC–MS for analysis of wine have been reported as the

technique is becoming more widely available. Untargeted metabolomics has been performed in wine [29], though we have focused on targeted methods as they are more reproducible and allow for absolute quantification. As with LC-UV, existing targeted LC–MS methods focus on either amines or phenols. Biogenic amine analysis has been limited to fewer than 10 amines while still requiring 20 min for separation [17,28]. Over 40 phenols have been detected in wine using 2D-LC–MS, but analysis time is over 60 min[12]. Our assay covers a combination of 56 amines and phenols with a 20 min gradient. Benzoyl chloride derivatization allows for accurate quantification using easily generated isotopically labeled internal standards, while adding minimal time for sample preparation per sample. Additionally, with the low limits of detection afforded by mass spectrometry and benzoyl chloride derivatization, we were able to detect trace metabolites, such as tryptamine, which are not routinely detected with other methods.4.

2.4.4. Conclusions

Benzoyl chloride derivatization with LC–MS/MS is a powerful technique for determination of amine and phenol metabolites in biological samples. To demonstrate its potential in wine, we have developed a quantitative assay for 56 metabolites in wine. It is likely that the method can be extended to many more amines and phenols in wine (and other foods) as needed for a given application. Combining phenols and amines in one assay is useful because they provide complementary information on the wine. Phenolic acids contribute to the flavor and aroma of wine, and are believed to have positive health benefits as well. High concentrations of biogenic amines are associated with spoilage and poor quality. As a proof of concept, we applied our method to four wines of two varietals and from two locations of production. We identified five metabolites which were significantly different based on varietal, and twenty-four which

were significantly different based on location. A broader, more rigorous study may allow for the distinction of wines by varietal and location of production using the observed metabolite profiles. As previously demonstrated with biological samples, BzCl derivatization with LC–MS/MS is a powerful technique for food analysis. The derivatization process improves sensitivity and quantification, which is well worth the minimal added sample preparation time. Wine was selected for analysis; however, this method could be easily adapted to other beverages or even solid foods following appropriate extraction techniques.

Appendix A. Supplementary data

Supplementary data associated with this article can be found, in the online version, at http://dx.doi.org/10.1016/j.chroma.2017.07.061.

REFERENCES

[1] D.M.A.M. Luykx, S.M. van Ruth, An overview of analytical methods for determining the geographical origin of food products, Food Chem. 107 (2008)897–911, http://dx.doi.org/10.1016/j.foodchem.2007.09.038.

[2] L.M. Reid, C.P. O'Donnell, G. Downey, Recent technological advances for the determination of food authenticity, Trends Food Sci. Technol. 17 (2006)344–353, http://dx.doi.org/10.1016/j.tifs.2006.01.006.

[3] I.S. Arvanitoyannis, M.N. Katsota, E.P. Psarra, E.H. Soufleros, S. Kallithraka, Application of quality control methods for assessing wine authenticity: use of multivariate analysis (chemometrics), Trends Food Sci. Technol. 10 (1999)321–336, http://dx.doi.org/10.1016/S0924-2244(99)00053-9.

[4] D.P. Makris, S. Kallithraka, P. Kefalas, Flavonols in grapes, grape products and wines: burden, profile and influential parameters, J. Food Compos. Anal.

19(2006) 396–404, http://dx.doi.org/10.1016/j.jfca.2005.10.003.

[5] C. Ancín-Azpilicueta, A. González-Marco, N. Jiménez-Moreno, Current knowledge about the presence of amines in wine, Crit. Rev. Food Sci. Nutr. 48(2008) 257–275, http://dx.doi.org/10.1080/10408390701289441.

[6] C. Manach, A. Scalbert, C. Morand, C. Rémésy, L. Jiménez, Polyphenols Food sources and bioavailability, Am. J. Clin. Nutr. 79 (2004) 727–747, http://dx.doi.org/10.1038/nature05488.

[7] A. Scalbert, C. Manach, C. Morand, C. Rémésy, L. Jiménez, Dietary polyphenols and the prevention of diseases, Crit. Rev. Food Sci. Nutr. 45 (2005) 287–306,http://dx.doi.org/10.1080/1040869059096.

[8] A. Bach-Faig, E.M. Berry, D. Lairon, J. Reguant, A. Trichopoulou, S. Dernini, F.X. Medina, M. Battino, R. Belahsen, G. Miranda, L. Serra-Majem, Mediterranean diet pyramid today. Science and cultural updates, Public Health Nutr. 14(2011) 2274–2284, http://dx.doi.org/10.1017/S1368980011002515.

[9] M. Antolovich, P. Prenzler, K. Robards, D. Ryan, Sample preparation in the determination of phenolic compounds in fruits, Analyst 125 (2000)989–1009, http://dx.doi.org/10.1039/b000080i.

[10] P. Dugo, F. Cacciola, M. Herrero, P. Donato, L. Mondello. Use of partially porous column as second dimension in comprehensive two-dimensional system for analysis of polyphenolic antioxidants, J. Sep. Sci. 31 (2008) 3297–3308, http://dx.doi.org/10.1002/jssc.200800281.

[11] P. Dugo, F. Cacciola, P. Donato, D. Airado-Rodríguez, M. Herrero, L. Mondello. Comprehensive two-dimensional liquid chromatography to quantify polyphenols in red wines, J. Chromatogr. A 1216 (2009) 7483–7487, http://dx.doi.org/10.1016/j.chroma.2009.04.001.

[12] P. Donato, F. Rigano, F. Cacciola, M. Schure, S. Farnetti, M. Russo, P. Dugo, L. Mondello. Comprehensive two-dimensional liquid chromatography-tandem mass spectrometry for the simultaneous determination of wine

polyphenols and target contaminants, J. Chromatogr. A 2016 (1458) 54–62, http://dx.doi.org/10.1016/j.chroma.2016.06.042.

[13] R. Romero, M. Sánchez-Vi˜nas, D. Gázquez, M.G. Bagur. Characterization of selected Spanish table wine samples according to their biogenic amine content from liquid chromatographic determination, J. Agric. Food Chem. 50(2002) 4713–4717, http://dx.doi.org/10.1021/jf025514r.

[14] E. Csomós, K. Héberger, L. Simon-Sarkadi. Principal component analysis of biogenic amines and polyphenols in Hungarian wines, J. Agric. Food Chem. 50(2002) 3768–3774, http://dx.doi.org/10.1021/jf011699a.

[15] K. Héberger, E. Csomós, L. Simon-Sarkadi, Principal component and linear discriminant analyses of free amino acids and biogenic amines in Hungarian wines, J. Agric. Food Chem. 51 (2003) 8055–8060, http://dx.doi.org/10.1021/JF034851C.

[16] J. Kiss, A. Sass-Kiss, Protection of originality of tokaji aszú: amines and organic acids in botrytized wines by high-performance liquid chromatography, J.Agric. Food Chem. 53 (2005) 10042–10050, http://dx.doi.org/10.1021/JF050394J.

[17] N. García-Villar, S. Hernández-Cassou, J. Saurina, Determination of biogenic amines in wines by pre-column derivatization and high-performance liquid chromatography coupled to mass spectrometry, J. Chromatogr. A 1216 (2009)6387–6393, http://dx.doi.org/10.1016/j.chroma.2009.07.029.

[18] A. Sass-Kiss, J. Kiss, B. Havadi, N. Adányi, Multivariate statistical analysis of botrytised wines of different origin, Food Chem. 110 (2008) 742–750, http://dx.doi.org/10.1016/j.foodchem.2008.02.059.

[19] S. Bodmer, C. Imark, M. Kneubühl, Biogenic amines in foods: histamine and food processing, Inflamm. Res. 48 (1999) 296–300, http://dx.doi.org/10.1007/s000110050463.

[20] Z. Kerem, B.A. Bravdo, O. Shoseyov, Y. Tugendhaft. Rapid liquid

chromatography-ultraviolet determination of organic acids and phenolic compounds in red wine and must, J. Chromatogr. A 1052 (2004) 211–215,http://dx.doi.org/10.1016/j.chroma.2004.08.105.

[21] V.M. Burin, S.G. Arcari, L.L.F. Costa, M.T. Bordignon-Luiz, Determination of some phenolic compounds in red wine by RP-HPLC: method development and validation, J. Chromatogr. Sci. 49 (2011) 647–651.

[22] Ó. Aznar, A. Checa, R. Oliver, S. Hernández-Cassou, J. Saurina, Determination of polyphenols in wines by liquid chromatography with UV spectrophotometric detection, J. Sep. Sci. 34 (2011) 527–535, http://dx.doi.org/10.1002/jssc.201000816.

[23] S. Gómez-Alonso, I. Hermosín-Gutiérrez, E. García-Romero, Simultaneous HPLC analysis of biogenic amines, amino acids, and ammonium ion as aminoenone derivatives in wine and beer samples, J. Agric. Food Chem. 55(2007) 608–613, http://dx.doi.org/10.1021/jf062820m.

[24] E.H. Soufleros, E. Bouloumpasi, A. Zotou, Z. Loukou, Determination of biogenic amines in Greek wines by HPLC and ultraviolet detection after dansylation and examination of factors affecting their presence and concentration, Food Chem. 101 (2007) 704–716, http://dx.doi.org/10.1016/j.foodchem.2006.02.028.

[25] R. Preti, M.L. Antonelli, R. Bernacchia, G. Vinci, Fast determination of biogenic amines in beverages by a core-shell particle column, Food Chem. 187 (2015)555–562, http://dx.doi.org/10.1016/j.foodchem.2015.04.075.

[26] T. Liu, B. Li, Y. Zhou, J. Chen, H. Tu, HPLC determination of (-aminobutyric acid in Chinese rice wine using pre-column derivatization, J. Inst. Brew. 121 (2015)163–166, http://dx.doi.org/10.1002/jib.196.

[27] Á.M. Alonso Borbalán, L. Zorro, D.A. Guillén, C. Garcı´ıa Barroso, Study of the polyphenol content of red and white grape varieties by liquid chromatography-mass spectrometry and its relationship to antioxidant power, J.

Chromatogr. A 1012 (2003) 31–38, http://dx.doi.org/10.1016/s0021-9673(03)01187-7.

[28] S. Millán, M.C. Sampedro, N. Unceta, M.A. Goicolea, R.J. Barrio, Simple and rapid determination of biogenic amines in wine by liquid chromatography-electrospray ionization ion trap mass spectrometry, Anal. Chim. Acta 584 (2007) 145–152, http://dx.doi.org/10.1016/j.aca.2006.10.042.

[29] M. Arbulu, M.C. Sampedro, A. Gómez-Caballero, M.A. Goicolea, R.J. Barrio, Untargeted metabolomic analysis using liquid chromatography quadrupole time-of-flight mass spectrometry for non-volatile profiling of wines, Anal.Chim. Acta 858 (2015) 32–41, http://dx.doi.org/10.1016/j.aca.2014.12.028.

[30] P. Song, O.S. Mabrouk, N.D. Hershey, R.T. Kennedy, In vivo neurochemical monitoring using benzoyl chloride derivatization and liquid chromatography-mass spectrometry, Anal. Chem. 84 (2012) 412–419.

[31] K. Guo, L. Li, Differential 12C-/13C-isotope dansylation labeling and fast liquid chromatography/mass spectrometry for absolute and relative quantification of the metabolome, Anal. Chem. 81 (2009) 3919–3932, http://dx.doi.org/10.1021/ac900166a.

[32] C.-L. Tseng, L. Li, High-performance isotope-labeling liquid chromatography mass spectrometry for investigating the effect of drinking Goji tea on urine metabolome profiling, Sci. China Chem. 57 (2014) 678–685, http://dx.doi.org/10.1007/s11426-014-5113-z.

[33] D. Achaintre, A. Buleté, C. Cren-Olivé, L. Li, S. Rinaldi, A. Scalbert, Differential isotope labeling of 38 dietary polyphenols and their quantification in urine by liquid chromatography electrospray ionization tandem mass spectrometry, Anal. Chem. 88 (2016) 2637–2644, http://dx.doi.org/10.1021/acs.analchem.5b03609.

[34] Y. Wu, F. Streijger, Y. Wang, G. Lin, S. Christie, J.-M. Mac-Thiong, S.

Parent, C.S. Bailey, S. Paquette, M.C. Boyd, T. Ailon, J. Street, C.G. Fisher, M.F. Dvorak, B.K. Kwon, L. Li, Parallel metabolomic profiling of cerebrospinal fluid and serum for identifying biomarkers of injury severity after acute human spinal cord injury, Sci. Rep. 6 (2016) 38718, http://dx.doi.org/10.1038/srep38718.

[35] E.K. Paleologos, S.D. Chytiri, I.N. Savvaidis, M.G. Kontominas. Determination of biogenic amines as their benzoyl derivatives after cloud point extraction with micellar liquid chromatographic separation, J. Chromatogr. A 1010 (2003)217–224, http://dx.doi.org/10.1016/S0021-9673(03)01068-9.

[36] J. Kirschbaum, K. Rebscher, H. Brückner, Liquid chromatographic determination of biogenic amines in fermented foods after derivatization with 3,5-dinitrobenzoyl chloride, J. Chromatogr. A 881 (2000) 517–530,http://dx.doi.org/10.1016/s0021-9673(00)00257-0.

[37] R. Sethi, S.R. Chava, S. Bashir, M.E. Castro. An improved high performance liquid chromatographic method for identification and quantization of polyamines as benzoylated derivatives, Am. J. Anal. Chem. 2 (2011) 456–469,http://dx.doi.org/10.4236/ajac.2011.24055.

[38] F. Aflaki, V. Ghoulipour, N. Saemian, M. Salahinejad. A simple method for benzoyl chloride derivatization of biogenic amines for high performance liquid chromatography, Anal. Methods. 6 (2014) 1482–1487, http://dx.doi.org/10.1039/c3ay41830h.

[39] J.M.T. Wong, P.A. Malec, O.S. Mabrouk, J. Ro, M. Dus, R.T. Kennedy, Benzoyl chloride derivatization with liquid chromatography-mass spectrometry for targeted metabolomics of neurochemicals in biological samples, J. Chromatogr. A 2016 (1446) 78–90, http://dx.doi.org/10.1016/j.chroma.2016.04.006.

[40] M.-Á. Rodrı´ıguez-Delgado, G. González-Hernández, J.-E. Conde-González, J.-P.Pérez-Trujillo. Principal component analysis of the polyphenol

content in young red wines, Food Chem. 78 (2002) 523–532, http://dx.doi.org/10.1016/S0308-8146(02)00206-6.

CHAPTER III
Building of a Linear Retention Index System in Liquid Chromatography

3.1. Proposal of a linear retention index system for improving identification reliability of triacylglycerol profiles in lipid samples by liquid chromatography methods

3.1.1. Introduction

The retention index system was proposed by Kováts [1] in 1958 with the aim to generate a uniform and universal scale describing the retention behaviour of a complete set of analytes. Prior to the introduction of such a system the relative retention time (expressed as ratio of the retention time of the analyte and that of a standard compound) was used as the main identification parameter; the basic shortcoming was the impossibility to fix a single standard for a great number of analytes, characterized by a wide range of physical-chemical properties. As a consequence, a change in the analytical conditions resulted in a significant variation of the relative retention time, since each analyte was differently affected by this change. On the other hand, Kováts suggested the use of a homologues series of standard compounds to fix the retention behaviour of the analytes relatively to the standards that elute in the same region of the chromatogram. The selected homologue series was the normal alkane one and the equation employed for retention index (*I*) calculation was the following [1]:

$$I = 100\left[z + \frac{\log t_{Ri} - \log t_{Rz}}{\log t_{R(z+1)} - \log t_{Rz}} \right] \qquad \text{Eq. 1}$$

where *z* and *z+1* are the carbon number of the alkane eluted immediately before and after the analyte (*i)* respectively, and t_R is the retention time of the analyte. This system made retention data dependent on the chromatographic phenomenon only, *viz.* on the three term interaction analyte-stationary phase-mobile phase, and as independent as possible from the operating conditions. Particularly in GC, because the mobile phase has a negligible influence, the retention of the analytes depends almost entirely on the stationary phase. The immediate derivation of Eq. 1 was that the retention index of *n*-alkanes is 100 times their carbon number, while a logarithmic relationship between *I* and the t_R of the analyte is kept under isothermal conditions. In 1963 van Den Dool and Kratz extended the applicability of retention indices to temperature-programmed GC analyses utilizing retention times instead of their logarithm, thus defining the linear retention index (LRI) as follows [2]:

$$LRI = 100\left[z + \frac{t_{Ri} - t_{Rz}}{t_{R(z+1)} - t_{Rz}} \right] \qquad \text{Eq. 2}$$

The advantages of the use of the *n*-alkane series are its easy, cheap and highly pure availability and its regular chromatographic profile under different analytical conditions. Moreover, one essential feature of the reference standard mixture is that its elution behaviour should change in a similar way to that of the analytes of interest. Other retention index systems have been described in the literature, which differ from the Kováts system in the selection of the standard compounds. Among them, the methyl esters of saturated even carbon number fatty acids (FAs), introduced almost simultaneously by Woodford and Gent [3] and Miwa *et al.* [4], were commonly employed for the characterization of FA samples. In this case, since only even carbon number FAs are employed, Eq. 2 needs to be adapted according to the following equation:

$$LRI = 100\left[z + 2\frac{t_{Ri} - t_{Rz}}{t_{R(z+2)} - t_{Rz}} \right] \qquad \text{Eq. 3.}$$

Within this context a generalization for LRI calculation can be performed according to Eq. 4:

$$LRI = 100\left[z + n\frac{t_{Ri} - t_{Rz}}{t_{R(z+n)} - t_{Rz}} \right] \qquad \text{Eq. 4}$$

where *z* is an arbitrary number associated to the reference compound eluted immediately before the analyte and *n* is the *z* unit difference of the reference compounds eluting immediately before and after the analyte.

In GC, the combination and complementarity of LRI and MS data, normally obtained by electron ionization (EI) MS sources, lead to an unequivocal identification, given the high reproducibility of both parameters [5-8]. Furthermore, the availability of commercial databases containing thousands of EI-MS spectra allows for a very fast and automatic identification process by means of commercially available software: compounds with a high spectra matching but with a LRI value falling out from a selected range are automatically excluded from the list of possible candidates.

Many attempts were done over the past years to establish an LRI system in LC, where qualitative analyses are much less robust and reliable than GC ones, since both the retention time and MS data reproducibility and the level of information arising from typical LC-MS interfaces are quite poorer [9,10]. A consistent literature refers about the employment of retention indices in LC during the decades ’80s-90s, sometimes combined with UV spectral information, mainly for the identification of drugs in toxicology studies. The first proposal by Baker and Ma in 1979 regarded the use of an alkan-2-one series, from acetone to 2-tricosanone, as homologue series and, since isocratic conditions were applied for the analyses, Eq. 1 was employed for *I* calculation

[11]. Three years later, Smith suggested the alkyl aryl ketones series, from acetophenone to heptanophenone, as the basis of the retention index scale, because of its higher UV absorption [12]. The influence of the stationary phase chemistry and packaging, as well as the mobile phase composition, was evaluated in these and later works [11-15] allowing to conclude that a standardization of the LC conditions is necessary to create a usable database [16]. From the end of ’80s to the beginning of the past decades, the standardization of LC methods and retention parameters centered the interest of other research groups; among them Bogusz *et al.* described the use of 1-nitroalkanes, from nitromethane to 1-nitrooctane, for retention index calculation, since, with respect to the alkyl aryl ketones series, has a better coverage of the chromatographic space under common reversed phase (RP) conditions [17-19]. Bogusz developed a general LC method for toxicology screening and, since a gradient elution was employed, he used Eq. 2 for LRI calculation. Nevertheless, nitroalkanes are not easily affordable neither highly stable at high pH [20]. The limitations encountered by the use of each homologue series, the low reproducibility experimented by any change of the analytical parameters and differences in instrumentation or even in column packaging hampered the widespread use of LRI databases at both intra- and interlaboratory levels [16,21].

The aim of this work was to reconsider the LRI system as a valuable identification tool in LC by exploiting the higher batch-to-batch reproducibility in LC instrumentation and columns achieved in the last decades. In particular, lipid species, namely triacylglycerols (TGs), were selected as target analytes, because of their extreme complexity [22], biological importance [23], very regular chromatographic RP-LC profile [24,25] and since they have never been considered before in similar studies.Within this context, one of the object of the present research was the development of an ultra high performance LC

(UHPLC) method, able to maximize the baseline separation of TG compounds in different real-world samples, ranging from very simple vegetable oil to much more complex fish oils, milk and milk-derived samples.

3.1.2. Experimental

3.1.2.1. Reagents and Materials

Acetonitrile, 2-propanol and water (HPLC grade and LC-MS grade), chloroform and methanol (reagent grade) and sodium sulphate were purchased fromMillipore Sigma (Milan, Italy), ammonium formate was obtained from Alfa Aesar GmbH & Co KG (Karlsruhe, Germany). Standard of trinonanoin ($C_9C_9C_9$), triundecanoin ($C_{11}C_{11}C_{11}$), tritridecanoin ($C_{13}C_{13}C_{13}$), tripentadecanoin ($C_{15}C_{15}C_{15}$), triheptadecanoin ($C_{17}C_{17}C_{17}$), trinonadecanoin ($C_{19}C_{19}C_{19}$) were purchased from MilliporeSigma. A standard mixture of the six compounds was prepared at a concentration of 1000 mg/L.

3.1.2.2. Samples and sample preparation

A total of 14 vegetable oils (peanut, corn, soybean, rapeseed, grapeseed, almond, hazelnut, sunflower, linseed, chia, sacha inchi, borage, castor, olive), 6 fish oils (menhaden, cod liver, sea bream, tuna fish, fish integrator, shrimps) and 5 milk and milk derived samples (goat, cow, whole biological milk, buffalo mozzarella, butter) were injected in the system. Vegetable oil samples were prepared by dissolving 10 mg of oil in 10 mL of 2-propanol, except for borage oil for which 10 mg were dissolved in 1 mL of the same solvent. Similarly menhaden oil, cod liver oil, fish integrator and butter were prepared at a concentration of 10 mg/mL. The other milk and fish samples underwent lipid extraction by Folch [26] and Bligh&Dyer [27] procedure, respectively, prior to injection at a concentration of 10 mg/mL. Briefly 10 mL of milk were treated with 40 mL of a chloroform: methanol mixture (1:2 *v/v*) and placed in an ice

bath under magnetic stirring for 30 minutes; the content was transferred to a separating funnel and shaken vigorously for 5 minutes; after, the mixture was collected into different tubes and centrifugated at 3000 rpm for 15 minutes. Once obtained the separation of phases, the phases below (containing the lipid fraction) were pooled together, the upper phases (aqueous) were added again to the separating funnel for a further extractions with 20 mL of chloroform: methanol mixture (2:1 *v:v*). The last step was replicated once again. The pooled organic phases were filtered on anhydrous sodium sulphate and evaporated using a rotary evaporator.

With regard to the Bligh&Dyer extraction, 10 g of fish tissue were weighed and reduced to small pieces. The sample was extracted with 30 mL of a mixture chloroform: methanol (1:2 *v:v*) and homogenized by using an Ultra Turrax apparatus for 10 min. Then, 10 mL of chloroform and 18 mL of distilled water were added and re-homogenized for 1 min; the mixture was collected into different tubes and centrifugated at 3000 rpm for 15 min. The lower organic phases were pooled, while the aqueous upper phases were extracted again with 20 mL 10% (*v/v*) methanol in chloroform.

Then, all the organic phases were pooled together, filtered on anhydrous sodium sulphate and evaporated using a rotary evaporator.

3.1.2.3. UHPLC-ELSD instrumentation and analytical conditions

Analyses were carried out by using a Nexera X2 system (Shimadzu, Kyoto, Japan), consisting of a CBM-20A controller, two LC-30AD dual-plunger parallel-flow pumps (120.0 MPa maximum pressure), a DGU-20A_5R degasser, a CTO-20AC column oven, a SIL-30AC autosampler, and a SPD-M30A PDA detector (1.8 μL detector flow cell volume). The UHPLC system was coupled to an ELSD (Evaporative Light Scattering Detector) detector (Shimadzu).

Separations were carried out on two serially coupled Titan C18 100 × 2.1 mm (L × ID), 1.9 μm *d.p.* columns (MilliporeSigma, Bellefonte, PA, USA). Mobile phases were (A) acetonitrile and (B) 2-propanol under gradient conditions: 0-105 min, 0-50% B (held for 20 min). The flow rate was set at 400 μL/min with oven temperature of 35 °C; injection volume was 5 μL. The following ELSD parameters were applied: evaporative temperature 60° C, nebulizing gas (N_2) pressure 270 KPa, detector gain <1 mV; sampling frequency: 10 Hz.

3.1.2.4. HPLC-ESI-MS instrumentation and analytical conditions

Analyses were carried out by using an Waters Alliance HPLC 2695 separation module consisting of a quaternary pump, autosampler and column thermostat, coupled to a Micromass Quattro micro API bench-top triple quadrupole mass spectrometer (Waters Associates Inc, Milford, MA, USA).

Separations were carried out on an Ascentis Express C18 100 × 2.1 mm (L × ID), 2.0 μm *d.p.* column (MilliporeSigma). Mobile phases were (A) acetonitrile: 10 mM aqueous ammonium formate 95:5 (*v:v*) and (B) 2-propanol under gradient conditions: 0-52.5 min, 0-55% B (held for 17.5 min). The flow rate was set at 400 μL/min with oven temperature of 35 °C; injection volume was 2 μL. MS acquisitions were performed using the Z-spray electrospray (ESI) source operating in positive ionization modes, under the following conditions: mass spectral range, 250-1250 *m/z*; event time, 1 s; desolvation gas (N_2) flow, 700.0 L hr^{-1}; no cone gas was applied; source temperature, 150 °C; desolvation temperature, 250 °C; capillary voltage, 3 KV; cone voltage, 80 V; extractor voltage, 3 V; RF lens, 0.2 V.

3.1.2.5. LRI calculation and data analysis

LRI were calculated according to Eq. 4, by using the odd carbon number TGs as reference homologue series from $C_9C_9C_9$ to $C_{19}C_{19}C_{19}$ and by assigning to *z* a value equal to the partition number (PN) of each TG, that is related to the carbon chain length (CN) and double bond number (DB): PN=CN-2DB [28]; therefore *z* is 27 for $C_9C_9C_9$, up to 57 for $C_{19}C_{19}C_{19}$, and *n* is equal to 6. The LRI database was built by using the Cromatoplus Spectra software (Chromaleont, Messina, Italy), that was also able to extrapolate LRI values for TGs eluted earlier than C9C9C9. Then analyses were processed by using the Cromatoplus Spectra software, which allowed to directly match the LRI automatically calculated for each peak with the LRI database previously created.

3.1.3. Results and Discussion

TG profiling is commonly investigated by considering in a complementary way the GC profiles of fatty acid methyl esters (FAMEs) and LC profiles of intact TGs. In such a way the identification of non-univocal lipid species can be driven by the FA composition; in other words isobars (identical MS spectra) can be distinguished by considering the relative abundance of FAs, which are combined in TGs [29-32]. Furthermore, for very simple samples, MS information could be not essential, being known FA composition and considering the typical elution profile of TGs under RP-LC. In fact, in RP-LC TGs are eluted according to the increasing PN, then a preliminary identification could be performed on the basis of the retention behavior. Nevertheless by considering very complex samples such as fish oils or milk, many exceptions from this rule can be observed for lipids containing the combination of highly polyunsaturated and short chain saturated FAs, which can be retained more weakly and elute in lower PN groups [33].

To this regard the LRI value associated to each TG could represent a reliable identification parameter, even more relevant if the total lack of LC-MS databases is considered. In fact, the embedding of the MS spectra in a single library is hampered by their non-repeatable nature and therefore the complementarity of LRI and MS data typical of the GC-MS systems, cannot be attained in LC, thus demonstrating the significance of such a work in providing an LRI database to be exploited in the identification process.

3.1.3.1. Chromatographic method development

The selection of proper chromatographic conditions was carried out aiming to develop a "universal" method able to provide maximum resolution for a large sphere of lipid samples. The choice of analytical parameters was driven by taking into account the high complexity of specific samples, *viz.* fish oils and milk. Starting from literature information, which report TG separation under RP-UHPLC conditions by multi-column set-up [31,34-37], two monodisperse sub-2μm columns (100×2.1 mm, L×ID) were serially coupled and operated at the optimal flow rate (400 μL/min, reference compound, byphenyl; k′, 9.7; N, ~ 43000; H, 4.6 μm) at a backpressure of 100 MPa, approaching the maximum potentialities of the UHPLC system employed (120 MPa).

However, the gradient program was carefully evaluated in order to compromise between chromatographic resolution and analysis time. Figure 1 (III-3.1) reports the main steps performed to enhance the separation for the most complex available samples, *viz.* a fish oil (cod liver oil) and a milk-related sample (butter); the identified PN region are highlighted in order to make evident the improvements and support the discussion. The final percentage of the stronger solvent (2-propanol) was the first delicate issue due to the high viscosity of such a solvent. For the same reason, the oven temperature represented a sensitive parameter in order to modulate solvent viscosity and

decrease system backpressure. The isocratic analysis at 40% solvent B (Figure 1A (III-3.1)) for cod liver oil showed that such a percentage was sufficient to completely elute all the TGs; therefore, 50% B was chosen as final B percentage to prevent any carry over in the following runs. Despite previous work demonstrated that room temperature (25-30° C) is an optimal condition to maximize TG separation [25,38-40], 35° C temperature needed to be applied to avoid overpressure issues. While almost no differences were evidenced between analyses obtained at 30 and 35° C, the separation of several critical pairs was impaired at 40° C (data not shown). Therefore, 35° C was set for the following test of the gradient mode. The first gradient program was 0-5 min, 20% B, 75 min to 50% B, achieving a good focusing at the head of the column by the initial isocratic step. The main problem of this program was the poor resolution at the low PN region (from 30 to 36) and the presence of several co-elutions in the richest PN region, namely PN 42 (Figure 1B (III-3.1)). The next step consisted in the decreasing of the initial B concentration, as follows: 0-30 min, 0-25% B, 30-105 min to 50% B. A clear separation between 30, 32 and 34 PN regions was achieved, as well as a major chromatographic resolution in each PN region (Figure 1C (III-3.1)). This two-step gradient was tried on the butter sample, leading to an unsatisfactory result, because of the presence of some co-elutions and the large peak width obtained (Figure 1D (III-3.1)). A linear gradient 0-50% B in 105 min, which resulted in a deceleration in the first step and an acceleration in the second one, was then tested on the butter sample, allowing to greatly improve the resolution and peak shape, by showing more uniform and narrower peak widths (Figure 1E (III-3.1)). Such a gradient was finally employed for the profiling of all the 25 samples.

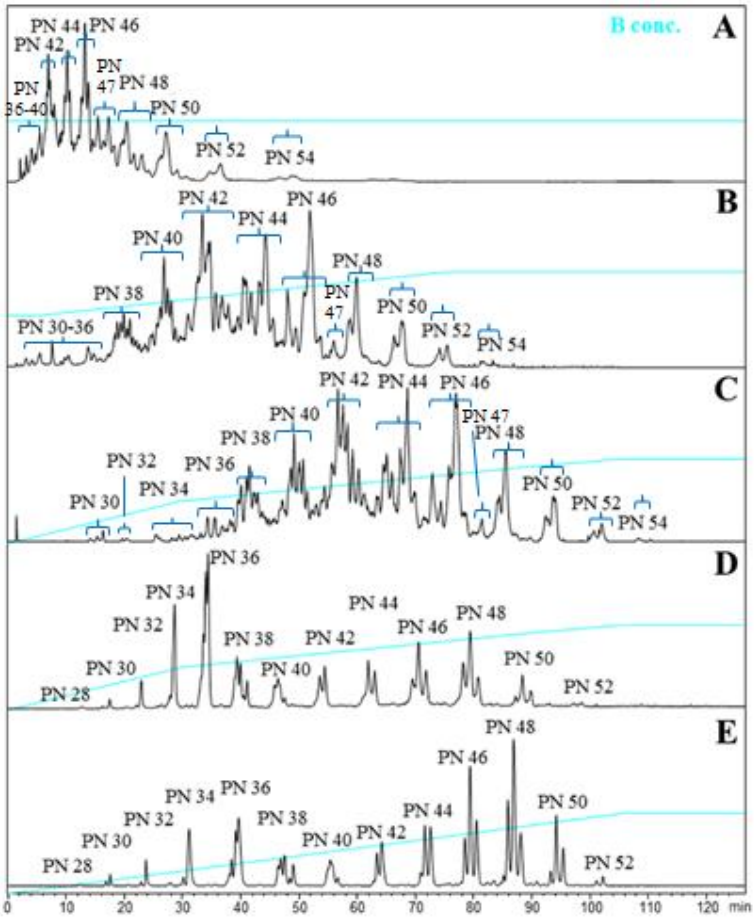

Figure 1 (III-3.1). UHPLC-ELSD method development steps: A) chromatogram of cod liver oil under isocratic conditions (40% solvent B); B) chromatogram of cod liver oil under 70 min linear gradient (20-50% B) with 5 min isocratic step (20% solvent B); C) chromatogram of cod liver oil under multi-step gradient elution (0-25% B in 30 min and 25-50% B in 75 min); D) chromatogram of butter sample under multi-step gradient elution (0-25% B in 30 min and 25-50% B in 75 min); E) chromatogram of butter sample under 105 min linear gradient (0-50% B).

For a practical estimation of the performance of the developed method, peak capacity was evaluated, by using the well-known approach by Neue [41], and

compared with previous methods [36,37]. Beccaria *et al.* dealt with the use of three serially coupled partially porous 150 × 4.6 mm (L × I.D.) columns, achieving a peak capacity of 170 at the expenses of 168 min analysis time (almost 1 peak *per* minute) [37]. In this work the use of two narrow-bore (2.1 mm I.D.) monodisperse sub-2μm columns allowed to obtain a peak capacity value of 162 in a considerably reduced analytical run (125 min, leading to detect 1.3 peak per minute). Dugo *et al.* reported the employment of four serially coupled partially porous 150 × 4.6 mm (L × I.D.) for menhaden oil separation, obtaining a peak capacity of 210 in 220 min (less than 1 peak per minute) [36]. Hence, the novel UHPLC method can represent an optimal compromise between chromatographic efficiency and analysis time; moreover the use of narrow-bore columns (2.1 mm I.D. *vs* 4.6 mm I.D. typically used in the previous works), operated at smaller flow rate (0.4 mL/min *vs* 1 mL/min or higher) allowed a more straightforward coupling with MS detectors, in addition to a significant solvent saving.

3.1.3.2. LRI database

The first step for LRI calculation was to find an adequate reference standard mixture that covered all the analysis time and shows a regular elution profile under the selected experimental conditions. The odd carbon number TG mixture from $C_9C_9C_9$ to $C_{19}C_{19}C_{19}$ was chosen since it occupies almost all the chromatogram, from 9 to 120 min with a homogenous distribution, as shown in Figure 2D (III-3.1).

The chromatograms of borage oil (the most complex vegetable oil injected), menhaden oil and goat milk are reported in in parts A, B, and C of Figure 2 (III-3.1), respectively, in direct comparison with the reference homologue series chromatogram Figure 2D (III-3.1); an immediate identification according to PN

is shown, in order to highlight the intersample repeatability in terms of retention time of each PN region, in spite of totally different elution profiles.

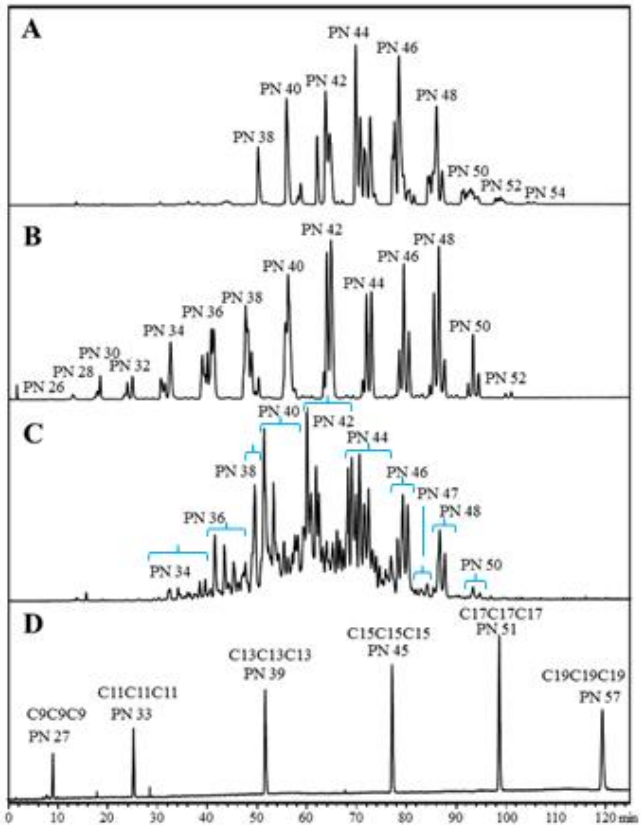

Figure 2 (III-3.1). UHPLC-ELSD selected chromatograms acquired by using the final developed method: A) borage oil; B) goat milk; C) menhaden oil; D) reference homologue series.

Supplementary Table 1S (III-3.1.) contains the list of all the tentatively identified TGs, ordered according to their elution time, along with their PN and calculated LRI reported as confidence interval around the intersample average. A total of 209 TGs are reported, identified according to their retention behaviour and literature data. Among them, 54 TGs representative of vegetable oils were confirmed by HPLC-ESI-MS analyses and are reported in Table 1

(III-3.1.) which represents an extract of the full LRI database reported in Supplementary Table 1S (III-3.1.); UHPLC-ESI-MS analyses will be necessary to confirm identification for fish and milk samples.

The absolute experimental maximum difference from the average is also reported and will be considered for the database search (ΔLRI). The confidence interval was estimated at the 95% confidence level using a normal probability distribution, assuming that the uncertainty of the method is equal to the average of all the standard deviations obtained for each LRI value. Such assumption derives from the fact that the standard deviation distribution can be approximated to a Pearson chi-square (χ^2) function. Therefore it is not related to the measured variable but only to its degrees of freedom, which correspond to the dimension or population of the same variable. In this specific situation the **population (p)** of the LRI value corresponds to the number of samples (each in duplicate since two analyses were performed for each sample) containing the specific TG and it is indicated in bracket in Table 1 (III-3.1.) and Supplementary Table 1S (III-3.1.).

Table 1 (III-3.1.). List of 54 identified TGs, along with their PN, LRI and ΔLRI value.

PN	Compound Name	LRI*	ΔLRI	PN	Compound Name	LRI*	ΔLRI	PN	Compound Name	LRI*	ΔLRI
36	LnLnLn (p=6)	3668±4	5	44	LLO(p=50)	4342±1	10	48	OOO (p=44)	4729±1	14
36	γLnγLnγLn (p=2)	3747±6	1	44	LLP(p=24)	4358±2	7	48	GLP (p=2)	4740±6	4
38	LnLLn (p=8)	3830±3	3	44	OOLn (p=14)	4360±6	11	48	POO (p=44)	4756±2	13
38	γLnLγLn (p=2)	3867±6	1	44	OOγLn (p=2)	4364±6	3	48	POP (p=26)	4776±2	14
38	PoγLnγLn(p=2)	3915±6	3	44	POLn (p=4)	4383±4	8	50	$C_{24:1}$LL (p=2)	4881±6	10
40	LLLn (p=10)	3993±3	6	44	PLnP (p=2)	4395±6	3	50	$C_{22:1}$LO (p=2)	4890±6	4
40	LLγLn (p=2)	3999±6	2	44	PγLnP (p=2)	4431±6	3	50	GOO(p=2)	4905±6	7
40	LnLnO (p=6)	4011±4	5	46	GLL (p=2)	4502±6	10	50	GOP(p=2)	4921±6	8
40	LnPLn (p=6)	4023±4	5	46	OOL (p=42)	4516±1	12	50	SLS (p=2)	4940±6	4
40	γLnγLnO (p=2)	4052±6	2	46	PLO (p=46)	4539±1	13	50	SOO (p=34)	4948±2	14
40	γLnPγLn (p=2)	4064±6	2	46	SLL (p=8)	4548±3	9	50	SOP (p=28)	4961±3	15
42	LLL (p=24)	4160±6	10	46	SOLn (p=6)	4563±4	7	50	SPP (p=12)	4978±3	8
42	γLnLO (p=2)	4181±6	2	46	PLP (p=24)	4571±2	14	52	$C_{22:1}$γLnC22:1 (p=2)	5069±6	4
42	LnLO (p=8)	4192±3	11	46	SOγLn (p=2)	4599±6	4	52	$C_{24:1}$OL (p=2)	5084±6	12
42	SLnLn (p=6)	4216±4	4	46	SγLnP (p=2)	4631±6	4	52	$C_{22:1}$OO (p=2)	5091±6	4
42	LnLP (p=6)	4217±6	3	48	$C_{22:1}$LL (p=2)	4690±6	4	52	SOS (p=20)	5103±2	15
42	γLnLP (p=2)	4221±6	2	48	OLG (p=2)	4703±6	4	54	$C_{22:1}$OG (p=2)	5238±6	5
42	SγLnγLn (p=2)	4221±6	2	48	$C_{24:1}$LγLn (p=2)	4723±6	9	54	$C_{22:1}$OS (p=2)	5271±6	5

* Intersample average; p: population; fatty acid abbreviations: P = palmitic acid, Ln = linolenic acid, L = linoleic acid, O = oleic acid, S = stearic acid, G = gadoleic acid, $C_{22:1}$ = erucic acid, $C_{24:1}$ = nervonic acid.

The length of the confidence interval was ≤ 12 units for all the compounds; as a consequence, a difference between subsequent TGs higher than 12 LRI units avoids any peak mismatching. Within this context the chromatographic resolution acquires special importance; it is strongly related to the so-called separation number (SN), that expresses the number of peaks which can be resolved between two consecutive TGs of the homologue series (z and z+6, respectively) [42]:

$$SN = \frac{t_{R(z+6)} - t_{Rz}}{w_{h(z+6)} + w_{hz}} - 1 \qquad \text{Eq. 5}$$

wherein, $t_{R(z+6)}$ and t_{Rz} are the retention times of two consecutive TGs of the homologue series and $w_{h(z+6)}$ and w_{hz} are the corresponding peak width at half height.

By considering Eq. 5 for z=39 (arbitarily chosen since a great number of TGs are contained in this region), SN is equal to 25 that means that 25 peaks can be satisfactorily resolved between $C_{13}C_{13}C_{13}$ and $C_{15}C_{15}C_{15}$ standard compounds;

as a consequence, the minimum retention index difference between two adjacent peaks must be δ=600/(SN+1), equal in the present situation to 23, which largely overcomes the obtained confidence interval length above described. In order to achieve accurate library search results the experimental LRI interval length (ΔLRI*2) must be also minor than δ value. For instance, within the 3900-4500 LRI region, for which δ is equal to 23, ΔLRI should not exceed a value of 11.5, that means that a larger variation will cause an overlapping between adjacent peaks. SN and δ calculations were carried out for all subsequent reference compound peaks, finding that for each region δ was found to be equal or even higher than the experimental LRI interval length. In particular, a total SN of 122 and an average δ of 30 units were obtained, meaning that ΔLRI values minor than 15 normally ensure a reliable identification.

A similar consideration can arise taking into account the average peak width of the analytes. In fact, being w_b = 0.8 min (48 s) and 1 LRI = 25 min/600 = 0.042 min (2.52 s), where 25 min is the difference time between $C_{13}C_{13}C_{13}$ and $C_{15}C_{15}C_{15}$ retention times, the LRI variability of ± 15 units corresponding to 0.63 min (37.8 s) results minor than w_b. Such a result indicates that each LRI corresponds only to the TG which occupies a specific position in the chromatogram in terms of retention time, pinpointing the reliability of a potential identification based only on the LRI concept.

It is noteworthy to mention that, based on the PN or equivalent carbon number (ECN) concept, serveral works deal with the prediction of relative t_R by using different empirical equations, taking into account the unsaturation degree, as well as factors related to the presence of other functional group [24,43-44]. Nevertheless, none of this methods lead to an automatic identification of TGs,

neither to the creation of a rich and reliable database, where species are confirmed by MS analyses.

3.1.3.3. LRI repeatability

In order to assess the LRI stability under a wide range of experimental conditions, a systematic study which involved all the analytical parameters playing a role in the chromatographic separation was accurately performed. Specifically, the influence of column dimension and stationary phase packing, flow rate, oven temperature, gradient and mobile phase composition was considered, by injecting three vegetable oils (borage, linseed and olive oils) containing a total of 54 TGs. Regarding the columns, three different technologies, all widely employed in the lipidomics field, were compared: monodisperse sub-2 μm (particle size 1.9 μm), partially porous (particle size 2.7 and 2.0 μm) and totally porous (particle size 3 μm) particles. All column dimensions were 100 × 2.1 mm, L × ID, operated at 400 μL/min, apart from one analytical columns of 4.6 mm ID, operated at 1.8 mL/min and used to evaluate the ID effect; the stationary phase bed length was changed by considering two serially coupled columns. The obtained results are reported in Supplementary Table 2S (III-3.1.), which contains the list of TGs along with their PN and LRI value on each column. The intersample average and ΔLRI are also provided. Since the LRI values on the totally porous column were totally different from the others, these values were placed in the last column of the table and discarded from the average. Such a difference was probably due to a different retention behaviour mediated by larger totally porous particles (particle size >> 2 μm) . Within this context, several studies report the evidence of similar kinetic and thermodynamic performances provided by sub-3 μm partially porous and sub-2 μm totally porous particles, pointing out comparable

loading capacity, retention factors and chromatographic efficiency [45,46]. In particular partially porous, as well as sub-2 μm, stationary phases allow very fast separation by reducing retention factors with respect to totally porous packed columns. Specifically, thermodynamic retention factor must be calculated taking into account only the volume of the active shell, excluding the solid core. On the other hand, from a kinetic point of view, due to the shallow pores in the thin active adsorbent layer, mass transfer phenomena are speeded up and the diffusion into the surface layer is reduced, thus significantly increasing chromatographic efficiency.

Other scientific contributions highlighted the higher performances of partially porous particles on totally porous packed material, specifically estimating the different contributions of all the Van Deemter terms on the column efficiency [47,48].

For all these reason and because of the experimental evidence of different LRI values obtained on the totally porous stationary phase, it is possible to assert that the analyte-stationary phase interaction is different between partially and totally porous columns, due to both thermodynamic and kinetic factors.

The partially porous 100 × 2.1 mm, L × ID, 2.0 μm *d.p.*, was selected for the evaluation of the effect of the other parameters.

Supplementary Tables 3S and 4S (III-3.1.) show the LRI values calculated at different flow rates and gradient steepness (the experimental conditions are reported in detail in the table captions), respectively, along with their average and ΔLRI, highlighting in both cases a perfect agreement between all the conditions.

The influence of column temperature (Supplementary Tables 5S (III-3.1.)) was more critical. Four temperatures were evaluated, in the range 30-50° C, leading to the conclusion that a variation of 10° C can significantly affect the LRI value, while 5° C difference could not have a strong influence. For this reason,

both the total average and the average between 30 and 35° C and 35 and 40° C are reported, along with their ΔLRI values. The LRI variability observed under different temperatures is probably related to the strict relationship between temperature and thermodynamic parameters that affect the retention behaviour.

As expected, the condition under which the LRI value is totally not repeatable was represented by the mobile phase composition, pointing out how even small variations of the mobile phase composition significantly change all LRI values (data not shown).

In conclusion, it is possible to assess that the LRI database can be used under different experimental conditions provided that the thermodynamic factors, mainly expressed by the partition coefficient, are not considerably altered. Therefore, column dimensions, flow rates and gradient steepness have almost no influence on LRIs, while mobile phase and column temperature need to be fixed to successfully use the LRI identification system.

Such a conclusion opens up new prospects for the use of LRI in LC, since, with respect to previous attempts [16-21], researchers can be now aware of which experimental conditions need to be standardized. On the other hand, thanks to the improvement in column packaging technology and instrumentation, it is now possible to obtain the same LRI by changing instrument (see next section), column lot or even analytical laboratory.

3.1.3.4. HPLC-ESI-MS analyses

The LRI value, by itself, is not an unambiguous system of identification because different compounds might have the same LRI if they are completely co-eluted. However, it is not probable that they present also the same mass spectrum. To this purpose, HPLC-ESI-MS analyses of borage, linseed and olive oils were carried out, providing the confirmation of the preliminary identification by UHPLC-ELSD method for 54 TGs common in vegetable oils.

Under the employed ESI-MS conditions, a highly informative fragmentation pattern was obtained. In particular, mono- and diacylglycerol (MG and DG, respectively) fragments were highlighted, so that each MG fragment correspond only to one fatty acid and each DG fragment is related to their combination. The molecule related ion (in this case the sodium adduct) represents the final confirmation of the right fatty acid combination in the TAG species and it is very helpful especially in the presence of co-elutions.

A comparison between the LRI values calculated on different instrumentation set-up, namely UHPLC-ELSD and HPLC-ESI-MS, was mandatory to verify the proper functioning of the LRI library search, *viz.* the use of the LRI database for achieving a reliable identification. Table 2 (III-3.1.) contains the comparison for the most abundant TGs identified in the three oils, along with the average and ΔLRI values, while Supplementary Figure 1S (III-3.1.) reports in a histogram the average values, each with the corresponding ΔLRI.

Table 2 (III-3.1.). Average LRI, ΔLRI and LRI values calculated by UHPLC-ELSD and HPLC-ESI-MS.

TG	LRI		LRI average	ΔLRI
	UHPLC-ELSD	HPLC-ESI-MS		
LnLnLn	3712	3709	3711	2
LnLLn	3859	3853	3856	3
γLnLγLn	3902	3884	3893	9
LLLn	4018	4017	4018	1
LLγLn	4040	4025	4033	8
LnLnO	4030	4036	4033	3
LnPLn	4057	4046	4052	6
γLnγLnO	4092	4077	4085	8
γLnPγLn	4111	4091	4101	10
LLL	4179	4169	4174	5
LnLO	4202	4190	4196	6
LLO	4352	4343	4348	5
LLP	4373	4363	4368	5
OOLn	4375	4372	4374	2
OOγLn	4397	4377	4387	10
PγLnP	4443	4419	4431	12
OOL	4524	4514	4519	5
PLO	4555	4538	4547	9
SOLn	4584	4575	4580	5
SOγLn	4609	4594	4602	8
$C_{22:1}$LL	4709	4704	4707	3
OOO	4732	4716	4724	8
POO	4764	4740	4752	12
POP	4782	4769	4776	7
SOO	4941	4940	4941	1
SOP	4959	4968	4964	5
$C_{22:1}$OO	5102	5072	5087	15
$C_{22:1}$OG	5239	5245	5242	3
$C_{22:1}$OS	5267	5280	5274	7

For fatty acid legend see Table 1 (III-3.1.).

Supplementary Figure 1S (III-3.1.) aims also to pinpoint the reliability of the new identification approach based only on the LRI values, since for the majority of the TGs no LRI superimposition occurs, thus avoiding ambiguous identification. Only for a few compounds, such as dilinoleyl-palmitoyl-glycerol (LLP) and dioleyl-linolenyl-glycerol (OOLn), the research in the LRI database can generate a list of several candidates. In this cases, the selection of the right candidate can be driven by the observed MS fragmentation pattern of each species. Figure 3 (III-3.1.) shows ESI-MS spectra of LLP (Figure 3A (III-3.1.)) and OOLn (Figure 3B (III-3.1.)) species, chromatographically co-eluted, along with fragment elucidation. Under the LC conditions described in the

experimental section, each TG showed a fragmentation profile characterized by the sodium adduct of the molecular species, diacylglycerol and monoacylglycerol fragments, leading to an unequivocal identification.

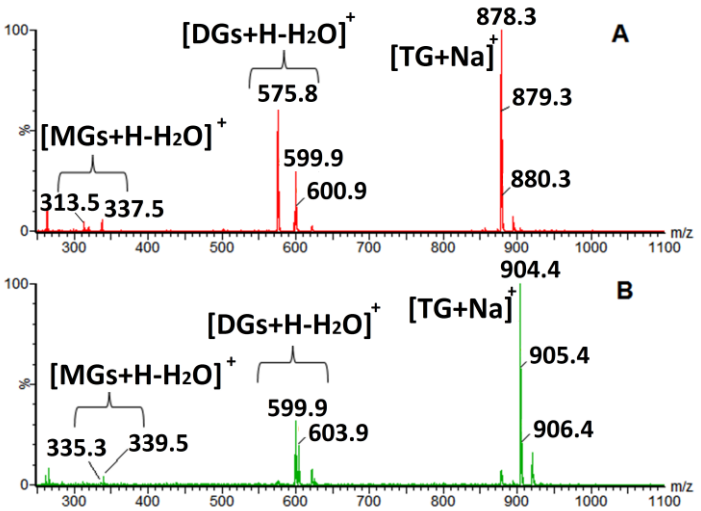

Figure 3 (III-3.1.). ESI-MS spectrum of A) LLP and B) OOLn, with fragment elucidation. $[MGs+H-H_2O]^+$: protonated monoacylglycerols which lost a water neutral molecule; $[DGs+H-H_2O]^+$: protonated diacylglycerols which lost a water neutral molecule; $[TG+Na]^+$: sodium adduct of triacylglycerol.

3.1.4. Conclusions

A total of 25 lipid samples were analyzed by the same chromatographic method and identified according to literature data, retention behaviour and MS spectra.

An LRI database, containing 209 TG species, was created. Further efforts will be required to extend it by including other lipid species, such as fatty acids, mono- and diacylglycerols, as well as sterols, for achieving a holistic lipid profile of different real-world samples.

LRI repeatability studies were carried out in order to assess the robustness of the novel identification approach and make the database usable at both intra- and interlaboratory levels.

Advancements in software able to perform an automatic identification on the basis of both LRI and MS data will be essential to perform a significant step forward in the field of identification reliability in LC. In particular, since MS spectra are strongly dependent from the ambient, sample and LC conditions, the software could consider only the MS fragment values rather than its relative intensity.

REFERENCES

[1] Kovats, E. Helv. Chim. Acta 1958, 41, 1915−1932.

[2] van Den Dool, H.; Kratz, P. D. J. Chromatogr. 1963, 11, 463−471.

[3] Woodford, F. P.; van Gent, C. M. J. Lipid Res. 1960, 1, 188−190.

[4] Miwa, T. K.; Mikolajczak, K. L.; Earle, F. R.; Wolff, I. A. Anal. Chem. 1960, 32, 1739−1742.

[5] Mondello, L.; Costa, R.; Tranchida, P. Q.; Dugo, P.; Lo Presti, M.; Festa, S.; Fazio, A.; Dugo, G. J. Sep. Sci. 2005, 28, 1101−1109.

[6] D'Acampora Zellner, B.; Bicchi, C.; Dugo, P.; Rubiolo, P.; Dugo, G.; Mondello, L. Flavour Fragrance J. 2008, 23, 297−314.

[7] Ragonese, C.; Sciarrone, D.; Tranchida, P. Q.; Dugo, P.; Dugo, G.; Mondello, L. Anal. Chem. 2011, 83, 7947−7954.

[8] Ragonese, C.; Sciarrone, D.; Tranchida, P. Q.; Dugo, P.; Mondello, L. J. Chromatogr. A 2012, 1255, 130−144.

[9] Smith, R. M.; Murilla, G. A.; Burr, C. M. J. Chromatogr. 1987, 388, 37−49.

[10] Trufelli, H.; Palma, P.; Famiglini, G.; Cappiello, A. Mass Spectrom. Rev. 2011, 30, 491−509.

[11] Baker, J. K.; Ma, C.-Y. J. Chromatogr. 1979, 169, 107−115.

[12] Smith, R. M. J. Chromatogr. A 1982, 236, 313−320.

[13] Smith, R. M.; Hurdley, T. G.; Gill, R.; Moffat, A. C. Chromatographia 1984, 19, 401−406.

[14] Smith, R. M.; Hurdley, T. G.; Gill, R.; Moffat, A. C. Chromatographia 1984, 19, 407−410.

[15] Smith, R. M.; Hurdley, T. G.; Gill, R.; Moffat, A. C. J. Chromatogr. A 1986, 355, 75−85.

[16] Smith, R. M. TrAC, Trends Anal. Chem. 1984, 3, 186−190.

[17] Bogusz, M.; Aderjan, R. J. Chromatogr. A 1988, 435, 43−53.

[18] Bogusz, M.; Neidl-Fischer, G.; Aderjan, R. J. Anal. Toxicol. 1988, 12, 325−329.

[19] Bogusz, M.; Wu, M. J. Anal. Toxicol. 1991, 15, 188−197.

[20] Smith, R. M.; Finn, N. J. Chromatogr. A 1991, 537, 51−60.

[21] Bogusz, M.; Hill, D. W.; Rehorek, A. J. Liq. Chromatogr. Relat. Technol. 1996, 19, 1291−1316.

[22] Belitz, H.-D; Grosch, W.; Shieberle, P. Food Chemistry; Springer- Verlag Berlin Heidelberg: Berlin Heidelberg, Germany, 2009; p 170, DOI: 10.1007/978-3-540-69934-7.

[23] Russo, G. L. Biochem. Pharmacol. 2009, 77, 937−946.

[24] Lin, J.-T.; Snyder, L. R.; McKeon, T. A. J. Chromatogr. A 1998, 808, 43−49.

[25] Ruiz-Gutiérrez, V.; Barron, L. J. R. J. Chromatogr., Biomed. Appl. 1995, 671, 133−168.

[26] Folch, J.; Lees, M.; Sloane Stanley, G. H. J. Biol. Chem. 1957, 726, 497−509.

[27] Bligh, E. G.; Dyer, W. J. Can. J. Biochem. Physiol. 1959, 37, 911−917.

[28] Wada, S. A.; Koizumi, C.; Nonaka, J. Yukagaku 1977, 26, 95−99.

[29] Costa, R.; Beccaria, M.; Grasso, E.; Albergamo, A.; Oteri, M.; Dugo, P.; Fasulo, S.; Mondello, L. Anal. Chim. Acta 2015, 875, 41−53.

[30] Beccaria, M.; Costa, R.; Sullini, G.; Grasso, E.; Cacciola, F.; Dugo, P.; Mondello, L. Anal. Bioanal. Chem. 2015, 407, 5211−5225.

[31] Fanali, C.; Dugo, L.; Cacciola, F.; Beccaria, M.; Grasso, S.; Dachà, M.; Dugo, P.; Mondello, L. J. Agric. Food Chem. 2011, 59, 13043−13049.

[32] Lísa, M.; Holčapek, M.; Řezanka, T.; Kabátová, N. J. Chromatogr. A 2007, 1146, 67−77.

[33] Ovčačíková, M.; Lísa, M.; Cífková, E.; Holčapek, M. J. Chromatogr. A 2016, 1450, 76−85.

[34] Holcapek, M.; Jandera, P.; Zderadička, P.; Hruba, L. J. Chromatogr. A 2003, 1010, 195−215.

[35] Lísa, M.; Lynen, F.; Holčapek, M.; Sandra, P. J. Chromatogr. A 2007, 1176, 135−142.

[36] Dugo, P.; Beccaria, M.; Fawzy, N.; Donato, P.; Cacciola, F.; Mondello, L. J. Chromatogr. A 2012, 1259, 227−236.

[37] Beccaria, M.; Sullini, G.; Cacciola, F.; Donato, P.; Dugo, P.; Mondello, L. J. Chromatogr. A 2014, 1360, 172−187.

[38] Herslöf, B.; Podlaha, O.; Toregard, B. J. Am. Oil Chem. Soc. 1979, 56, 864−876.

[39] Cárdenas, S.; Gallego, M.; Valcárcel, M. Anal. Chim. Acta 1999, 402, 1−5.

[40] Cunha, S. C.; Oliveira, M. B. P. P. Food Chem. 2006, 95, 518− 524.

[41] Neue, U. W. J. Chromatogr. A 2005, 1079, 153−161.

[42] Ettre, L. S. Pure Appl. Chem. 1993, 65, 819−879.

[43] López-Hernández, A.; Torres, C. F.; García, H. S.; Hill, C. G., Jr. J. Am. Oil Chem. Soc. 2004, 81, 743−747.

[44] Solaesa, A. G.; Bucio, S. L.; Sanz, M. T.; Beltran, S.; Rebolleda, S. J. Oleo Sci. 2014, 63, 449−460.

[45] Ruta, J.; Zurlino, D.; Grivel, C.; Heinisch, S.; Veuthey, J.-L.; Guillarme, D. J. Chromatogr. A 2012, 1228, 221−231.

[46] Jandera, P.; Hajek, T.; Ruzickova, M. J. AOAC Int. 2017, 100, 1636−1646.

[47] Broeckhoven, K.; Cabooter, D.; Desmet, G. J. Pharm. Anal. 2013, 3, 313−323.

[48] Gonzalez-Ruiz, V.; Olives, A. I.; Martìn, M. A. J. Chromatogr. A 2014, 1364, 83−95.

CHAPTER IV
Multidimensional Liquid Chromatography

4.1. Comprehensive lipid profiling in the Mediterranean mussel (*Mytilus galloprovincialis*) using hyphenated and multidimensional chromatography techniques coupled to mass spectrometry detection

4.1.1. Introduction

Lipid analysis and profiling is a crucial task to separation scientists working in many different fields, including pharmaceutical and cosmetic, clinical, biological, and food [1,2]. The complete clinical lipidomics workflow includes selection of the subjects, the sample type, the sample pre-processing conditions, the analytical method/s, and data processing [3].

Given the high complexity of many lipid matrices and the great structural diversity of these molecules, no single analytical technique is capable to afford thorough knowledge of all the lipid classes and species in a given sample. A variety of chromatographic techniques have been employed to this purpose, coupled to mass spectrometry (MS) and other types of detectors [4,5]. Reversed-phase HPLC (RP-LC) has been widely applied to accomplish rapid separation of saturated and unsaturated fatty acids (FAs) differing in chain length and number of degree of unsaturation. In RP-LC, retention of FAs and, hence, of triacylglycerols (TGs) increases with the increasing degree of hydrophobicity, commonly identified by partition number (PN), as given by the sum of the total carbon number (CN), minus twice the number of double bonds (DB) in the acyl chain, i.e.: PN=CN-2DB [6,7]. Normal-phase HPLC (NP-LC) separates neutral lipids like TGs, cholesterol and cholesteryl esters (CEs), as

well as phospholipids (PLs) on the basis of their polarity, regardless of their FA composition [8]. A fair limitation of NP-LC is that mobile phases are commonly used, which are not compatible with MS due to their low polarity and dielectric constant. Likewise, hydrophilic interaction HPLC (HILIC) can be regarded as a version of NP-LC, in which class-type separation of lipids can be performed by passing a hydrophobic or mostly organic mobile phase across a neutral hydrophilic stationary phase. By this means, HILIC is an electrospray ionization (ESI)-MS compatible separation tool for PL separation according to the polar head group; the elution order will be roughly the reverse of that in RP-LC mode [9].

The benefits to be attained by the coupling of two independent (orthogonal) separation mechanisms in a multidimensional (MD) chromatographic system are evident, as resolving power may be boosted greatly, and subsequent detection made easier and more reliable [10]. The maximum gain in separation will result from the implementation of two-dimensional comprehensive techniques where, unlike in the case of heart-cutting approaches, the whole column effluent is directed from a first (^{1}D) to a second (^{2}D) chromatographic dimension, usually by means of one or more switching valves, equipped with symmetrical (empty or packed) loops for sample storage. Among the possible arrangements, continuous on-line techniques (LC×LC) have clear advantages over off-line and stop-flow techniques (2D-LC), involving fraction collection after ^{1}D, and/or flow-interruption. Major advantages of LC×LC techniques consist in capability for full automation, faster analysis time, reduced risk of sample loss, sample deterioration, and artefact formation; however the coupling of different stationary phases may be challenging [11], and a number of technical issues must be taken into consideration [12]. Specifically, stop-flow HILIC×RP-LC has been employed to achieve separation of individual molecular species of PLs [13] and other lipids [14] in biological tissues, NP-

LC×RP-LC has allowed for comprehensive lipid profiling in plasma [15]. Remarkably, all online LC×LC techniques relied on RP-LC as the final dimension of separation, due to the use of MS-compatible solvents [16], with the noteworthy exceptions of the work carried out by the research groups of Holčapek [17] and Schoenmakers [18].

As far as detection is concerned, MS represents the most versatile and powerful tool for lipid detection, definitely, since it combines the capability for structural information with high sensitivity; acquisition of mass spectral data can be conducted in an untargeted (full spectra acquisition), class-specific (neutral-loss scanning, precursor-ion scanning, product-ion scanning) or targeted (multiple-reaction monitoring) way [19].

On the other hand, GC allows for flame ionization detection (FID) to be employed universally, and to obtain reliable quantification according to organic carbon of lipid molecules; usually after conversion of the FAs into their corresponding methyl esters (FAMEs). Non-polar (e.g., 5% diphenyl/95% methylsiloxane) and mid-polarity (e.g., polyethylene glycol, PEG) stationary phases afford FAME separation on the basis of their CN, while high-polarity (e.g., 100% cyanopropylsiloxane phase, CPS) columns provide more detailed separation of positional and geometric isomers of unsaturated FAs [20,21]. Since their invention by Armstrong almost two decades ago [22], room temperature ionic liquids (RTIL) have been widely employed as stationary phases for FAME separation, showing comparable or even better selectivity than CPS, along with reduced column bleed [23]. Delmonte *et al.* [24] demonstrated the feasibility of the use of a dicationic, imidazolium-based IL phase for the separation of *cis* and *trans* isomers of monounsaturated FAs (MUFAs) and conjugated linoleic acid (CLA) isomers. Due to their engineered orthogonality and high thermal stability, IL columns have been also exploited as either ^{1}D or ^{2}D in multidimensional comprehensive GC (GC×GC)

approaches focused on FAME profiling in different samples [25,26], this topic has been recently reviewed, thoroughly [27]. The present research aimed to implement a multi-technique approach, focused on the comprehensive characterization of the total lipid profile in a complex marine organism, namely *Mytilus galloprovincialis* (Mediterranean mussel). These molluscan bivalves, native from the Mediterranean sea, are recommended as bioindicator organisms to elucidate the relationship between environment and health in contaminated sites [28]. Major lipid classes in mussels comprise FFAs, TGs, sterols and sterol esters, and polar lipids; unlike most terrestrial organisms, mussels are rich in ω-3 long-chain polyunsaturated FAs PUFAs (20:4, 20:5 (EPA), 22:5, 22:6 (DHA)). Lipid content and composition in mussels may vary depending on the geographical site, season, animal's life cycle, sex, and spawning; furthermore the composition of TGs, who represent the main depot lipids, will be affected by the feeding conditions [29,30].

Class-type separation and side chain composition of neutral and polar lipids were obtained by online HILIC×RP, providing for the first time a global fingerprint of the lipidome without the common drawbacks associated to the use of NP-LC or the stop-flow approaches; hyphenation to ion trap-time of flight (IT-ToF) MS allowed for further characterization of the lipid fraction, in terms of molecular species within each class. In addition, GC-MS data obtained for the off-line collected fractions of individual PL species afforded qualitative information about the FA distribution within the PC class, providing unambiguous evidence of the different FA positional and geometric isomers.

4.1.2. Materials and Methods

4.1.2.1. Solvents and Chemicals

Chloroform ($CHCl_3$), methanol (MeOH), water (H_2O), *n*-hexane, diethyl ether (Et_2O), acetic acid (CH_3COOH), and potassium hydroxide (KOH) employed for

extraction of the mussel lipids, solid-phase extraction (SPE) and derivatization of the FAs were from Carlo Erba (Milan, Italy). LC-MS grade acetonitrile (ACN), H_2O, ammonium formate ($HCOONH_4$), MeOH, isopropyl alcohol (IPA) and tetrahydrofuran (THF) were from Sigma-Aldrich/Supelco (Milan, Italy). Cholesterol, cholesteryl palmitate (CE(16:0)), cholesteryl stearate (CE(18:0)), cholesteryl oleate (CE(18:1)), cholesteryl linoleate (CE(18:2)), glyceryl trilinoleate (LLL, TG(18:2/18:2/18:2)), 1,2-dilinoleoyl-3-palmitoyl-rac-glycerol (LLP, TG(18:2/18:2/16:0)), 1,2-dioleoyl-3-linoleoyl-rac-glycerol (OOL, TG(18:1/18:1/18:2)), 1,3-dipalmitoyl-2-oleoylglycerol (POP, TG(16:0/18:1/16:0)), phosphatidylcholine (PC), phosphatidylethanolamine (PE), phosphatidylserine (PS), phosphatidylinositol (PI), sphingomyelin (SM) and L-α-phosphatidylcholine (LPC) standard materials were from Millipore Sigma/Supelco (Bellefonte, PA, USA). The following standard materials were used for optimization of the GC conditions: linoleic acid methyl esters, *cis/trans*-isomers; linolenic acid methyl ester isomer mix; Supelco 37 Component FAME Mix; Polyunsaturated Fatty Acid Mix (PUFA No.1, PUFA No.2, PUFA No.3); bacterial acid methyl ester (BAME) mix; AOCS official method margarine FAMEs (provided by Millipore Sigma/Supelco).

4.1.2.2. Samples and sample preparation

Standard solutions. For the preparation of the standard solutions, around 10 mg of each standard were dissolved in a $CHCl_3$:MeOH (2:1, *v/v*) mixture up to 1 mL volume, filtered through 0.22 μm nylon membrane (Acrodisc, Pall Life Sciences, Ann Arbor, MI, USA), and stored at -18 °C until use.

Mussel tissue homogenization and lipid extraction. Adult specimens of *Mytilus galloprovincialis* (Mediterranean mussel) were obtained from an aquaculture farm in the coastal area of Brucoli (Sicily, Italy). The organisms were randomly selected, transported to the laboratory in aerated seawater, and immediately

subjected to lipid extraction. The shells were gently opened and, after removal of the excess inter-valvar liquid, the whole tissue was removed; around 30 g of mussel tissues were pooled and homogenized (IKA 3720000 T-18 Ultra Turrax Digital Homogenizer, Cole-Parmer, Vernon Hills, IL, USA); lipids were then extracted using the method from Bligh and Dyer [31] recommended by the Technical Guidelines of the Organization for Economic Cooperation and Development (OECD) for complete extraction of total lipids from marine species [32]. Total lipids were extracted with 90 mL of a $CHCl_3$:MeOH (1:2 *v/v*) mixture in a separating funnel, upon homogenization for 2 min, the homogenate was filtered and the solid residue set aside. Afterwards, 30 mL $CHCl_3$ were added to the liquid mixture and, after blending for 30 s, 30 mL of H_2O were added, and blending continued for 30 more seconds. After centrifugation at 3000 rpm for 15 min, the lower $CHCl_3$ phase was collected, and the whole extraction procedure was applied twice to the upper phase combined with the solid residue. The three extracted phases were pooled together, filtered through 0.22 μm nylon membrane and brought to dryness in an Envi (EZ-2 Envi) Evaporator (Genevac, Ipswich, Suffolk, UK). The sample was stored at -18 °C until use.

SPE procedure. Three main lipid fractions were separated on a Supelclean LC-NH_2SPE tube (bed wt. 500 mg, volume 6 mL, Millipore Sigma/Supelco, Bellefonte, PA, USA): neutral lipids, free fatty acids (FFAs), and polar lipids. Around 70 mg of the dried lipid extract were reconstituted in 1 mL of a MeOH:$CHCl_3$:*n*-hexane (2:1:1, *v/v/v*) mixture prior to isolation and purification by SPE. The SPE cartridge was preconditioned with *n*-hexane, and then the lipid extract was loaded. Neutral lipids (TGs, diacylglycerols (DGs), monoacylglycerols (MGs), cholesterol, and CEs) were eluted first with 4 mL of $CHCl_3$:IPA (2:1,*v/v*) mixture; the following fraction, containing the FFAs, was collected upon elution with 8 mL of Et_2O:CH_3COOH (98:2,*v/v*) mixture, while

PLs were eluted last with 4 mL of MeOH. The samples were stored at -18 °C until use.

Preparation of FAMEs. For the preparation of FAMEs, 250 µL of 2 N KOH in methanol and 1 mL of *n*-hexane were added to 5 mg of the neutral lipid and the polar lipid fractions. After vortexing for 5 min, the mixtures were allowed to stand for about 5 min, then the hexane upper layer was transferred into a vial and injected for the GC-MS analyses of FAMEs. All measurements were performed in triplicate. Knowledge about the free fatty acid composition of mediterranean mussel had been gained in a previous study using nanoLC-EI-MS [28].

For identification of the fatty acid substituent in a given lipid species, the same procedure was applied to the offline collected PC species, after RP-LC analysis of the PC class obtained by HILIC separation of the SPE-fractionated polar lipids.

4.1.2.3. Instrumentation and software

2D-LC and LC×LC instrument. Two-dimensional LC analyses were performed on a Nexera LC system (Shimadzu, Kyoto, Japan), consisting of a CBM-20A controller, four LC-30AD dual-plunger parallel-flow pumps, a DGU-20 A_{5R} degasser, a CTO-20A column oven, a SIL-30AC autosampler, and a SPD-M20A photodiode array (PDA) detector (2.5 µL flow cell volume). The two separation dimensions were connected by means of two high speed/high pressure two-position, six-ports switching valves with micro-electric actuator (model FCV-32 AH, 1.034 bar; Shimadzu), placed inside the column oven and equipped with two 0.254 mm I.D. stainless steel sample loops of identical volume (100 µL). The LC×LC system was interfaced to an LCMS-IT-TOF spectrometer through an ESI source (Shimadzu). The instrument and the switching valves were controlled by the LCMSsolution version 3.50.346

software (Shimadzu). The LC×LC data were visualized and elaborated into two and three dimensions using Chromsquare version 2.2 software (Shimadzu). A schematic of the LC×LC instrumentation is shown Figure 1 (IV-4.1.).

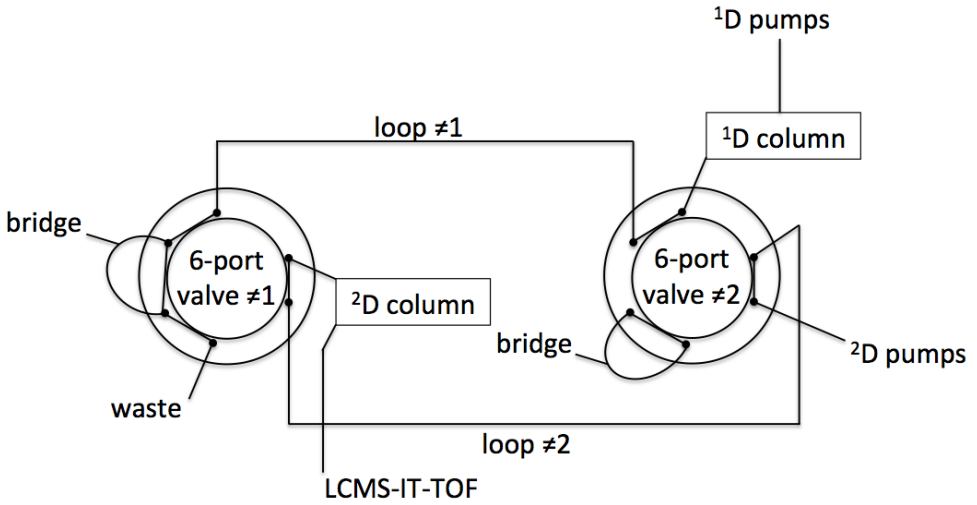

Figure 1 (IV-4.1.). A schematic of the two-dimensional instrumentation employed for the HILIC×RP-LC-MS/MS analysis of the mussel lipidome.

GC instruments. GC-MS analyses were carried out on a GCMS-QP2010 (Shimadzu, Kyoto, Japan) equipped with a split-splitless injector, an AOC-20i autosampler, and a single quadrupole MS analyzer, with electron impact (EI) ionization. The GCMSsolution software (Shimadzu) was used for data collection and handling. The Shimadzu Lipids Library (Shimadzu) was used for compound identification.

4.1.2.4. Analytical conditions

Online HILIC×RP-LC analyses. Optimization of the analytical conditions for the first (HILIC) and second (RP) dimension separation was carried out on

standard material; two-dimensional comprehensive separation of the mussel lipid extract (≈ 10 mg/mL in $CHCl_3$:MeOH, 2:1 *v/v*) was then obtained using the two columns, connected online. In ^{1}D, an Ascentis Express HILIC, 150 mm×2.1 mm I.D., 2.7 μm *d.p.* column was used. The mobile phases were: (A) ACN:10mM $HCOONH_4$ (98:2, *v/v*), (B) ACN:MeOH:10 mM $HCOONH_4$ (55:35:10, *v/v/v*). The gradient program was: 0-15 min 0% B, 40 min 100% B, held for 40 min. The mobile phase flow rate was 50 μL/min, and the injection volume 5 μL. In ^{2}D, a Titan C18, 50 mm×4.6 mm I.D., 1.9 μm *d.p.* column was used. The mobile phases were: (A) ACN:MeOH:10mM $HCOONH_4$ (55:35:10, *v/v/v*), (B) IPA + 0.1% formic acid. The segmented gradient (SG) conditions were: 0.01–0.35 min 0% B, 1.00 min 20% B, 1.70 min 70% B, 1.75 min 100% B (held for 0.10 min), 1.86 min 0% B (held for 0.14 min), repeated for the initial 40 min of the ^{1}D run; 0.01–0.75 min 0% B, 1.00 min 20% B, 1.70 min 70% B, 1.75 min 100% B (held for 0.10 min), 1.86 min 0% B (held for 0.14 min), for the subsequent 40-62 min of the ^{1}D run; 0.01–1.00 min 0% B, 1.85 min 20% B, 1.86 min 0% B (held for 0.14 min), for the final 62-80 min of the ^{1}D run. The mobile phase flow rate was 3.0 mL/min, with column oven temperature of 55 °C. The modulation time of the switching valves was 120 s. Data were averaged from three consecutive runs. Acquisition was occasionally performed by PDA, using a detection wavelength range of 300-500 nm.

MS and MS/MS parameters. A flow of 0.25 mL/min from the LC unit was directed to the MS by means of a stainless steel, 1/16″ O.D. tee Valco fitting (VICI AG International, Schenkon, Switzerland). Resolution, sensitivity, and mass number calibration of the IT and the TOF analyzer were adjusted using a standard sample solution of trifluoroacetic acid (approx. 0.25 mL/L) and sodium hydrate (approx. 0.1 g/L). After the calibrant had flowed, cleaning operation of the tube and ESI probe was made by flowing ACN (0.2 mL/min, 20 min). MS acquisition was performed using an ESI interface simultaneously

operated in both positive and negative ionization modes, under the following conditions: curved desolvation line (CDL) temperature, 250 °C; heat block temperature, 250 °C; nebulizer gas flow, N_2, 1.5 L/min; detector voltage, 1.55 kV; acquisition, 250-1000 *m/z* (positive polarity) or 150-1000 *m/z* (negative polarity); ion accumulation, 30 ms; repeat, 3. For MS/MS: acquisition, 50-800 *m/z*; ion accumulation, 50 ms; precursor ion isolation (width: 1, time: 50 ms). Collision-induced dissociation (CID) parameters: energy, 100%; collision gas, 100%; time, 50 ms.

Data were averaged from three consecutive runs.

Offline HILIC-RP-LC analyses. Separation of the PL fraction obtained upon SPE of the mussel lipid extract (≈ 27 mg dissolved in 600 μL of MeOH) into classes was achieved on an Ascentis Express HILIC, 250 mm×4.6 mm I.D., 5.0 μm *d.p.* column, with mobile phases consisting of: (A) ACN:10 mM $HCOONH_4$ (98:2, *v/v*), (B) ACN:MeOH:10 mM $HCOONH_4$ (55:35:10, *v/v/v*), in gradient mode (0-15 min 0% B, 15-40 min 0-100% B, 40-80 min 100% B), at a flow rate of 0.8 mL/min. The column oven was set at 35 °C, and the injection volume was 20 μL. The chromatographic peak corresponding to the PC class was collected after consecutive runs, evaporated to dryness, and re-dissolved in MeOH (≈ 1 mg/mL) for subsequent separation of the individual molecular species. RP-LC separation of the PC species was achieved using an Ascentis Express C18, 250 mm×4.6 mm I.D., 5.0 μm *d.p.* column, with mobile phases consisting of: (A) IPA:10 mM $HCOONH_4$:THF (55:30:15, *v/v*), (B) ACN, isocratically (40% B), at a flow rate of 0.6 mL/min. The column oven was set at 35 °C, and the injection volume was 50 μL. The PDA detection wavelength was set at 205 nm.

GC-MS analyses. GC separations of the FAMEs were achieved on a Supelco SLB-IL 111, 200 m×0.25 mm I.D., 0.20 μm d_f, fused silica capillary column. The programmed oven temperature was: 50 °C (1 min) to 160 °C (33 min) at 10

°C/min, then up to 185 °C (8 min) at 6 °C/min, and finally up to 260 °C at 3 °C/min. Injector temperature: 260 °C; injection volume: 0.5 µL; injection mode: splitless. Helium (He) was used as the carrier gas at a constant linear velocity of 20.9 cm/s and a pressure of 492.3 KPa. MS parameters were as follows: mass range, 40-650 amu; scan interval, 0.20 s; ion source temperature, 200 °C; interface temperature, 220 °C. Data were averaged from three consecutive runs.

All the chromatographic columns were kindly donated by Millipore Sigma/Supelco (Bellefonte, PA, USA).

4.1.3. Results and Discussion

4.1.3.1. Online HILIC×RP-MS

The separation in the two chromatographic dimensions was first optimized using a mixture of standard material, representative of the main lipid classes, i.e.: TGs (LLL, LLP, OOL, POP), PLs (PC, PE, PS, PI, SM, LPC), sterols and CEs (cholesterol, CE(16:0), CE(18:0), CE(18:1), CE(18:2)). The class-type separation of neutral and polar lipid species was achieved on a 150 mm-long, narrow bore (2.1 mm) HILIC column, packed with 2.7 µm-partially porous particles; the choice of such a stationary phase was the outcome of a number of considerations. HILIC can be described as a kind of liquid–liquid partition chromatography, which separates compounds by passing an organic-dominant mobile phase across an hydrophilic stationary phase, causing solutes to elute in order of increasing hydrophilicity; thus, the elution order of analytes in HILIC will be the reverse of that in RP mode, more or less. To this concern, HILIC can be regarded as a version of NP-LC, which is also used for PL classes separation, but performed with water-miscible solvents, which are both RP- and ESI-compatible. On-line hyphenation to MS is therefore straightforward, and furthermore the high organic content in a mobile phase promotes enhanced ESI-

MS response, thus increasing the sensitivity of detection. ESI-IT-TOF MS detection was chosen because of the possibility to perform exact measurement of intact molecule-related ions (very little fragmentation), and at the same time obtain structural information (MS^n capabilities), to help in identification of unknown structures and sometimes discrimination of isomers/isobars. The column was operated at 30 °C and at a mobile phase flow rate of 300 μL/min, at which the minimum plate height and thus the maximum efficiency was achieved. Complete elution of the standard lipid mixture was obtained within 15 min (as shown in Supplementary Figure 1S (IV-4.1.) in Supplementary material), with mobile phases consisting of 2% $HCOONH_4$ in ACN (A), and (B) 10% $HCOONH_4$ in a ACN:MeOH mixture (55:35 *v/v*), under the following gradient: 0-5 min 0% B, 5-10 min to 100% B, held for 25 min. Individual lipid classes were identified using total ion current in positive ion mode, detected as $[M+NH_4]^+$ or $[M+Na]^+$ adducts (TGs and CEs, respectively), or as protonated molecular ions $[M+H]^+$ (PLs), the only exception being PI, detected as $[M-H]^-$ in the negative ion mode only; also for PS a better signal was obtained, as $[M+H]^-$ (Supplementary Figure 2S (IV-4.1.) in Supplementary material).

As expected, HILIC did not enable baseline separation of all the neutral lipids (TGs, cholesterol, and CEs), as most of them co-eluted in one chromatographic peak, before the starting of the gradient (isocratically, at 0% B). Baseline separation of all the PLs was obtained, according to the nature of the polar head group, in order of decreasing polarity: PI>PS>PE>PC>SM>LPC. During method development, it was found that the higher organic solvent composition in the eluent resulted in more retention of polar compounds, and that the addition of $HCOONH_4$ as mobile phase modifier was helpful to obtain well-shaped peaks of each PL class, and higher ESI-MS sensitivity. According to a previous work [33], the separation of neutral and charged phospholipids in HILIC mode showed a different behaviour: retention of the former (PE, PC,

SM, LPC) was higher with the increasing polarity of the molecules; elution of the latter classes of PLs (PI, PS) probably resulted from combined effect of hydrophilic and electrostatic interactions, since their retention times decreased by increasing the $HCOONH_4$ percentage. Accordingly, PI and PS gave peak shapes very similar to those of neutral lipids (a single, sharp peak), while for PE, PC, SM, and LPC also a partial separation of the individual lipid species within each class occurred, as visible from the crested peaks.

After HILIC-ESI-MS, next step was the separation of individual species inside the lipid classes, this was accomplished by the coupling of RP-LC; the latter was first optimized for each standard lipid class in monodimensional analyses, and then adapted to the real sample. In view of the subsequent online coupling to HILIC, a number of requirements needed to be fulfilled, including mobile phase miscibility and operational (flow rate, transfer loop size/volume) compatibility. A clear advantage of online approaches with no interruption of flow is that the second dimension analysis is run in parallel to the first separation, with no increase in the overall analysis time, with respect to a monodimensional LC analysis. In this LC×LC approach, all the fractions eluted from ^{1}D were continuously transferred to the secondary column, and this posed stringent demands for the separation in ^{2}D. The latter needed to be very fast, since in the time allotted for the collection of each ^{1}D fraction into the loop of the switching valve, analytes transferred during the previous modulation had to undergo complete elution, and reconditioning of the column from the gradient had to be accomplished, before occurring of the next transfer (modulation). While too slow a ^{2}D run may not ensure sufficient time for complete elution of all the compounds contained in a given fraction, on the other hand, too fast a ^{2}D separation may not provide adequate resolution. Following these considerations, a short (50 mm) octadecylsilica column of 4.6 mm I.D. was chosen for ^{2}D-RP, consisting of monodisperse material. Being the limited ^{2}D

separation time proportional to the column hold-up time, with such a column, fast repetitive gradients could be run at higher mobile phase flow rates, *viz.* 3.0 mL/min, without any loss in efficiency and with very fast re-equilibration (8.4 s); the latter was confirmed by the superimposition of repetitive sample injections in ^{2}D (data not shown), and the absence of wraparound effects in the final 2D plot [34]. In order to avoid any mismatch issues and ensure full compatibility of the mobile phases used in the two dimensions, solvent A) used for the ^{2}D gradient was exactly the same as solvent B) in ^{1}D (ACN:MeOH:$HCOONH_4$, 55:35:10 *v/v/v*), while the addition of 0.1% of formic acid in IPA (solvent B of ^{2}D) resulted in improved peak shapes and ESI-MS sensitivity. Under a repetitive ^{2}D gradient going to 100% of IPA in 1.75 min, complete elution of all the lipid species was achieved, for each class of lipid standard, within 2.00 min, at a column oven temperature of 55 °C; an example is illustrated in Supplementary Figure 3S (IV-4.1.) (Supplementary material), showing the RP-LC-ESI-MS separation of individual PC species, detected as $[M+H]^+$ ions. Thus, a modulation time equal to 2 min was fixed for the 2D-LC approach, while the HILIC column flow rate was reduced from 300 to 50 µL/min, to allow for total emptying of the 100-µL loops of the valves, at each switching. By operating the ^{1}D column at sub-optimal flow rates, the amount of solvent transferred onto the secondary column was substantially reduced, facilitating peak compression and peak focusing; moreover, increased ^{1}D peak widths were obtained, allowing for better fractionation of the transferred peaks (e.g., 3-5 min for the more complex PL classes).

In the HILIC×RP approach, 5 µL (≈ 10 mg/mL in $CHCl_3$:MeOH, 2:1 *v/v*) of the mussel lipid extract were injected under the optimized conditions discussed above, and the ESI-MS plot obtained in the positive ion mode is shown in Figure 2 (IV-4.1.). Complete elution of the sample components was achieved in 72 min, using ACN (solvent A) and 55:35 ACN:MeOH (solvent B), both

containing ammonium formate as an additive, with the following gradient: 0-15 min 0% B, 15-40 min to 100% B (held for 40 min). According to what previously observed for the separation of the standard compounds, neutral lipids, which are the most hydrophobic components of the lipid extract (and therefore, the less retained on the polar ^{1}D column) were the first-eluted class, appearing at the beginning of the HILIC trace before the starting of the gradient (8-12 min). Along with TGs and sterol lipids (cholesterol, CEs, and secosteroids), also FFAs, wax esters (WEs), prenol lipids and polyketides were observed, the latter two classes comprising natural antioxidants like flavonoids and carotenoids belonging to different classes. The highest amounts of solvent B were required for elution of the polar PL classes, according to the increasing polarity of the polar head group, together with their corresponding lyso forms: PE, LPE, PC, LPC. The assignment of chromatographic blobs in the 2D plot in Figure 2 (IV-4.1.) to specific lipid classes was performed by careful interpretation of MS and MS/MS spectra averaged under each chromatographic peak in the raw data file, as explained in the section that follows. A preliminary investigation performed by the neutral loss scan survey confirmed the literature data available on the PL distribution in mussels [35], reporting PC species as the most abundant PL class (chromatographic band centred at 57 min), followed by PE (band centred at 45 min); also the corresponding lyso forms LPC and LPE were found (at 66 and 46 min, respectively) which, lacking one acyl chain with respect to the parent classes have higher polarity and thus were more retained. Together with diacylic PC and PE, also the plasmanyl and plasmenyl forms phosphonocholine (PnC) and phosphonoethanolamine (PnE) were also detected, in which one of the acyl chains is replaced by an alkyl (O-PC, O-PE) or alkenyl (P-PC, P-PE) side chain. Plasmanyl and plasmenyl analogues of LPC (O-LPC, P-LPC) were observed as well (blob centred at 70 min), but not of LPE. In addition, ceramide lipids belonging to the aminoethylphosphonate

(CAEP) class were observed, as a separate chromatographic band eluting between those of LPE and PC (at 51 min); these compounds, called sphingophosphonolipids (SPnL), are sphingolipids with a direct C-P bond and a phosphoethanolamine polar head group, and have been reported in marine invertebrates such as bivalve molluscs, including mussels [36]. Among the polar lipids, PS and PI were by far the least abundant, the latter partially co-eluting with species belonging to the diacylglycerophosphate sub-class, i.e. phosphatidic acid (PA); all these lipids were detected in negative polarity.

The separation of lipid individual species within each class was obtained, in the ^{2}D RP-LC, according to their hydrophobicity, on a C18 phase operated under a gradient of IPA (containing 0.1% formic acid) into a mixture of ACN:MeOH:$HCOONH_4$ (55:35:10, *v/v/v*) and at a column oven temperature of 55 °C; such high temperature led to accelerated diffusion of the species and to reduction in the solvent viscosity, thus ensuring fast elution of the analytes to be completed in each 2-min modulation, with improved separation efficiency and peak capacity, and not exceeding the backpressure limit of the instrumentation and the column. Conditions for the separation needed to be revised, given the high complexity of the mussel lipid extract; specifically, the presence of species with different hydrophobicity, thus spanning in a much wider range of PN values with respect of those of the standard mixture, and the presence of compounds belonging to additional categories, in the neutral fraction (wax esters, prenol lipids, and polyketides). The initial and final concentrations of solvent B), as well as the gradient steepness, were adapted for the ^{2}D RP-LC separation of each neutral and polar lipid class, according to their different complexity and hydrophobicity. The type of gradient program in fact controls the range of lipophilicity of sample compounds that can be separated in the ^{2}D RP-LC short run and, to this concern, the use of a repetitive (sometimes referred to as “full in fraction”) ^{2}D gradient would have provided limited

coverage of the 2D plane (poor orthogonality) and therefore limited separation of the lipid species within each class [37-39]. A "segmented in fraction" ^{2}D gradient was then designed, in order to cover sufficient mobile phase range in the different time segments, providing adequate retention span for the compounds of the individual fractions, and at the same time avoid sample carry-over to the next fraction arising from elution outside the gradient time range. In more detail, in the ^{2}D gradient adopted for the initial 40 min of the ^{1}D run, an isocratic initial step at 0% B for 0.35 min was suitable to avoid the co-elution of free cholesterol, FFAs, WEs, polyketides, and secosteroids, with the more hydrophobic CEs and TGs (chromatographic bands at 6-14 min in the 2D plot in Figure 2 (IV-4.1.)). Elution of the latter lipid compounds required higher amounts of IPA and was completed at 60% B for CEs, while TGs eluted at the end of the ^{2}D gradient, i.e. at %B spanning from 70 to 100%; for both classes, separation occurred following the PN rule. For the subsequent 40-62 min of the ^{1}D run, in which the more polar lipids eluted (including PLs and ceramides), the employment of a longer initial isocratic step of the ^{2}D gradient (at 0% B for 0.75 min) was beneficial for subsequent resolution of the several species contained into each class, again, eluted according to decreasing polarity and increasing PN. In the final 62-80 min of the ^{1}D HILIC separation, LPC species (band centred at 66 min in the 2D plot in Figure 2 (IV-4.1.)) together with plasmanyl and plasmenylic analogues (band centred at 70 min) eluted, in the first 1 min of the ^{2}D gradient, i.e. isocratically, at 0% B; for the most hydrophilic compounds in the mussel lipid extract, the ^{2}D gradient was ended at 20% B. The HILIC×RP approach implemented rendered a 2D plot of the mussel lipid species, in which the different compounds are characteristically distributed along the two retention time (r_T) axes, so that hydrophilicity of the separated lipid classes increases going from the left to the right of the ^{1}D HILIC axis, while hydrophobicity of the individual species increases with retention in

the ^{2}D RP axis, from the bottom up. Even though the resolution in ^{2}D RP-LC analysis could not be fully exploited due to the limited run time available (and made worse by the complexity of the sample), yet the 2D plot obtained allows for a quick visual fingerprinting of the mussel lipid composition.

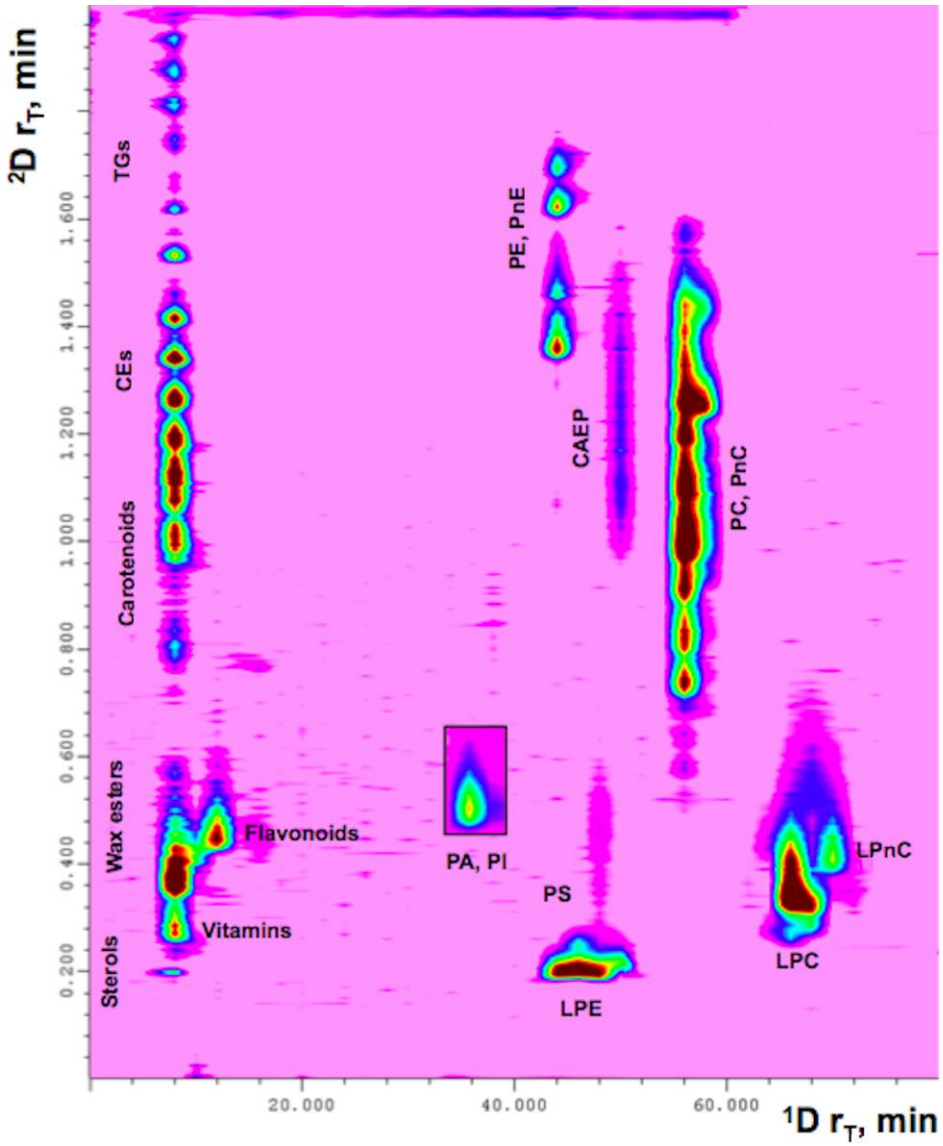

Figure 2 (IV-4.1.). 2D plot obtained from the HILIC×RP separation of the mussel lipidome, recorded in the ESI($^{+}$) mode by IT-ToF detection.

Abbreviations: FFA, free fatty acids; Chol, cholesterol; WE, wax esters; CE, cholesteryl esters; TG, triacylglycerols; PA, phosphatidic acid; PI, phosphatydylinositol; PS, phosphatydylserine; PE, phosphatydylethanolamine; PnE, phosphonoethanolamine; LPE, lysophosphatydylethanolamine; CAEP, ceramide 2-aminoethylphosphonate; PC, phosphatydylcholine; PnC, phosphonocholine; LPC, lysophosphatydylcholine; LPnC, lysophosphonocholine.

4.1.3.2. MS and MS/MS analyses

ESI-IT-ToF MS detection allowed untargeted identification through exact measurement of intact lipid-related ions, and at the same time perform targeted experiments, to discriminate between isobaric species. Conditions for MS and MS/MS analyses were first optimized using a standard lipid mixture; an ESI-compatible ^{2}D mobile phase consisting of ACN:MeOH:$HCOONH_4$ (55:35:10, *v/v/v*) and IPA (with 0.1% formic acid) as solvent A) and B), respectively, was found adequate to support ionization of all the lipid species extracted from the mussel sample, spanning a wide range of polarities. Identification was afterwards performed by gathering the complementary data of retention times in the two chromatographic dimensions, MS and MS/MS data, and further supported by the data attained by GC-MS analysis, on the FA composition of the neutral and polar lipid mussels, after SPE fractionation (described later). Accurate *m/z* ratios retrieved from IT-ToF MS spectra were first searched on the LIPID MAPS Lipidomics Gateway (freely accessible at: http://www.lipidmaps.org/); since the typical mass accuracy delivered by manual predicted flight time adjustment after autotune was <2.5 ppm (in the mass range 400-2000 Da), a tight mass tolerance could be set on the *m/z* ratio

matching, equal to (±)0.001. The described approach led to the identification of over 200 species in the mussel lipidome, which are distributed along 19 different classes/categories, spanning a wide range of hydrophilicity/hydrophobicity (plot in Figure 2 (IV-4.1.)), as discussed below. The lipid species identified are grouped in Table 1 (IV-4.1.) into classes (listed according to the increasing retention time in the two dimensions), along with their chemical formula, observed and calculated *m/z*, observed ion, and PN (if applicable).

Identification of the neutral lipids

Neutral lipids were the less retained by the ^{1}D HILIC column, eluted within the first 14 min of the HILIC×RP analysis (2D plot in Figure 2 (IV-4.1.)); as expected, the most represented classes were FFAs, TGs and CEs, apart from WEs, secosteroids, prenol lipids, and polyketides (detected in the positive polarity, except for FFAs, not visible in the 2D plot). Among the less hydrophobic compounds in the neutral lipid fraction, a total of 24 FFAs were recorded in the negative ion mode as deprotonated molecular ions, from the long-chain PUFA docosahexaenoic acid (DHA, C22:6) to the long-chain saturated (SFA) one, i.e. behenic acid (C22:0), eluted according to increasing PN values, ranging from 10 to 22 (#1-23 in Table 1 (IV-4.1.)). Identification of the SFAs (i.e., 14:0, 15:0, 16:0, 17:0, 18:0, 19:0, 20:0, and 22:0) through database search was straightforward, given the presence of only one possible candidate (matched mass) at the tight *m/z* tolerance (±0.001). Conversely, in the case of MUFAs and PUFAs, two candidates were obtained upon database search, for each observed *m/z* value; e.g., for an input mass of 281.2492, FA(18:1) and FA(18:0(cyclo)) are found, both with matched mass of 281.2486. These two compounds would show nearly identical fragmentation patterns in tandem ESI-MS spectra (even at high collision energy), however the presence

of isobaric carbocyclic FAs could be excluded, on the basis of further analysis by GC-MS and what reported in the literature [28-30]. Thus, compound #13 in Table 1 (IV-4.1.) was identified as octadecenoic acid (18:1), and not as 18:0(cyclo). For compounds with up to two unsaturated bonds, the ESI-MS spectra also showed very low-intensity peaks generated from the loss of H_2O and formation of triple bond(s), e.g. for FA 18:1 observed as $[M-H]^-$ at *m/z* 281.2492, also $[M-H-H_2O]^-$ was observed, at *m/z* 263.2374. On the other hand, PUFAs containing 3 to 6 DBs showed in their ESI-MS spectra also a characteristic fragment generated from the loss of CO_2, e.g. for FA 22:6 observed as $[M-H]^-$ at *m/z* 327.2335, also $[M-H-COO]^-$ was observed, at *m/z* 283.2436.

Free sterols were also early eluted, before the beginning of the ^{2}D gradient (blob centred at total retention time, Tr_T 8.2, as given by the sum of ^1Dr_T and ^2Dr_T), and detected as $[M+H]^+$ ions; in accordance with data from the literature [40 and references therein], a total of 8 compounds were identified (#24-31 in Table 1 (IV-4.1.)), as sterol lipids, on the basis of their ESI-MS spectra and MS/MS fragmentation of selected precursor ions. In detail: cholesterol (observed at *m/z* 387.3628, MS/MS ion at *m/z* 369.3511 resulting from the loss of H_2O); brassicasterol ($[M+H]^+$ at 399.3618, $[M+H-H_2O]^+$ at 381.3521); campesterol ($[M+H]^+$ at 401.3783, $[M+H-H_2O]^+$ at 383.3681); isofucosterol ($[M+H]^+$ at 413.3774, $[M+H-H_2O]^+$ at 395.3668); dinosterol ($[M+H]^+$ at 429.4094, $[M+H-H_2O]^+$ at 411.3994); occelasterol, desmosterol, and 22-dehydrocholesterol were all observed as $[M+H]^+$ in ESI-MS and $[M+H-H_2O]^+$ ions in ESI-MS/MS, at *m/z* 385.3471 and *m/z* 367.3363, respectively. Discrimination between the isobaric structures was possible on the basis of the distinctive product ions generated from a common fragmentation pattern; i.e. the low-intensity peaks generated from bond cleavage at site of unsaturation in the alkyenyl chain linked to the cyclopentane ring of cholesterol

(http://cfmid.wishartlab.com). Occelasterol (27-nor-(24S)-methylcholest-5,22E-dien-3β-ol) and 22-dehydrocholesterol (cholesta-5,22E-dien-3β-ol) gave a common fragment at *m/z* 71 (C_5H_{11}), arising from cleavage of the double bond between C22 and C23. Such a product ion was not observed in the ESI-MS/MS spectrum of desmosterol (cholest-5,24-dien-3β-ol), in which the double bond is located between C24 and C25; a fragment at *m/z* 55 showed up (C_4H_7), corresponding to 2-methylprop-1-en-1-ylium. Detection of a product ion at *m/z* 73 allowed to further identify a 24-methyl substituted sterol, as occelasterol (see Supplementary Figure 4S (IV-4.1.) in Supplementary material).

WEs, CEs, and TGs being more hydrophobic, were more retained on the ^{2}D C18 column, and separated according to the length and degree of unsaturation of the linked acyl chain/s. As esters of long chain FAs and fatty alcohols, WEs are lacking polar groups for cation adduct formation, and are sometimes disregarded in ESI-MS lipidomic studies, since they are more difficult to be detected; however, they can be conveniently ionized using additives such as sodium or ammonium acetate. WEs eluted within the first 0.5 min of the ^{2}D gradient, and showed up in ESI-IT-ToF MS as $[M+Na]^+$ ions; lipid assignment for these compounds was straightforward due to the presence of a single candidate, while tandem MS was necessary to infer the exact lipid composition. As an example, for the observed *m/z* 599.4802, only WE(40:8) was found, with a matched mass of 599.4798 (delta 0.0004). In ESI-MS/MS, the following ions were observed: $[M+Na]^+$, $[M+H]^+$ at *m/z* 581, and $[M+H-H_2O]^+$ at *m/z* 563. In addition, fragments at *m/z* 281, 303, 307, and 329 were detected, corresponding to different $[RCOOH_2]^+$ and $[R'COOH_2]^+$ ions, and namely deriving from four different FAs: 18:2, 20:5, 20:3, and 22:6, respectively. The only two possible combinations for a PN equal to 24 (calculated from CN=40 and 2×DB=16) are: 18:2/22:6 and 20:3/20:5 (peaks #33 and #34 in Table 1 (IV-4.1.), respectively).

On these basis, a total of 14 fatty acyl compounds were identified, (#33-46 in Table 1 (IV-4.1.)), eluted according to their increasing PN (in the 24-34 range). Cholesteryl esters are listed in Table 1 (IV-4.1.) as peaks #72-81, eluting within the 1.2-1.5 min duration of the ^{2}D gradient, at IPA percentages increasing from 30 to 50%. For these lipid compounds, the ESI process generated strong signal intensity of precursor ions corresponding to $[M+Na]^+$ ions, regardless of the number of carbon chains and double bonds in CEs. In the ESI-MS/MS analysis, all CEs lost their FA, as well as created a specific fragment at *m/z* 369 derived from cholesterol, which produces this specific daughter ion upon its dehydration ($[M-H_2O+H]^+$). For each observed *m/z* value, a unique candidate was found, and thus identification of 10 CEs compounds was straightforward, from the species CE(20:5) with a PN of 10, to CE(20:1) with a PN of 18.

Triacylglycerols were the most hydrophobic species in the lipid extract, and thus eluted during the final step of the ^{2}D gradient, requiring high amounts of isopropanol in the RP-LC mobile phase (55-100%). These lipids were detected by ESI-MS as ammonium adducts, and analysis of the tandem mass spectra allowed identification of the individual species in the sample, by the characteristic fragment ions, reflecting their FA composition. As an example, for the observed *m/z* 962.7237, the lipid assignment is TG(60:15) was found (PN=30), with a matched mass of 962.7232 (delta 0.0005); possible FA combinations for identification of the species were: 18:4/20:5/22:6 and 20:5/20:5/20:5. The ESI-MS/MS spectra from precursor ion $[M+NH_4]^+$ contained the $[M+H]^+$ ion at *m/z* 945 and the $[M+H-H_2O]^+$ ion at *m/z* 927. Moreover, three distinct fragments were observed, deriving from the neutral loss of the FA substituents, at *m/z* 669, 643, and 617. This observation permitted assignment of the masses of FA substituents, confirming the existence of TG species 18:4/20:5/22:6, being *m/z* 669 the fragment generated upon the neutral loss of *sn1* $RCOOH+NH_3$ from $[M+NH_4]^+$, *m/z* 643 the

fragment generated upon the neutral loss of *sn2* RCOOH+NH_3 from $[M+NH_4]^+$, and *m/z* 617 the fragment generated upon the neutral loss of *sn3* RCOOH+NH_3 from $[M+NH_4]^+$. Moreover, intense signal of comparable abundances were observed, corresponding to the three acyl chains $[RC=O]^+$: *sn1* at *m/z* 259, *sn2* at *m/z* 285, *sn3* at *m/z* 311. On these basis, the co-elution of the isobaric TG species 20:5/20:5/20:5 could be reasonably excluded, on the basis of the relative abundances of these ions, unless in traces. A total of 34 TGs are listed in Table 1 (IV-4.1.) (#82-115), eluted according to their increasing PN (in the 30-48 range).

Apart from the expected lipid species investigated, also metabolites of vitamin D_3 (#32 in Table 1 (IV-4.1.)) and several pigments were co-extracted from the mussels, the latter being responsible for their intense (from pale yellow to dark orange) coloration. In accordance with findings from previous research, carotenoids (C40 isoprenoids/tetraterpenes #47-71 in Table 1 (IV-4.1.)) and flavonoids (polyketides #116-120 in Table 1 (IV-4.1.)) were identified, from their MS spectra and characteristic absorption wavelengths in the visible region. It is known that bivalves accumulate carotenoids obtained from their dietary microalgae and modify them through metabolic reactions; in addition several classes of environmental pollutants are known to enhance the intracellular formation of reactive oxygen species in molluscs, with consequences on their antioxidant system [41 and references therein].

Identification of the polar lipids

Phosphatidic acid species were detected in the negative ion mode as $[M-H]^-$ ions, and are shown in the inset in the Plot of Figure 2 (IV-4.1.) (co-eluted with PI species); a total of 6 species were identified, listed as #121-126 in Table 1 (IV-4.1.), with PN values comprised in the 20-34 range. Identification through database search was immediate for the first representative of this

diacylglycerophosphates sub-class, as for the observed mass at *m/z* 791.4662, a unique species was identified as PA(44:12), i.e. 22:6/22:6 (#121) with a matched mass of 791.4657 (error 0.0005). The situation was far more complicated for the PA #122, since for an input mass of 719.4661, five different candidates were matched, all within the tight ±0.001 tolerance, with common lipid assignment PA(38:6), and namely: 16:0/22:6, 18:1/20:5, 18:2/20:4, 18:3/20:3, 18:4/20:2. However, the latter two species could be excluded on the basis of the fragmentation pattern, as observed in ESI-MS/MS analysis; e.g. for PA(16:0/22:6) (#122) the most abundant daughter ions corresponded to the neutral losses of FA(22:6) at *m/z* 255 and FA(16:0) at *m/z* 327.

A total of eight different classes were identified in the mussel phospholipidome, in good agreement with data from the literature [35,36], being more retained on the ^{1}D HILIC column according to the polar character of their characteristic head group: PI (#127-132), PS (#133-136), PE (#137-139), PnE (#140-159), LPE (#160-162), CAEP (#163-172), PC (#173-203), PnC (#204-213), LPC (#214-222), LPnC (#223-226). The corresponding blobs in Figure 2 (IV-4.1.) were all detected under positive polarity, except for PI and PS (showed as $[M-H]^-$ ions). Unambiguous class identification was also achieved in ESI-MS/MS performing the neutral loss scan (NLS), and generation of the diagnostic ions occurred both from the diacylic, and the alkyl- and alkyenyl-acylic PL; e.g., the neutral loss of *m/z* 183 (phosphocholine head group) was observed from PC, O-PC, and P-PC (the latter two listed in Table 1 (IV-4.1.) under the PnC class).

Identification of the monoacylglycerophosphocholines and their plasmanyl/plasmenyl derivatives, i.e. LPE (#160-162), LPC (#214-222), and LPnC (#223-226) was straightforward, given the presence of a unique candidate species for each observed mass (and lipid assignment); to make an example, for the observed mass at *m/z* 542.3238, a unique species was identified as LPC(20:5) with a matched mass of 542.3241 (error 0.0003).

Conversely, careful interpretation of the ESI-MS/MS spectra was deemed as necessary to achieve the exact lipid composition of all the diacylic species and their derivatives; the class of PC will be taken as an illustrative example, illustrating the identification of one of the most abundant species, also of nutritional relevance, i.e. PC(16:0/22:6). Upon database search (±0.001 tolerance) of an observed mass at *m/z* 806.5699, PC(38:6) and PE(41:6) are found, as isobaric species with a matched mass of 806.5695 (error 0.0004). However, the second candidate could be readily excluded, on the basis of the chromatographic elution on the ^{1}D HILIC column, and was furthermore excluded from the results from NLS. Once the PC class was selected, six possible FA combinations are shown, with chemical formula $C_{46}H_{80}NO_8P$ (neutral mass); further structural elucidation was achieved by interpretation of the tandem MS spectra, and the spectral features resulting from the preferential losses permitted identification and also assignment of the FAs linked at the glycerol backbone. Under the positive ionization mode (as shown in Supplementary Figure 5S (IV-4.1.) of Supplementary material), fragmentation of the $[M+H]^+$ precursor ion showed the characteristic phosphocholine ion at *m/z* 184 $[C_5H_{15}NO_4P]^+$, and also a signal of lower abundance *m/z* 623 was detected, generated from the diacylglycerol-like fragment ions $[C_{41}H_{66}NO_4]^+$. A very intense signal was generated from the neutral loss of the external FA, i.e. $[M+H\text{-}R_2COOH]^+$ at *m/z* 478, while the loss of *sn-1* FA was less favoured, i.e. $[M+H\text{-}R_1COOH]^+$ at *m/z* 550. In addition, the neutral losses of a "ketene" was observed, as $[M+H\text{-}R_2CH{=}C{=}O]^+$ at *m/z* 496 (loss of *sn-2* favoured) and as $[M+H\text{-}R_1CH{=}C{=}O]^+$, at *m/z* 568 [36]. Further confirmation was attained by examining the corresponding ESI-MS/MS spectra, recorded under negative polarity (see Supplementary Figure 6S (IV-4.1.) in Supplementary material). Under these conditions, PC was detected as formate adduct at *m/z* 850.5611, while in the MS/MS experiment the most abundant signal was detected at *m/z*

790 (resulting from the loss of CH_3 and formate from precursor ion), and noticeably the two FAs showed up, as $[RCOO]^-$, at *m/z* 327 (higher intensity) and *m/z* 255. On the basis of these results, substructure annotation was possible, as PC(16:0/22:6), which was by far the most abundant species eluting according to a PN value of 26; while in a similar way, PC(14:0/16:1) and PC(16:0/20:4) were identified as the most represented species later co-eluted according to increasing hydrophobicity, i.e. with a PN value of 28. These two peaks will be the object of further investigation, and will be regarded as peaks 8 and 11, in the section devoted to GC-MS analysis.

Briefly, all CAEP lipids were detected as protonated forms, and exhibited the neutral loss of their head group as a common feature, i.e. (2-aminoethyl)phosphonic acid (125.02 Da), followed by generation of a C=C bond between carbons C_1 and C_2 of the sphingoid chain and subsequent loss of water. Taking as an example compound #165 in Table 1 (IV-4.1.), identified as CAEP(d18:3/16:0), the overall composition, in terms of carbon atoms and C=C bonds, of the sphingoid backbone and of the acyl chain could be retrieved from accurate mass measurement of $[M+H]^+$ ion at m/z 640.5021, as 34:3. The neutral loss of phosphoethanolamine gave a product ion at 516, and the subsequent rearrangement of the C=C bonds and loss of water led to the m/z 498 ion. Furthermore, the loss of a 16:0 amide-linked acyl chain was observed, as a ketene, at m/z 260 and, thus, assumption of a 18:3 sphingoid backbone was straightforward. Regarding the plasmalogen phospholipid structures, positive ion MS/MS analysis of the protonated molecular ions enabled non ambiguous class identification, due to the generation of the diagnostic phosphocholine ion at m/z 184. Negative ion MS/MS spectra obtained for the corresponding $[M-CH_3]$ precursor ions showed signals corresponding to the loss of a ketene or fatty acid, for the chain linked through an ester bond to glycerol. In the MS_3

spectra, ions generated from the loss of the ether-linked chain, as a vinyl alcohol, were observed.

Table 1 (IV-4.1.). Lipid compounds identified by HILIC×RP-ESI-MS/MS analysis of a mussel lipidome.

#	Class	PN	Chemical Formula	Species	Observed *m/z*	Calculated *m/z*	Ion
1	FFA	10	$C_{22}H_{31}O_2$	22:6	327.2335	327.2330	[M-H]-
2	FFA	10	$C_{20}H_{29}O_2$	20:5	301.2176	301.2173	[M-H]-
3	FFA	10	$C_{18}H_{27}O_2$	18:4	275.2022	275.2017	[M-H]-
4	FFA	12	$C_{20}H_{31}O_2$	20:4	303.2338	303.2330	[M-H]-
5	FFA	12	$C_{22}H_{33}O_2$	22:5	329.2491	329.2486	[M-H]-
6	FFA	12	$C_{18}H_{29}O_2$	18:3	277.2178	277.2173	[M-H]-
7	FFA	14	$C_{22}H_{35}O_2$	22:4	331.2649	331.2643	[M-H]-
8	FFA	14	$C_{20}H_{33}O_2$	20:3	305.2492	305.2486	[M-H]-
9	FFA	14	$C_{14}H_{27}O_2$	14:0	227.2022	227.2017	[M-H]-
10	FFA	14	$C_{16}H_{29}O_2$	16:1	253.2180	253.2173	[M-H]-
11	FFA	14	$C_{18}H_{31}O_2$	18:2	279.2335	279.2330	[M-H]-
12	FFA	15	$C_{15}H_{29}O_2$	15:0	241.2181	241.2173	[M-H]-
13	FFA	16	$C_{18}H_{33}O_2$	18:1	281.2492	281.2486	[M-H]-
14	FFA	16	$C_{16}H_{31}O_2$	16:0	255.2339	255.2330	[M-H]-
15	FFA	16	$C_{20}H_{35}O_2$	20:2	307.2650	307.2643	[M-H]-
16	FFA	16	$C_{22}H_{37}O_2$	22:3	333.2804	333.2799	[M-H]-
17	FFA	17	$C_{17}H_{33}O_2$	17:0	269.2491	269.2486	[M-H]-
18	FFA	18	$C_{18}H_{35}O_2$	18:0	283.2650	283.2643	[M-H]-
19	FFA	18	$C_{20}H_{37}O_2$	20:1	309.2802	309.2799	[M-H]-
20	FFA	18	$C_{22}H_{39}O_2$	22:2	335.2961	335.2956	[M-H]-

#	Class	PN	Chemical Formula	Species	Observed *m/z*	Calculated *m/z*	Ion
21	FFA	19	$C_{19}H_{37}O_2$	19:0	297.2806	297.2799	[M-H]-
22	FFA	20	$C_{20}H_{39}O_2$	20:0	311.2959	311.2956	[M-H]-
23	FFA	22	$C_{22}H_{43}O_2$	22:0	339.3274	339.3269	[M-H]-
24	Chol		$C_{27}H_{44}O$	Occelasterol	385.3471	385.3465	$[M+H]^+$
25	Chol		$C_{27}H_{44}O$	Desmosterol	385.3471	385.3465	$[M+H]^+$
26	Chol		$C_{27}H_{44}O$	22-dehydrocholesterol	385.3471	385.3465	$[M+H]^+$
27	Chol		$C_{27}H_{46}O$	Cholesterol	387.3628	387.3621	$[M+H]^+$
28	Chol		$C_{28}H_{46}O$	Brassicasterol	399.3618	399.3621	$[M+H]^+$
29	Chol		$C_{28}H_{48}O$	Campesterol	401.3783	401.3778	$[M+H]^+$
30	Chol		$C_{29}H_{48}O$	Isofucosterol	413.3774	413.3778	$[M+H]^+$
31	Chol		$C_{30}H_{52}O$	Dinosterol	429.4094	429.4091	$[M+H]^+$
32	Vit. D3		$C_{33}H_{52}O_8Na$	Hydroxyvitamin D3-glucoside	599.3562	599.3554	$[M+Na]^+$
33	WE	24	$C_{40}H_{64}O_2Na$	18:2/22:6	599.4802	599.4798	$[M+Na]^+$
34	WE	24	$C_{40}H_{64}O_2Na$	20:3/20:5	599.4802	599.4798	$[M+Na]^+$
35	WE	25	$C_{37}H_{62}O_2Na$	15:0/22:6	561.4650	561.4642	$[M+Na]^+$
36	WE	26	$C_{36}H_{62}O_2Na$	16:1/20:4	549.4647	549.4642	$[M+Na]^+$
37	WE	26	$C_{36}H_{62}O_2Na$	18:3/18:2	549.4647	549.4642	$[M+Na]^+$
38	WE	26	$C_{36}H_{62}O_2Na$	16:0/20:5	549.4647	549.4642	$[M+Na]^+$
39	WE	27	$C_{37}H_{64}O_2Na$	17:0/20:5	563.4802	563.4798	$[M+Na]^+$
40	WE	29	$C_{33}H_{64}O_2Na$	16:1/17:0	515.4791	515.4798	$[M+Na]^+$
41	WE	32	$C_{38}H_{70}O_2Na$	18:2/20:1	581.5273	581.5268	$[M+Na]^+$
42	WE	32	$C_{38}H_{70}O_2Na$	18:1/20:2	581.5273	581.5268	$[M+Na]^+$

#	Class	PN	Chemical Formula	Species	Observed *m/z*	Calculated *m/z*	Ion
43	WE	32	$C_{32}H_{64}O_2Na$	16:0/16:0	503.4789	503.4798	$[M+Na]^+$
44	WE	32	$C_{32}H_{64}O_2Na$	14:0/18:0	503.4789	503.4798	$[M+Na]^+$
45	WE	33	$C_{42}H62O_2Na$	22:6/20:5	621.4651	621.4642	$[M+Na]^+$
46	WE	34	$C_{42}H_{78}O_2Na$	22:2/20:1	637.5903	637.5894	$[M+Na]^+$
47	Tetraterpene		$C_{40}H_{52}$	Tetradehydro-β-carotene	532.4073	532.4069	$[M]^{+\cdot}$
48	Tetraterpene		$C_{40}H_{56}$	β-carotene	536.4386	536.4382	$[M]^{+\cdot}$
49	Tetraterpene		$C_{40}H_{58}$	7,8-Dihydro-β-carotene	538.4543	538.4539	$[M]^{+\cdot}$
50	Tetraterpene		$C_{40}H_{64}$	Phytoene	544.5011	544.5008	$[M]^{+\cdot}$
51	Tetraterpene		$C_{40}H_{54}O$	Echinenone	550.4178	550.4175	$[M]^{+\cdot}$
52	Tetraterpene		$C_{40}H_{56}O$	β-cryptoxanthin	552.4327	552.4331	$[M]^{+\cdot}$
53	Tetraterpene		$C_{40}H_{58}O$	3-Hydroxy-β-zeacarotene	554.4481	554.4488	$[M]^{+\cdot}$
54	Tetraterpene		$C_{40}H_{60}O$	Chloroxanthin	556.4653	556.4644	$[M]^{+\cdot}$
55	Tetraterpene		$C_{40}H_{52}O_2$	Alloxanthin	564.3964	564.3967	$[M]^{+\cdot}$
56	Tetraterpene		$C_{40}H_{54}O_2$	Diatoxanthin	566.4129	566.4124	$[M]^{+\cdot}$
57	Tetraterpene		$C_{40}H_{56}O_2$	Zeaxanthin	568.4285	568.4280	$[M]^{+\cdot}$
58	Tetraterpene		$C_{40}H_{56}O_2$	Lutein	568.4285	568.4280	$[M]^{+\cdot}$
59	Tetraterpene		$C_{40}H_{58}O_2$	Dihydrozeaxanthin	570.4444	570.4437	$[M]^{+\cdot}$
60	Tetraterpene		$C_{40}H_{58}O_2$	7,8-Dihydrozeaxanthin	570.4439	570.4437	$[M]^{+\cdot}$
61	Tetraterpene		$C_{40}H_{60}O_2$	7,8,7',8'- Tetrahydrozeaxanthin	572.4601	572.4593	$[M]^{+\cdot}$
62	Tetraterpene		$C_{40}H_{54}O_3$	Diadinoxanthin	582.4077	582.4073	$[M]^{+\cdot}$
63	Tetraterpene		$C_{40}H_{56}O_3$	19-Hydroxylutein	584.4236	584.4229	$[M]^{+\cdot}$
64	Tetraterpene		$C_{40}H_{56}O_3$	Capsanthin	584.4236	584.4229	$[M]^{+\cdot}$

#	Class	PN	Chemical Formula	Species	Observed *m/z*	Calculated *m/z*	Ion
65	Tetraterpene		$C_{40}H_{54}O_4$	Mytiloxanthin	598.4025	598.4022	$[M]^{+\cdot}$
66	Tetraterpene		$C_{40}H_{56}O_4$	Capsanthin 3,6-epoxide	600.4171	600.4179	$[M]^{+\cdot}$
67	Tetraterpene		$C_{40}H_{56}O_4$	Auroxanthin	600.4171	600.4179	$[M]^{+\cdot}$
68	Tetraterpene		$C_{40}H_{56}O_4$	Neoxanthin	600.4171	600.4179	$[M]^{+\cdot}$
69	Tetraterpene		$C_{40}H_{56}O_4$	Violaxanthin	600.4171	600.4179	$[M]^{+\cdot}$
70	Tetraterpene		$C_{40}H_{56}O_4$	Luteoxanthin	600.4171	600.4179	$[M]^{+\cdot}$
71	Tetraterpene		$C_{42}H_{58}O_6$	Fucoxanthin	658.4227	658.4233	$[M]^{+\cdot}$
72	CE	10	$C_{47}H_{74}O_2Na$	20:5	693.5590	693.5581	$[M+Na]^+$
73	CE	10	$C_{49}H_{76}O_2Na$	22:6	719.5741	719.5737	$[M+Na]^+$
74	CE	12	$C_{45}H_{74}O_2Na$	18:3	669.5587	669.5581	$[M+Na]^+$
75	CE	14	$C_{41}H_{72}O_2Na$	14:0	619.5431	619.5424	$[M+Na]^+$
76	CE	14	$C_{43}H_{74}O_2Na$	16:1	645.5573	645.5581	$[M+Na]^+$
77	CE	14	$C_{45}H_{76}O_2Na$	18:2	671.5731	671.5737	$[M+Na]^+$
78	CE	16	$C_{43}H_{76}O_2Na$	16:0	647.5735	647.5737	$[M+Na]^+$
79	CE	16	$C_{45}H_{78}O_2Na$	18:1	673.59.1	673.5894	$[M+Na]^+$
80	CE	18	$C_{45}H_{80}O_2Na$	18:0	675.6047	675.605	$[M+Na]^+$
81	CE	18	$C_{47}H_{82}O_2Na$	20:1	701.6211	701.6207	$[M+Na]^+$
82	TG	30	$C_{63}H_{96}NO_6$	18:4/20:5/22:6	962.7237	962.7232	$[M+NH_4]^+$
83	TG	32	$C_{63}H_{98}NO_6$	18:3/20:5/22:6	964.7395	964.7389	$[M+NH_4]^+$
84	TG	34	$C_{61}H_{98}NO_6$	16:1/20:5/22:6	940.7381	940.7389	$[M+NH_4]^+$
85	TG	34	$C_{59}H_{96}NO_6$	16:1/20:5/20:5	914.7236	914.7232	$[M+NH_4]^+$
86	TG	36	$C_{57}H_{96}NO_6$	14:0/18:3/22:6	890.7227	890.7232	$[M+NH_4]^+$

#	Class	PN	Chemical Formula	Species	Observed *m/z*	Calculated *m/z*	Ion
87	TG	36	$C_{55}H_{94}NO_6$	14:0/18:3/20:5	864.7074	864.7076	$[M+NH_4]^+$
88	TG	36	$C_{61}H_{100}NO_6$	16:0/20:5/22:6	942.7541	942.7545	$[M+NH_4]^+$
89	TG	36	$C_{61}H_{100}NO_6$	18:1/20:5/20:5	942.7541	942.7545	$[M+NH_4]^+$
90	TG	36	$C_{63}H_{102}NO_6$	16:0/22:6/22:6	968.7708	968.7702	$[M+NH_4]^+$
91	TG	36	$C_{63}H_{102}NO_6$	18:1/20:5/22:6	968.7708	968.7702	$[M+NH_4]^+$
92	TG	38	$C_{57}H_{98}NO_6$	14:0/18:2/22:6	892.7393	892.7389	$[M+NH_4]^+$
93	TG	38	$C_{57}H_{98}NO_6$	16:1/18:2/20:5	892.7393	892.7389	$[M+NH_4]^+$
94	TG	38	$C_{59}H_{100}NO_6$	16:0/18:3/22:6	918.7545	918.7545	$[M+NH_4]^+$
95	TG	38	$C_{59}H_{100}NO_6$	18:1/18:3/20:5	918.7545	918.7545	$[M+NH_4]^+$
96	TG	40	$C_{55}H_{98}NO_6$	14:0/16:0/22:6	868.7396	868.7389	$[M+NH_4]^+$
97	TG	40	$C_{59}H_{102}NO_6$	16:1/18:3/22:4	920.7705	920.7702	$[M+NH_4]^+$
98	TG	42	$C_{53}H_{98}NO_6$	14:0/16:0/20:4	844.7391	844.7389	$[M+NH_4]^+$
99	TG	42	$C_{59}H_{104}NO_6$	16:0/18:1/22:6	922.7865	922.7858	$[M+NH_4]^+$
100	TG	42	$C_{61}H_{106}NO_6$	18:0/18:3/22:5	948.8017	948.8015	$[M+NH_4]^+$
101	TG	42	$C_{57}H_{102}NO_6$	14:0/18:0/22:6	896.7699	896.7702	$[M+NH_4]^+$
102	TG	42	$C_{57}H_{102}NO_6$	16:0/16:0/22:6	896.7699	896.7702	$[M+NH_4]^+$
103	TG	44	$C_{59}H_{106}NO_6$	16:0/18:0/22:6	924.8009	924.8015	$[M+NH_4]^+$
104	TG	44	$C_{59}H_{106}NO_6$	16:1/20:2/20:3	924.8009	924.8015	$[M+NH_4]^+$
105	TG	44	$C_{51}H_{98}NO_6$	14:0/16:0/18:2	820.7394	820.7389	$[M+NH_4]^+$
106	TG	44	$C_{61}H_{108}NO_6$	18:0/18:1/22:6	950.8177	950.8171	$[M+NH_4]^+$
107	TG	46	$C_{53}H_{102}NO_6$	16:0/16:0/18:2	848.7703	848.7702	$[M+NH_4]^+$
108	TG	46	$C_{53}H_{102}NO_6$	14:0/18:0/18:2	848.7703	848.7702	$[M+NH_4]^+$

#	Class	PN	Chemical Formula	Species	Observed *m/z*	Calculated *m/z*	Ion
109	TG	46	$C_{57}H_{106}NO_6$	16:0/18:0/20:4	900.8022	900.8015	$[M+NH_4]^+$
110	TG	46	$C_{57}H_{106}NO_6$	18:0/18:1/18:3	900.8022	900.8015	$[M+NH_4]^+$
111	TG	48	$C_{51}H_{102}NO_6$	16:1/18:0/18:2	824.7710	824.7702	$[M+NH_4]^+$
112	TG	48	$C_{51}H_{102}NO_6$	15:0/16:0/17:0	824.7710	824.7702	$[M+NH_4]^+$
113	TG	48	$C_{51}H_{102}NO_6$	16:0/16:0/16:0	824.7710	824.7702	$[M+NH_4]^+$
114	TG	48	$C_{59}H_{110}NO_6$	18:0/18:2/20:2	928.8333	928.8328	$[M+NH_4]^+$
115	TG	48	$C_{53}H_{104}NO_6$	16:0/16:0/18:1	850.7862	850.7858	$[M+NH_4]^+$
116	Polyketide		$C_{24}H_{21}O_9$	Epigallocatechin coumarate	453.1195	453.1186	$[M+H]^+$
117	Polyketide		$C_{21}H_{25}O_{11}$	Epicatechin galactoside	453.1403	453.1397	$[M+H]^+$
118	Polyketide		$C_{23}H_{23}O_{11}$	Kaempferol 3-(4"-acetylrhamnoside)	475.1232	475.1240	$[M+H]^+$
119	Polyketide		$C_{25}H_{25}O_{14}$	Myricetin 3-(3",4"-diacetylrhamnoside)	549.1236	549.1244	$[M+H]^+$
120	Polyketide		$C_{24}H_{23}O_{14}$	Quercetin 3-(4"-malonylrhamnoside)	535.1091	535.1088	$[M+H]^+$
121	PA	20	$C_{47}H_{68}O_8P$	22:6/22:6	791.4662	791.4657	$[M-H]^-$
122	PA	26	$C_{41}H_{68}O_8P$	16:0/22:6	719.4661	719.4657	$[M-H]^-$
123	PA	26	$C_{41}H_{68}O_8P$	18:1/20:5	719.4661	719.4657	$[M-H]^-$
124	PA	26	$C_{41}H_{68}O_8P$	18:2/20:4	719.4661	719.4657	$[M-H]^-$
125	PA	28	$C_{41}H_{70}O_8P$	18:0/20:5	721.4822	721.4814	$[M-H]^-$
126	PA	34	$C_{45}H_{80}O_8P$	20:2/22:2	779.5589	779.5596	$[M-H]^-$
127	PI	28	$C_{45}H_{78}O_{13}P$	16:0/20:4	857.5180	857.5185	$[M-H]^-$
128	PI	28	$C_{45}H_{78}O_{13}P$	18:1/18:3	857.5180	857.5185	$[M-H]^-$
129	PI	30	$C_{41}H_{76}O_{13}P$	14:0/18:1	807.5032	807.5029	$[M-H]^-$
130	PI	30	$C_{41}H_{76}O_{13}P$	16:0/16:1	807.5032	807.5029	$[M-H]^-$

#	Class	PN	Chemical Formula	Species	Observed *m/z*	Calculated *m/z*	Ion
131	PI	30	$C_{43}H_{78}O_{13}P$	14:0/20:2	833.5186	833.5185	$[M-H]^-$
132	PI	30	$C_{43}H_{78}O_{13}P$	16:1/18:1	833.5186	833.5185	$[M-H]^-$
133	PS	25	$C_{43}H_{71}NO_{10}P$	15:0/22:6	792.4823	792.4821	$[M-H]^-$
134	PS	32	$C_{42}H_{77}NO_{10}P$	14:0/22:2	786.5296	786.5290	$[M-H]^-$
135	PS	32	$C_{42}H_{77}NO_{10}P$	16:0/20:2	786.5296	786.5290	$[M-H]^-$
136	PS	32	$C_{42}H_{77}NO_{10}P$	18:0/18:2	786.5296	786.5290	$[M-H]^-$
137	PE	26	$C_{43}H_{75}NO_8P$	16:0/22:6	764.5221	764.5225	$[M+H]^+$
138	PE	26	$C_{43}H_{75}NO_8P$	18:1/20:5	764.5221	764.5225	$[M+H]^+$
139	PE	28	$C_{45}H_{79}NO_8P$	18:0/22:6	792.5533	792.5538	$[M+H]^+$
140	PnE		$C_{43}H_{77}NO_7P$	P-18:0/20:5	750.5428	750.5432	$[M+H]^+$
141	PnE		$C_{43}H_{77}NO_7P$	P-18:1/20:4	750.5428	750.5432	$[M+H]^+$
142	PnE		$C_{43}H_{77}NO_7P$	O-16:0/22:6	750.5428	750.5432	$[M+H]^+$
143	PnE		$C_{45}H_{81}NO_7P$	P-18:0/22:5	778.5744	778.5745	$[M+H]^+$
144	PnE		$C_{43}H_{79}NO_7P$	P-18:0/20:4	752.5593	752.5589	$[M+H]^+$
145	PnE		$C_{39}H_{77}NO_7P$	O-14:0/20:2	702.5430	702.5432	$[M+H]^+$
146	PnE		$C_{39}H_{77}NO_7P$	O-16:0/18:2	702.5430	702.5432	$[M+H]^+$
147	PnE		$C_{39}H_{77}NO_7P$	P-14:0/20:1	702.5430	702.5432	$[M+H]^+$
148	PnE		$C_{39}H_{77}NO_7P$	P-16:0/18:1	702.5430	702.5432	$[M+H]^+$
149	PnE		$C_{39}H_{77}NO_7P$	P-16:1/18:0	702.5430	702.5432	$[M+H]^+$
150	PnE		$C_{41}H_{79}NO_7P$	P-18:2/18:0	728.5596	728.5589	$[M+H]^+$
151	PnE		$C_{41}H_{79}NO_7P$	P-16:0/20:2	728.5596	728.5589	$[M+H]^+$
152	PnE		$C_{41}H_{81}NO_7P$	P-18:1/18:0	730.5744	730.5745	$[M+H]^+$

#	Class	PN	Chemical Formula	Species	Observed *m/z*	Calculated *m/z*	Ion
153	PnE		$C_{41}H_{81}NO_7P$	P-16:0/20:1	730.5744	730.5745	$[M+H]^+$
154	PnE		$C_{41}H_{81}NO_7P$	O-16:0/20:2	730.5744	730.5745	$[M+H]^+$
155	PnE		$C_{43}H_{83}NO_7P$	P-18:0/20:2	756.5909	756.5902	$[M+H]^+$
156	PnE		$C_{43}H_{83}NO_7P$	P-18:1/20:1	756.5909	756.5902	$[M+H]^+$
157	PnE		$C_{43}H_{85}NO_7P$	P-18:0/20:1	758.6055	758.6058	$[M+H]^+$
158	PnE		$C_{45}H_{87}NO_7P$	P-18:0/22:2	784.6217	784.6215	$[M+H]^+$
159	PnE		$C_{45}H_{87}NO_7P$	P-20:1/20:1	784.6217	784.6215	$[M+H]^+$
160	LPE	10	$C_{25}H_{43}NO_7P$	20:5	500.2778	500.2772	$[M+H]^+$
161	LPE	10	$C_{27}H_{45}NO_7P$	22:6	526.2932	526.2928	$[M+H]^+$
162	LPE	18	$C_{23}H_{49}NO_7P$	18:0	482.3239	482.3241	$[M+H]^+$
163	CAEP	24	$C_{38}H_{68}N_2O_5P$	d18:3/18:3	663.4861	663.4865	$[M+H]^+$
164	CAEP	27	$C_{39}H_{72}N_2O_5P$	d20:5/17:0	679.5177	679.5178	$[M+H]^+$
165	CAEP	28	$C_{36}H_{70}N_2O_5P$	d18:3/16:0	641.5021	641.5017	$[M+H]^+$
166	CAEP	28	$C_{38}H_{72}N_2O_5P$	d18:3/18:1	667.5171	667.5178	$[M+H]^+$
167	CAEP	29	$C_{37}H_{72}N_2O_5P$	d18:3/17:0	655.5173	655.5173	$[M+H]^+$
168	CAEP	29	$C_{39}H_{74}N_2O_5P$	d20:4/17:0	681.5339	681.5335	$[M+H]^+$
169	CAEP	30	$C_{34}H_{70}N_2O_5P$	d16:1/16:0	617.5014	617.5017	$[M+H]^+$
170	CAEP	30	$C_{38}H_{74}N_2O_5P$	d18:3/18:0	669.5327	669.5330	$[M+H]^+$
171	CAEP	32	$C_{36}H_{74}N_2O_5P$	d18:1/16:0	645.5325	645.5330	$[M+H]^+$
172	CAEP	32	$C_{38}H_{76}N_2O_5P$	d18:2/18:0	671.5488	671.5486	$[M+H]^+$
173	PC	20	$C_{46}H_{75}NO_8P$	18:4/20:5	800.5229	800.5225	$[M+H]^+$
174	PC	20	$C_{50}H_{79}NO_8P$	20:5/22:6	852.5542	852.5538	$[M+H]^+$

#	Class	PN	Chemical Formula	Species	Observed *m/z*	Calculated *m/z*	Ion
175	PC	22	$C_{44}H_{75}NO_8P$	18:3/18:4	776.5229	776.5225	$[M+H]^+$
176	PC	22	$C_{46}H_{77}NO_8P$	18:3/20:5	802.5381	802.5381	$[M+H]^+$
177	PC	24	$C_{42}H_{75}NO_8P$	14:0/20:5	752.5228	752.5225	$[M+H]^+$
178	PC	24	$C_{44}H_{77}NO_8P$	14:0/22:6	778.5379	778.5382	$[M+H]^+$
179	PC	24	$C_{44}H_{77}NO_8P$	16:1/20:5	778.5379	778.5382	$[M+H]^+$
180	PC	25	$C_{46}H_{79}NO_8P$	18:2/20:5	804.5532	804.5538	$[M+H]^+$
181	PC	25	$C_{45}H_{79}NO_8P$	15:0/22:6	792.5533	792.5538	$[M+H]^+$
182	PC	25	$C_{43}H_{77}NO_8P$	15:0/20:5	766.5388	766.5382	$[M+H]^+$
183	PC	26	$C_{44}H_{79}NO_8P$	16:0/20:5	780.5531	780.5538	$[M+H]^+$
184	PC	26	$C_{44}H_{79}NO_8P$	16:1/20:4	780.5531	780.5538	$[M+H]^+$
185	PC	26	$C_{46}H_{81}NO_8P$	16:0/22:6	806.5699	806.5695	$[M+H]^+$
186	PC	26	$C_{42}H_{77}NO_8P$	16:1/18:3	754.5378	754.5382	$[M+H]^+$
187	PC	27	$C_{45}H_{81}NO_8P$	17:0/20:5	794.5701	794.5695	$[M+H]^+$
188	PC	28	$C_{42}H_{79}NO_8P$	16:0/18:3	756.5533	756.5538	$[M+H]^+$
189	PC	28	$C_{42}H_{79}NO_8P$	16:1/18:2	756.5533	756.5538	$[M+H]^+$
190	PC	28	$C_{38}H_{75}NO_8P$	14:0/16:1	704.5227	704.5225	$[M+H]^+$
191	PC	28	$C_{44}H_{81}NO_8P$	16:0/20:4	782.5691	782.5694	$[M+H]^+$
192	PC	28	$C_{44}H_{81}NO_8P$	18:4/18:0	782.5691	782.5694	$[M+H]^+$
193	PC	28	$C_{44}H_{81}NO_8P$	18:3/18:1	782.5691	782.5694	$[M+H]^+$
194	PC	30	$C_{40}H_{79}NO_8P$	14:0/18:1	732.5531	732.5538	$[M+H]^+$
195	PC	30	$C_{40}H_{79}NO_8P$	16:0/16:1	732.5531	732.5538	$[M+H]^+$
196	PC	30	$C_{42}H_{81}NO_8P$	16:0/18:2	758.5701	758.5695	$[M+H]^+$

#	Class	PN	Chemical Formula	Species	Observed *m/z*	Calculated *m/z*	Ion
197	PC	30	$C_{42}H_{81}NO_8P$	16:1/18:1	758.5701	758.5695	$[M+H]^+$
198	PC	32	$C_{42}H_{83}NO_8P$	16:0/18:1	760.5859	760.5851	$[M+H]^+$
199	PC	32	$C_{42}H_{83}NO_8P$	16:1/18:0	760.5859	760.5851	$[M+H]^+$
200	PC	32	$C_{44}H_{85}NO_8P$	16:1/20:1	786.6011	786.6008	$[M+H]^+$
201	PC	32	$C_{40}H_{81}NO_8P$	16:0/16:0	734.5702	734.5695	$[M+H]^+$
202	PC	34	$C_{46}H_{89}NO_8P$	18:0/20:2	814.6322	814.6321	$[M+H]^+$
203	PC	34	$C_{44}H_{87}NO_8P$	16:1/20:0	788.6159	788.6164	$[M+H]^+$
204	PnC		$C_{43}H_{79}NO_7P$	O-15:0/20:5	752.5591	752.5594	$[M+H]^+$
205	PnC		$C_{44}H_{81}NO_7P$	O-16:0/20:5	766.5739	766.5745	$[M+H]^+$
206	PnC		$C_{44}H_{79}NO_7P$	P-16:0/20:5	764.5591	764.5589	$[M+H]^+$
207	PnC		$C_{44}H_{79}NO_7P$	O-14:0/22:6	764.5598	764.5594	$[M+H]^+$
208	PnC		$C_{45}H_{81}NO_7P$	P-17:0/20:5	778.5748	778.5751	$[M+H]^+$
209	PnC		$C_{46}H_{83}NO_7P$	P-18:0/20:5	792.5909	792.5902	$[M+H]^+$
210	PnC		$C_{46}H_{85}NO_7P$	P-18:0/20:4	794.6054	794.6058	$[M+H]^+$
211	PnC		$C_{48}H_{87}NO_7P$	P-20:0/20:5	820.6221	820.6215	$[M+H]^+$
212	PnC		$C_{40}H_{81}NO_7P$	P-16:0/16:0	718.5744	718.5745	$[M+H]^+$
213	PnC		$C_{40}H_{83}NO_7P$	O-16:0/16:0	720.5903	720.5902	$[M+H]^+$
214	LPC	10	$C_{28}H_{49}NO_7P$	20:5	542.3238	542.3241	$[M+H]^+$
215	LPC	10	$C_{30}H_{51}NO_7P$	22:6	568.3394	568.3398	$[M+H]^+$
216	LPC	12	$C_{28}H_{51}NO_7P$	20:4	544.3395	544.3398	$[M+H]^+$
217	LPC	12	$C_{26}H_{49}NO_7P$	18:3	518.3239	518.3241	$[M+H]^+$
218	LPC	16	$C_{24}H_{51}NO_7P$	16:0	496.3396	496.3398	$[M+H]^+$

#	Class	PN	Chemical Formula	Species	Observed *m/z*	Calculated *m/z*	Ion
219	LPC	16	$C_{26}H_{53}NO_7P$	18:1	522.3551	522.3554	$[M+H]^+$
220	LPC	17	$C_{25}H_{53}NO_7P$	17:0	510.3558	510.3554	$[M+H]^+$
221	LPC	18	$C_{26}H_{55}NO_7P$	18:0	524.3713	524.3711	$[M+H]^+$
222	LPC	18	$C_{28}H_{57}NO_7P$	20:1	550.3869	550.3867	$[M+H]^+$
223	LPnC		$C_{26}H_{55}NO_6P$	P-18:0	508.3768	508.3762	$[M+H]^+$
224	LPnC		$C_{28}H_{59}NO_6P$	P-20:0	536.4077	536.4075	$[M+H]^+$
225	LPnC		$C_{26}H_{57}NO_6P$	O-18:0	510.3911	510.3918	$[M+H]^+$
226	LPnC		$C_{24}H_{53}NO_6P$	O-16:0	482.3611	482.3605	$[M+H]^+$

4.1.3.3. Offline HILIC-RP-LC

Under the separation/analysis conditions employed, it was not possible to infer the exact FA composition of the lipid species identified, in terms of structural isomers and stereoisomers. Thus, in a next step, the separated PC species have been selected as a case study, and subjected to further investigation by GC-MS, to demonstrate the capability of the technique to handle such a task. To this purpose, a HILIC column of conventional I.D. (for higher load capacity with respect to the one used in the online approach) was employed to achieve class-type separation of the PCs, from the whole polar lipids obtained upon SPE-fractionation of the mussel lipid extract. Once collected and evaporated to dryness, the PC fraction was reinjected onto a long C18 column, for subsequent separation of the individual molecular species, which was achieved isocratically.

4.1.3.4. GC-MS analyses

In order to highlight the FAs composition of the different species belonging to the PC class, and eventually elucidate the *cis/trans* geometry, the offline collected fractions, as separated according to their partition number by RP-LC (Supplementary Figure 7S (IV-4.1.) in Supplementary Material), were analysed by GC-MS. To this purpose, a 200-m highly polar ionic liquid stationary phase has been employed, as previously reported in the literature [42], a dedicated MS database of the standard FAMEs was constructed in lab, and the linear retention indices (LRI) of the separated lipid species were calculated. A total of 74 different FAMEs have been included in the MS database, together with their LRIs calculated against an homologue series of C4-C24 ethyl esters fatty acids (FAEEs). In more detail, 10 compounds from C4-C24 even carbon saturated FAMEs, 4 linoleic acid methyl esters, *cis/trans*-isomers; 8 linolenic acid methyl

esters isomer mix; 22 from Supelco 37 Components FAME Mix; 4 from PUFA No.1 marine source FAMEs; 2 from PUFA No.2 animal source FAMEs; 4 from PUFA No.3 menhaden oil FAMEs; 6 from bacterial acid methyl esters (BAME) mix; 14 from the AOCS official method margarine FAMEs. The chromatographic conditions were optimized with the aim to obtain the separation of the geometric isomers using the splitless mode followed by isothermal steps, and the following conditions were selected: after 1 min of splitless, the oven temperature was rapidly increased to a first isothermal step at 160 °C, followed by a second isothermal step at 185 °C, at the end of which a temperature gradient allowed elution of the most retained components. In such a way, the total run time was conveniently shortened, as well. All the peaks separated within the PC fraction, with PN values in the 20-34 range (Supplementary Figure 7S (IV-4.1.) in Supplementary Material), have been subjected to transesterification prior to injection in GC. For the preparation of the FAME derivatives, special attention has been paid on the selection of the most suitable methylating agent and the reaction conditions; given that the sample is characterized by the presence of PUFAs, mostly represented by EPA (20:5 ω-3) and DHA (22:6 ω-3), vigorous conditions have been avoided, to prevent their degradation [43]. It has been shown that simple lipids like TGs can be completely transesterified in less than 5 min, and PCs in only 1 min, at room temperature [44,45]. Commonly, using basic reagents, the esters will form an anionic intermediate, and to this regard the use of dehydrated reagents is crucial for the transesterification, since the presence of water could lead to the formation of free acids from the anionic intermediate, as a side reaction. In the light of such premises, derivatization of the offline collected PC fractions was carried out in a basic medium, at room temperature, by using dehydrated potassium hydroxide in the presence of a large excess amount of methanol. After 2 min, the reaction was stopped by addition of a diluted acid to neutralize

the base. As illustrative examples, Supplementary Figures 8S and 9S (IV-4.1.) (in Supplementary Material) show the GC-MS chromatograms of the FAMEs obtained from the two most abundant peaks isolated from the PC fraction, eluting in RP-LC according to PN=26 and PN=28, respectively. The GC separation and identification of peak 8 showed evidence of the presence of Me.C16:0 (MS similarity 99%, LRI_{Theor}1563, LRI_{Exp}1560) and Me.C22:6n3 (4Z,7Z,10Z,13Z,16Z,19Z) (MS similarity 99%, LRI_{Theor}2652, LRI_{Exp}2654). From the combination of the two, a PN value of 26 could be derived for PC(16:0/22:6) (Supplementary Figure 8S (IV-4.1.) in Supplementary Material). Me.C14:0 (MS similarity 99%, LRI_{Theor}1362, LRI_{Exp}1361), Me.C16:0 (MS similarity 99%, LRI_{Theor}1563, LRI_{Exp}1560), Me.C16:1n7 (9Z) (MS similarity 99%, LRI_{Theor}1662, LRI_{Exp}1663), and Me.C20:4n6 (5Z,8Z,11Z,14Z) (MS similarity 92%, LRI_{Theor}2334, LRI_{Exp}2337) have been identified, as co-eluted within peak 11 (Supplementary Figure 9S (IV-4.1.) in Supplementary Material), given the presence of individual PC species with the same PN value of 28, and namely: PC(14:0/16:1) and PC(16:0/20:4).

4.1.4. Conclusions

In this research, an "omic" approach was developed for quick fingerprinting of total lipids in complex samples, and demonstrated for the separation and identification of the lipidome extracted from bivalve molluscs. To the best of our knowledge, this represents the first online HILIC×RP-LC-MS/MS method, allowing for the simultaneous analysis of both the polar and neutral lipids. The two-dimensional comprehensive approach afforded both class-type and individual species separation, with no increase of the overall analysis time, with respect to monodimensional approaches. As a practical restraint, the separation capability of the RP-LC separation is sacrificed in ^{2}D, due to the limited time (2-min) allotted for analysis and subsequent injection of each transferred

fraction eluted from ^{1}D; nevertheless it was possible to achieve lipid assignment and structure annotation for the separated lipid compounds. The use of a soft ionization mode (ESI) has the advantage of negligible in-source dissociation of ions during MS analysis of different classes of intact lipids (unlike more commonly employed APCI-MS), thus enabling more reliable quantization of labile compounds, if desired.

Furthermore, it is demonstrated how the combined use of LRI values on a highly polar ionic liquid column is practicable to achieve unambiguous identification of the FAs contained in the lipid species through database search, whereas the use of spectral similarity alone would fail. Noticeably, the experimental LRI values derived on the IL stationary phase were in good agreement with the theoretical ones, and comparable to those obtained on the most widespread apolar column.

REFERENCES

[1] Teslovich TM, Musunuru K, […], Kathiresan S. Biological, clinical and population relevance of 95 loci for blood lipids. Nature. 2010;466:707-13.

[2] Akoh CC. Food lipids: chemistry, nutrition, and biotechnology. 4th ed. Boca Raton: CRC Press; 2017.

[3] Hyötyläinen T, Orešič M. Optimizing the lipidomics workflow for clinical studies - practical considerations. Anal Bioanal Chem. 2015;407:4973-93.

[4] Donato P, Cacciola F, Beccaria M, Dugo P, Mondello L. Lipidomics. In: Picò Y, editor. Advanced mass spectrometry for food safety and quality. Amsterdam: Elsevier; 2015. pp. 395-439.

[5] Donato P, Inferrera I, Sciarrone D, Mondello L. Supercritical fluid chromatography for lipid analysis in foodstuffs. J Sep Sci. 2017;40:361-82.

[6] Beccaria M, Sullini G, Cacciola F, Donato P, Dugo P, Mondello L. High performance characterization of triacylglycerols in milk and milk-related

samples by liquid chromatography and mass spectrometry. J Chromatogr A. 2014;1360:172-87.

[7] Lísa M, Holčapek M. Triacylglycerols profiling in plant oils important in food industry, dietetics and cosmetics using high performance liquid chromatography-atmospheric pressure chemical ionization mass spectrometry. J Chromatogr A. 2008;1198:115-30.

[8] Hutchins PM, Barkley RM, Murphy RC. Separation of cellular non polar neutral lipids by normal-phase chromatography and analysis by electrospray ionization mass spectrometry. J Lipid Res. 2008;49:804-13.

[9] Donato P, Cacciola F, Cichello F, Russo M, Dugo P, Mondello L. Determination of phospholipids in milk samples by means of hydrophilic interaction liquid chromatography coupled to evaporative light scattering and mass spectrometry detection. J Chromatogr A. 2011;1218:6476-82.

[10] Tranchida PQ, Donato P, Dugo P, Dugo G, Mondello L. Comprehensive chromatographic methods for the analysis of lipids. TrAC Trends Anal Chem. 2007;26:191-205.

[11] Jandera P. Column selectivity for two-dimensional liquid chromatography. J Sep Sci. 2006;29:1763-83.

[12] Jandera P. Comprehensive two-dimensional liquid chromatography - practical impacts of theoretical considerations. A review. Cent Eur J Chem. 2012;10:844-75.

[13] Dugo P, Fawzy N, Cichello F, Cacciola F, Donato P, Mondello L. Stop-flow comprehensive two-dimensional liquid chromatography combined with mass spectrometric detection for phospholipid analysis. J Chromatogr A. 2013;1278:46-53.

[14] Lísa M, Cífková E, Holčapek M. Lipidomic profiling of biological tissues using off-line two-dimensional high-performance liquid chromatography-mass spectrometry. J Chromatogr A. 2011;1218:5146-56.

[15] Li M, Tong X, Lv P, Feng B, Yang L, Wu Z, Cui X, Bai Y, Huang Y, Liu H. A not-stop-flow online normal-/reversed-phase two-dimensional liquid chromatography–quadrupole time-of-flight mass spectrometry method for comprehensive lipid profiling of human plasma from atherosclerosis patients. J Chromatogr A. 2014;1372:110-9.

[16] Donato P, Cacciola F, Tranchida PQ, Dugo P, Mondello L. Mass spectrometry detection in comprehensive liquid chromatography: basic concepts, instrumental aspects, applications and trends. Mass Spectr Rev. 2012;31:523-59.

[17] Holčapek M, Ovčačíková M, Lísa M, Cífková E, Hájek T. Continuous comprehensive two-dimensional liquid chromatography–electrospray ionization mass spectrometry of complex lipidomic samples. Anal Bioanal Chem. 2015;407:5033–43.

[18] Baglai A, Gargano AFG, Jordens J, Mengerink Y, Honing M, van der Wal S, Schoenmakers PJ. Comprehensive lipidomic analysis of human plasma using multidimensional liquid- and gas-phase separations: two-dimensional liquid chromatography-mass spectrometry vs. liquid chromatography-trapped-ion-mobility-mass spectrometry. J Chromatogr A. 2017;1530:90-103.

[19] Cajka T, Fiehn P. Comprehensive analysis of lipids in biological systems by liquid chromatography-mass spectrometry. TrAC Trends Anal Chem. 2014;61:192-206.

[20] Zoccali M, Schug KA, Walsh P, Smuts J, Mondello L. Flow-modulated comprehensive two-dimensional gas chromatography combined with a vacuum ultraviolet detector for the analysis of complex mixtures. J Chromatogr A. 2017;1497:135-43.

[21] Delmonte P, Fardin-Kia AR, Rader JI. Separation of fatty acid methyl esters by GC-online hydrogenation×GC. Anal Chem. 2013;85:1517-24.

[22] Anderson JL, Armstrong DW. High-stability ionic liquids. A new class of stationary phases for gas chromatography. Anal Chem. 2003;75:4851-8.

[23] Amaral MSS, Marriott PJ, Bizzo HR et al. Ionic liquid capillary columns for analysis of multi-component volatiles by gas chromatography-mass spectrometry: performance, selectivity, activity and retention indices. Anal Bioanal Chem. 2017; doi:10.1007/s00216-017-0718-7.

[24] Delmonte P, Fardin-Kia AR, Kramer JKG, Mossoba MM, Sidisky L, Rader, J. Separation characteristics of fatty acid methyl esters using SLB-IL111, a new ionic liquid coated capillary gas chromatographic column. J Chromatogr A. 2011;1218:545-54.

[25] Zapadlo Michal, Krupcik J, Májek P, Armstrong DW, Sandra P. Use of a polar ionic liquid as second column for the comprehensive two-dimensional GC separation of PCBs. J Chromatogr A. 2010;1217:5859-67.

[26] Seeley JV, Seeley SK, Libby EK, Breitbach ZS, Armstrong DW. Comprehensive two-dimensional gas chromatography using a high-temperature phosphonium ionic liquid column. Anal Bioanal Chem. 2008;390:323-32.

[27] Fanali C, Micalizzi G, Dugo P, Mondello L. Ionic liquids as stationary phases for fatty acid analysis by gas chromatography. Analyst. 2017; doi:10.1039/c7an01338h.

[28] Albergamo A, Rigano F, Purcaro G, Mauceri A, Fasulo S, Mondello L. Free fatty acid profiling of marine sentinels by nanoLC-EI-MS for the assessment of environmental pollution effects. Sci Tot Environ. 2016;571:955-62.

[29] Martínez-Pita I, Sánchez-Lazo C, Ruíz-Jarabo R, Herrera M, Mancera JM. Biochemical composition, lipid classes, fatty acids and sexual hormones in the mussel Mytilus galloprovincialis from cultivated populations in south Spain. Aquaculture. 2012;358-359:274-83.

[30] Rigano F, Albergamo A, Sciarrone D, Beccaria M, Purcaro G, Mondello L. Nano liquid chromatography directly coupled to electron ionization mass spectrometry for free fatty acid elucidation in mussel. Anal. Chem. 2016;88:4021-28.

[31] Bligh EG, Dyer WG. A rapid method of total lipid extraction and purification. Can J Biochem Phys. 1959;37:911-7.

[32] OECD, Test No. 305: Bioaccumulation in Fish: Aqueous and Dietary Exposure, OECD Publishing, Paris, 2012; doi:10.1787/9789264185296-en

[33] Zhu C, Dane A, Spijksma G, Wang M, van der Greef J, Luo G, Hankemeier T, Vreeken RJ. An efficient hydrophilic interaction liquid chromatography separation of 7 phospholipid classes based on a diol column. J Chromatogr A. 2012;1220:26-34.

[34] Facchini L, Losito I, Cataldi TR, Palmisano F. Seasonal variations in the profile of main phospholipids in Mytilus galloprovincialis mussels: a study by hydrophilic interaction liquid chromatography-electrospray ionization Fourier transform mass spectrometry. J Mass Spectrom. 2017; doi: 10.1002/jms.4029.

[35] Facchini L, Losito I, Cataldi TR, Palmisano F. Ceramide lipids in alive and thermally stressed mussels: an investigation by hydrophilic interaction liquid chromatography-electrospray ionization Fourier transform mass spectrometry. J Mass Spectrom. 2016;51:768-81.

[36] Jandera P. Programmed elution in comprehensive two-dimensional liquid chromatography. J Chromatogr A. 2012;1255:112-29.

[37] Jandera P, Hájek T, Cesla P. Comparison of various second-dimension gradient types in comprehensive two-dimensional liquid chromatography. J Sep Sci. 2010;33:1382-97.

[38] Pirok BWJ, Gargano AFG, Schoenmakers PJ. Optimizing separations in online comprehensive two-dimensional liquid chromatography. J Sep Sci. 2017;1-30. doi: 10.1002/jssc.201700863.

[39] Donato P, Rigano F, Cacciola F, Schure M, Farnetti S, Russo M, Dugo P, Mondello L. Comprehensive two-dimensional liquid chromatography–tandem mass spectrometry for the simultaneous determination of wine polyphenols and target contaminants. J Chromatogr A. 2016;1458:54-62.

[40] Murphy KJ, Mooney BD, Mann NJ, Nichols PD, Sinclair AJ. Lipid, FA, and sterol composition of New Zealand green lipped mussel (Pernacanaliculus) and Tasmanian blue mussel (Mytilusedulis). Lipids. 2002;37:587-95.

[41] Gorinstein S, Moncheva S, Katrich E, Toledo F, Arancibia P, Goshev I, Trakhtenberg S. Antioxidants in the black mussel (Mytilus galloprovincialis) as an indicator of black sea coastal pollution. Mar Pollut Bull. 2003;46:1317-25.

[42] Delmonte P, Fardin-Kia AR, Kramer JKG, Mossoba MM, Sidisky L, Tyburczy C, Rader JI. Evaluation of highly polar ionic liquid gas chromatographic column for the determination of the fatty acids in milk fat. J Chromatogr A. 2012;1233:137-46.

[43] Christie WW. Preparation of ester derivatives of fatty acids for chromatographic analysis. In: Christie WW, editor. Advances in Lipid Methodology – Two. Dundee: Oily Press; 1993.pp. 69-111.

[44] Marinetti GV. Hydrolysis of lecithin with sodium methoxide. Biochemistry 1962;1:350-3.

[45] Marinetti GV. Low temperature partial alcoholysis of triglycerides. J Lipid Res. 1966;7:786-8.

CHAPTER V
Carbon-dioxide based techniques for the analysis of lipids and lipid-like compounds

5.1. Supercritical fluid chromatography×ultrahigh pressure liquid chromatography for red chilli pepper fingerprinting by photodiode array, quadrupole-time-of-flight and ion mobility mass spectrometry (SFC×RP-UHPLC-PDA-QToF MS-IMS)

5.1.1. Introduction

Applications based on two-dimensional separation techniques have grown exponentially over the last decade, along with the increased demand for deeper and more precise analysis. For the investigation of non volatile compounds, the coupling of two liquid chromatography dimensions (LC) has succeeded to meet the high complexity of many natural and synthetic samples, especially in the comprehensive mode (LC×LC) in which the whole effluent is transferred from a first (^{1}D) to a second (^{2}D) separation dimension. Although being more difficult to implement, on-line approaches bring a series of fair advantages with respect to off-line methods: first, the fully automated solute transfer between the two separation dimensions, with no flow interruption, this implies no increase in the analysis time, and also greater analytical repeatability. Moreover, sample handling is minimized and, as a consequence, risks of sample deterioration, loss, or artifact formation. A number of theoretical and practical issues and restraints must be considered, when developing on-line 2D methods; these include the choice of column stationary phase and dimensions, the mobile phase flow rate and composition, the design of optimum gradient profiles (in terms of compatibility and peak capacity generation), the fraction volume and

the transfer frequency (both affecting peak focusing at the head of the ^{2}D column). Last but not least, dedicated software for processing of 2D data is needed, as well as an interface for the coupling of the two separation dimensions [1]. Most LC×LC systems implemented so far were based on the use of two-position, 10-, 8-, or 6-port switching valves equipped with symmetrical sample loops of identical volumes, alternately filled with the effluent from the first column at each sampling period (modulation time). Since at each valve switching the loop content will be transferred onto the ^{2}D column by the ^{2}D mobile phase, a stringent requirement is that the sampling period be equal to the ^{2}D analysis time; the latter thus need to be fast enough to avoid incomplete analyte elution and wrap-around phenomena. To this regard, the use of sub- 2 □ m or partially porous particles [2], as well as monodisperse material [3], even operated at high temperature, may be helpful. Two-dimensional LC systems based on the coupling of identical or similar stationary phases are easily implemented, given the full compatibility of mobile phases, however the correlation of retention mechanisms will afford little orthogonality, i.e., coverage of the 2D space available for the separation [4].

On the other hand, the maximum gain in separation power will result from the selection of two orthogonal (independent) retention mechanisms; narrow- or microbore columns are often used as ^{1}D, and operated at sub-optimum mobile phase flow rates to reduce the occurrence of possible solvent strength mismatch and band broadening connected to the transfer from ^{1}D to ^{2}D [5]. From a detection standpoint, the hyphenation to mass spectrometry (MS) offers additional degrees of freedom, either employing tandem MS techniques to obtain structure elucidation, or using high- or ultra-high mass resolution [6,7]. Analysis of food and food-related compounds has been one major field of application of LC×LC-MS platforms, devoted to the evaluation of sample quality and authenticity, and possibly to the identification of molecules with

beneficial or toxic effects on human health [8]. Among the latter, carotenoids have attracted a great deal of interest, because of their potential beneficial health properties, such as antioxidant activity [9], prevention of metabolic disorders [10], cardiovascular diseases [11] and cancer [12]. Carotenoids are natural pigments widely diffuse in plants, algae, fungi and bacteria; moreover animals and human rely on food-borne carotenoids as visual pigments, antioxidants, or colorants. Their basic structure consist of a C_{40}-tetraterpenoid symmetrical skeleton, from which different modifications can occur, giving rise to a wide array of compounds: addition of oxygen functions, hydrogenation and dehydrogenation, cyclization at one or both ends, rearrangement. Formally, two types of carotenoids can be discerned: carotenes (hydrocarbon carotenoids) such as β-carotene and lycopene, and xanthophylls (oxygenated carotenoids) such as lutein and β-cryptoxanthin; mono- or dihydroxylated carotenoids may occur in their free from or in the more stable esterified form [13]. Analysis of the intact carotenoid esters, i.e. the unsaponified carotenoid fraction in food samples is a multifaceted concept, as they may be useful markers of product authenticity or may be used as a ripeness index; moreover carotenoids are commonly used as food and food additives ingredients and, thus, valuable information may be derived to help in dosing formulations and in predicting the bio-availability after intake [14]. Despite the obvious interest in such an investigation, a saponification step is instead often employed to reduce sample complexity prior to separation/analysis of the carotenoid fraction; apart from the loss of informative data, common drawbacks of this procedure consist in the likelihood of loss of compound, or isomerisation. The high variability in their chemical structure, their poor stability to air and light, and the scarcity of commercially available standards further contribute to make carotenoid analysis a quite challenging task [15].

Conventional techniques for carotenoid analysis have consisted in reversed

phase liquid chromatography (RP-LC) on C_{18} or C_{30} stationary phases, affording molecule separation according to hydrophobicity [16], whereas normal-phase LC (NP-LC) on silica-based columns is largely employed for carotenoid class separation, according to different polarity [17]. However, the huge number of carotenoids found in foodstuffs, with high degree of structural similarity, often lead to chromatographic co-elutions, when using mono-dimensional LC techniques. As a consequence, several LC×LC approaches have been developed, in order to achieve enhanced separation efficiency, and render identification more reliable; the majority of them consisted in the coupling of NP-LC to RP-LC [18], the latter also conveniently operated under ultra-high pressure conditions (RP-UHPLC), with fair advantages in terms of analysis, speed, sampling, and resolving power [19,20]. Although providing the best results in terms of orthogonality of the two chromatographic dimensions and peak capacity, this kind of coupling is quite cumbersome to implement, due to mobile phase incompatibility and peak focusing issues (solvents used for ^{1}D separation are strong eluent for the ^{2}D column). Since its inception, supercritical fluid chromatography (SFC) has proven to be a viable alternative to LC-based techniques, for the separation of low- to-medium polarity analytes, including carotenoids, with most applications devoted to analysis of foodstuffs [21-24]. As the primary component of the mobile phase in SFC, carbon dioxide (CO_2) offers superior solubility for carotenoids and promotes non-polar interactions between analytes and the mobile phase, thereby reducing the retention time. Moreover, the high diffusivity of CO_2 allows for high chromatographic efficiency at reduced pressure drop and with less organic solvent consumption.

In the present contribution, a novel SFC×RP-UHPLC system has been developed, configured around two 2-position, six-port switching valves equipped with octadecylsilica cartridges for effective trapping and focusing of

the analytes eluted from ^{1}D. In addition to photodiode array (PDA) and quadrupole-time-of-flight mass spectrometry (QToF MS) detection, ion mobility separation (IMS) based on analyte mass, shape and size added a fourth separation dimension for carotenoid fingerprinting in a red chilli pepper sample.

5.1.2. Materials and methods

5.1.2.1. Chemicals

Reagent grade methanol (MeOH), ethyl acetate, methyl tert-butyl ether (MTBE), petroleum ether (for sample preparation), LC-MS grade acetonitrile (ACN), isopropanol (IPA), methanol and water (H_2O) (for SFC×RP-UHPLC analyses) were supplied by Merck (Milan, Italy). Carbon dioxide (CO_2) 4.8 quality was from Rivoira (Milan, Italy).

Carotenoid standard, namely β-carotene, capsanthin, lutein, physalein, zeaxanthin were purchased from Extrasynthese (Genay, France).

5.1.2.2. Sample and sample preparation

The red chilli pepper sample (*Capsicum annuum L.*) was purchased in a local market. For extraction of the intact carotenoids, 200 g of red chilli pepper homogenate were treated with three consecutive 300-mL aliquots of a MeOH/ethyl acetate/petroleum ether (1:1:1, *v/v/v*) mixture. Combined extracts were then dissolved in 4 mL of MeOH/ MTBE (1:1, *v/v*) and afterward subjected to filtration through a 0.45 μm Acrodisc nylon membrane filter (Pall Life Sciences, Ann Arbor, MI, USA).

5.1.2.3. SFC×RP-UHPLC-QToF MS-IMS instrument

Instrumentation for the SFC analyses consisted of: Acquity UPC^2 Convergence Manager, Acquity UPC^2 Binary Solvent Manager, Acquity UPC^2 Sample Manager-FL, Acquity UPLC 30 cm Column Heater. Instrumentation for the

UHPLC analyses consisted of: Acquity Column Manager, Acquity UPLC Class Binary Solvent Manager, Isocratic Solvent Manager. The SFC×RP-UHPLC interface consisted of two 2-position/six-port switching valves (CM-A Acquity) equipped with two 1-μL empty sample loop (bridges) and two packed loops, controlled by an electronic device for the programmed actuation of the switching valves and the synchronization of the second dimension pump(s) and detector(s). The system was on-line hyphenated to Acquity UPLC PDA eλ Detector (with 500 nL flow cell) and Synapt G2-S*i* HDMS. All the instruments and devices were from Waters Corporation (Milford, MA, USA).

5.1.2.4. Columns

For the first dimension analysis, an Ascentis ES Cyano, 250×1.0 mm, 5.0 μm *d.p.* column was employed (MilliporeSigma/Supelco, Bellefonte, PA, USA), and thermostated at 40 °C. For the second dimension analysis, an Acquity UPLC BEH C18, 50×2.1 mm, 1.7 μm *d.p.* column was employed, and thermostated at 60 °C. The packed loops used for the trapping of the analytes from the SFC effluent were Xbridge C18, 2.1×20 mm, 5 μm *d.p.* cartridges (Waters Corp., Milford, MA, USA).

5.1.2.5. SFC×RP-UHPLC-PDA-QToF MS-IMS analyses

SFC analysis in ^{1}D was performed at a mobile phase flow rate of 0.05 mL/min, under the following gradient of MeOH into compressed CO_2: 0-2 min 0% B, 2-27 min to 20% B. The outlet pressure was 310 bar. The injection volume was 2 μL. The ^{2}D UHPLC separation was achieved with a mobile phase consisting of A) ACN/H_2O, 8:2 (*v/v*) and B) IPA at a flow rate of 0.7 mL/min, under the following gradient: 0-0.5 min, 20-50% B (hold for 0.3 min), 0.8-1.0 min to 80% B (hold for 0.6 min), 1.61 min to 20% B (hold for 0.39 min for column reconditioning). The outlet pressure was 419 bar.

For SFC×RP-UHPLC analyses, water was added as make-up solvent to the ^{1}D effluent prior to the interface, and delivered isocratically at a flow rate of 1.3 mL/min (at a pressure of 245 bar). The modulation time of the 2D switching valves was set at 2.00 min. Data were acquired using MassLynx software V4.1 (Waters Corp., Milford, MA, USA) and processed using Chromsquare software V2.2 (Shimadzu, Kyoto, Japan). All the analyses were made in triplicate, and retention time RSD% calculated on selected peaks from each different class were lower than 4.

PDA detection was performed in the 330-550 nm scan range, at a sampling frequency of 40 Hz and a resolution of 1.2 mm. Q-ToF MS detection was performed through an atmospheric pressure ionization interface in negative ion mode, and source parameters were set as follows: capillary voltage, 3.0 kV; sampling cone voltage, 40 V; corona current, 5 μA; cone gas flow rate, 50 L/h; desolvation gas flow rate, 600 L/h; nebulizer gas flow rate, 4.5 bar; source temperature, 150 °C; desolvation temperature, 400 °C; probe temperature, 400 °C. The lock mass compound used was leucine enkephaline with a reference mass at *m/z* 554.2615 in negative ion mode. Mass range was set at 400-1200 Da with a scan speed of 0.2 s per scan using the MassLynx software V4.1 (Waters Corp., Milford, MA, USA). Ion mobility MS (IMS) was optimized by injecting an all-*trans*-β-carotene standard solution (20 μg/mL in MeOH/MTBE 1:1, *v/v*) directly into the MS in IMS mode using direct infusion at a flow of 10 μL/min. The traveling wave ion mobility cell was operated at a wave velocity ramping of 800-300 m/s and a wave height of 40 V. In this approach, intact ions were allowed to pass through the trap cell and separated in the drift tube. The transfer cell was used to fragment the isomers at *m/z* 536.4378 by applying a collision energy of 4 V. IMS data were processed using DriftScope software V2.1 (Waters Corp., Milford, MA, USA).

5.1.3. Results and discussion

The objective of this work was to develop a two-dimensional comprehensive separation platform, in which the first dimension is represented by SFC. This, as an alternative to NP-LC separation commonly employed as ^{1}D in LC×LC, to afford enhanced resolving power and allow for reliable identification of carotenoids extracted from a complex real-world sample. Despite the obvious advantages of using SFC as at least one of the separation dimensions in comprehensive chromatography techniques, only few applications have been reported, so far. SFC×SFC was first implemented by Sandra and David in automated off-line mode [25], and afterwards exploited by Hirada and co-workers in stopped flow mode [26,27]; the selectivity was tuned in the two separation dimensions by the choice of different stationary phases or a variation in the column temperature. A valuable option for the analysis of low polarity compounds consisted in the implementation of SFC and RP-LC in a comprehensive configuration [28,29,30], in which the two dimensions were coupled on-line through an interface for solid-phase trapping. The design and functioning of the SFC×RP-UHPLC interface developed in this work is very similar, except for the use of two 2-position/six-port switching valves, equipped with symmetrical cartridges composed of C18 silica (see a schematic in Figure 1a-b (V-5.1.)). At each 2-min modulation time, switching of the two valves occurs asymmetrically: when the left valve is in position 2 and the right valve is in position 1, analytes eluted from ^{1}D SFC are trapped into the solid phase of cartridge 1, while at the same time analytes trapped in the previous modulation are eluted from cartridge 2 to the RP-LC analytical column, by the ^{2}D mobile phase (Figure 1a (V-5.1.)). Loading and trapping occur in opposite flow direction with respect to elution, so that after 2 min, the left valve will be in position 1 and the right valve will be in position 2 (Figure 1b (V-5.1.)). After the backpressure regulator, the sample compounds were contained in a spray of

decompressed CO_2, which would cause detrimental effects of on the LC pump and detector performance. In order to maintain the mobile phase gas-free, the 'solvent displacement' method was adopted [31], by using an auxiliary isocratic pump for rinsing the trap prior to transfer, by displacing the residual CO_2 with a flow of pure water, supplied by a tee-union. The effect of the addition of H_2O as a make-up solvent was tested by off-line analyses, by injecting a standard carotenoid solution, under the same chromatographic conditions, and set at 1.3 mL/min. This flushing step before entering the loops and the stationary phase inside the same loops, were also of utmost importance for effective focusing of the solutes at the head of the secondary column, avoiding the transfer of solvents which could cause peak deterioration and loss of resolution. In this way, the fractions transferred from ^{1}D SFC were composed of solvents fully compatible with the ^{2}D mobile phase and column packing, in comparison to the use of NP-LC, and moreover column re-equilibration was faster. Another advantage featured by the use of SFC instead of liquid-based separation consisted in the employment of a low-viscosity, high-diffusivity mobile phase resulting in shorter retention times; this in turn allowed for increasing the separation efficiency, by the use of a longer stationary phase, due to a lower pressure drop [32].

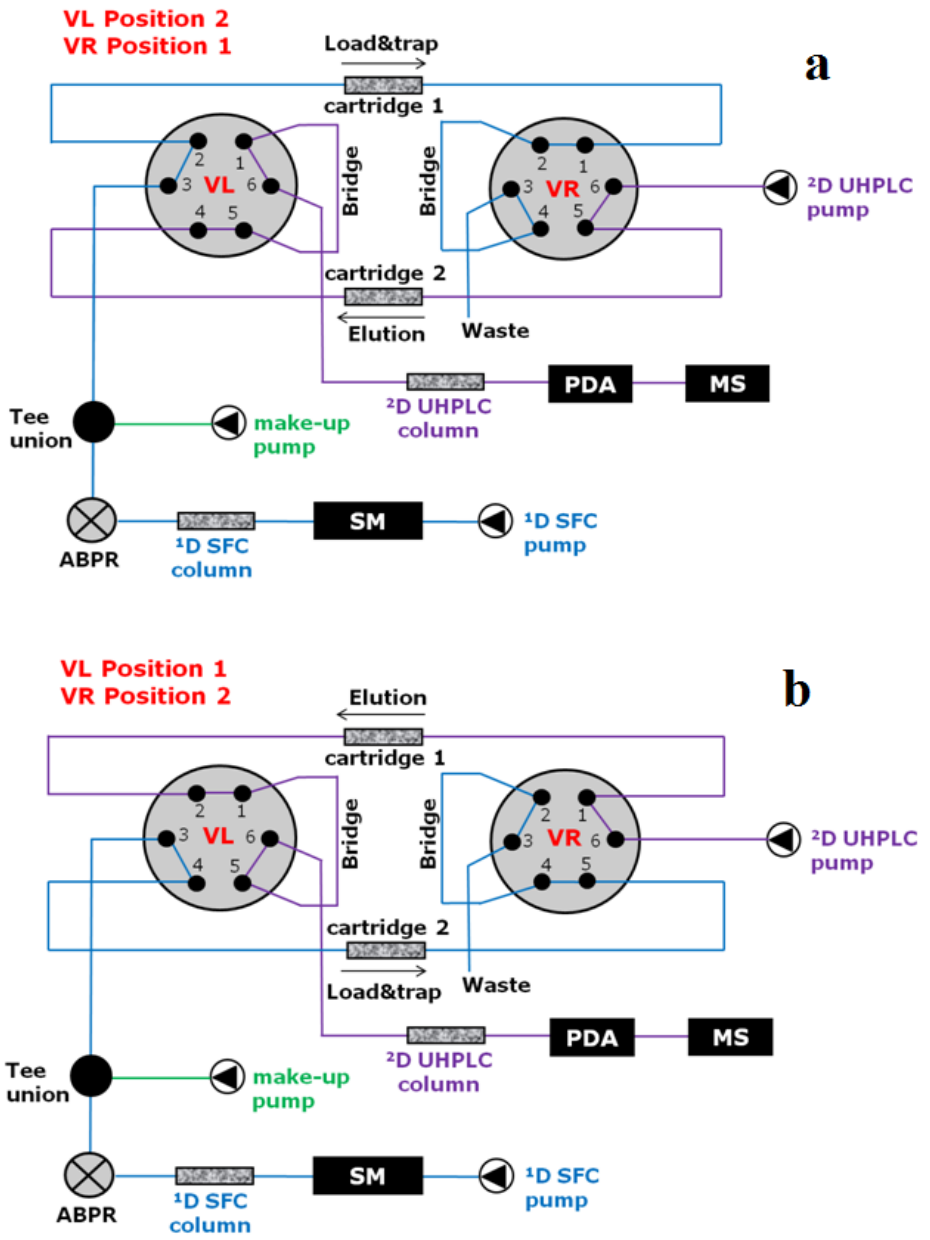

Figure 1 (V-5.1.). Schematic of the two-dimensional SFC×RP-UHPLC-PDA-Q-ToF-MS instrument with detail of the interface functioning. VL: valve left; VR: valve right; ABPR: active backpressure regulator; SM: sample manager. (a) and (b) show the different position of the two-position, 6-port switching valves during each modulation.

A 250×1.0 mm, 5 μm *d.p.* cyano column was used in the first dimension, and operated at 40 °C under a linear gradient of MeOH into compressed CO_2, going from 0 to 20% of organic modifier in 27 min, at a mobile phase flow rate of 0.05 mL/min. The latter was optimized for the microbore column, in terms of efficiency and analysis time, for carotenoid separation into classes of increasing polarity (as discussed later on). The use of MeOH as co-solvent improved the solubility of more polar analytes, resulting in better peak shape (reduced peak tailing) and less retention; moreover the selectivity was affected as well by the modifier, which introduced additional hydrogen bonding or dipole-dipole interactions, between the analytes and the stationary phase (data not shown). Most remarkably, the critical point of the mobile phase was modified, with respect to pure CO_2, depending on the increasing amount of the modifier in the gradient. It is known that the critical temperature (31° C) and pressure (73 bar) of pure CO_2 will rapidly increase with the addition of a co-solvent, to reach already 40° C and 83 bar upon addition of 3.5% MeOH to CO_2; the conditions required to maintain CO_2 in the supercritical state at 20% of MeOH would be unfeasible for the analysis. As a practical consequence, under the gradient program and at the mild temperatures adopted for this separation, a subcritical fluid was obtained very quickly.

The second dimension separation of the red chilli pepper carotenoids was achieved on a short ODS column with sub-2 μm particles, and namely 50×2.1 mm, 1.7 μm *d.p.*, thermostated at 60 °C. Since the whole effluent from ^{1}D was transferred on-line to the ^{2}D column, the modulation time of the switching valves needed to correspond exactly to the ^{2}D analysis time. The cycle time and gradient profile were optimized so that each fraction injected onto the ^{2}D column was completely eluted before the following transfer; moreover undersampling was kept to a minimum, by obtaining a high number of cuts from ^{1}D. Fast ^{2}D analyses were obtained at a mobile phase flow rate of 0.7

mL/min (the maximum allowed by the system), and by running a fast ramp up to 80% of the stronger solvent (IPA) at the end of the gradient, to ensure the elution of all the components. The elution profiles obtained after repetitive runs of the sample under these conditions were perfectly comparable, demonstrating that an isocratic step of 0.39 min was sufficient for column re-conditioning after the gradient (data not shown). Investigation of the breakthrough on the C18 packed loops was made by injecting a carotenoid standard solution, and switching the valves manually at different times after ^{1}D elution. A comparison of the peak areas obtained under SFC and RP-UHPLC demonstrated that, at the modulation time set of 2 min, the compound was still effectively trapped in the cartridge.

Results obtained from the SFC×RP-UHPLC analysis of free carotenoids and carotenoid esters in the red chilli pepper extract are shown in the contour plot of Figure 2 (V-5.1.), extracted at a wavelength of 450 nm. Orthogonality of the separation, as provided by two independent retention mechanisms operating in ^{1}D and ^{2}D, is clear from a visual inspection of the 2D plot, in which all the compounds (blobs) are widely spread over the 2D retention plane (great space coverage), and distributed along characteristic chemical patterns. It can be appreciated how chromatography on the cyano stationary phase allowed separation of the carotenoids into 15 different chemical classes, eluted according to their increasing polarity in ^{1}D (dashed circles in Figure 2 (V-5.1.)), in the order: acyclic hydrocarbons < cyclic hydrocarbons < free monools < monool-esters < diol-diesters < *cis*-diol-monoepoxide-monoesters < *cis*-diol-monoketo-diesters < *trans*-diol-monoketo-diesters < diol-monoketo-monoesters < diol-diketo-diesters < polyoxygenated free xanthophylls < diol-monoepoxide-diesters < *trans*-diol-monoepoxide-monoesters < *cis*-diol-diketo-monoesters < *trans*-diol-diketo-monoesters.

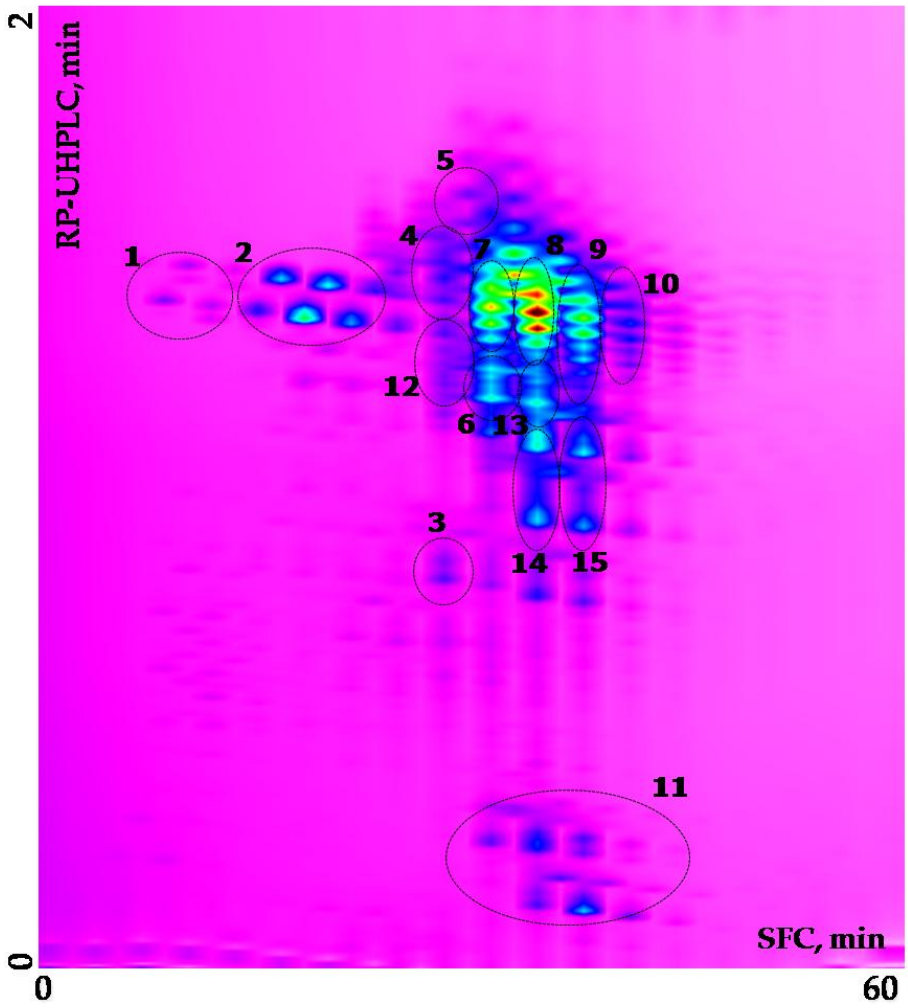

Figure 2 (V-5.1.). 2D Plot of the SFC×RP-UHPLC-PDA-Q-ToF-MS separation of a red chilli pepper sample (PDA detection at 450 nm). The dashed circles group the different carotenoids compounds into classes, further identified as in Table 1 (V-5.1.): 1) Acyclic hydrocarbons (No. 1-3); 2) Cyclic hydrocarbons (No. 4-8); 3) Free monools (No. 9); 4) Monool-esters (No. 12-15); 5) Diol-diesters (No. 16,17); 6) *cis*-Diol-monoepoxide-monoesters (No. 19,20); 7) *cis*-Diol-monoketo-diesters (No. 21-25); 8) *trans*-Diol-monoketo-diesters (No. 32-36); 9) Diol-monoketo-monoesters (No. 41-45); 10) Diol-diketo-diesters (No. 46-50); 11) Polyoxygenated free xanthophylls (No. 18,26,27,37,38); 12) Diol-monoepoxide-diesters (No. 10,11); 13) *trans*-Diol-monoepoxide-monoesters (No. 30,31); 14) *cis*-Diol-diketo-monoesters (No. 28,29); 15) *trans*-Diol-diketo-monoesters (No. 39,40).

Individual species within each class were further separated by the ^{2}D ODS column, on the basis of their increasing hydrophobicity and decreasing polarity; i.e., for components of the *trans*-diol-monoketo-diester class, the elution order increased with the number of carbon atoms of the fatty acid chains. The combined use of PDA and MS data allowed identifying a total of 50 carotenoids contained in the sample, either in their free, or in the esterified form. The identified carotenoids are listed in Table 1 (V-5.1.), numbered within each class according to increasing total retention time (T_{tR}, given by the sum of individual retention times in the first and second dimension), together with the compound respective spectral PDA data, the theoretical and experimental masses of pseudomolecular ions obtained by APCI under negative polarity, and the experimental error (internal calibration of the Q-ToF mass spectrometer yielded mass accuracy within ± 2 ppm).

Analysis by APCI MS operated under negative polarity offered improved sensitivity for the identification of unknown carotenoids, since very little (if any) fragmentation of parent ions occurred, and thus the spectra obtained were dominated by the presence of very intense pseudomolecolar ions $[M]^{\cdot-}$, making identification/quantization of low-abundant components easier. It is noteworthy that the complementary information gathered from the two detectors allowed discriminating between compounds showing similar (or nearly identical) UV-absorption properties, or isobaric compounds, giving the same *m/z* values. An example is represented by the four monool-esters listed in Table 1 (V-5.1.) as No. 12-15, all showing a characteristic three-band spectrum with absorption at 451 (max), 471 and 426 (shoulder), given the presence of identical chromophores. On the other hand, the pseudo molecular ions detected at *m/z* 706.5393, 7 *m/z* 34.6011, *m/z* 762.6322 and *m/z* 790.6625 allowed to easily distinguishing one from the other. Conversely, carotenoids numbered as 4-8, belonging to the cyclic hydrocarbon class, showing the same pseudomolecolar

ions $[M]^{\cdot-}$ at *m/z* 536 (averaged), could be differentiated by the different PDA spectra.

Table 1 (V-5.1.). Carotenoid compounds identified by SFC×RP-UHPLC-PDA-Q-ToF-MS analysis of a red chilli pepper sample.

Class	No.	Compound	Tt_R	$[M]^{\cdot}$- theor.	$[M]^{\cdot}$- exp.	Error (ppm)	PDA (nm)
Acyclic hydrocarbons	1	1,2-Dihydrophytofluene	17.30	544.5008	544.5011	-0.55	332, 349, 367
	2	Neurosporene	19.35	538.4538	538.4541	-0.56	417, 440, 468
	3	Phytofluene	21.29	542.4851	542.486	-1.66	334, 348, 368
Cyclic hydrocarbons	4	13*Z*-β-Carotene	25.28	536.4382	536.4389	-1.30	337,446,469
	5	α-Carotene	27.33	536.4382	536.4390	-1.49	(422), 445,473
	6	β-Carotene	29.27	536.4382	536.4378	0.75	(427), 452, 477
	7	9*Z*-α-Carotene	31.32	536.4382	536.4373	1.68	331,418,441,469
	8	9*Z*-β-Carotene	33.26	536.4382	536.4389	-1.30	336, (423), 447, 473
Free monools	9	β-Cryptoxanthin	40.86	552.4331	552.4341	-1.81	426, 451, 477
Diol-monoepoxide-diesters	10	Mutatoxanthin-C12:0,C14:0	41.15	976.7884	976.7888	-0.41	406, 429, 454
	11	Mutatoxanthin-C12:0,C16:0	41.21	1004.8197	1004.8202	-0.50	406, 429, 454
Monool-esters	12	β-Cryptoxanthin-C10:0	41.30	706.5689	706.5693	-0.57	426,451,477
	13	β-Cryptoxanthin-C12:0	41.33	734.6002	734.6011	-1.23	425,451,478
	14	β-Cryptoxanthin-C14:0	41.36	762.6315	762.6322	-0.92	426,450,478
	15	β-Cryptoxanthin-C16:0	41.40	790.6628	790.6625	0.38	426,451,477
Diol-diesters	16	Zeaxanthin-C14:0, C14:0	43.42	988.8248	988.8256	-0.81	424, 450, 478
	17	Zeaxanthin-C16:0, C16:0	43.46	1044.8873	1044.8883	-0.96	424, 450, 477

Polyoxygenated free xanthophylls	18	*cis*-Antheraxanthin	44.45	584.4229	584.4219	1.71	332, 424,443,469
cis-Diol-monoepoxide-monoesters	19	*cis*-Antheraxanthin-C12:0	45.09	766.5900	766.5913	-1.70	330, 418, 444, 470
	20	*cis*-Antheraxanthin-C14:0	45.14	794.6213	794.6207	0.76	332, 418, 443, 472
cis-Diol-monoketo-diesters	21	*cis*-Capsanthin-C10:0, C12:0	45.24	920.7258	920.7248	1.09	330, 467
	22	*cis*-Capsanthin-C12:0, C12:0	45.36	948.7570	948.7578	-0.84	332, 469
	23	*cis*-Capsanthin-C12:0, C14:0	45.29	976.7884	976.7896	-1.23	330, 467
	24	*cis*-Capsanthin-C14:0, C14:0	45.31	1004.8197	1004.8188	0.90	331, 469
	25	*cis*-Capsanthin-C14:0, C16:0	45.35	1032.8510	1032.8523	-1.26	330, 467
Polyoxygenated free xanthophylls	26	*cis*-Capsanthin	48.35	584.4229	584.4221	1.37	336, 467
	27	Lutein	48.45	568.4280	568.4291	-1.94	423, 444, 469
cis-Diol-diketo-monoesters	28	*cis*-Capsorubin-C12:0	48.96	782.6213	782.6228	-1.92	339, 478
	29	*cis*-Capsorubin-C14:0	49.08	810.6526	810.6533	-0.86	338, 476
trans-Diol-monoepoxide-monoesters	30	Antheraxanthin-C12:0	49.13	766.5900	766.5891	1.17	424, 445, 474
	31	Antheraxanthin-C14:0	49.17	794.6213	794.6202	1.38	423, 446, 474
trans-Diol-monoketo-diesters	32	Capsanthin-C10:0, C12:0	49.23	920.7258	920.7264	-0.65	474
	33	Capsanthin-C12:0, C12:0	49.25	948.7570	948.7556	1.48	474
	34	Capsanthin-C12:0, C14:0	49.28	976.7884	976.7896	-1.23	473
	35	Capsanthin-C14:0, C14:0	49.31	1004.8197	1004.8216	-1.89	473

	36	Capsanthin-C14:0, C16:0	49.34	1032.8510	1032.8502	0.77	474
Polyoxygenated free xanthophylls	37	Capsanthin	52.34	584.4229	584.4238	-1.54	474
	38	Zeaxanthin	52.44	568.4280	568.4285	-0.88	426,451,477
trans-Diol-diketo-monoesters	39	*trans*-Capsorubin-C12:0	52.83	782.6213	782.6228	-1.92	476
	40	*trans*-Capsorubin-C14:0	52.94	810.6526	810.653	-0.49	478
Diol-monoketo-monoesters	41	Capsanthin-C10:0	53.20	738.5587	738.5578	1.22	473
	42	Capsanthin-C12:0	53.22	766.5900	766.5914	-1.83	474
	43	Capsanthin-C14:0	53.25	794.6213	794.6228	-1.89	473
	44	Capsanthin-C16:0	53.27	822.6526	822.6531	-0.61	474
	45	Capsanthin-C18:0	53.30	850.6839	850.6833	0.71	473
Diol-diketo-diesters	46	Capsorubin-C12:0, C12:0	57.20	964.7520	964.7536	-1.66	479
	47	Capsorubin-C12:0, C14:0	57.22	992.7833	992.7845	-1.21	480
	48	Capsorubin-C14:0, C14:0	57.24	1020.8146	1020.8157	-1.08	480
	49	Capsorubin-C14:0, C16:0	57.27	1048.8460	1048.8472	-1.14	479
	50	Capsorubin-C16:0, C16:0	57.29	1076.8772	1076.8765	0.65	481

The scatter plot in Figure 3 (V-5.1.) displays the *m/z* 400-1200 distribution over the first (SFC, *x*) and second (RP-UHPLC, *y*) separation dimensions; the relative abundances (intensities) are rendered by colour map.

Although LC×LC-MS provides excellent resolving power and identification capabilities, the time required for fully optimized separations of carotenoid isomers in such complex samples can be long, and MS detection is not always able to distinguish *cis/trans* isomers. On the other hand, resolving and possibly quantifying carotenoid geometrical isomers in biological specimens would help in understanding their physiological functions, and furthermore help in dose formulations. To this purpose, the feasibility of using IMS and IM-MS/MS was investigated, as an additional dimension of high speed separation added to MS analysis. Because of thermal instability, carotenoids are known to isomerize during the ionization process, and the possibility of in-source *cis/trans* isomerization of carotenoids has been investigated previously. The experiments were first optimized by direct infusion of an all-*trans*-β-carotene standard solution into the ion source at a flow of 10 μL/min, for tuning of the IMS conditions in terms of gas flow rate, height and velocity of the travelling wave, and ramping the last produced the best separations.

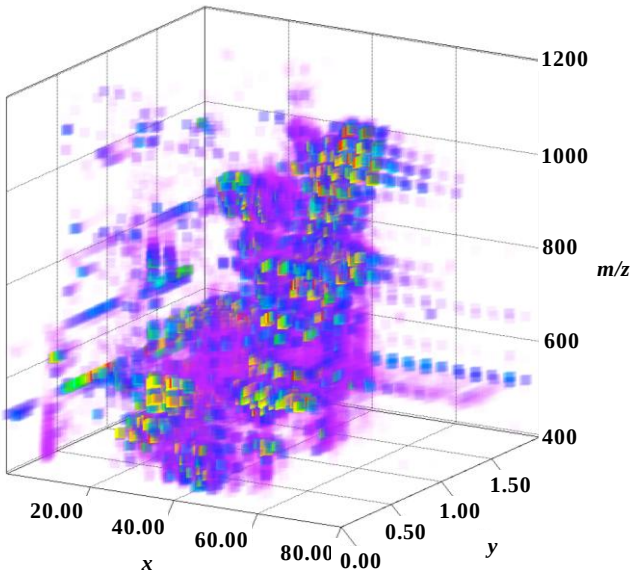

Figure 3 (V-5.1.). 4D Scatter plot of the SFC×RP-UHPLC-PDA-Q-ToF-MS separation of a red chilli pepper sample. Q-ToF-MS detection by APCI(-) in the 400-1200 *m/z* range. Mass distribution (*m/z*) is displayed over the first (*x*) and second (*y*) retention time. Intensity is rendered by colour map.

Afterwards, to determine if the geometric isomers of β-carotene could be distinguished using IM-MS/MS, the positive ion tandem mass spectra were obtained, by using argon for collision induced dissociation in the transfer cell of the spectrometer, after separation into the IMS cell. The results obtained from SFC×RP-UHPLC-IM-MS/MS analysis of the all-*trans*-β-carotene standard solution are shown in Figure 4 (V-5.1.). As shown in Figure 4a (V-5.1.), only one chromatographic peak was eluted at a retention time of 29.4 min, while two β-carotene peaks were observed during IM-MS (Figure 2b (V-5.1.)), with drift times differing by 1.30 ms for the isomers of *m/z* 536.4378. IM MS drift time distributions of the $[M]^{\cdot -}$ ions of *m/z* 536.4378 and the relative abundances are shown in Figure 4c (V-5.1.), where the peak with drift time of 5.06 ms was identified as a *cis*-isomer of β-carotene, and the peak with drift time of 6.36 ms

was identified as the all-*trans* isomer. Such findings, in accordance with the literature [33], were suggested by the IM-MS/MS CID spectra of the $[M]^{\cdot -}$ ions of *m/z* 536.4378 shown in Figure 4d-e (V-5.1.). The base peak of the tandem mass spectrum of the *cis*-β-carotene isomer (Figure 4d (V-5.1.)) was the molecular ion measured at *m*/*z* 536.4378 (theoretical *m*/*z* 536.4382 with formula $C_{40}H_{56}$), whereas the base peak of the tandem mass spectrum of the all-*trans*-β-carotene isomer (Figure 4e (V-5.1.)) was observed at *m*/*z* 444.3724 and corresponded to the loss of toluene (theoretical *m*/*z* 444.3756 with formula $C_{33}H_{48}$).

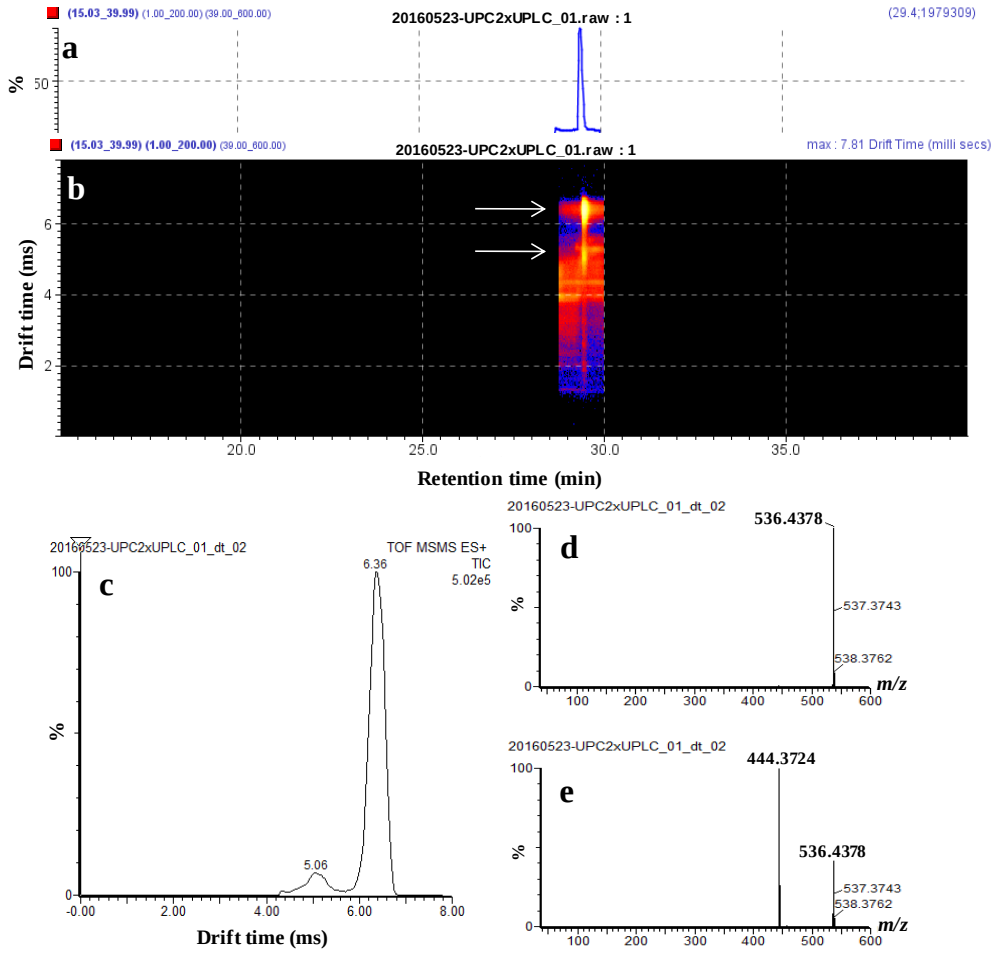

Figure 4 (V-5.1.). 2D SFC×RP-UHPLC-IM-MS/MS analysis of β-carotene isomers. a: SFC×RP-UHPLC-IMS chromatogram; b: 2D map showing ion mobility drift time (ms) *vs* SFC×RP-UHPLC retention time (min); c: IM-MS drift time distributions of the [M]·- ions of *m/z* 536.4378 and the relative abundances of *cis*- (peak at 5.06 ms) and *trans*- (peak at 6.36 ms) isomers of β-carotene; d-e: IM-MS/MS CID spectra of the [M]·- ions of *m/z* 536.4378 corresponding to *cis*-β-carotene (d) and all-*trans*-β-carotene (e).

The 3D plot obtained from SFC×RP-UHPLC-IM-MS/MS analysis of the whole intact carotenoid fraction extracted from the red chilli pepper sample is

illustrated in Figure 5 (V-5.1.), where the relative intensities of the *m/z* values are showed, as a function of the ion mobility drift time (bins). Identification of geometric isomers of carotenoid compounds in the sample anlyzed is currently in progress.

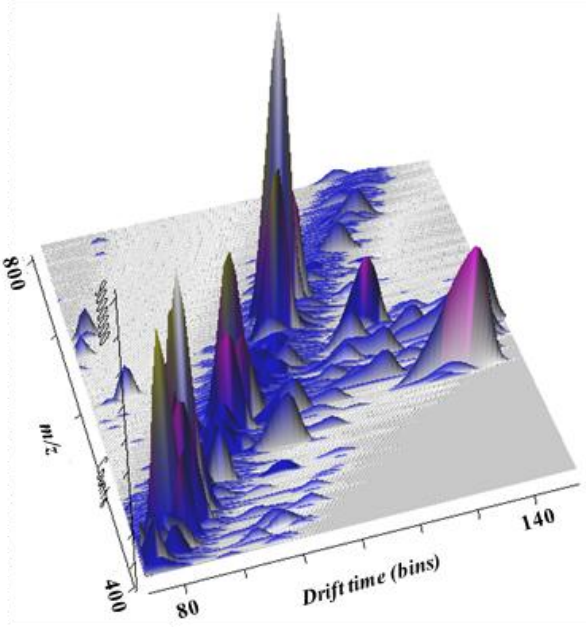

Figure 5 (V-5.1.). 3D plot of the SFC×RP-UHPLC-PDA-IM-MS/MS separation of a red chilli pepper sample, showing the mass distribution (*m/z*) *vs.* ion mobility drift time (bins).

5.1.4. Conclusions

In this research, the first on-line coupling of SFC to RP-UHPLC was implemented, hyphenated to PDA, QToF MS and IM MS/MS detection. As a proof of principle, the system was employed for the separation and identification of the intact carotenoid fraction in a red chilli pepper sample. Compared to a previously developed application, based on the use of NP-LC in the first dimension [19], the selectivity was increased in both chromatographic dimensions, in terms of class-type separation (15 *vs* 10) and compound

identification (50 *vs* 33). Remarkably, carotenoids fingerprint by SFC×RP-UHPLC was obtained in half the analysis time with respect to NP×RP-UHPLC (60 *vs* 120), and with solvent consumption in ^{2}D reduced by 90% (42 mL *vs* 480 mL). Moreover, the second dimension column performance is preserved, since the RP stationary phase is now not exposed to hazardous solvents used for NP-LC separations. The separation of geometric isomers like *cis/trans* carotenoids differing in collision cross-sections was demonstrated, using travelling wave ion mobility.

REFERENCES

[1] Jandera P (2012) Comprehensive two-dimensional liquid chromatography-practical impacts of theoretical considerations. A review. Cent Eur J Chem 10:844-875.

[2] Mondello L, Donato P, Cacciola F, Fanali C, Dugo P (2010) RP-LC×RP-LC analysis of a tryptic digest using a combination of totally porous and partially porous stationary phases. J Sep Sci 33:1454–1461.

[3] Donato P, Micalizzi G, Oteri M, Rigano F, Sciarrone D, Dugo P, Mondello L (2018) Comprehensive lipid profiling in the Mediterranean mussel (*Mytilus galloprovincialis*) using hyphenated and multidimensional chromatography techniques coupled to mass spectrometry detection. Anal Bioanal Chem 410:3297-3313.

[4] Donato P, Cacciola F, Sommella E, Fanali C, Dugo L, Dachà M, Campiglia P, Novellino E, Dugo P, Mondello L (2011) On-line comprehensive RPLC×RPLC with mass spectrometry detection for the analysis of proteome samples. Anal Chem 83:2485-2491.

[5] François I, Sandra K, Sandra P (2009) Comprehensive liquid chromatography: fundamental aspects and practical considerations: a review. Anal Chim Acta 641:14-31.

[6] Donato P, Cacciola F, Tranchida P Q, Dugo P, Mondello L (2012) Mass spectrometry detection in comprehensive liquid chromatography: basic concepts, instrumental aspects, applications and trends. Mass Spectr Rev 31:523-559.

[7] Donato P, Rigano F, Cacciola F, Schure M, Farnetti S, Russo M, Dugo P, Mondello L (2016) Comprehensive two-dimensional liquid chromatography-tandem mass spectrometry for the simultaneous determination of wine polyphenols and target contaminants. J Chromatogr A 1458:54-62.

[8] Tranchida P Q, Donato P, Cacciola F, Beccaria M, Dugo P, Mondello L (2013) Potential of comprehensive chromatography in food analysis. TRAC-Trends Anal Chem 52:186-205.

[9] Young A, Lowe G L (2018) Carotenoids-Antioxidant Properties. Antioxidants (Basel) 7:28-31.

[10] Murillo A G, Fernandez M L (2016) Potential of dietary non-provitamin A carotenoids in the prevention and treatment of diabetic microvascular complications. Adv Nutr 7:14-24.

[11] Di Pietro N, Di Tomo P, Pandolfi A (2016) Carotenoids in cardiovascular disease prevention. JSM Atheroscler 1:1002-1014.

[12] Martí R, Roselló S, Cebolla-Cornejo J (2016) Tomato as a source of carotenoids and polyphenols targeted to cancer prevention. Cancer 8:58-86.

[13] Rodriguez-Amaya D B (2016) Structures and analysis of carotenoid molecules. Subcell Biochem 79:71-108.

[14] Giuffrida D, Dugo P, Salvo A, Saitta M, Dugo G (2010) Free carotenoid and carotenoid ester composition in native orange juices of different varieties. Fruits 65:277–284.

[15] Dugo P, Herrero M, Giuffrida D, Kumm T, Dugo G, Mondello L (2008) Application of comprehensive two-dimensional liquid chromatography to elucidate the native carotenoid composition in red orange essential oil. J Agric

Food Chem 56:3478-3485.

[16] Herrero M, Cacciola F, Donato P, Giuffrida D, Dugo G, Dugo P, Mondello L (2008) Serial coupled columns reversed-phase separations in high-performance liquid chromatography. Tool for analysis of complex real samples. J Chromatogr A 1188:208-215.

[17] Panfili G, Fratianni A, Irano M (2004) Improved normal-phase high-performance liquid chromatography procedure for the determination of carotenoids in cereals. J Agric Food Chem 52:6373-6377.

[18] Dugo P, Giuffrida D, Herrero M, Donato P, Mondello L (2009) Epoxycarotenoids esters analysis in intact orange juices using two-dimensional comprehensive liquid chromatography. J Sep Sci 32:973-980.

[19] Cacciola F, Donato P, Giuffrida D, Torre G, Dugo P, Mondello L (2012) Ultra high pressure in the second dimension of a comprehensive two-dimensional liquid chromatographic system for carotenoid separation in red chili pepper. J Chromatogr A 1255:244-251.

[20] Cacciola F, Giuffrida D, Utczas M, Mangraviti D, Dugo P, Menchaca D, Murillo E, Mondello L (2016) Application of comprehensive two-dimensional liquid chromatography for carotenoid analysis in red mamey (Pouteria sapote) fruit. Food Anal Meth 9:2335-2341.

[21] Donato P, Inferrera V, Sciarrone D, Mondello L (2017) Supercritical Fluid Chromatography for Lipid Analysis in Foodstuffs. J Sep Sci 40:361-382.

[22] Bernal J L, Martin M T, Toribio L (2013) Supercritical fluid chromatography in food analysis. J Chromatogr A 1313:24-36.

[23] Giuffrida D, Zoccali M, Giofre S V, Dugo P, Mondello L (2017) Apocarotenoids determination in Capsicum chinense Jacq. cv Habanero by supercritical fluid chromatography-mass spectrometry. Food Chem 231:316-323.

[24] Zoccali M, Giuffrida D, Dugo P, Mondello L (2017) Direct online

extraction and determination, by supercritical fluid extraction supercritical fluid chromatography-mass spectrometry of targeted carotenoids from red Habanero peppers (Capsicum chinense Jacq.). J Sep Sci 40:3905-3913.

[25] Sandra P, Medvedovici A, David F (2003) Comprehensive pSFC×pSFC-MS for the characterization of triglycerides in vegetable oils. LC GC Europe 16(12A):32-34.

[26] Hirata Y, Hashiguchi T, Kawata E (2003) Development of comprehensive two-dimensional packed column supercritical fluid chromatography. J Sep Sci 26:531-535.

[27] Hirata Y, Sogabe I (2004) Separation of fatty acid methyl esters by comprehensive two-dimensional supercritical fluid chromatography with packed columns and programming of sampling duration. Anal Bioanal Chem 378:1999-2003.

[28] François I, dos Santos Pereira A, Lynen F, Sandra P (2008) Construction of a new interface for comprehensive supercritical fluid chromatography×reversed phase liquid chromatography (SFC×RPLC). J Sep Sci 31:3473-3478.

[29] François I, Sandra P (2009) Comprehensive supercritical fluid chromatography×reversed phase liquid chromatography for the analysis of the fatty acids in fish oil. J Chromatogr A 1216:4005-4012.

[30] Cacciola F, Donato P, Sciarrone D, Dugo P, Mondello M (2017) Comprehensive liquid chromatography and other liquid- based comprehensive techniques coupled to mass spectrometry in food analysis. Anal Chem 89:414-429.

[31] Mougin C, Dubroca J, Barriuso E (1996) On-line supercritical fluid extraction and high performance liquid chromatography for determination of triazine compounds in soil. J High Resolut Chromatogr 19:700-702.

[32] Brunelli C, Zhao Y, Brown M H, Sandra P (2008) Development of a

supercritical fluid chromatography high-resolution separation method suitable for pharmaceuticals using cyanopropyl silica. J Chromatogr A 1185:263-272.
[33] Dong L, Shion H, Davis R G, Terry-Penak B, Castro-Perez J, van Breemen R B (2010) Collision cross-section determination and tandem mass spectrometric analysis of isomeric carotenoids using electrospray ion mobility time-of-flight mass spectrometry. Anal Chem 82:9014-9021.

5.2. Triacylglycerol Fingerprinting in Edible Oils by Subcritical Solvent Chromatography

5.2.1 Introduction

Triacylglycerols (TAGs) are neutral lipids synthesized by enzymatic esterification of glycerol with saturated and unsaturated fatty acids (FAs), differing in their acyl chain length, number and position of double bonds, and *cis/trans* configuration of the latter. The number of possible FA combinations and, thus, TAG compounds, is further increased by the different stereochemical position (*sn*-1, 2, or 3) of FAs at the glycerol backbone. TAGs may consist of three repetitive FA units, or contain two or three different acyl chains, in the last case *R/S* optical isomerism may also occur. TAGs are commonly designated by the initial of the FAs trivial names, ordered according to their position at the glycerol skeleton, for most purposes not distinguishing between the 1 and 3 positions [1-3].

The task of TAGs analysis and profiling is of concern in different fields, including metabolomic studies, pharmaceutical, cosmetic, and food industry. These molecules play a crucial role in human organism for energy storage, membrane cell composition, and a number of metabolic processes; to this concern, several studies have given insight into the relation between TAGs imbalances in human diet and the onset of metabolic diseases or disorders, like obesity, dyslipidaemia, diabetes, and atherosclerosis [4-7]. TAGs dietary intake represents the main source of fat-soluble vitamins and other non-polar and polar compounds, like free fatty acids. The latter exert a functional role as essential components of all membranes, gene regulators, and direct substrates for energy production via the beta oxidation pathway. In addition, polyunsaturated fatty acids (PUFAs) that cannot be synthesized by the human body, are precursors of biologically active metabolites, i.e. the eicosanoids; α-linolenic acid (ALA,

C18:3, omega-3) and linoleic acid (LA, C18:2, omega-6) are two essential FAs for humans, whose deficiency can result in retarded growth, dermatitis, kidney diseases, and several brian disorders [8].

TAGs account almost wholly for the composition of most animal fats (e.g., butter, tallow, lard and processed products like margarine) and vegetable oils (e.g., olive, palm, corn, and soybean) of commercial relevance, therefore determining the functionalities of these lipid substances either as food ingredients or for the physiological effects resulting from food intake. For such reasons, profiling of the intact TAGs in fats and oils, without pre-saponification, is a key tool for their characterization, allowing confirming authenticity or detecting adulterations, as well as for the prediction of their physical/physiological properties and those of derived food products. In many foods TAGs play a major role in determining the overall physical characteristics, such as flavour, texture, mouthfeel and appearance; apart from food quality and health, TAG analysis is of concern in food industry, for a number of other reasons: legal (conform to standards of identity and nutritional labelling), economic (recovery of expensive ingredients from waste products), and processing (processing conditions will considerably effect the quality of lipids in the final commodity) [9, 10].

Since a large number of species may arise from all the different combinations of possible FAs at the glycerol backbone, TAG analysis and separation is a challenging task, and to this purpose a variety of chromatographic techniques have been employed [11], including thin layer chromatography (TLC) [12], high-performance liquid chromatography (HPLC) [13], capillary electrochromatography (CEC), gas chromatography (GC), and supercritical fluid chromatography (SFC) [14]. As for detection, the coupling to MS may provide additional resolution and bring complementary information [15].

HPLC methods using reversed-phase (RP) and silver ion (SI) columns have

been widely applied for the separation of intact TAGs, either independently [16,17], or in offline or online combinations, the latter exploiting the complementary nature of the two retention mechanisms and, thus, of the information attainable. In RP-HPLC, retention of TAGs increases with the increasing degree of hydrophobicity, commonly identified by their equivalent carbon number (ECN) or partition number (PN), as given by the sum of the total carbon number (CN), minus twice the number of double bonds (DB) in the acyl chain, i.e.: ECN=CN-2DB. Under properly optimized conditions, the separation of critical TAG pairs within the same ECN group is also feasible, as well as of TAGs differing only in the position of double bond(s); on the other hand, the technique does not allow to discriminate between *R/S* optical isomers, and regioisomers, and *cis/trans* isomers. The latter two issues may be addressed by the use of SI columns, on which TAG separation is controlled by the unsaturation degree, and the distribution of DBs in the FA chains. Both RP- and silver ion HPLC rely on the use of non-aqueous (NA) mobile phase components of low polarity, well suited to the non polar nature of TAGs; one main advantage of both techniques consist in the use of mild temperatures, so that degradation risks of the more labile long-chain PUFAs are alleviated. One major issue related remains detection, since the commonly use of UV is precluded from the lack of suitable chromophores in TAG molecules, while the universal refractive index (RI) is not practicable under the gradient conditions commonly employed for TAG elution.

Unlike LC, capillary GC (cGC), usually performed on phenyl-methylsilicone stationary phases, offers the possibility of flame ionization detection (FID) to be employed universally, and to obtain reliable quantification according to organic carbon of TAGs; however the low volatility of the analytes and the high temperatures required often preclude direct analysis of TAGs and, thus, analysis of the fatty acid methyl esters (FAMEs) obtained upon transesterification of

TAGs is usually performed. Drawbacks of this procedure consist in the loss of information about the intact TAG composition and, moreover, in the case of PUFAs reliable quantification is sometimes hampered from incomplete transesterification of the sample. Conversely, for the analysis of matrices containing high amounts of PUFAs, the use of SFC have shown some advantages over cGC, since mild temperatures are employed, and almost identical response factors are obtained for saturated and unsaturated TAGs, by employing FID detection. Advantages of the use of SFC over other chromatographic techniques practised for lipid analysis, and notably for TAG analysis, consist in: feasibility for separation of high molecular and thermally labile TAGs (in contrast to GC) under the mild operating temperatures employed; feasibility for direct analysis, without the need for a derivatization step (often needed prior to GC analysis); likelihood of hyphenation to different universal detectors, i.e. FID, mass spectrometry (MS), evaporative light scattering (ELSD). Moreover, SFC is fully compatible with injection of samples in pure organic solvents, and is much suitable for lipid analysis, especially the more hydrophobic TAGs. These aspects have been discussed in a number of reviews, focusing on food lipids [18,19] and TAGs [20,21].

A major benefit of SFC, whatever the application, is related to the low mobile phase viscosity and higher diffusion coefficients, that allow for faster or more efficient separations to be attained, by the use of high linear velocities or longer columns, respectively (moderate pressure falls through the column). With respect to LC, in SFC organic solvent consumption is considerably reduced, and this implies reduced toxicity, costs, and environmental impact. Moreover, shorter re-equilibration times are needed, after each gradient elution in SFC, and this allows for faster separations and better resolution to be achieved.

Most of the earlier work focused on lipid separation by SFC used fused-silica capillary columns with cross-linked chemically bonded stationary phases, and

namely TAG separation was achieved on the same columns employed for high-resolution GC (HRGC), consisting of either non-polar (e.g., phenyl-methylsiloxane, polymethylsiloxane) or polar (e.g., cyanopropyl-phenyl-methylpolysiloxane, polyethyleneglycol) stationary phases. In capillary SFC (cSFC), the mobile phase consists of neat CO_2 under a gradient of density, and separations were therefore achieved under a program of temperature and pressure ramps. Separation is mainly ruled by CN, and the data obtained were very similar to those attained by cGC, except for the lower resolution, pertaining to non optimal operation of the narrow bore SFC columns, since linear velocities higher than the optimum were employed. The degree of unsaturation also influences the elution of TAGs within the same CN, however the separation of complex matrices was fair insufficient, due to the many co-elutions. First introduced by Lee [22] and Novotny [23], open tubular SFC was successfully exploited for the separation of edible oils and fats by carbon number and degree of unsaturation [24] on a very polar, siloxane-based stationary phase (25% cyanopropyl, 50% phenyl), at temperature as low as 70° C. The same material allowed for the separation of γ- and α-linolenic acid-containing TAGs, by combining two 50 μm i.d., 10 m long columns to enhance the separation of one critical pair [25]. All these approaches used atmospheric pressure chemical ionization (APCI) MS detection, affording spectra characterized by the presence of $[M+H]^+$ and $[M-RCOO]^+$ ions. The protonated molecular ion was more intense with the increase in unsaturation, while the loss of an acyl moiety was dependent on the degree of unsaturation and the regiospecific distribution of the FA moiety between the *sn*-1/3 and the *sn*-2 positions, the latter being less favoured; thus the resolution of TAGs within the same CN and DB value was possible. On the other hand, chromatographic separation of TAG regioisomers is only feasible by SI-SFC, in which retention is ruled by the degree of unsaturation, and DB distribution in the FA chains. In

the analysis of fish and vegetable oils reported by Sandra et al. [17] additional separation of TAGs within the same DB value was also attained, based on the CN; since multiple retention mechanisms act in SI columns, separation according to the FA distributions in TAGs (positional isomers) may be observed, as well. Key aspects and applications of capillary column SFC for the analysis of oils and fats have been discussed by David et al. [26].

Most recent SFC techniques are based on packed columns, and small (2-40%) percentages of a polar organic solvent (co-solvent or modifier) are added to the CO_2 mobile phase; increased amounts of acetonitrile, methanol, ethanol, or isopropanol typically employed to allow the solubility of more polar analytes favour result in less retention and better peak shape. The improved solubility also reduces peak tailing phenomena, and moreover the presence of a modifier will minimize undesired interactions between analytes and active residual silanol groups on the stationary phase. The selectivity will be affected as well by the co-solvent, which introduces additional hydrogen bonding or dipole-dipole interactions, and most important the critical point of the mobile phase will be modified, with respect to pure CO_2. The critical temperature (31° C) and pressure (73 bar) of pure CO_2 will rapidly increase, depending on the amount (and the nature) of the modifier, i.e. to reach already 40° C and 83 bar upon addition of 3.5% MeOH to CO_2; a practical consequence is that, under a typical gradient program and at the mild temperatures adopted for separations, a subcritical fluid will be obtained very quickly since the conditions required to ensure a supercritical mobile phase would be impracticable (e.g., 135 °C and 168 bar for a 70:30 CO_2:MeOH mixture). The many faces of packed column SFC have been critically reviewed by Lessellier & West [27], also concerning most recent instrumental developments that have contributed to make efficiency and sensitivity of modern SFC comparable to that of LC or ultra-high pressure LC (UHPLC). Minimized void volumes, higher pressure capabilities, and novel

design of backpressure regulator have made SFC operation with sub-2 μm and superficially porous particles feasible [28]. At the same time, a number of packing materials specifically tailored for SFC have been introduced, affording improved selectivity, peak shape, and sample capacity [29].

Applications of packed SFC (pSFC) to the task of TAG profiling in foodstuffs have been reviewed recently [30], using octadecylsilica (ODS) columns. Retention of TAGs on ODS stationary phases closely resembles that observed under NARP-LC conditions, as ECN is the main factor ruling a separation; moreover for TAGs within the same ECN group, a linear relationship has been demonstrated between retention and TAG DB values. Also in a similar way, temperature has a stronger effect on selectivity than mobile phase density, as TAG retention increases at decreasing temperature. TAG profiling by pSFC on ODS columns has been reported, in plant oils, using either neat CO_2 as a mobile phase [31,32], or a gradient of organic modifier [33-36].

In this work, TAG profiling in edible oils of vegetable origin was achieved, by means of SFC analysis on ODS columns with superficially porous particles, under subcritical conditions. Characterization of the intact lipid fraction of borage, maize, hazelnut, olive, palm, peanut, and soybean oils was attained, by the complementary information given by the retention behaviour, and the mass spectral data obtained by quadrupole time-of-flight (Q ToF) and ion mobility (IM) mass spectrometry (MS) detection.

5.2.2. Materials and Method

5.2.2.1. Chemicals and materials

Compressed CO_2 (99.9% grade) used as the main mobile phase was from Rivoira (Milan, Italy); LC-MS grade methanol (MeOH), ethanol (EtOH), isopropyl alcohol (IPA), *n*-hexane, and acetonitrile (ACN) used as the modifier or sample diluent were from Sigma-Aldrich (Milan, Italy). TAG standard

trilinolein (C18:2/C18:2/C18:2) and 1,3-palmitin-2-olein (C16:0/C18:1/C16:0) from Sigma-Aldrich (Milan, Italy).

5.2.2.2. Samples and sample preparation

Samples of Borage oil (*Borago officinalis*), Corn oil (*Zea mays*), refined Hazelnut oil (*Corylus colurna*), Extra Virgin Olive Oil (*Olea europaea*), Palm oil (*Elaeis guineensis*), Peanut oil (*Arachis hypogaea*), and Soybean oil (*Glycine max*) were purchased from the market. All samples were diluted (1000 ppm in IPA) and filtered through 0.45 μm Acrodisc nylon membrane filter (Pall Life Sciences, Ann Arbor, MI, USA) prior to SFC-MS analyses.

5.2.2.3. Instruments

SFC-MS analyses were performed on a Acquity UPC^2 (Ultra Performance Convergence Chromatography) system (Waters Co., Manchester, England) with a UPC^2 Binary Solvent Manager (BSM), Sample Manager –FL, UPC^2 Convergence Manager, Column Manager-A. The system was hyphenated to Synapt G2-S mass spectrometer (Waters Co., Manchester, England) through an atmospheric pressure chemical ionization (APCI) interface. The SFC and MS systems were controlled by separate processors, both using MassLynx V4.1 SCN916 software for data acquisition and processing; an external trigger was set, to start MS acquisition right after SFC analysis start.

5.2.2.4. Analytical conditions

Chromatographic separations of TAGs were carried out on Ascentis Express C18 (100×30 mm i.d., 2.0 μm *d.p.*, partially porous) column (Supelco, Bellefonte, PA), at a constant mobile phase flow rate of 1.0 mL/min. The injection volume was 2 μL. The following experimental parameters were studied: nature of modifier (ACN, EtOH, IPA) into compressed CO_2, type of

elution (isocratic *vs.* gradient), gradient stepness, pressure of the active backpressure regulator (ABPR, 1500 psi and 3000 psi), and column temperature (20° C and 30° C). Under optimized experimental conditions, SFC separation of the vegetable oil samples was achieved under the following conditions: column temperature, 20° C; ABPR set, 1500 psi; gradient elution of ACN into CO_2, 0-5 min, 5% B, 5-20 min, to 30% B, hold for 3 min.

Q-ToF-MS spectra were acquired under the following conditions: ionization mode, APCI positive; scan range, 100 to 1200 *m/z*; source temperature, 120° C; probe temperature, 400° C; desolvation gas (N_2) flow, 400 L/h; nebulizer gas flow (N_2), 4.5 bar; corona current, 4 μA; sampling cone, 40 V.

Leucine enkephaline was used as the lock mass for all experiments.

For ion mobility experiments: IMS gas flow rate (N_2), 90 mL/min, IMS wave velocity, 501 m/s, and wave height, 40 V. Typical acquisition of an ion mobility experiment consisted of 200 bins with each bin having a mobility drift time of 50 μs (10 ms for a complete ion mobility experiment). ToF MS data were acquired and analyzed with MassLynx V4.1 SCN916 software, while IMS data were processed with DriftScope 2.7 (Waters Corp.).

5.2.3. Results and discussion

5.2.3.1. Optimization of chromatographic conditions

The aim of this research work was the development of a chromatographic method for the comprehensive characterization of TAG profile in different edible oils of vegetal origin, using CO_2 as the main mobile phase solvent, under subcritical conditions, and Q-ToF MS detection. For optimization of the separation method, in terms of resolution, peak shape, and analysis time, the effect of selected parameters was investigated, i.e.: nature of the organic modifier, type of elution, and outlet column pressure (as controlled by the ABPR). All chromatographic experiments were carried out at a selected

temperature of 20° C, on the basis of previous results on the retention behaviour of TAGs on RP ODS columns, as a function of the temperature [31,32]. It was demonstrated that, with neat CO_2 as the mobile phase (at a pressure of 150 atm), in the supercritical region (35-45° C) the retention increased with increasing temperature, due to the decrease of density. On the other hand, in the subcritical region (0-30° C) an opposite behaviour was observed since, in a similar way to HPLC, the retention decreased with increasing temperature, and the selectivity changed, allowing more peaks to be resolved. Under the subcritical conditions employed in this work, an identical behaviour was to be expected, since the extension of the relationships between retention properties of TAGs and chemical structures generally observed in HPLC and subcritical chromatography with neat CO_2 have been demonstrated, afterwards [15,35].

Different modifiers including 2-propanol, ethanol, methanol, acetonitrile, and acetonitrile/methanol (1:1, *v/v*) were evaluated. The best result was obtained using the solvent mixture CO_2/acetonitrile, with a linear gradient elution mode. It is well known that pressure is an important factor on the density of supercritical CO_2. The setting of backpressure obviously influences the eluotropic strength of supercritical fluid. An optimal backpressure of 1500 psi was selected for the UPC^2 analysis. In order to improve the separation, an Ascentis Express C18 Column (100 mm × 3 mm I.D., 2 μm *d.p.*, Supelco) was used; it resulted good for the resolution and the really short analysis time, as shown in Figure 1 (V-5.2.) for Extra Virgin Olive Oil (EVOO), reported as an example.

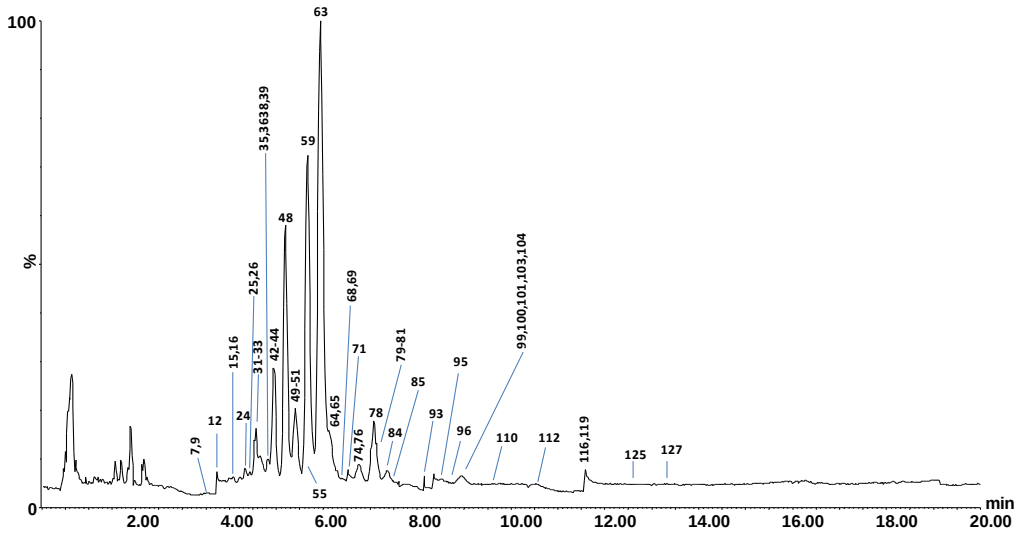

Figure 1 (V-5.2.). UHPSFC-APCI-MS chromatograms of TAGs in EVOO on Ascentis Express C18 column, 100 mm ×3.0 mm, 2 μm. (The peak numbers are correlated to TAGs reported in Table 1 (V-5.2.)).

5.2.3.2. Chromatographic separation and identification of triacylglycerols

As shown in Figure 1 (V-5.2), Figure 2 (V-5.2.) and Table 1 (V-5.2.), a total of 133 TAGs were separated under the present UPC^2-ToF MS conditions. The elution order of such compounds increases with increasing PN, reflecting the relation between CNs and DBs in acyl chains, like in NARP-LC. As can be seen, TAGs are eluted within 14 min gradient, according to their increasing hydrophobicity, with a calculated PN number ranging from 36 to 56 for the more complex borage oil sample. The retention behaviour of TAGs within one single PN group is strongly influenced by the FA composition in individual TAGs, mainly by the unsaturation degree and acyl chain lengths. TAG retention, within one PN group, increases with increasing DB number in the acyl chains. Despite the shorter analysis time, the separation in all the samples was satisfactory, except for the borage oil where some co-elutions still occur. However the identification of the co-elution peaks was mainly based on the

accurate ionic mass.

In analyzed samples, TAGs have been identified using positive ion APCI-MS based on protonated molecules $[M+H]^+$ and sodium adduct $[M+Na]^+$, used for the molecular weight assignment, and fragment ions $[M+H-R_iCOOH]^+$, formed by cleavage of FAs from the glycerol backbone, used for the identification of individual FAs. The standard notation of TAGs uses initials of FA trivial names, listed in the order of *sn*-1, *sn*-2, and *sn*-3. Since an achiral approach cannot differentiate *sn*-1 and *sn*-3 enantiomers, we regarded them as equivalent and arranged them in the order of decreasing molecular weight. The FA in *sn*-2 position, instead, can be determined because the neutral loss of FA from the inner position is less favored compared to *sn*-1 and *sn*-3 positions and thus it produces fragment ions of lower intensity. Considering that in nature regioisomers are present in mixtures and relative abundances of fragment ions resulted from fragment ions of all isomers, only predominant FAs in the *sn*-2 position are defined. According to literature data, unsaturated FAs, mainly linoleic acid, preferentially occupy the *sn*-2 position in plant oils [37].

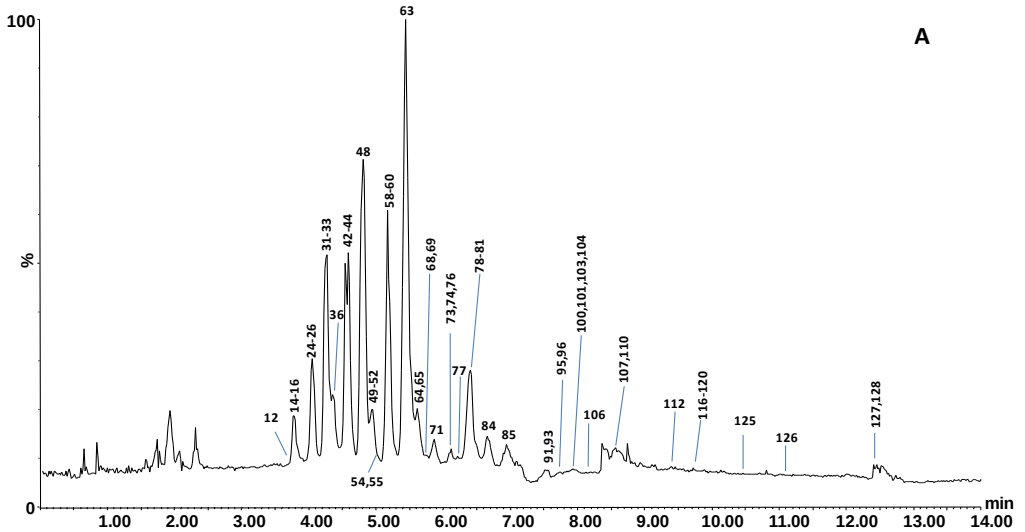

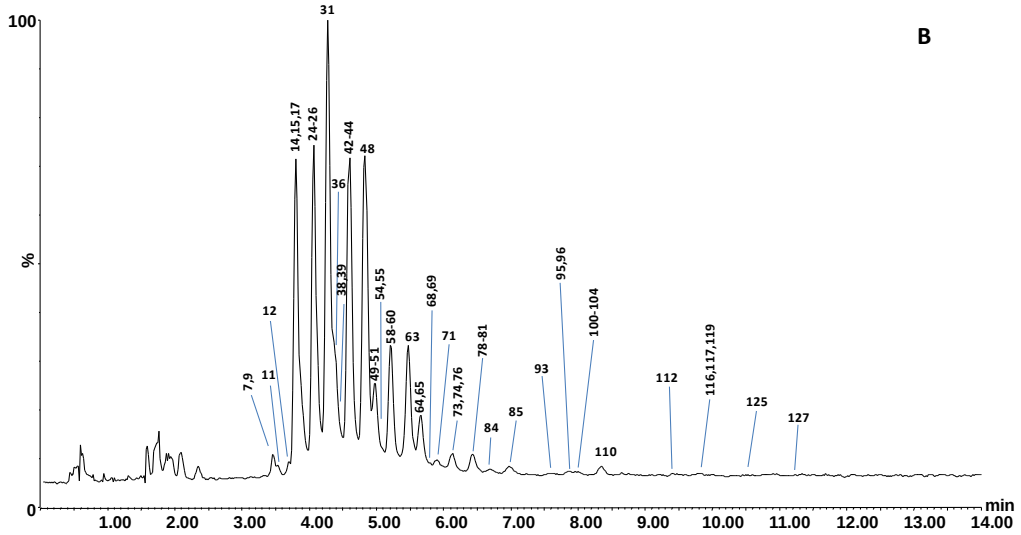
B
100
%
0
min
1.00
2.00
3.00
4.00
5.00
6.00
7.00
8.00
9.00
10.00
11.00
12.00
13.00
14.00
31
14,15,17
24-26
42-44
48
36
38,39
54,55
58-60
63
68,69
71
78-81
95,96
100-104
7,9
11
12
49-51
64,65
73,74,76
84
85
93
110
112
116,117,119
125
127

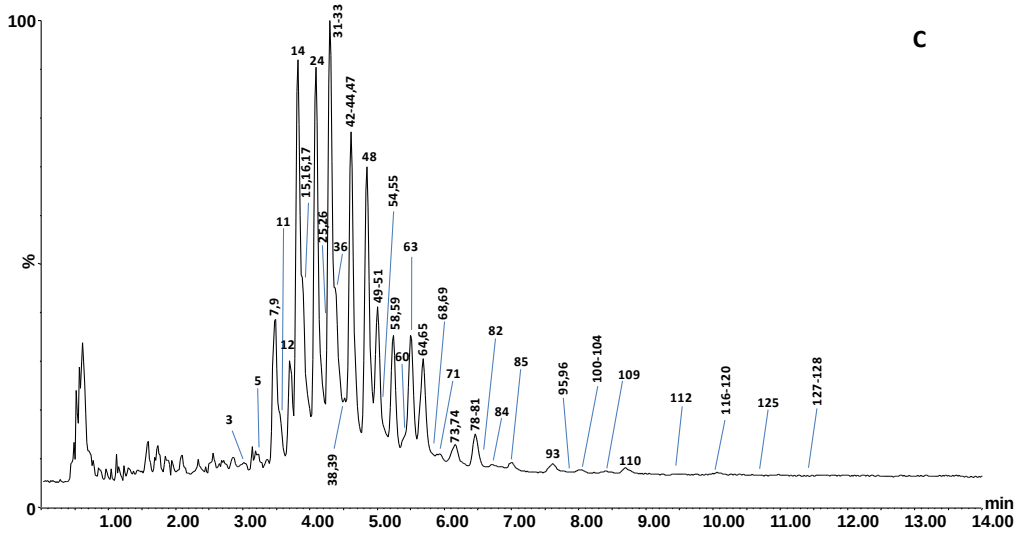
C
100
%
0
min
1.00
2.00
3.00
4.00
5.00
6.00
7.00
8.00
9.00
10.00
11.00
12.00
13.00
14.00
31-33
14
24
42-44,47
48
54,55
15,16,17
11
25,26
36
63
49-51
7,9
58,59
68,69
12
60
64,65
82
85
71
5
3
38,39
73,74
78-81
84
93
95,96
100-104
109
110
112
116-120
125
127-128

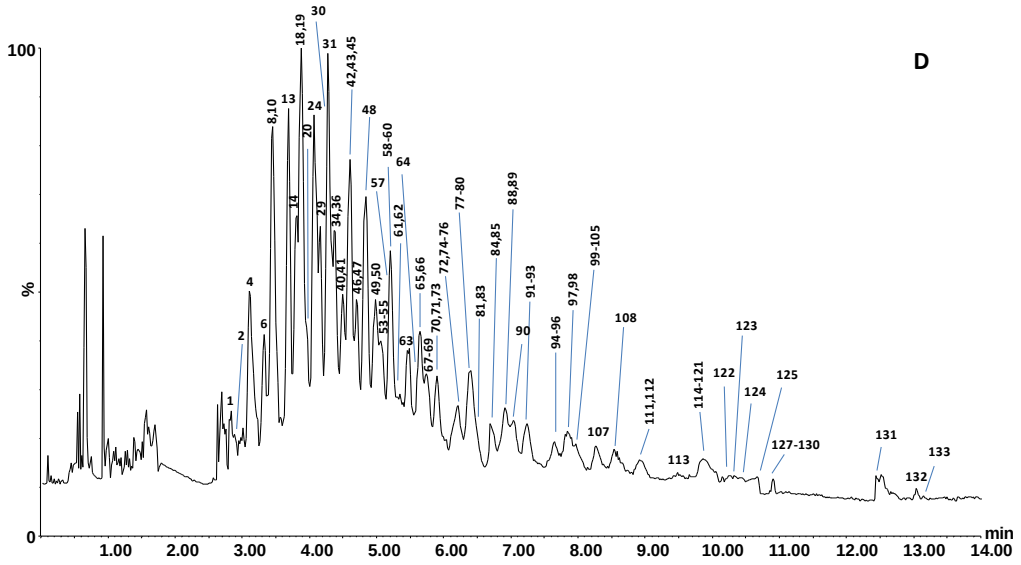
D
100
%
0
1.00
2.00
3.00
4.00
5.00
6.00
7.00
8.00
9.00
10.00
11.00
12.00
13.00
14.00
min
1
2
4
6
8,10
13
18,19
30
31
42,43,45
48
58-60
64
57
24
20
14
29
34,36
40,41
46,47
49,50
53-55
63
61,62
65,66
67-69
70,71,73
72,74-76
77-80
81,83
84,85
88,89
90
91-93
94-96
97,98
99-105
107
108
111,112
113
114-121
122
123
124
125
127-130
131
132
133

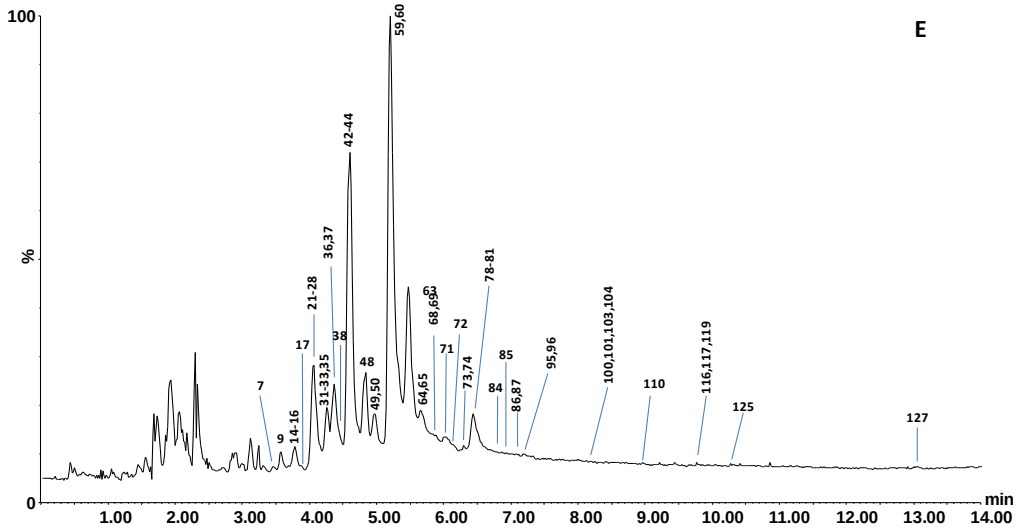
E
100
%
0
1.00
2.00
3.00
4.00
5.00
6.00
7.00
8.00
9.00
10.00
11.00
12.00
13.00
14.00
min
7
9
14-16
17
21-28
31-33,35
36,37
38
42-44
48
49,50
59,60
63
64,65
68,69
71
72
73,74
78-81
84
85
86,87
95,96
100,101,103,104
110
116,117,119
125
127

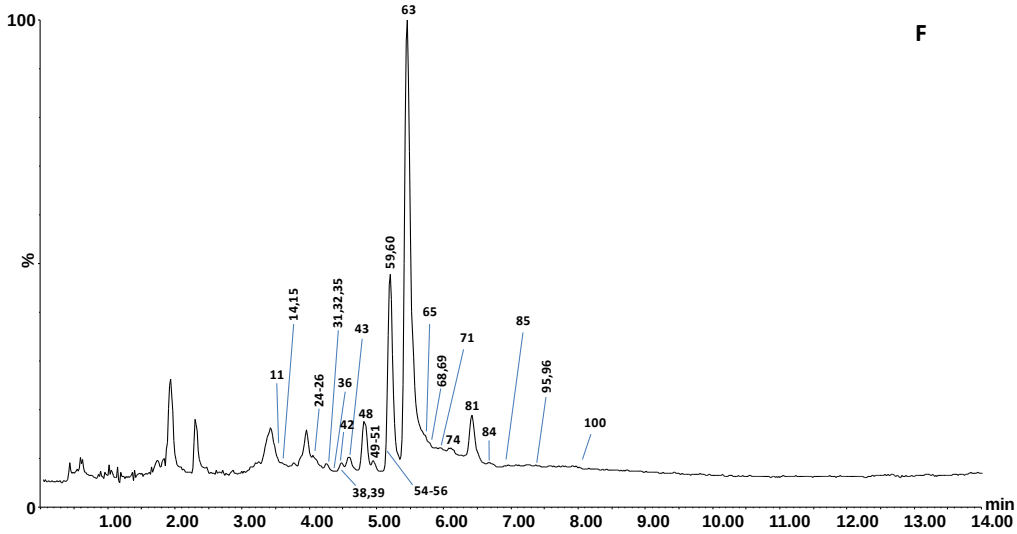

Figure 2 (V-5.2.). UHPSFC-APCI-MS analysis of Peanut oil (A), Corn oil (B), Soybean oil (C), and Borage oil (D), Palm oil (E), Hazelnut oil (F). (The peak numbers are correlated to TAGs reported in Table 1 (V-5.2.)).

Table 1 (V-5.2.). TAGs identified in the vegetable oils analyzed. The PN value, DB and theorical *m/z* are also reported.

N°	TAGs	PN	DB	$[M+H]^+_{Theo}$	Peanut	Corn	EVOO	Soybean	Borage	Palm	Hazelnut
1	γLnγLnγLn	36	9	873.6967					*		
2	γLnγLnPo	38	7	849.6967					*		
3	LnLLn	38	8	875.7123				*			
4	γLnLγLn	38	8	875.7123					*		
5	LnLnP	40	6	851.7123				*			
6	γLnγLnP	40	6	851.7123					*		
7	LLLn	40	7	877.7280		*	*	*		*	
8	LLγLn	40	7	877.7280					*		
9	LnOLn	40	7	877.7280		*	*	*		*	
10	γLnOγLn	40	7	877.7280					*		
11	LLPo	42	5	853.7280		*		*			*
12	LnLP	42	5	853.7280	*	*	*	*			
13	γLnLP	42	5	853.7280					*		
14	LLL	42	6	879.7436	*	*	*	*	*	*	*
15	OLLn	42	6	879.7436	*	*	*	*		*	*
16	SLnLn	42	6	879.7436	*		*	*		*	
17	PLnP	44	3	829.7280		*		*		*	
18	OLγLn	42	6	879.7436					*		
19	SγLnγLn	42	6	879.7436					*		
20	PγLnP	44	3	829.7280					*		
21	PLM	44	2	803.7123						*	
22	OLM	44	3	829.7280						*	
23	PPoL	44	3	829.7280						*	
24	LLP	44	4	855.7436	*	*	*	*	*	*	*
25	OLPo	44	4	855.7436	*	*	*	*		*	*
26	LnOP	44	4	855.7436	*	*	*	*		*	*
27	POM	46	1	805.728						*	
28	PPM	46	0	779.7123						*	
29	γLnOP	44	4	855.7436					*		
30	GγLnγLn	42	7	905.7593					*		
31	OLL	44	5	881.7593	*	*	*	*	*	*	*
32	OOLn	44	5	881.7593	*		*	*		*	*
33	SLLn	44	5	881.7593	*		*	*		*	
34	OOγLn	44	5	881.7593					*		
35	POPo	46	2	831.7436			*			*	*
36	PLP	46	2	831.7436	*	*	*	*	*	*	*
37	OOM	46	2	831.7436						*	
38	LLC17:0	45	4	869.7593		*	*	*		*	*
39	OLC17:1	45	4	869.7593		*	*	*			*
40	SLγLn	44	5	881.7593					*		
41	C17:1LP	45	3	843.7436					*		
42	OOPo	46	3	857.7593	*	*	*	*	*	*	*
43	OLP	46	3	857.7593	*	*	*	*	*	*	*
44	SLnP	46	3	857.7593	*	*	*	*		*	
45	SγLnP	46	3	857.7593					*		
46	GLγLn	44	6	907.7749					*		
47	C20:2LL	44	6	907.7749				*	*		
48	OLO	46	4	883.7749	*	*	*	*	*	*	*
49	POP	48	1	833.7593	*	*	*	*	*	*	*
50	SLL	46	4	883.7749	*	*	*	*	*	*	*
51	SOLn	46	4	883.7749	*	*	*	*			*
52	PPP	48	0	807.7436	*						
53	SOγLn	46	4	883.7749					*		

N°	TAGs	PN	DB	$[M+H]^+_{Theo}$	Peanut	Corn	EVOO	Soybean	Borage	Palm	Hazelnut
54	OLC17:0	47	3	871.7749	*	*		*	*		*
55	OOC17:1	47	3	871.7749	*	*	*	*	*		*
56	C17:1OP	47	2	845.7593							*
57	GγLnP	46	4	883.7749					*		
58	GLL	46	5	909.7906	*	*		*	*		
59	OOP	48	2	859.7749	*	*	*	*	*	*	*
60	SLP	48	2	859.7749	*	*		*	*	*	*
61	GOγLn	46	5	909.7906					*		
62	ALγLn	46	5	909.7906					*		
63	OOO	48	3	885.7906	*	*	*	*	*	*	*
64	GLP	48	3	885.7906	*	*	*	*	*	*	
65	SLO	48	3	885.7906	*	*	*	*	*	*	*
66	SγLnS	48	3	885.7906					*		
67	C22:1LγLn	46	6	935.8062					*		
68	OOC17:0	49	2	873.7906	*	*	*	*	*	*	*
69	SLC17:0	49	2	873.7906	*	*	*	*	*	*	*
70	GγLnS	48	4	911.8062					*		
71	GLO	48	4	911.8062	*	*	*	*	*	*	*
72	SPP	50	0	835.7749					*	*	
73	ALL	48	4	911.8062	*	*		*	*	*	
74	SOP	50	1	861.7906	*	*	*	*	*	*	*
75	C22:1γLnP	48	4	911.8062					*		
76	C17:0OP	49	1	847.7749	*	*	*		*		
77	C22:1LL	48	5	937.8219	*				*		
78	GOP	50	2	887.8062	*	*	*	*	*	*	
79	ALP	50	2	887.8062	*	*	*	*	*	*	
80	SLS	50	2	887.8062	*	*	*	*	*	*	
81	SOO	50	2	887.8062	*	*	*	*	*	*	*
82	BLLn	48	5	937.8219				*			
83	BLγLn	48	5	937.8219					*		
84	GOO	50	3	913.8219	*	*	*	*	*	*	*
85	ALO	50	3	913.8219	*	*	*	*	*	*	*
86	APP	52	0	863.8062						*	
87	SSP	52	0	863.8062						*	
88	GLS	50	3	913.8219					*		
89	BγLnP	50	3	913.8219					*		
90	C24:1LγLn	48	6	963.8375					*		
91	C22:1LO	50	4	939.8375	*				*		
92	GLG	50	4	939.8375					*		
93	BLL	50	4	939.8375	*	*	*	*	*		
94	C24:1γLnP	50	4	939.8375					*		
95	AOP	52	1	889.8219	*	*	*	*	*	*	*
96	SOS	52	1	889.8219	*	*	*	*	*	*	*
97	C24:1OγLn	50	5	965.8532					*		
98	C24:1LL	50	5	965.8532					*		
99	GOS	52	2	915.8375			*		*		
100	AOO	52	2	915.8375	*	*	*	*	*	*	*
101	BLP	52	2	915.8375	*	*	*	*	*	*	
102	ALS	52	2	915.8375		*		*	*		
103	BOP	54	1	917.8532	*	*	*	*	*	*	
104	AOS	54	1	917.8532	*	*	*	*	*	*	
105	C22:1OP	52	2	915.8375					*		
106	C23:0LL	51	4	953.8532	*						

N°	TAGs	PN	DB	$[M+H]^+_{Theo}$	Peanut	Corn	EVOO	Soybean	Borage	Palm	Hazelnut
107	C22:1OO	52	3	941.8532	*				*		
108	C24:1LP	52	3	941.8532					*		
109	LgLLn	50	5	965.8532				*			
110	BLO	52	3	941.8532	*	*	*	*		*	
111	C24:1LO	52	4	967.8688					*		
112	LgLL	52	4	967.8688	*	*	*	*	*		
113	C24:1γLnS	52	4	967.8688					*		
114	C22:1OS	54	2	943.8688					*		
115	C24:1OP	54	2	943.8688					*		
116	BOO	54	2	943.8688	*	*	*	*	*	*	
117	LgLP	54	2	943.8688	*	*		*	*	*	
118	BLS	54	2	943.8688	*			*	*		
119	LgOP	56	1	945.8845	*	*	*	*	*	*	
120	BOS	56	1	945.8845	*			*	*		
121	C22:1γLnC22:1	52	5	993.8845					*		
122	C24:1OO	54	3	969.8845					*		
123	C24:1LS	54	3	969.8845					*		
124	C22:1OG	54	3	969.8845					*		
125	LgLO	54	3	969.8845	*	*	*	*	*	*	
126	C23:0OO	55	2	957.8845	*						
127	LgOO	56	2	971.9001	*	*	*	*	*	*	
128	LgLS	56	2	971.9001	*			*	*		
129	C24:1OS	56	2	971.9001					*		
130	C22:1GS	56	2	971.9001					*		
131	C22:1GG	56	3	997.9158					*		
132	C22:1OC22:1	56	3	997.9158					*		
133	C24:1OG	56	3	997.9158					*		

Fatty acid abbreviations: M = miristic acid, P = palmitic acid, Po = palmitoleic acid, $C_{17:0}$ = margaric acid, $C_{17:1}$ = eptadecenoic acid, Ln = linolenic acid, L = linoleic acid, O = oleic acid, S = stearic acid, A = arachidic acid, G = gadoleic acid, B = behenic acid, $C_{22:1}$ = erucic acid, Lg = lignoceric acid, $C_{24:1}$ = nervonic acid.

5.2.3.3. IMS separation of triacylglycerols

The combination of retention times, MS and MS/MS spectra allows to identify the sample components, except than in the presence of co-eluting, isobaric compounds which would also render indistinguishable collision MS/MS spectra. On the other hand, the mobility of an ion passing through the IMS assembly and governed by the size, shape and mass to charge ratio (*m/z*) can afford further separation.

Figure 3 (V-5.2.) shows the UPC^2-IM-MS analysis of borage oil. As can be noted, for TAGs species IMS distribution is very similar, and it is critical to obtain structural insight without any preliminar chromatographic separation. However, the combination of the retention times, MS spectra, together with the

additional drift times, gives supplementary insight into the identity of the compounds of interest.

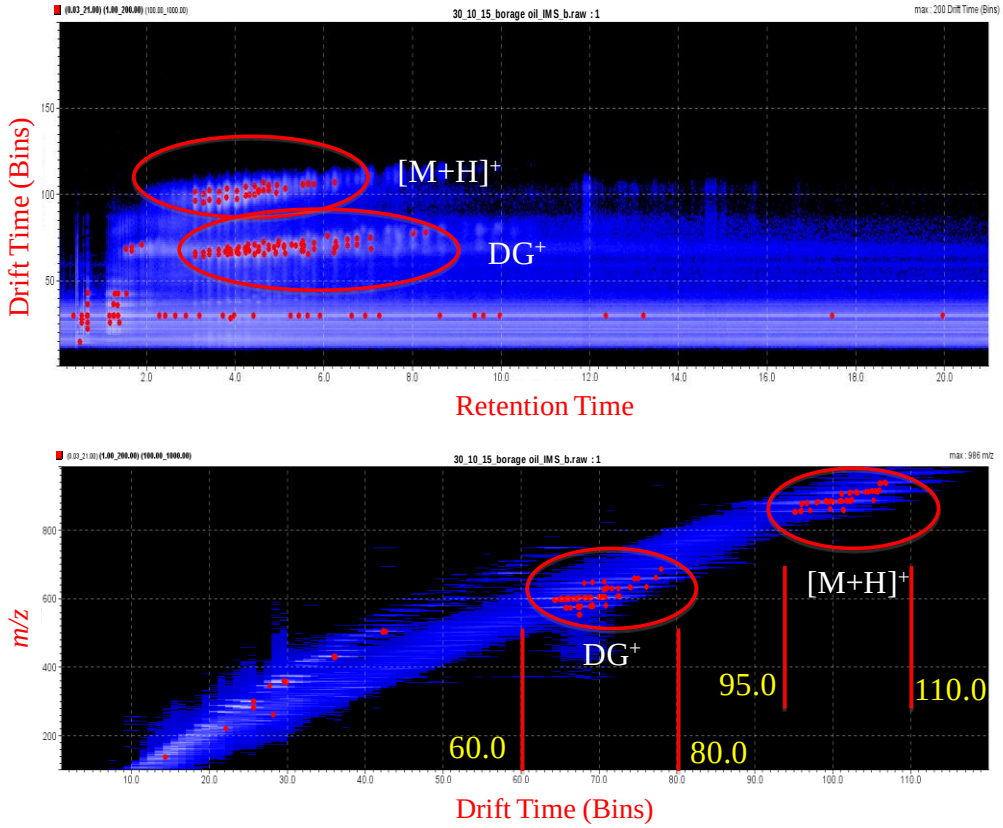

Figure 3 (V-5.2.). UPC^2-IM-MS plots of borage oil: (A) drift time vs.r_T; (B) m/z vs. drift time.

5.2.4. Conclusions

From the perspective of current applied lipid research, UPC^2 is enabling new ways of separating non-polar lipids. Good resolution was achieved on a single end-capped C18 column, in less of 14 min analysis time, for the separation of TAGs in a variety of vegetable oils with excellent repeatability (average retention time CV 0.21%). While the number of positive identifications was comparable to what reported in the literature, run time was drastically reduced

(up to >10 times) and also the organic solvent consumption (up to >30). Remarkably, the use of APCI interface alleviates the need for a post-column make-up solvent/pump, retaining the advantages of less toxic, environmental-friendly technique.

REFERENCES

[1] Christie, W.W., Han, X., Lipid Analysis. 4th Edition, Oily Press, Bridgewater 2010.

[2] Gunstone, F. D., Harwood, J. L., Dijkstra, A. J., The Lipid Handbook with CD ROM. 3rd Edition, CRC Press, Boca Raton 2007.

[3]http://www.lipidmaps.org/data/classification/LM_classification_exp.php (updated on March 20th, 2017).

[4] Brown, H.A., Marnett, L.J., to Introduction lipid biochemistry, metabolism, and signaling. Chem Rev. 2011, 111, 5817-5820.

[5] Orešič, M., Hänninen, V. A., Vidal-Puig, A., Lipidomic: a new window to biomedical frontiers. Trends Biotech. 2008, 26, 647–652.

[6] Vance, J. E., Vance, D. E., Biochemistry of Lipids, Lipoproteins and Membranes. 4th Edition, Elsevier, Amsterdam 2002.

[7] Lusis, A. J., Atherosclerosis. Nature 2000, 407, 233–241.

[8] Bazinet, R. P., Layé, S. Polyunsaturated fatty acids and their metabolites in brain function and disease. Nat Rev Neurosc 2014, 15, 771–785

[9] Gunstone, F. D., Vegetable Oils in Food Technology: Composition, Properties and Uses, Second Edition, 2011 Blackwell Publishing Ltd.

[10] FEDIOL, The European Vegetable Oil and Proteinmeal Industry, Brussells, http://www.fediol.be/.

[11] Andrikopoulos, N.K. Chromatographic and spectroscopic methods in the analysis of triacylglycerol species and regiospecific isomers of oils and fats. critical Reviews In Food Science And Nutrition, 2002, 42, 473-505.

[12] Rejsek, J., Vrkoslav, V., Vaikkinen, A., *et al.* Thin-Layer Chromatography/Desorption Atmospheric Pressure Photoionization Orbitrap Mass Spectrometry of Lipids. Anal Chem, 2016, 88, 12279-12286.

[13] Idrus, S. I. S., Latiff, A. A., Ismail, M. N. Determination of triacylglycerols in food by high-performance liquid chromatography. Instrumentation Science & Technology, 2017, 45, 577-591.

[14] Rezanka, T., Padrova, K., Sigler, K. Regioisomeric and enantiomeric analysis of triacylglycerols. Analytical Biochemistry, 2017, 524, 3-12.

[15] Kallio, H., Nylund, M., Bostrom, P. *et al.* Triacylglycerol regioisomers in human milk resolved with an algorithmic novel electrospray ionization tandem mass spectrometry method. Food Chemistry, 2017, 233, 351-360.

[16] Dermaux, A., Medvedovici, A., Ksir, M., Van Hove, E., Talbi, M., Sandra, P. Elucidation of the triglycerides in fish oil by packed-column supercritical fluid chromatography fractionation followed by capillary electrochromatography and electrospray mass spectrometry. J. Microcolumn Sep. 1999, 11, 451–459.

[17] Sandra, P., Medvedovici, A., Zhao, Y., David, F., Characterization of triglycerides in vegetable oils by silver-ion packed-column supercritical fluid chromatography coupled to mass spectroscopy with atmospheric pressure chemical ionization and coordination ion spray. J. Chromatogr. A 2002, 974, 231–241.

[18] Bernal, J. L., Martín, M. T., Toribio, L., Supercritical fluid chromatography in food analysis. J. Chromatogr. A 2013, 1313, 24–36.

[19] Laboureur, L., Ollero, M., Touboul, D., Lipidomics by supercritical fluid chromatography. Int. J. Mol. Sci.2015, 16, 13868–13884.

[20] Buchgraber, M., Ulberth, F., Emons, H., Anklam, E., Triacylglycerol profiling by using chromatographic techniques. Eur. J. Lipid Sci. Technol. 2004, 106, 621–648.

[21] Laakso, P., Analysis of triacylglycerols – approaching the molecular composition of natural mixtures. Food Rev. Int. 1996, 12, 199–250.

[22] Lee, M. L., Markides, K. E., Chromatography with supercritical fluids. Science 1987, 235, 1342–1347.

[23] Novotny, M. V., Recent developments in analytical chromatography. Science 1989, 246, 51–57.

[24] Manninen, P., Laakso, P., Kallio, H., Method for characterization of triacylglycerols and fat-soluble vitamins in edible oils and fats by supercritical fluid chromatography. J. Am. Oil Chem. Soc. 1995, 72, 1001–1008.

[25] Manninen, P., Laakso, P., Kallio, H., Separation of γ - and (α; -linolenic acid containing triacylglycerols by capillary supercritical fluid chromatography. Lipids 1995, 30, 665–671.

[26] David, F., Medvedovici, A., Sandra, P., Oils, Fats and Waxes: Supercritical Fluid Chromatography. Academic Press, Cambridge, MA 2000, 3567–3575.

[27] Lesellier, E., West, C., The many faces of packed column supercritical fluid chromatography—a critical review. J. Chromatogr. A 2015, 1382, 2–46.

[28] Nováková, L., Perrenoud, A. G.-G., François, I., West, C., Lesellier, E., Guillarme, D., Modern analytical supercritical fluid chromatography using columns packed with sub-2 μm particles: A tutorial. Anal. Chim. Acta 2014, 824, 18–35.

[29] Poole, C. F., Stationary phases for packed-column supercritical fluid chromatography. J. Chromatogr. A 2012, 1250, 157–171.

[30] Donato, P., Inferrera, V., Sciarrone, D., Mondello, L., Supercritical fluid chromatography for lipid analysis in foodstuffs. J. Sep. Sci. 2017, 40, 361–382.

[31] Funada, Y., Hirata, Y., Analysis of plant oils by subcritical fluid chromatography using pattern fitting. J. Chromatogr. A 1998, 800, 317–325.

[32] Funada, Y., Hirata, Y., Retention behavior of triglycerides in subcritical

fluid chromatography with carbon dioxide mobile phase. J. Chromatogr. A 1997, 764, 301–307.

[33] Lesellier, E., Latos, A., Lopes de Oliveira, A., Ultra high efficiency/low pressure supercritical fluid chromatography with superficially porous particles for triglyceride separation. J. Chromatogr. A 2014,1327, 141–148.

[34] Lesellier, E., Bleton, J., Tchapla, A., Use of relationships between retention behaviors and chemical structures in subcritical fluid chromatography with CO_2/modifier mixtures for the identification of triglycerides. Anal. Chem. 2000, 72, 2573–2580.

[35] Lesellier, E., Tchapla, A., Retention behavior of triglycerides in octadecyl packed subcritical fluid chromatography with CO_2/modifier mobile phases. Anal. Chem. 1999, 71, 5372–5378.

[36] Lee, J. W., Uchikata, T., Matsubara, A., Nakamura, T., Fukusaki, E., Bamba, T., Application of supercritical fluid chromatography/mass spectrometry to lipid profiling of soybean. J. Biosci. Bioeng. 2012, 113, 262–268.

[37] Lísa M., Holčapek M., J. Chromatogr. A 2008, 1198-1199, 115-130.

This page was intentionally left blank

CHAPTER VI
Application of matrix assisted laser desorption/ ionization time-of-flight mass spectrometry in lipid research

6.1. Structural analysis of triacylglycerols in vegetable oil by using high-resolution MALDI-ToF/ToF mass spectrometry

6.1.1. Introduction

MALDI-TOF MS (Matrix Assisted Laser Desorption/Ionization Time-of-Flight Mass Spectrometry) can provide both qualitative and quantitative determinations of lipids from food and biological samples, and is generally more sensitive and less affected by impurities such as buffer salts and polarities of analytes compared with other MS methods. Additionally, MALDI do allow for direct tissue analysis for the investigation of the spatial distribution of the species within the tissue. Despite its potential being recognized for lipid analysis, it is surprising how little attention has so far attracted in this field. However, it has been shown that triacylglycerols (TAGs) can be easily and accurately analyzed by MALDI-TOF MS, and that 2,5-dihydrobenzoic acid (DHB) is the matrix of choice [1]. An important advantage of MALDI-TOF MS in lipid analysis arises from the fact that both the lipid and the matrix are soluble in organic solvents, thus all manipulations can be performed in a single organic phase.

This results in extremely homogeneous matrix/analyte co-crystals and an excellent reproducibility in comparison to water-soluble compounds such as proteins.

Aim of the research work carried out in Messina was centered onto the evaluation of the capabilities of a novel MALDI-TOF/TOF mass spectrometer

with high –sensitivity, throughput, resolution – in the field of lipid research.

A detailed description of an in-depth structural analysis of different (individual and mixtures) triacylglycerol species of nutritional and cosmetic interest is presented.

Triacylglycerols (TAG) are important for the storage of energy (fat tissues in living organisms), while diacylglycerols (DAG) are important lipid-derived second messengers; the latter are normally generated from glycerophospholipids by cleavage of the polar headgroup under the influence of the enzyme phospholipase C [2]. The positive ion MALDI-TOF mass spectra of both, DAGs [3] as well as TAGs [4] can be easily recorded with standard DHB. The MALDI mass spectra give always exclusively the Na^+ adducts, whereas H^+ adducts are never detected, even if the solutions are acidified [5]. Using MALDI MS in combination with high energy collisionally-induced dissociation (CID), the losses of the fatty acyl residues, from glycerol backbone, can be used for structural elucidation of TAGs [6], i.e. the determination which fatty acyl residue is located in which position.

The applied matrix has only a relatively weak impact on the spectral quality, whereas strongly different sensitivities are achieved in dependence on the used solvents.

The MALDI process can be briefly described in Figure 1 (VI-6.1.). In a former step, the compound to be analyzed is dissolved in a solvent containing small organic molecules, called matrix.

A droplet of such an analyte/matrix solution is the deposited onto a dedicated plate and dried before analysis. This results in the formation of a “solid” bed of matrix/analyte crystals, in which the analyte molecules are embedded throughout the matrix in the way that they are completely isolated from one another. The second step occurs under the vacuum conditions inside the source of the mass spectrometer. Upon firing a laser pulse over a short duration, the

following rapid heating causes the ablation and sublimation of a portion of the solid surface, and the expansion of the matrix into the gas phase, entraining intact analytes in the expanding matrix plume. The formed analyte ions move then towards the entrance of the mass analyzer for mass separation.

Although the processes of absorption of the laser energy are easily understood, rather surprisingly the overall processes of desorption and ionization have not yet been fully clarified.

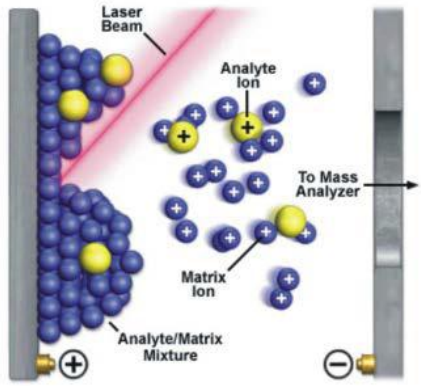

Figure 1 (VI-6.1.). Representation of the MALDI process

A well-known disadvantage which affects MALDI is represented by the low shot-to-shot reproducibility of mass spectra.

In fact, each laser shot ablates a few layers of the matrix/analyte bed, and depending on the position on the surface irradiated, a significant variation of the shot-by-shot spectra can be observed.

Therefore, improvement of the sample preparation protocols (which, however, are still empirical) leading to a more homogeneous surface has a beneficial effect on the reproducibility of mass spectra. This is very important if precise quantitative results must be obtained. Another way for compensating such an unavoidable poor reproducibility is to acquire several single-shot spectra from

one spot.

The standard method of sample preparation in the MALDI technique is the *"dried-droplet"* method; a very simple and rapid execution method, which provides the mixing of an almost saturated solution of the matrix with a solution of known concentration of analyte. Generally, 1 μL of matrix and analyte is deposited on the sample holder (plate), it is left to air dry, or under forced flow of hot air, to encourage the evaporation of the solvent and the crystallization of the sample.

The other deposition method used is the *"sandwich"* method. This sample preparation method provides that, a drop of saturated solution of matrix is first deposited on the plate, immediately after, a drop of the solution, with known concentration of analyte, is subsequently deposited, and after crystallization, another drop of saturated solution of matrix is deposited on the target.

The present work shows the evaluation of MALDI-TOF MS in the qualitative analysis of the main components of two different vegetable oils, i.e. triacylglycerols. Extra Virgin Olive (EVO) and Borage oils were analyzed by MALDI-TOF.

EVOO is one of the main ingredients of the Mediterranean diet; while Borage oil is mainly used in cosmetic industry.

Although chromatographic methods are useful in providing structural information on this class of molecules, they have the disadvantage of requiring more time and substantial amounts of organic solvents.

During the present work, we tried to obtain spectral information useful to provide a structural description, as complete as possible, of these molecules.

The structural features investigated include: (i) the specific nature of individual fatty acids linked to glycerol backbone; (ii) the position of each fatty acid in the triacylglycerol in order to evaluate the position isomers.

In a first step of the work, the analysis of standard materials was carried out, in

order to obtain information on the typical fragmentation *patterns* of triacylglycerols.

For this purpose, two species of TAGs, were analyzed:

- ✓ C52: 1 corresponding to the pair of POP (1,3-dipalmitoyl-2-oleyl-glycerol) and OPP (1-oleyl-2,3-dipalmitoyl-glycerol) position isomers;
- ✓ C54: 1 corresponding to the pair of SOP (1-sterayl-2-oleyl-3-palmitoyl-glycerol) OPS (1-oleyl-2-palmitoyl-3-sterayl-glycerol) and OSP (1-oleyl-2-sterail) -3-palmitoyl-glycerol) isomers.

The choice of these TAGs was made in order to identify the typical fragmentation *patterns*, useful to obtain complete structural information and to identify the exact position of the hypothetical unsaturations. Furthermore, the identification of the fatty acid in position *sn-2* allowed to distinguish position isomers. After acquiring the mass spectra, each TAG was subjected to mass/ mass analysis (MSMS) in order to obtain more structural information. Once the fragmentation *patterns* have been obtained, the same analytical approach has been applied to the EVOO and Borage oil.

6.1.2. Experimental

6.1.2.1. Samples and sample preparation

All TAGs (POP: 1,3-dipalmitoyl-2-oleyl-glycerol; OPP: 1-oleyl-2,3-dipalmitoyl-glycerol; SOP: 1-sterayl-2-oleyl-3-palmitoyl-glycerol; OPS: 1-oleyl-2-palmitoyl-3-sterayl-glycerol; OSP (1-oleyl-2-sterail)-3-palmitoyl-glycerol) used in this study were purchased from Supelco/Sigma Aldrich. 2,5-Dihydroxybenzoic (DHB) acid and was purchased from Shimadzu GLC (Kyoto, Japan).

Individual TAG solutions were obtained in concentration 10 mg/mL in chloroform.

2,5-DHB was used as matrix, and was prepared in methanol (10 mg/mL).

Before depositing the sample, it is necessary to wash the sample holder (plate): the washing involves several phases, while the solvents used are generally isopropanol , methanol and distilled water. The washing is necessary in order to eliminate contaminants, or residues of the sample used in the analysis previously carried out.

Sample preparation was carried out following the *sandwich* method: a first thin layer of matrix crystals was prepared by placing a droplet of matrix solution (0.35 μL) onto a MALDI target spot and allowed to dry. A sample droplet (0.35 μL) was afterwards placed on the top of the preformed matrix layer, followed by an equal amount of a 10 mM (in methanol) NaCl solution. A final (second) matrix droplet was then deposited onto the target.

6.1.2.2. MALDI-ToF MS analyses

All mass spectrometric analyses were performed on a MALDI 7090 (Shimadzu) with a solid state UV-laser (ʎ = 355 nm), for the ions generation, operating at a 2 kHz acquisition repetition rate. The instrument was operated at an acceleration voltage of 20 KeV, and .

In order to enhance the spectral resolution, the analyzes were performed in reflectron mode with detection of positive mode spectra of all analytes.

The mass range has been set from 200 to 1200 Da, and the pulsed extraction function, to improve mass resolution, was carefully applied (850 m/z).

The power and diameter of the laser, and other instrumental parameters have been optimized in real time, adapting them to the nature of the sample.

The laser power was adjusted for each experiment to obtain the best signal-to-noise ratio and to maximize the number and intensity of structural fragments.

During the optimization phase, the sensitivity (signal-to-noise ratio) and the mass resolution are evaluated, in fact, to enhance the ratio, 100 single shots were averaged for each mass spectrum.

MS/MS experiments are performed after selecting the precursor ion, setting a well defined ion gate range. The fragmentation of the precursor ion was induced by collision (collision induced dissociation - CID) with Helium gas (the pressure during the CID process is 2.8 * 10-6). The spectra related to the precursor ion fragments were acquired by operating always in reflectron mode and in positive mode.

The TOF analyzer was calibrated using the TOFmix standards solution using.

All mass spectrometric data were acquired and analyzed by using the MALDI Solution software (Kratos Analytical, Manchester, UK).

6.1.3. Results and discussion

In order to obtain information about the TAG fragmentation *patterns*, POP and OPP (isomers) and the SOP, OSP and OPS (isomers) standard TAGs were analyzed. Mass spectra were acquired in *reflectron* mode with positive ion detection, in mass range from 200 to 1200 *m/z*, with laser power equivalent to 70. Figure 2 (VI-6.1.) shows MALDI-TOF mass spectrum of POP.

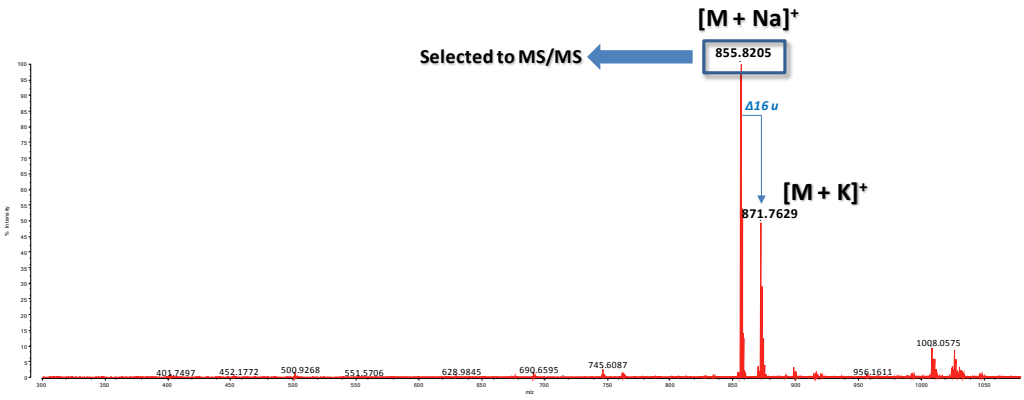

Figure 2 (VI-6.1.). MALDI-TOF mass spectrum of POP.

The two most abundant ions, one at *m/z* 855.3205 and the other at *m/z*

871.7629, show a difference of 16 u.m.a.; 855.3205 ion is sodium adduct $[M+Na]^+$ of POP. The ion at 871.7629 *m/z* relative to the potassium adduct $[M+K]^+$ with the POP ion.

In MALDI-TOF experiments, the production of sodium and potassium (ubiquitous metals) adducts is very common. In protonated adduct (not revealed in this experiment), the proton is supplied by the DHB matrix. This is probably due to the lower half-life of the protonated adduct, compared to the sodium or potassium adduct. In fact, only the ions sufficiently stable to reach the analyzer without first decomposing, are detected [7].

The ion at *m/z* 855.3205 was selected for MS/MS experiment; the fragmentation of the precursor ion was induced by CID and the spectrum relative to its fragments was acquired in reflectron positive mode using laser power setted at 80. Figure 3 (VI-6.1.) shows MS/MS spectrum related to the fragmentation of the precursor ion (POP); it is possible to distinguish three different spectral regions.

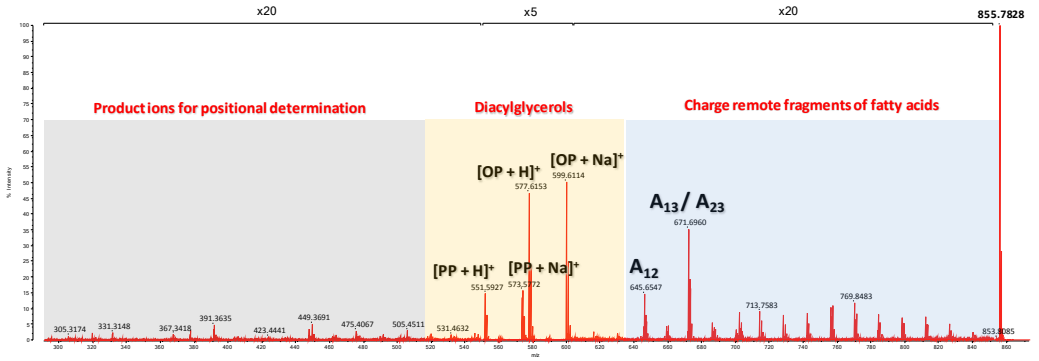

Figure 3 (VI-6.1.). MS/MS spectrum of the precursor ion *m/z* 855.8205 (POP).

On the left of the spectrum region there is the zone corresponds to the monoacylglycerol ions deriving from the loss of two fatty acids from the TAG standard; the middle spectral region corresponds to the diacylglycerol ions,

each deriving from the loss of one of the fatty acid of the TAG; the spectral region on the right represents the zone of *charge remote* fragments. More information about the fragmentation *patterns* [8] are shown below in Figure 4 (VI-6.1.).

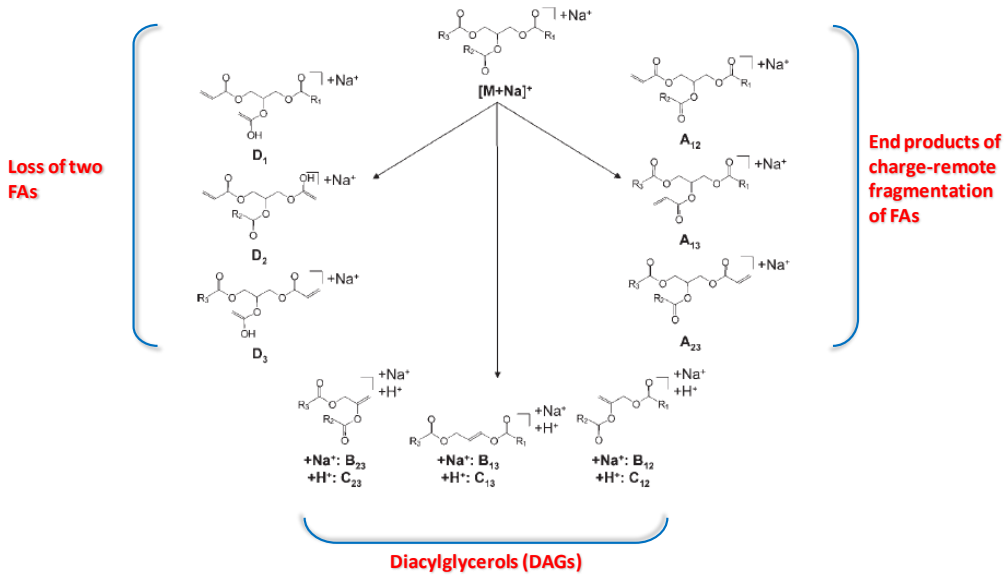

Figure 4 (VI-6.1.). Typical triacylglycerol fragmentation *patterns*

In the left spectral region (monoacylglycerol region), there are three types of fragments, indicated (in Figure 4 (VI-6.1.)) respectively as D_1, D_2 and D_3. The D_1 and D_3 fragments derive from the loss of one of the external fatty acids (*sn-1/3*) and the loss of the fatty acid in the central position (*sn-2*).

D_2 ion product indicates the monoacylglycerol obtained from the loss of both fatty acids that occupy the external positions; it maintains the fatty acid in central position (*sn-2*).

The fragment ions, in the diacylglycerol zone, can be conventionally indicated

to as; $B_{2,3}$, $B_{1,3}$ and $B_{1,2}$, (sodium adducts); $C_{2,3}$, $C_{1,3}$ and $C_{1,2}$ (protonated adducts).

Fragments deriving from the charge-remote reactions, in the right region of the spectrum, are designated as $A_{1,2}$, $A_{2,3}$ and $A_{1,3}$.

Figure 5 (VI-6.1.) shows an expansion of middle spectral region, i.e. diacylglycerols region of OPP and POP TAGs fragmentation.

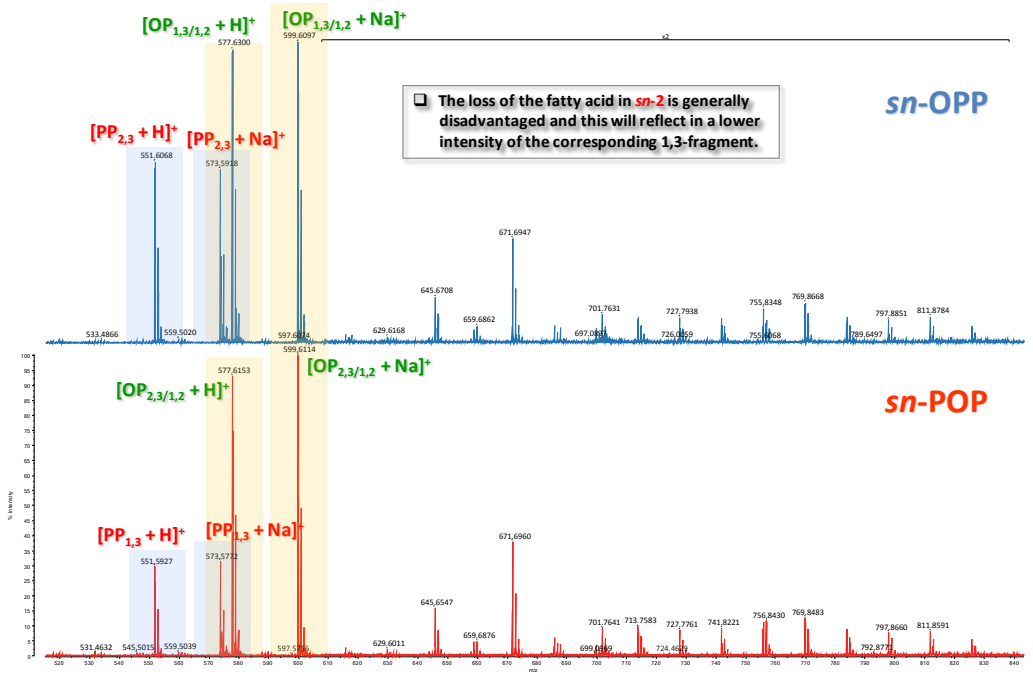

Figure 5 (VI-6.1.). Expansion of diacylglycerols spectral region in MALDI MS/MS analysis of (*sn*-OPP and *sn*-POP)

1-oleyl-2,3-dipalmitoyl-glycerol (OPP) and (1,3-dipalmitoyl-2-oleyl-glycerol) (POP) are positional isomers differing in the oleic acid position in glycerol backbone (*sn-1* position in OPP) and (*sn-2* position in POP).

Observing the diacylglycerols region, for both TAGs, the peaks relative to the corresponding diacylglycerols are detected; in particular both the protonated

and sodium adducts are detected, (for example: $[PP_{1,3}+Na]^+$ and $[PP_{2,3}+Na]^+$, $[OP_{1,3}+Na]^+$ and $[OP_{2,3}+Na]^+$). For both TAGs, we have the diacylglycerol deriving from the loss of oleic acid, that is identified by formation of the diacylglycerol proton adduct at *m/z* 551.6068 $[PP_{1,3}/_{2,\ 3}+H]^+$, regardless of the position oleic acid occupies the glycerol backbone; if we have the sodium adduct, the diacylglycerol has *m/z* 573.5918 $[PP_{1,3}/_{2,\ 3}+Na]^+$.

The intensity of the ions at *m/z* 551.6068 $[PP_{1,3}/_{2,\ 3}+H]^+$ and *m/z* 573.5918 $[PP_{1,3}/_{2,\ 3}+Na]^+$ is smaller than the other diacylglycerol ions because of the loss of the fatty acid linked in the *sn-2* position is disadvantaged compared to the loss of the fatty acid which occupies an external position.

The peak corresponding to the diacylglycerol deriving from the loss of the central fatty acid ($B_{1,3}$ or $C_{1,3}$ fragment) will be less intense than the peak related to the loss of fatty acid which occupies an external position ($B_{2,3}$ or $C_{2,3}$ fragment).

A right spectral region is occupied by ions deriving from *charge remote* fragmentation reactions. Many studies have shown that the fragmentation of gaseous ions can occur as a result of the breaking of the bonds located far from the site of the molecule charge. This type of fragmentation, called *charge remote fragmentation* (CFR), is useful for the structural characterization of many natural and synthetic molecules [9].

The reactions can be defined *charge remote* only when there is no involvement of the charge to the fragmentation process; in fact, the reactions that will lead to the fragmentation of the ion will be independent of the state of charge. The charge must be stable in its position and must not "migrate".

CRF reactions are observed for both anionic and cationic species, and generally, the energy required to promote such reactions is considerable.

The usefulness of the CFR for analytical purposes lies in the production of characteristic fragmentation *patterns*, which make possible structural

identification of different molecules, offering the possibility to trace the length of alkyl chains present in various molecules of interest, and also to identify the exact position of ipotetical unsaturation and substituents.

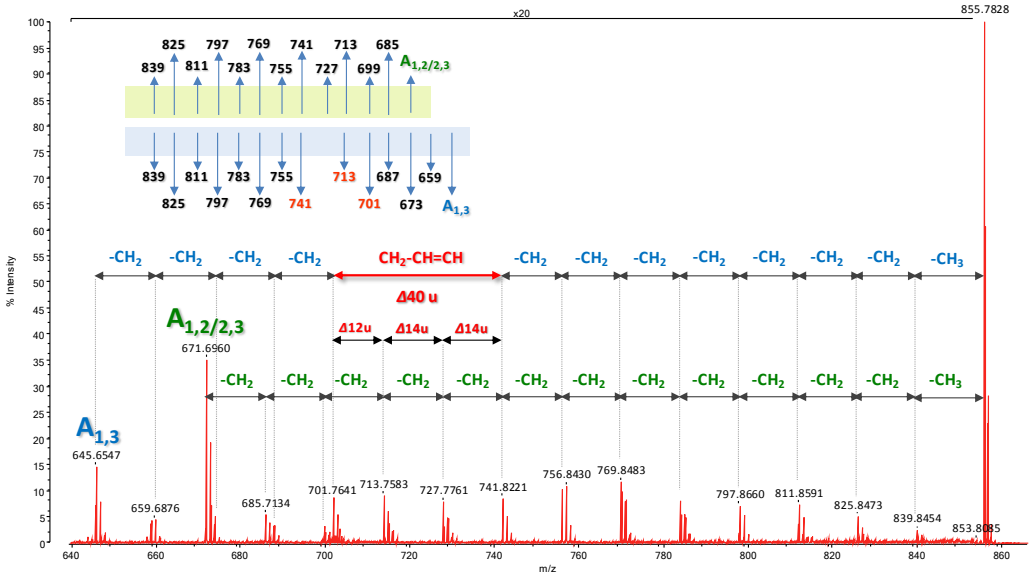

Figure 6 (VI-6.1.). Expansion of the *charge remote* spectral region (MS/MS spectrum of *sn*-POP)

As shown in Figure 6 (VI-6.1.), in the *charge remote* spectral region (MS/MS spectrum of POP) the most abundant peaks are: the peak at *m/z* 671.6960, corresponding to the $A_{1,2/2,3}$ fragment and the peak at *m/z* 645.6547, corresponding to the $A_{1,3}$ fragment. The $A_{1,2/2,3}$ fragment derives from the *charge remote* fragmentation of palmitic acid (16: 0), which occupies the external positions; it refers to palmitic acid in both *sn*-1 and *sn*-3 positions.

Palmitic acid is a saturated fatty acid, so the *charge remote* fragmentation will lead to the elimination of methylene units ($-CH_2$), resulting from the breaking of individual consecutive C-C bonds in the carbon chain, identifiable, in the MS/MS spectrum, from the presence of a series of fragment ions that differ by

14 u.m.a. The presence of these fragments allows to know the length of the carbonic chain of fatty acid present in the external positions *sn*-1/3, and it indicates if it is a saturated fatty acid. The peak at *m/z* 645.6547 corresponds to the $A_{1,3}$ fragment, which derives from the *charge remote* fragmentation of the oleic acid in position *sn*-2. The latter differs from the palmitic acid, for the length of the carbon chain, and also for the presence of unsaturation. The presence of the unsaturation as well as its exact position can both be deduced from a careful observation of the fragments present in the spectral region of *charge remote fragments*.

The spectrum in this area shows the presence of a series of fragment ions (which differ from each other by 14 u.m.a.) resulting from the splitting of individual consecutive C-C bonds of the alkyl chain of fatty acid; the fragmentation near to the double bond will take place in a different way, in fact in the latter case, the elimination of olefin hydrogen (hydrogen linked to one of the carbons involved in the double bond) is energetically disadvantaged, so that the C-C bond adjacent to the double bond will be split. This will lead to the elimination of the double bond as vinyl group ($-CH_2-CH=CH-$); this loss can be identified in the spectrum by the presence of two fragments that differ from each other of 40 u.m.a.

The presence of these two fragments allows the univocal identification of the position of the unsaturation in the alkyl chain of fatty acid. Considering what has been said, in Figure 6 (VI-6.1.), the position of the unsaturation will be obtained from the fragments at *m/z* 741.8221 and 701.7641.

The positions where the individual fatty acids bind to glycerol can be determined by the presence of designated fragments such as E_1, E_3, F_1, F_3, G_1 and G_3 and J_2 (Figure 7 (VI-6.1.)). In particular the $E_{1/3}$, $F_{1/3}$ and $G_{1/3}$ fragments provide useful information about the fatty acids present in the external positions *sn*-1/3 of triacylglycerol; while the J_2 fragment is useful to determinate the fatty

acid present in the central position *sn*-2. Thanks to the presence of such fragments it is possible to distinguish isomeric triacylglycerols.

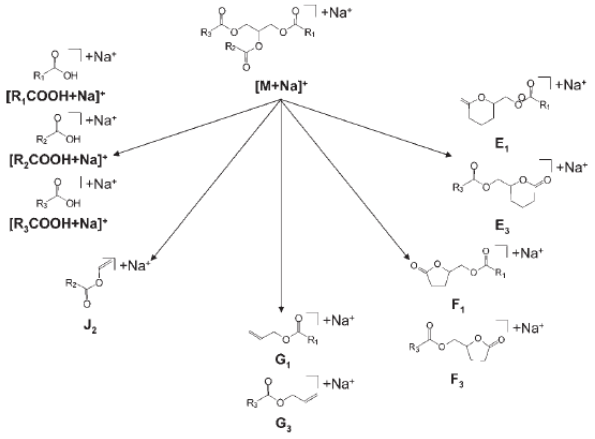

	Loss of two FAs		*sn*-1/3		*sn*-2
FA	**D-fragment**	**E-fragment**	**F-fragment**	**G-fragment**	**J-fragment**
C16:0	$C_{24}H_{42}NaO_6^+$ **449.2874**	$C_{22}H_{40}NaO_4^+$ **391.2819**	$C_{21}H_{38}NaO_4^+$ **377.2662**	$C_{19}H_{36}NaO_2^+$ **319.2608**	$C_{18}H_{34}NaO_2^+$ **305.2451**
C18:0	$C_{26}H_{46}NaO_6^+$ **477.3192**	$C_{24}H_{44}NaO_4^+$ **419.3137**	$C_{23}H_{42}NaO_4^+$ **405.2981**	$C_{21}H_{40}NaO_2^+$ **347.2926**	$C_{20}H_{38}NaO_2^+$ **333.2770**
C18:1	$C_{26}H_{44}NaO_6^+$ **475.3036**	$C_{24}H_{42}NaO_4^+$ **417.2981**	$C_{23}H_{40}NaO_4^+$ **403.2824**	$C_{21}H_{38}NaO_2^+$ **345.2770**	$C_{20}H_{36}NaO_2^+$ **331.2613**
C18:2	$C_{26}H_{42}NaO_6^+$ **473.2879**	$C_{24}H_{40}NaO_4^+$ **415.2824**	$C_{23}H_{38}NaO_4^+$ **401.2668**	$C_{21}H_{36}NaO_2^+$ **343.2613**	$C_{20}H_{34}NaO_2^+$ **329.2456**

Figure 7 (VI-6.1.). *Charge remote* fragments

Figure 8 (VI-6.1.) shows the comparison of MS/MS spectra of POP and OPP, highlighting the D, E, F, G and J_2 fragments useful for the exact identification of the positions of fatty acids and useful to distinguish the two isomers. In the upper portion of the Figure 8 (VI-6.1.), the MS/MS spectrum of OPP TAG is shown: the peak at *m/z* 305.3263 corresponds to the J_2 fragment; its presence indicates the presence of palmitic acid in *sn*-2 position. The peak at *m/z* 417.3670 is present in case of OPP TAG, but not in its POP isomer, because it indicates the presence of oleic acid in *sn*-1 position and it corresponds to the E_1

fragment.

Considering POP TAG, there is no peak at *m/z* 345.3389 which indicates the presence of oleic acid in the external positions and it corresponds to the G_1 fragment. However, the peak at *m/z* 391 is present in both spectra: in the case of the OPP, it corresponds to the E_3 fragment (*m/z* 391.3473), and it indicates the presence of palmitic acid in the external position *sn*-3; while in POP isomer the signal is more intense (*m/z* 391.3635) because it is due to the contribute of palmitic acid in both the *sn*-1 and *sn*-3 positions (E_3/E_1 fragment); similar considerations must be made for fragments F_3 and F_2.

To understand the identification of these fragments, is necessary to evaluate the data shown in the table present in the lower portion of (Figure 7 (VI-6.1.).

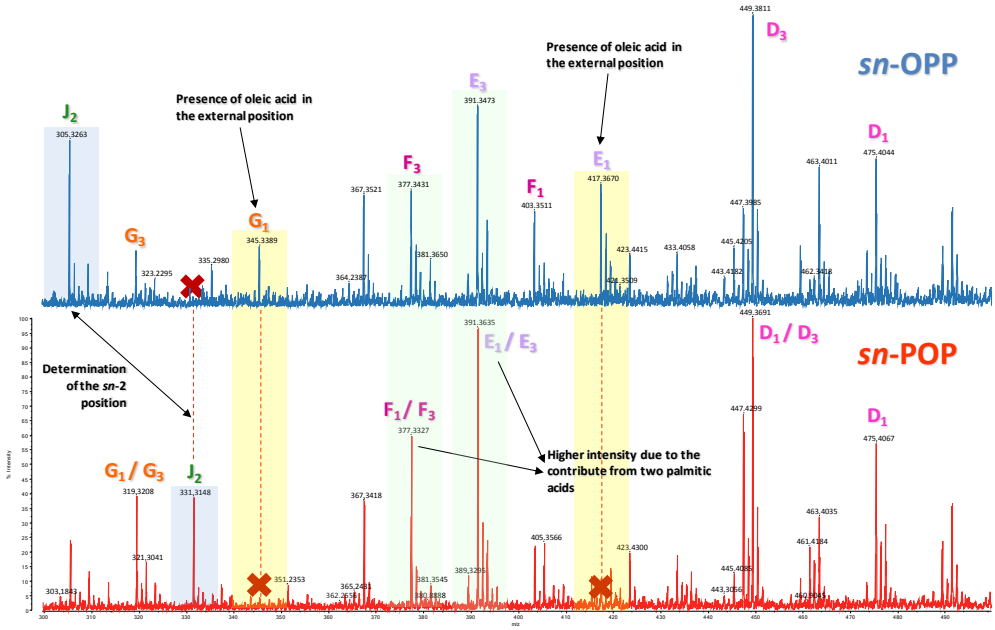

Figure 8 (VI-6.1.). Expansion of the *charge remote* spectral region (*sn*-OPP and *sn*-POP).

The same approach has been used for SOP (1-stearyl-2-oleyl-3-palmitoyl-

glycerol), OSP (O-stearyl-2-oleyl-2-oxylate-3-palmitoyl-glycerol), and SPO (1-sterayl-2-) palmitoyl-3-oleyl-glycerol) isomers. Figure 9 (VI-6.1.) shows the spectral regions of diacylglycerols. Also in this case, the signals corresponding to $B_{1,3}$ or $C_{1,3}$ fragments, namely diacylglycerols deriving from the loss of the fatty acid in central position, will be less intense because the loss of the fatty acid in *sn*-2 position is unfavorable. In OSP TAG, the signal at *m/z* 577.5986, corresponding to the diacylglycerol formed by the loss of stearic acid in the central position; the signal will be less intense than the diacylglycerol signals formed by the loss of one of the fatty acids in *sn*-1/3 position.

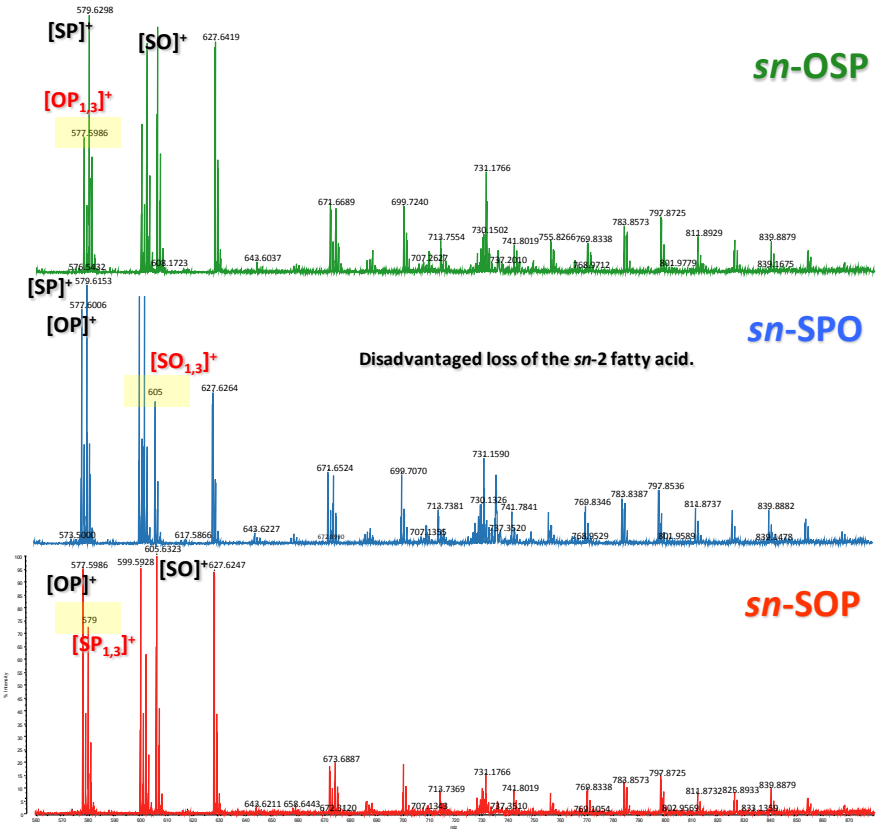

Figure 9 (VI-6.1.). Expansion of the diacylglycerols spectral region (*sn*-OSP, *sn*-SPO and *sn*-SOP).

The assignment of *sn*-1, *sn*-2 and *sn*-3 positions, by identifying the E_1, E_3, F_1,

F_3, G_1 and G_3 and J_2 fragments, allows to distinguish the positional isomers. Figure 10 (VI-6.1.) shows MS/MS spectra of OSP, SPO and SOP TAG isomers. The E_1, E_3, F_1, F_3, G_1 and G_3 fragments are diagnostic for the determination of fatty acids linked in *sn*-1/3. The peak at *m/z* 419 is present in both the SPO (*m/z* 419.3794) and SOP (*m/z* 419.3907) isomers, and it is identified as E_1 fragment, it indicates that *sn*-1 position is occupied by stearic acid in both the isomers; the same consideration can be done about the peaks that identify the F_1 and G_1 fragments. The J_2 fragment for SPO isomer corresponds to the peak at *m/z* 305.3199 and it indicates the presence of palmitic acid in *sn*-2; while in SOP isomer, this position is occupied by the oleic acid and shows the J_2 fragment at *m/z* 331.3282. The J_2 fragment for OSP isomer is at *m/z* 333.3360 and it identifies the stearic acid in *sn*-2 position; while peaks at *m/z* 417.3673 and *m/z* 403.3316 are respectively E_1 and F_1 fragments, both indicating the presence of oleic acid in position *sn*-1.

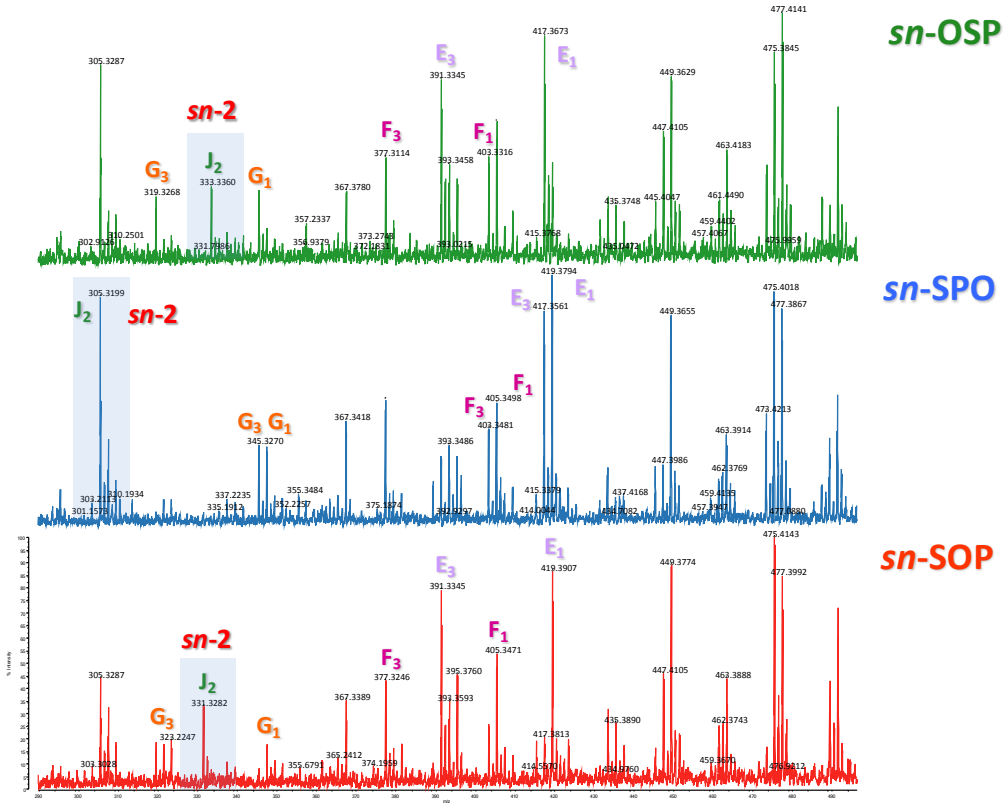

Figure 10 (VI-6.1.). Expansion of the *charge remote* spectral region (*sn*-OSP, *sn*-SPO and *sn*-SOP).

Once the information about the fragmentation *patterns* of the TAGs was obtained, the same analytical approach was applied to the two samples of interest: EVOO and Borage oil. Mass spectra, in both cases, were acquired in reflectron positive mode, and laser power was set at 70. In Figure 11 (VI-6.1.) the MALDI-ToF mass spectrum of EVOO sample is reported. The peak at *m/z* 883.7711 indicates the presence, in the sample, of TAGs belonging to the species C52:1: 16:0/18:1/18:0 (POS) and 18:0/16:1/18:0 (SPoS). The presence of TAGs belonging to the species C54:3, as sodium adducts, is shown by the presence of the peak at *m/z* 907.7742: 18:0/18:3/18:0 (SLnS), 18:0/18:1/18:2 (SOL) and 18:1/18:1/18:1 (OOO).

The qualitative identification was tentative, on the base of fatty acids present in EVOO usually reported in literature. For the real identification is necessary to do MS/MS analysis.

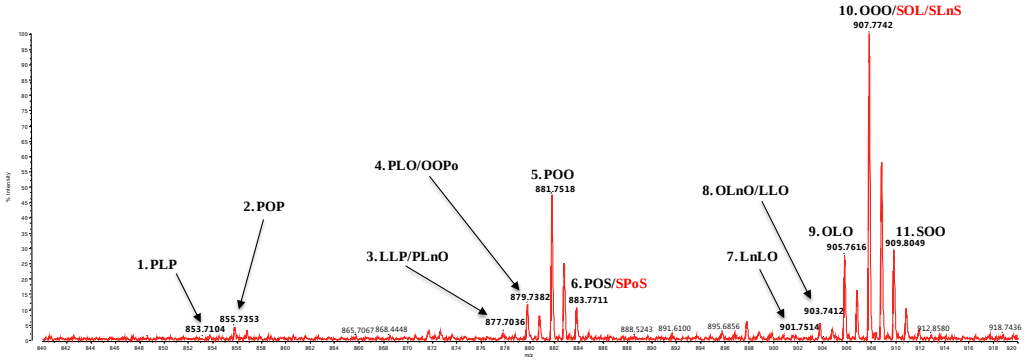

Figure 11 (VI-6.1.). MALDI-ToF mass spectrum of EVOO sample.

The spectra related to the analysis of Borage oil were acquired by setting a mass range from *m/z* 700 to 1200 and laser power equivalent to 70. The Figure 12 (VI-6.1.) shows the most abundant sodium ion $[M+Na]^+$ adducts at *m/z* 875.7592, 877.7714, 899.7747, 901.7885 and 903.7418; while the corresponding protonated adducts $[M+H]^+$ were not detected.

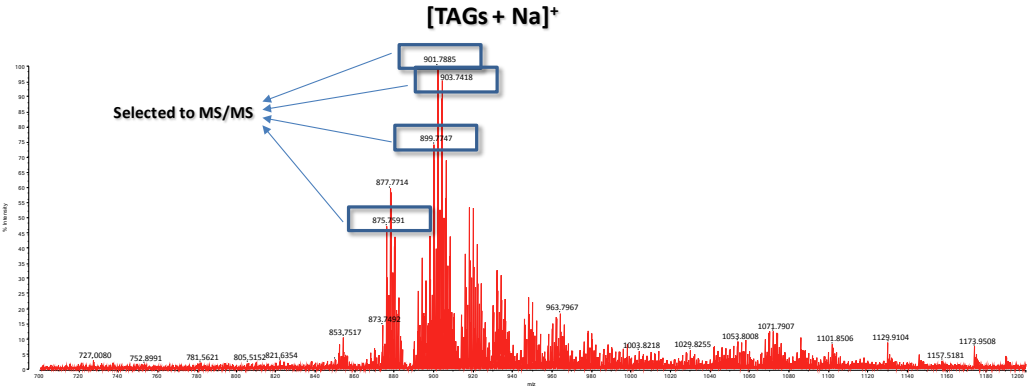

Figure 12 (VI-6.1.). MALDI-ToF mass spectrum of Borage oil.

Because of the complexity, in terms of qualitative composition, of Borage oil, MS/MS analyses were carried out. After the initial MALDI-ToF-MS analysis, the most abundant ions were selected and subjected to MS/MS experiments; the MS/MS spectra were acquired always operating in reflectron positive mode, but the laser power was set at 80.

As an example, in Figure 13 (VI-6.1.) is reported the spectrum relative to the MS/MS analysis of the ion at *m/z* 899.7747.

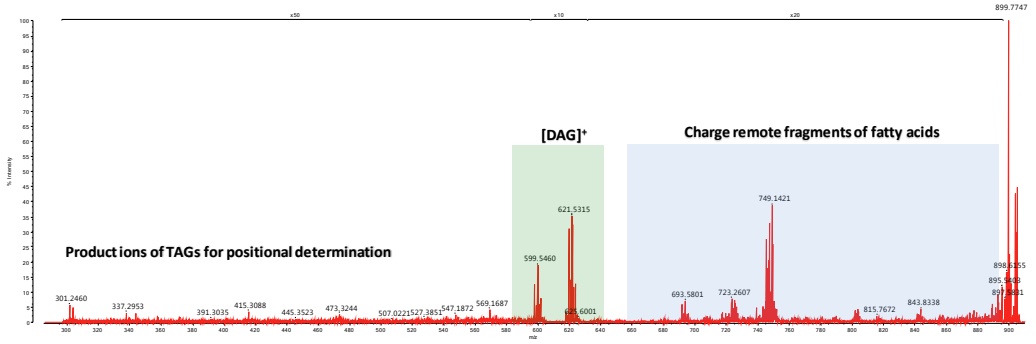

Figure 13 (VI-6.1.). MS/MS analysis of the *m/z* ion 899.7747.

The expansion of the left region of the spectrum, reported in Figure 14 (VI-6.1.), shows the fatty acid sodium adducts; *m/z* 301.2460 $[Ln+Na]^+$; *m/z* 303.2644 $[L+Na]^+$; *m/z* 305.2659 $[O+Na]^+$. In this region, D_1, D_2 and D_3 fragments can be identified. In addition, diagnostic fragments are highlighted to determine the exact position of each fatty acid linked to the glycerol backbone.

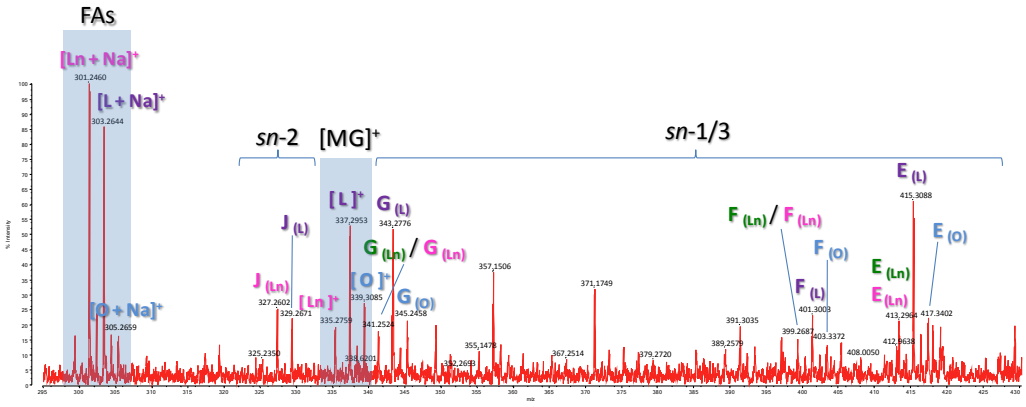

Figure 14 (VI-6.1.). Expansion of the spectral region of fatty acids and monoacylglycerols.

The peaks at *m/z* 327.2602 and 329.2671 are identified in J_2 fragments and they are diagnostic for the determination of fatty acid present in *sn*-2 position.

Ion at *m/z* 327.2602 is indicative of the presence of linolenic acid (C18:3) in *sn*-2 position; the ion *m/z* 329.2671 indicates the presence of linoleic acid (C18:2) in *sn*-2 position. The peaks at *m/z* 415.3088, 401.3003, and 343.2776, respectively indicate the fragments E, F and G, which are indicative of the presence of linoleic acid in positions *sn*-1 or *sn*-3. The peaks at *m/z* 413.2964, 399.2687 and 341.2524 (fragments E, F and G, respectively) are indicative of the presence of linolenic acid (18:3) in *sn*-1 or *sn*-3 positions. The peaks at *m/z* 417.3402, 403.3372 and 345.2458 indicate the presence of oleic acid (18:1) in *sn*-1 or *sn*-3 positions.

Therefore, in this spectral region, identified fragments indicate the possibility of TAGs with oleic acid, linoleic acid and linolenic acid in *sn*-1/3 positions.

About the last two fatty acids, the relative J_2 fragments have been detected, but the relative J_2 fragment for the oleic acid has not been detected, this means that there is no evidence of oleic acid in *sn*-2 position. Figure 15 (VI-6.1.) shows the

expansion of the other two spectral regions, one related to the diacylglycerols and one related to the *charge remote* fragments.

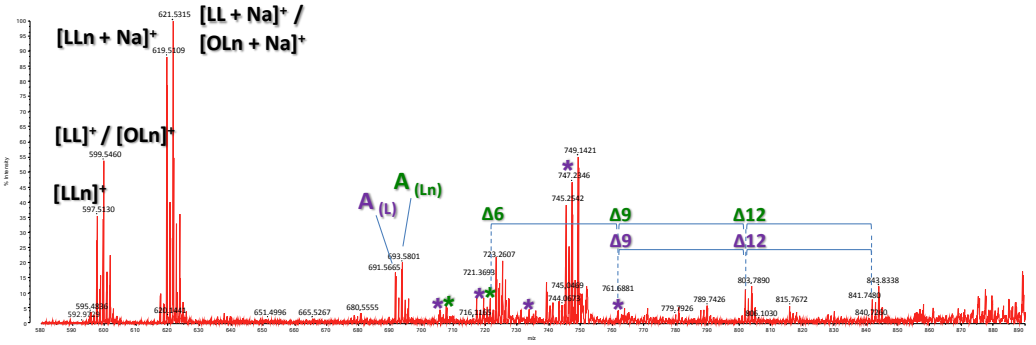

Figure 15 (VI-6.1.). Expansion of the spectral region of diacylglycerols and *charge remote* (right side).

On the left of the spectrum (Figure 15 (VI-6.1.)), the diacylglycerols zone is illustrated: $[LLn+Na]^+$, $[LL]^+/[OLn]^+$, $[LLn]^+$, $[LL+Na]^+$, $[OLn+Na\ ]^+$. In the *charge remote* area, the identification of the fragments allowed us to identify the degree of unsaturation of fatty acids linked to backbone glycerol and the exact position of the unsaturations. The peak at *m/z* 693.5801 corresponds to the $A_{1.2}$, that is detected as a result of *charge remote* fragment of the fatty acid in *sn*-3 position.

The presence of the following fragment ions: *m/z* 843.8338 and 803.7890, differing from each other by 40 u.m.a., indicates a first unsaturation in C_{12} position; the fragment ions at *m/z* 803.7890 and 763.6881 (Δ40 u.m.a.) indicate the presence of a second unsaturation, in C_9 position; the fragment ions at *m/z* 763.6881 and 723.2607 (Δ40 u.m.a.) indicate the presence of a third unsaturation in C_6 position. The identification of these fragments and the fragments deriving from the cleavage of C-C bonds (therefore, deriving from the loss of methylene units ($-CH_2$)), allowed us to trace the presence of a fatty

acid with 18 carbon atoms and three unsaturations in *sn*-3 position; these fragments allowed us to assign the exact positions of the unsaturations in the alkyl chain, being able to distinguish between α-linolenic acid and γ-linolenic acid.

α-linolenic acid, is an ω3-fatty acid with three unsaturations located respectively at C_9, C_{12} and C_{15}.

While, γ-linolenic acid (GLA), is a fatty acid isomer of the α-linolenic acid and it belongs to the ω6 series. Their unsaturations are located respectively at C_6, C_9 and C_{12}. On the basis of these considerations, the fatty acid identified in *sn*-3 position corresponds to the γ-linolenic acid (GLA - C18:3ω6).

The fragment ion at *m/z* 691.5665, reported as fragment $A_{(L)}$ in Figure 15 (VI-6.1.), derives from the *charge remote* fragmentation of linoleic acid (C18:2). In fact, fragments at *m/z* 843.8388 and 803.7890 (Δ40 u.m.a.) are detected and they indicate the presence of a double bond in C_{12}; the fragment at *m/z* 761.6881, which shows a difference of 40 u.m.a. with respect to the fragment at *m/z* 803.7890, indicates the presence of a double bond in C_9.

Considering the information obtained from the fragments present in the *charge remote* spectral region, together with the other information obtained from the MS/MS experiment of the ion at *m/z* 899.7747, (such as the identification of the $E_{1/3}$, $F_{1/3}$, $G_{1/3}$ and J_2 fragments), the possible triacylglycerols present in the Borage Oil correspond to the pair of isomers LLLn and LLnL (Ln = α-linolenic) and to the OLnγLn triacylglycerol.

REFERENCES

[1] D.J. Harvey. Matrix assisted laser desorption ionization mass spectrometry of phospholipids. J. Mass Spectrom. 30 (1995) 1333.

[2] B. Fuchs, R. Sus, J. Schiller. An update of MALDI-TOF mass spectrometry in lipid research. Progress in Lipid Research 49 (2010) 450.

[3] S. Carrasco, I. Merida. Diacylglycerol, when simplicity becomes complex. Trends Biochem Sci 32 (2007) 27.

[4] S Benard, J. Arnhold, M. Lehnert, J. Schiller, K. Arnold. Experiments towards quantification of saturated and polyunsaturated diacylglycerols by matrix assisted laser desorption and ionization time-of-flight mass spectrometry (MALDI-TOF MS). Chem Phys Lipids 100 (1999) 115.

[5] G.R. Asbury, K. Al-Saad, W.F. Siems, R.H. Hannan, H.H. Hill Jr. Analysis of triacylglycerols and whole oils by matrix-assisted laser desorption/ionization time of flight mass spectrometry. J Am Soc Mass Spectrom 10(1999) 983.

[6] J. Gidden, R. Liyanage, B. Durham, J.O. Lay Jr. Reducing fragmentation observed in the matrix-assisted laser desorption/ionization time-of-flight mass spectrometric analysis of triacylglycerols in vegetable oils. Rapid Commun Mass Spectrom 21 (2007) 1951.

[7] B. Fuchs, J. Schiller, Eur, J. Lipid Sci. Technol. 111 (2009) 83.

[8] E. Pittenauer, G. Allmaier. The renaissance of high-energy CID for structural elucidation of complex lipids: MALDI-TOF/RTOF-MS of alkali cationized triacylglycerols. J Am Soc Mass Spectrom 20 (2009) 1037.

[9] J. Wiley & Sons. Inc, R, Mass Spectr. 19 (2000) 398.

APPENDIX I
Supplementary Materials

Chapter II - Liquid Chromatography coupled to Mass Spectrometry and Statistical Analyisis

2.1. Reuse of dairy product: evaluation of the lipid profile evolution during and after their shelf-life

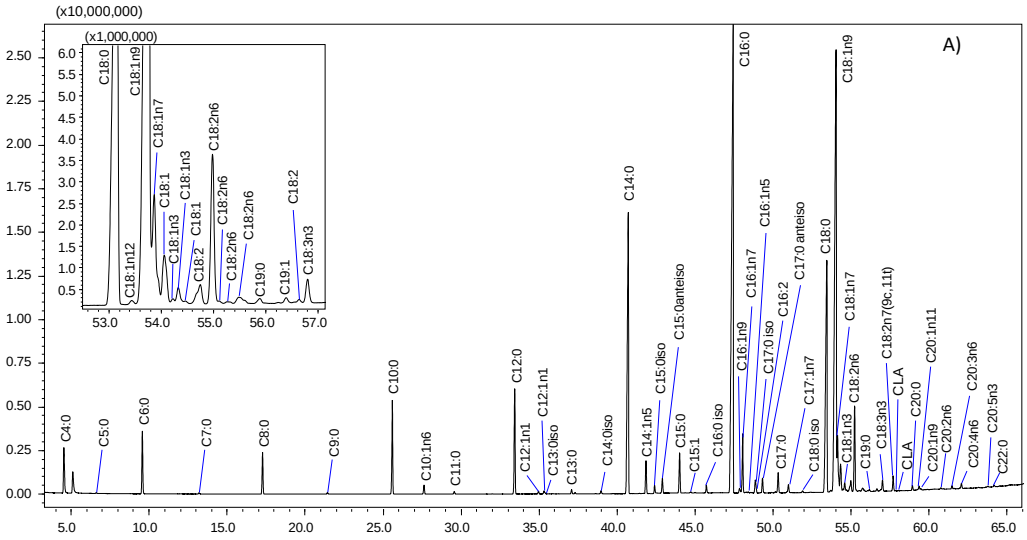

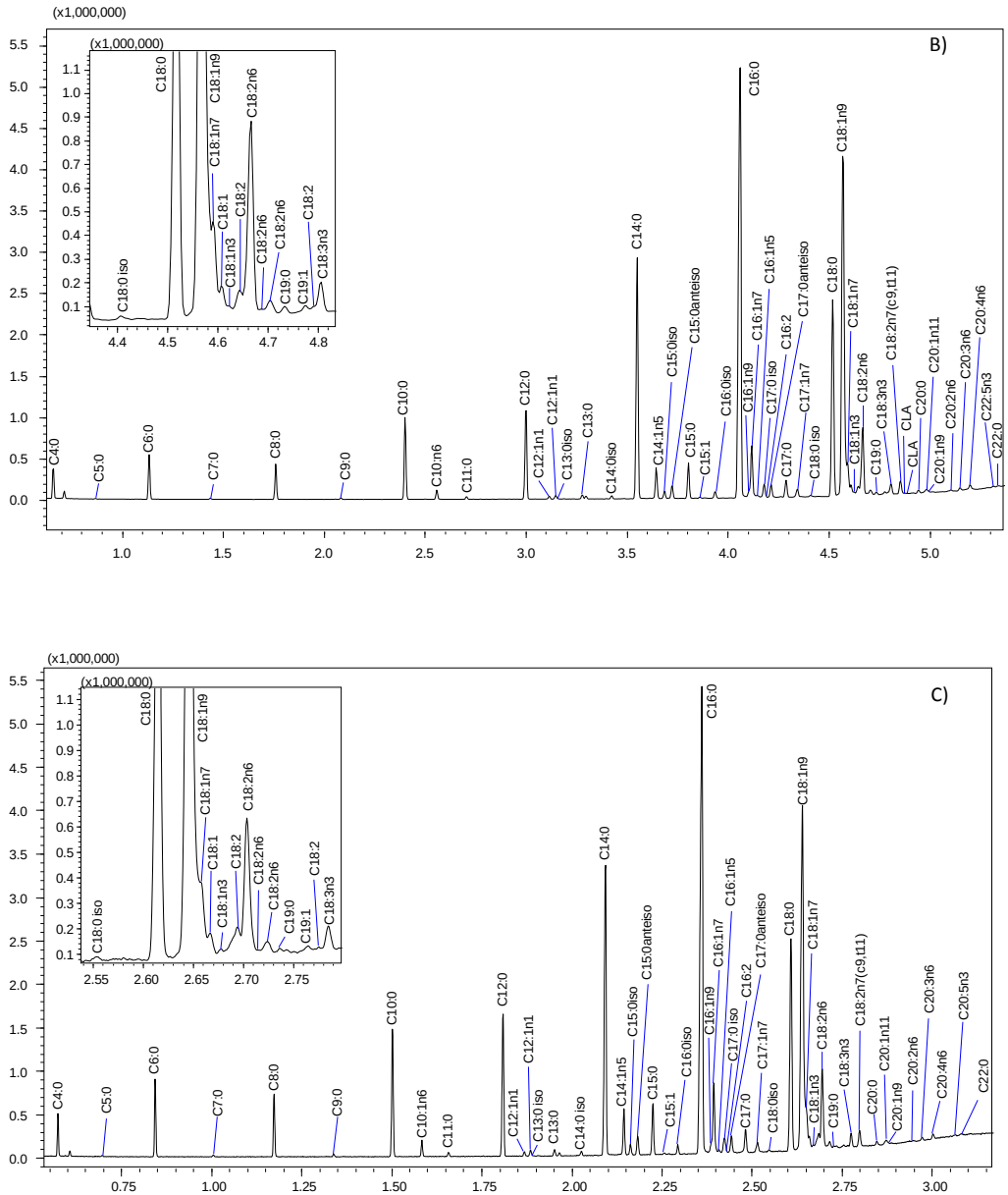

Figure 1S (II-2.1.). GC-FID FAMEs profile of SY sample, obtained using different chromatographic conditions. A) conventional run (80 min); B) fast run (8 min); and C) faster run (5 min).

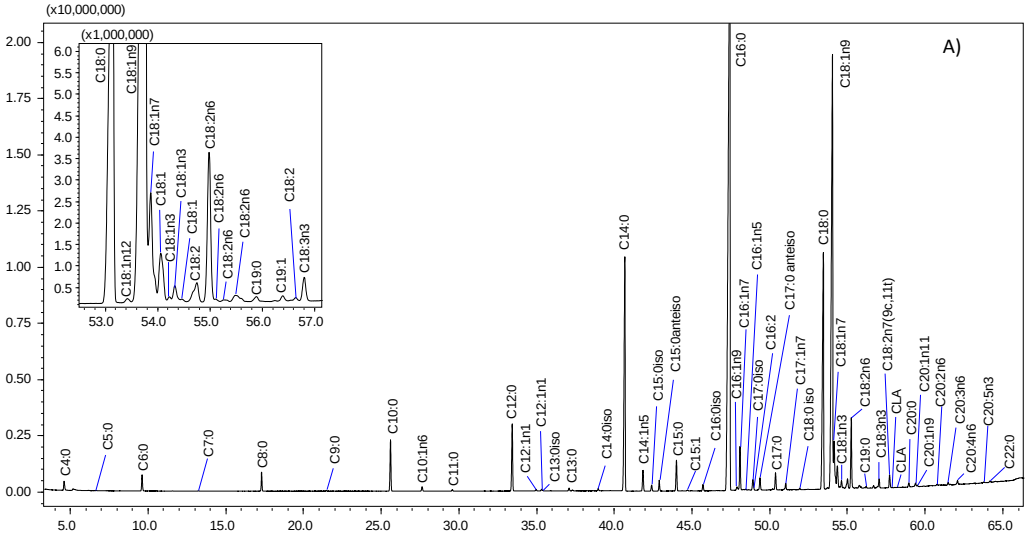
(x10,000,000)
(x1,000,000)
A)
C4:0
C5:0
C6:0
C7:0
C8:0
C9:0
C10:0
C10:1n6
C11:0
C12:0
C12:1n1
C13:0iso
C13:0
C14:0iso
C14:0
C14:1n5
C15:0iso
C15:0anteiso
C15:0
C15:1
C16:0iso
C16:0
C16:1n9
C16:1n7
C17:0iso
C16:1n5
C16:2
C17:0
C17:0anteiso
C17:1n7
C18:0iso
C18:0
C18:1n9
C18:1n7
C18:2n6
C18:1n3
C18:3n3
C18:2n7(9c,11t)
CLA
C20:0
C20:1n11
C20:1n9
C20:2n6
C20:3n6
C20:4n6
C20:5n3
C22:0
C18:0
C18:1n9
C18:1n12
C18:1n7
C18:1
C18:1n3
C18:2
C18:2n6
C19:0
C19:1
C18:2
C18:3n3

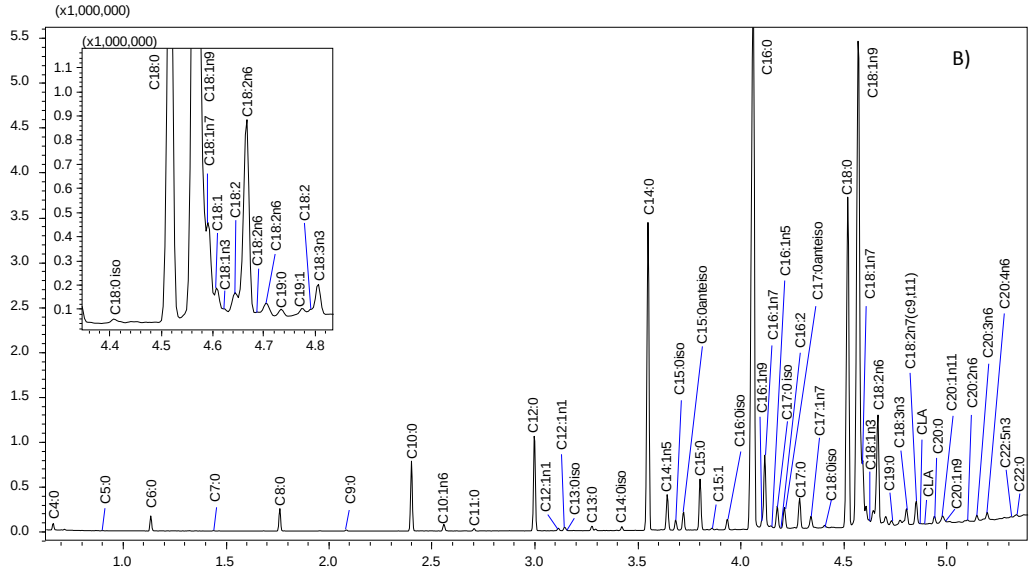
(x1,000,000)
B)
C4:0
C5:0
C6:0
C7:0
C8:0
C9:0
C10:0
C10:1n6
C11:0
C12:0
C12:1n1
C13:0iso
C13:0
C14:0iso
C14:0
C14:1n5
C15:0iso
C15:0anteiso
C15:0
C15:1
C16:0iso
C16:0
C16:1n9
C16:1n7
C17:0iso
C16:1n5
C16:2
C17:0
C17:0anteiso
C17:1n7
C18:0iso
C18:0
C18:1n9
C18:1n7
C18:2n6
C18:1n3
C18:3n3
C18:2n7(c9,t11)
CLA
C20:0
C20:1n11
C20:1n9
C20:2n6
C20:3n6
C20:4n6
C22:5n3
C22:0
C18:0iso
C18:0
C18:1n9
C18:1n7
C18:1
C18:2
C18:1n3
C18:2n6
C18:2n6
C19:0
C19:1
C18:2
C18:3n3

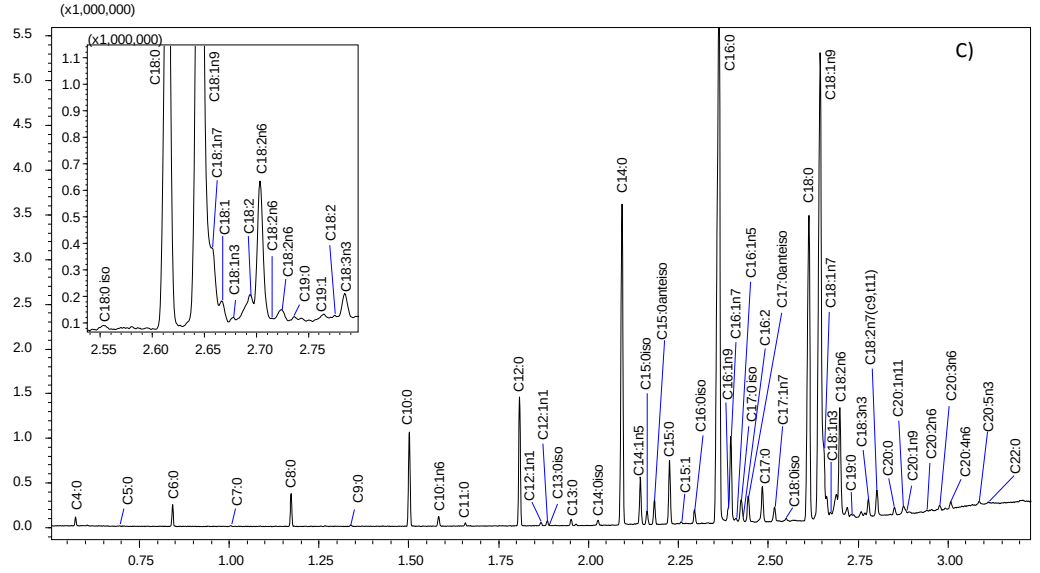

Figure 2S (II-2.1.). GC-FID FAMEs profile of SP sample, obtained using different chromatographic conditions. A) conventional run (80 min); B) fast run (8 min); and C) faster run (5 min).

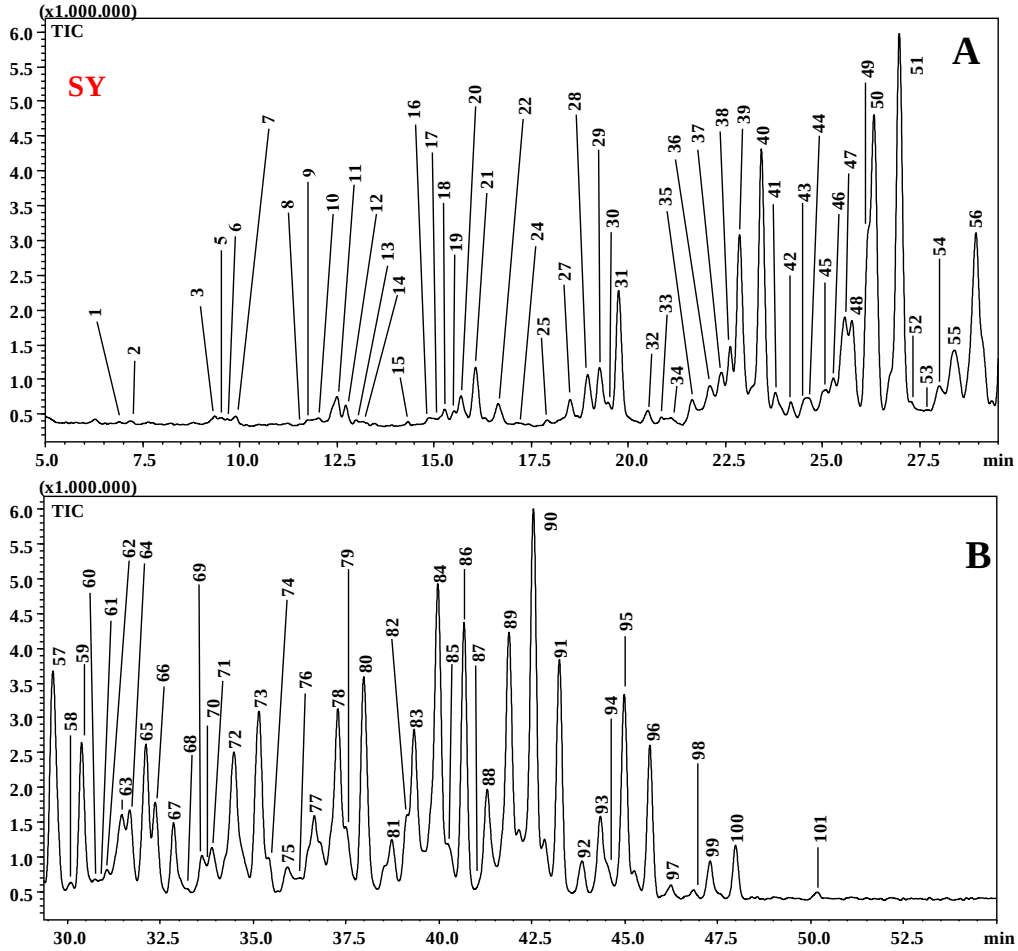

Figure 3S (II-2.1.). Enlargement of TIC chromatogram of SY sample by NARP-HPLC-APCI-MS. a) min 5.0-29.5; b) min 29.5-55.0.

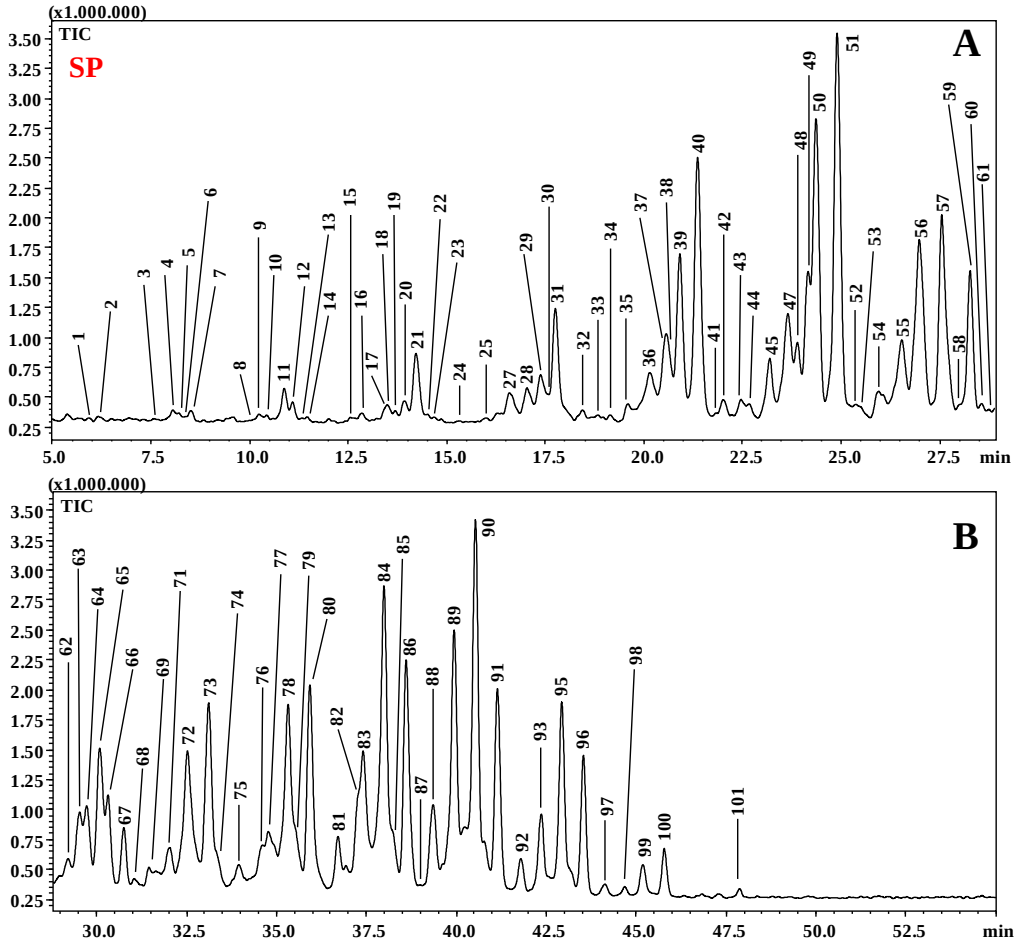

Figure 4S (II-2.1.). Enlargement of TIC chromatogram of SP sample by NARP-HPLC-APCI-MS. a) min 5.0-29.5; b) min 29.5-55.0.

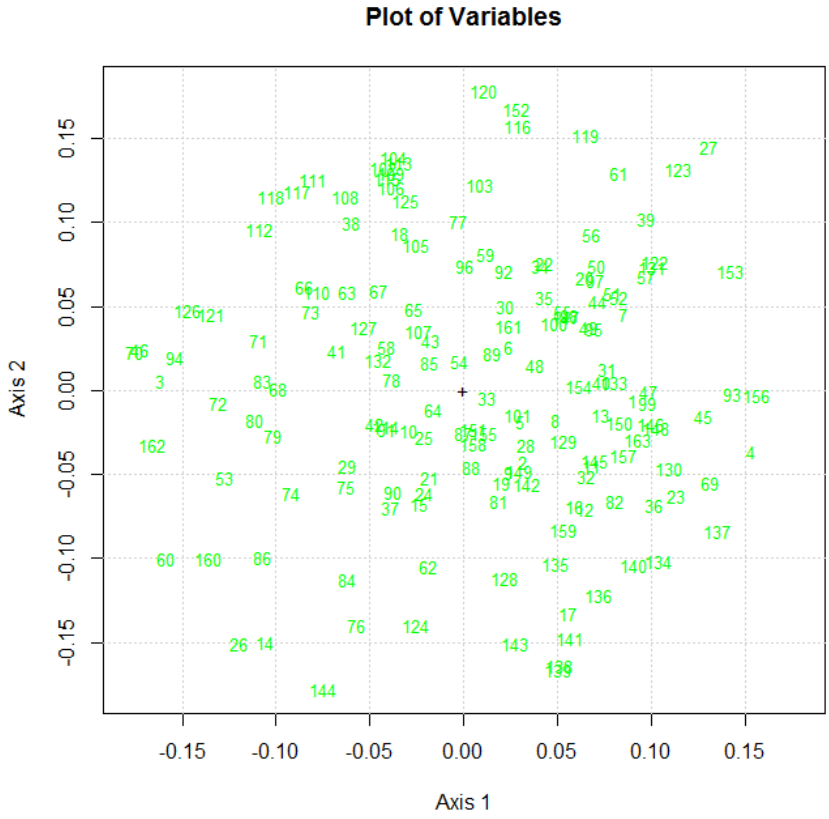

Figure 5S (II-2.1.). Plot of Variables obtained by performing the three-way PCA on the entire data set of FAMEs and TAGs.

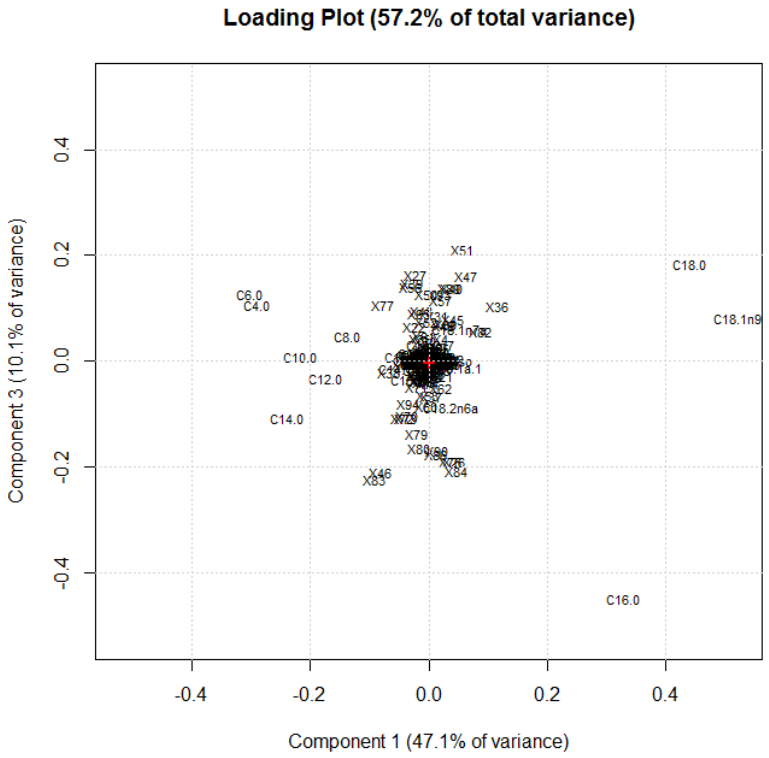

Figure 6S (II-2.1.). Loading plot on PC1 and PC3 of FAMEs and TAGs of the SC, SY, and SP samples analyzed during the project.

Table 1S (II-2.1.). FAMEs quantitative data of SC, SY, and SP.

	Stracchino Classic (SC)						Stracchino Probiotic (SP)						Stracchino with Yogurt (SY)					
	80 min		8 min		5 min		80 min		8 min		5 min		80 min		8 min		5 min	
NAME	Area (n=3)	CV%	Area (n=3)	CV%	Area (n=3)	CV%	Area (n=3)	CV%	Area (n=3)	CV%	Area (n=3)	CV%	Area (n=3)	CV%	Area (n=3)	CV%	Area (n=3)	CV%
C4:0	1.43	1.14	1.52	17.03	2.15	13.43	0.38	4.12	0.51	13.10	0.45	1.76	0.92	4.26	0.69	4.97	0.59	3.48
C5:0	0.02	5.53	0.02	9.21	0.04	1.96	0.01	7.20	0.01	8.79	0.02	12.46	0.02	1.31	0.02	6.91	0.01	3.50
C6:0	1.67	1.31	2.46	14.18	2.33	5.74	3.01	3.27	3.24	6.95	3.12	4.34	2.13	0.43	3.11	7.07	2.66	0.16
C7:0	0.02	6.71	0.03	7.35	0.05	4.36	0.01	10.38	0.04	12.20	0.06	10.93	0.03	2.65	0.03	8.99	0.04	10.18
C8:0	1.32	12.82	1.74	14.92	2.23	13.41	2.18	6.18	2.82	8.43	2.83	2.11	2.14	1.28	2.64	7.35	2.22	2.90
C9:0	0.04	8.45	0.05	15.66	0.07	10.29	0.03	7.61	0.08	9.77	0.10	1.27	0.05	7.66	0.08	1.44	0.07	11.02
C10:0	3.72	3.84	3.73	12.91	4.04	9.10	4.76	3.47	6.20	10.87	6.00	3.46	6.17	0.76	6.05	6.74	5.15	1.84
C10:1	0.29	1.99	0.39	13.11	0.59	4.98	0.21	3.98	0.69	7.67	0.66	3.18	0.34	6.49	0.62	7.69	0.53	2.43
C11:0	0.06	3.52	0.08	10.96	0.11	9.00	0.06	6.41	0.14	6.90	0.14	5.57	0.08	7.40	0.15	10.17	0.13	3.95
C12:0	3.40	3.60	3.92	8.87	4.16	0.93	5.51	3.64	5.60	11.03	5.47	3.41	5.52	7.34	5.86	5.49	5.15	4.23
C12:1n3	0.07	1.00	0.10	9.70	0.12	7.13	0.08	2.83	0.14	5.86	0.14	13.46	0.10	7.69	0.16	7.84	0.12	7.12
C12:1n2	0.09	8.31	0.12	10.51	0.14	1.53	0.09	5.01	0.15	6.54	0.16	3.79	0.11	0.89	0.17	2.57	0.15	1.69
C13:0 iso	0.02	6.69	0.03	8.51	0.04	5.82	0.02	2.77	0.05	9.17	0.03	9.05	0.03	10.29	0.05	9.62	0.04	4.65
C13:0	0.11	6.76	0.08	9.02	0.28	1.53	0.12	1.58	0.18	10.08	0.19	5.47	0.13	1.14	0.19	5.63	0.18	13.23
C14:0 iso	0.09	4.78	0.11	6.21	0.12	3.17	0.10	4.60	0.10	11.90	0.11	5.08	0.09	2.24	0.13	3.39	0.12	2.27
C14:0	11.79	4.16	11.68	3.85	12.43	2.73	12.69	2.70	13.34	6.45	13.23	1.47	11.71	2.34	13.90	3.04	13.30	1.03
C14:1n5	0.94	1.57	1.02	3.06	1.11	2.81	1.04	2.86	1.24	7.63	1.21	1.25	1.10	2.56	1.33	4.84	1.25	1.73
C15:0 iso	0.24	1.65	0.21	4.60	0.23	2.01	0.27	5.02	0.21	5.14	0.21	1.34	0.23	6.99	0.21	3.75	0.23	1.11
C15:0 anteiso	0.43	2.98	0.44	2.01	0.41	5.58	0.50	3.48	0.44	3.80	0.44	0.73	0.43	3.22	0.47	1.55	0.47	0.96
C15:0	1.12	1.13	1.17	1.16	1.12	4.06	1.45	2.84	1.19	2.60	1.19	0.57	1.22	1.82	1.23	1.61	1.23	1.30
C15:1	0.04	8.04	0.03	10.62	0.03	13.76	0.03	3.90	0.03	1.44	0.03	2.61	0.02	0.96	0.03	7.27	0.03	2.50
C16:0 iso	0.25	3.30	0.25	9.73	0.27	8.08	0.27	5.05	0.20	2.66	0.22	5.45	0.22	0.33	0.21	1.41	0.25	1.10
C16:0	31.79	1.20	31.93	1.63	31.69	2.29	28.05	2.74	29.45	5.03	30.39	0.55	30.60	2.75	30.13	1.30	31.71	1.18
C16:1n9	0.17	6.41	0.17	1.92	0.14	3.42	0.20	3.62	0.15	5.21	0.14	7.23	0.16	7.54	0.16	10.05	0.17	7.54
C16:1n7	1.59	0.43	1.62	1.10	1.44	6.32	2.06	2.29	1.53	2.86	1.54	0.73	1.80	3.03	1.61	0.89	1.70	0.57
C16:1n5	0.02	6.17	0.01	8.80	0.03	11.24	0.03	7.02	0.02	12.99	0.01	12.95	0.05	10.77	0.02	10.17	0.02	7.59
C17:0 iso	0.46	5.75	0.40	4.00	0.35	5.50	0.84	3.12	0.39	5.46	0.36	1.67	0.66	2.48	0.39	3.20	0.40	0.46
C17:0 anteiso	0.41	0.96	0.38	3.38	0.30	7.39	0.55	2.34	0.33	7.65	0.33	1.72	0.37	0.24	0.34	3.95	0.36	2.37
C17:0	0.58	2.13	0.52	3.39	0.42	4.98	0.76	3.84	0.44	11.04	0.44	2.26	0.53	3.84	0.44	2.76	0.48	0.92
C17:1[a]	0.03	8.97	0.02	7.67	*	*	0.03	12.78	0.01	13.41	*	*	0.01	5.22	0.02	5.07	*	*
C17:1[a]	0.24	4.95	0.23	1.42	0.21	7.63	0.31	7.81	0.21	13.18	0.23	1.29	0.24	6.81	0.21	4.62	0.25	0.58

C18:0 iso	0.05	9.51	0.05	6.42	0.06	10.29	0.06	5.13	0.03	6.46	0.01	7.08	0.04	9.19	0.03	5.54	0.01	8.85
C18:0	9.24	3.32	8.84	4.68	8.48	2.78	7.91	1.19	7.40	7.40	7.55	2.15	8.01	6.82	7.24	4.83	8.14	1.08
C18:1n12	0.08	8.59	0.04	5.94	0.03	10.83	0.13	8.20	0.06	10.96	0.06	2.03	0.08	5.50	0.06	5.15	0.06	12.25
C18:1n9	19.56	2.22	19.36	4.83	19.37	4.17	15.92	2.79	16.97	4.93	16.57	2.31	16.39	2.81	15.93	5.13	16.25	3.77
C18:1n7[a]	1.87	1.96	1.68	4.10	1.07	9.38	2.42	4.36	1.55	9.63	1.46	5.74	1.61	0.09	1.41	1.82	1.25	4.02
C18:1[a]	0.32	2.00	*	*	*	*	0.46	6.60	*	*	*	*	0.26	0.83	*	*	*	*
C18:1[a]	1.05	2.18	0.90	9.29	0.69	8.91	1.51	3.98	0.92	11.64	0.94	7.77	1.01	0.80	0.86	3.73	0.94	2.45
C18:1[a]	0.09	11.30	*	*	*	*	0.13	9.04	*	*	*	*	0.07	10.00	*	*	*	*
C18:1[a]	0.32	3.55	0.23	12.18	0.15	7.94	0.44	5.28	0.26	14.73	0.28	4.31	0.30	11.02	0.22	6.07	0.29	5.26
C18:1[a]	0.07	5.11	*	*	*	*	0.09	11.36	*	*	*	*	0.05	7.88	*	*	*	*
C18:2[a]	0.51	3.88	0.37	2.27	0.18	6.13	0.70	3.60	0.28	11.91	0.24	6.76	0.52	1.74	0.28	5.00	0.24	8.68
C18:2n6[a]	2.48	1.71	2.30	3.38	1.88	4.83	2.22	5.97	1.99	13.62	2.14	2.98	2.70	2.12	1.98	4.13	2.36	1.54
C18:2[a]	0.03	7.41	*	*	*	*	0.04	7.28	*	*	*	*	0.03	6.87	*	*	*	*
C18:2[a]	0.03	5.79	0.03	8.71	0.01	10.39	0.05	2.65	0.01	5.47	0.01	3.47	0.02	13.62	0.02	4.97	0.01	4.31
C18:2[a]	0.15	3.49	0.12	1.94	0.11	10.62	0.19	4.53	0.07	10.96	0.09	10.12	0.14	2.30	0.07	4.35	0.07	5.43
C18:2[a]	0.03	6.10	0.04	8.27	*	*	0.05	6.26	0.02	6.89	*	*	0.02	3.35	0.02	1.60	*	*
C19:0	0.04	7.66	0.02	9.37	0.02	6.70	0.04	8.54	0.01	10.78	0.02	9.99	0.04	2.63	0.01	13.89	0.01	4.47
C19:1	0.09	3.42	0.03	4.16	0.02	12.37	0.11	8.96	0.06	8.79	0.02	10.64	0.07	3.04	0.04	9.43	0.03	5.90
C18:2[a]	0.03	2.26	0.07	7.78	0.06	11.18	0.03	10.08	0.04	10.82	0.04	7.28	0.03	3.52	0.04	6.57	0.04	3.62
C18:3n3	0.39	2.36	0.44	3.48	0.34	3.91	0.44	2.61	0.34	12.92	0.35	1.86	0.39	2.51	0.32	0.81	0.38	3.09
C18:2n7	0.53	0.78	0.46	7.74	0.34	6.33	0.60	3.13	0.39	5.04	0.35	4.62	0.45	1.87	0.37	4.73	0.40	0.69
C18:2[a]	0.01	8.86	*n.q.*	*n.q.*	*n.q.*	*n.q.*	0.01	2.53	*n.q.*	*n.q.*	*n.q.*	*n.q.*	0.01	8.30	*n.q.*	*n.q.*	*n.q.*	*n.q.*
C18:2[a]	0.01	5.32	*n.q.*	*n.q.*	*n.q.*	*n.q.*	0.02	1.70	*n.q.*	*n.q.*	*n.q.*	*n.q.*	0.02	5.27	*n.q.*	*n.q.*	*n.q.*	*n.q.*
C20:0	0.16	4.21	0.11	6.22	0.07	6.42	0.18	2.04	0.10	11.97	0.07	6.21	0.10	2.68	0.07	8.61	0.10	5.49
C20:1n11	0.10	4.93	0.09	3.48	0.09	5.19	0.14	3.07	0.06	9.88	0.10	2.84	0.06	6.05	0.07	4.62	0.10	0.52
C20:1n9	0.02	10.30	0.04	9.41	*	*	0.03	6.75	0.03	7.08	*	*	0.03	2.55	0.02	7.13	*	*
C20:2n6	0.04	3.57	0.02	4.78	0.04	3.36	0.07	8.76	0.03	10.31	0.03	10.29	0.05	2.40	0.03	15.60	0.03	1.32
C20:3n6	0.09	9.83	0.08	6.89	0.07	2.99	0.14	6.40	0.06	10.34	0.06	3.91	0.12	4.17	0.09	8.36	0.07	7.28
C20:4n6	0.13	2.75	0.15	10.06	0.21	5.91	0.18	4.29	0.10	10.62	0.12	8.61	0.13	2.74	0.11	9.99	0.16	6.30
C20:5n3	0.03	2.61	0.03	6.42	0.03	9.03	0.06	7.71	0.02	6.40	0.02	10.75	0.08	10.31	0.02	5.74	0.02	1.32
C22:0	0.05	4.91	0.04	6.71	0.04	0.98	0.06	7.96	0.04	8.56	0.03	6.78	0.02	9.60	0.04	7.71	0.04	3.64
		4.6		7.1		6.4		5.1		8.6		5.0		4.4		5.7		3.9
[a] isomers		0.43		1.10		0.93		1.19		1.44		0.55		0.09		0.81		0.16
*** Coelution**		12.82		17.03		13.76		12.78		14.73		13.46		13.62		15.60		13.23

n.q. Not quantified

Table 2S (II-2.1.). PCA data elaboration.

	1	2	3	4	5	6	7	8	9	10	11	12	13	14	15	16	17	18	19	20
SC, t0	0.05	0.04	0.04	0.13	0.09	0.04	0.13	0.02	0.07	0.06	0.47	0.21	0.06	0.00	0.03	0.13	0.09	0.18	0.13	0.32
SY, t0	0.02	0.03	0.11	0.00	0.08	0.05	0.10	0.02	0.07	0.12	0.41	0.19	0.05	0.04	0.03	0.10	0.06	0.20	0.12	0.35
SP, t0	0.05	0.06	0.04	0.11	0.11	0.08	0.09	0.02	0.09	0.08	0.47	0.21	0.09	0.03	0.05	0.10	0.10	0.16	0.09	0.35
SC, exp	0.05	0.06	0.04	0.12	0.10	0.07	0.14	0.04	0.08	0.07	0.53	0.21	0.06	0.00	0.05	0.13	0.09	0.21	0.12	0.40
SY, exp	0.05	0.04	0.14	0.00	0.08	0.07	0.12	0.04	0.09	0.07	0.44	0.20	0.04	0.06	0.06	0.04	0.10	0.12	0.16	0.36
SP, exp	0.06	0.08	0.06	0.11	0.16	0.10	0.08	0.05	0.10	0.04	0.54	0.21	0.10	0.05	0.05	0.09	0.11	0.21	0.22	0.35
SC, t exp 1	0.05	0.05	0.03	0.11	0.08	0.05	0.14	0.03	0.06	0.08	0.44	0.20	0.05	0.00	0.02	0.10	0.05	0.25	0.12	0.41
SY, t exp 1	0.03	0.06	0.10	0.00	0.08	0.07	0.07	0.02	0.03	0.10	0.38	0.17	0.04	0.05	0.04	0.06	0.05	0.27	0.06	0.30
SP, t exp 1	0.03	0.03	0.03	0.09	0.08	0.04	0.10	0.04	0.04	0.06	0.42	0.19	0.05	0.05	0.03	0.07	0.20	0.11	0.07	0.18
SC, t exp 2	0.04	0.02	0.04	0.12	0.07	0.04	0.18	0.03	0.08	0.10	0.46	0.19	0.10	0.00	0.06	0.11	0.10	0.23	0.10	0.29
SY, t exp 2	0.04	0.05	0.10	0.00	0.09	0.06	0.10	0.02	0.09	0.06	0.46	0.18	0.04	0.06	0.04	0.04	0.06	0.28	0.11	0.32
SP, t exp 2	0.07	0.06	0.04	0.14	0.10	0.05	0.14	0.03	0.09	0.05	0.50	0.22	0.06	0.05	0.05	0.07	0.13	0.16	0.15	0.35
SC, t exp 3	0.09	0.09	0.03	0.15	0.12	0.09	0.12	0.04	0.08	0.08	0.51	0.25	0.06	0.00	0.03	0.04	0.06	0.34	0.08	0.47
SY, t exp 3	0.03	0.03	0.10	0.00	0.09	0.05	0.13	0.05	0.09	0.06	0.50	0.21	0.07	0.06	0.04	0.06	0.07	0.32	0.13	0.30
SP, t exp 3	0.10	0.09	0.06	0.18	0.08	0.08	0.17	0.09	0.12	0.13	0.64	0.23	0.14	0.07	0.05	0.12	0.25	0.15	0.20	0.36
SC, t exp 4	0.09	0.07	0.06	0.17	0.10	0.10	0.14	0.10	0.07	0.07	0.62	0.21	0.15	0.00	0.05	0.05	0.10	0.29	0.17	0.49
SY, t exp 4	0.04	0.06	0.12	0.00	0.10	0.05	0.12	0.03	0.09	0.08	0.47	0.20	0.05	0.06	0.06	0.06	0.06	0.29	0.14	0.30
SP, t exp 4	0.04	0.04	0.05	0.14	0.09	0.04	0.09	0.04	0.07	0.12	0.60	0.29	0.11	0.11	0.07	0.15	0.21	0.23	0.22	0.35
SC, t exp 5	0.03	0.03	0.03	0.10	0.08	0.05	0.10	0.03	0.08	0.05	0.41	0.18	0.08	0.00	0.03	0.06	0.14	0.13	0.17	0.27
SY, t exp 5	0.03	0.03	0.10	0.00	0.08	0.02	0.10	0.03	0.06	0.05	0.41	0.19	0.06	0.03	0.03	0.08	0.07	0.21	0.17	0.27
SP, t exp 5	0.04	0.08	0.05	0.17	0.08	0.03	0.12	0.04	0.11	0.06	0.45	0.21	0.04	0.05	0.05	0.15	0.13	0.18	0.11	0.29

21	22	23	24	25	26	27	28	29	30	31	32	33	34	35	36	37	38	39	40
0.75	0.23	0.06	0.04	0.07	0.15	0.37	0.56	0.64	0.24	1.56	0.18	0.11	0.07	0.33	0.94	0.53	1.07	2.41	3.56
0.71	0.31	0.00	0.06	0.07	0.43	0.00	0.62	0.67	0.18	1.51	0.17	0.11	0.08	0.33	0.64	0.63	0.74	2.21	3.33
0.66	0.27	0.06	0.05	0.06	0.38	0.00	0.68	0.56	0.25	1.51	0.13	0.09	0.05	0.31	0.65	0.68	0.72	2.44	3.59
0.74	0.32	0.02	0.03	0.06	0.12	0.38	0.60	0.68	0.20	1.57	0.17	0.10	0.07	0.46	0.64	0.52	0.79	2.57	3.74
0.70	0.32	0.00	0.07	0.09	0.47	0.00	0.54	0.60	0.21	1.64	0.13	0.14	0.09	0.38	0.62	0.52	0.78	2.55	3.45
1.05	0.07	0.11	0.08	0.13	0.48	0.00	0.74	0.60	0.36	1.86	0.19	0.11	0.05	0.21	1.11	0.95	0.51	2.44	3.91
0.73	0.40	0.04	0.03	0.05	0.09	0.32	0.48	0.69	0.24	1.67	0.17	0.10	0.08	0.34	0.71	0.74	0.75	2.70	3.38
0.73	0.09	0.00	0.03	0.13	0.51	0.00	0.41	0.64	0.30	1.18	0.12	0.06	0.05	0.18	0.34	0.81	1.02	2.07	2.90
0.97	0.08	0.05	0.02	0.05	0.54	0.00	0.41	0.59	0.19	1.58	0.17	0.08	0.05	0.16	1.11	0.69	0.60	2.27	3.41
0.59	0.50	0.06	0.02	0.06	0.07	0.37	0.42	0.62	0.33	1.62	0.16	0.13	0.08	0.20	1.31	0.55	0.82	2.41	3.73
0.66	0.25	0.00	0.10	0.06	0.48	0.00	0.60	0.56	0.26	1.63	0.14	0.10	0.07	0.20	0.28	0.75	1.41	2.28	3.81
0.86	0.12	0.05	0.06	0.08	0.56	0.00	0.55	0.68	0.19	1.57	0.14	0.09	0.05	0.19	1.01	0.72	0.63	2.21	3.60
0.70	0.19	0.09	0.03	0.08	0.23	0.32	0.49	0.64	0.23	1.64	0.14	0.08	0.08	0.21	1.13	0.31	1.00	2.32	3.74
0.96	0.21	0.00	0.05	0.06	0.62	0.00	0.46	0.82	0.14	1.72	0.17	0.13	0.09	0.22	0.42	0.88	1.35	2.50	3.73
0.95	0.12	0.06	0.10	0.12	0.65	0.00	0.64	0.73	0.22	1.56	0.21	0.10	0.09	0.20	1.25	0.71	0.75	2.22	3.86
0.99	0.05	0.07	0.10	0.16	0.20	0.46	0.74	0.54	0.16	1.73	0.19	0.10	0.23	0.23	0.44	0.88	1.42	2.59	3.88
0.96	0.21	0.00	0.05	0.08	0.59	0.00	0.56	0.80	0.19	1.65	0.16	0.10	0.07	0.18	0.38	0.68	1.54	2.27	3.87
0.51	0.37	0.15	0.12	0.11	0.53	0.00	0.60	0.68	0.17	1.52	0.21	0.12	0.08	0.29	0.95	0.67	0.58	2.15	3.61
0.66	0.29	0.03	0.04	0.07	0.13	0.26	0.57	0.52	0.30	1.44	0.14	0.11	0.07	0.29	0.82	0.52	0.82	2.29	3.63
0.93	0.05	0.00	0.04	0.05	0.54	0.00	0.51	0.71	0.18	1.44	0.14	0.10	0.07	0.26	0.93	0.37	1.01	2.16	3.54
0.96	0.08	0.06	0.02	0.06	0.70	0.00	0.57	0.75	0.12	1.65	0.16	0.15	0.07	0.23	1.18	0.82	0.82	2.25	3.74

41	42	43	44	45	46	47	48	49	50	51	52	53	54	55	56	57	58	59
0.13	0.23	0.27	0.30	0.94	0.00	1.70	1.03	1.54	3.93	5.27	0.28	0.00	0.60	1.54	3.39	3.22	0.17	1.87
0.45	0.25	0.28	0.26	0.52	0.47	1.40	1.15	1.38	3.52	4.87	0.37	0.15	0.63	1.40	3.55	2.97	0.23	1.82
0.09	0.23	0.19	0.23	0.87	0.00	1.54	0.98	1.47	3.96	4.53	0.33	0.10	0.58	1.35	3.49	2.83	0.19	1.58
0.13	0.20	0.24	0.27	0.88	0.00	1.65	0.99	1.57	3.76	5.16	0.37	0.00	0.57	1.35	3.33	3.14	0.20	1.77
0.29	0.25	0.32	0.19	0.37	0.53	1.46	1.10	1.34	3.89	5.23	0.32	0.09	0.61	1.44	3.47	3.03	0.20	1.82
0.04	0.29	0.29	0.21	0.91	0.00	1.83	1.00	1.63	3.88	5.58	0.15	0.06	0.49	1.54	3.22	3.20	0.17	1.72
0.14	0.24	0.28	0.29	0.97	0.00	1.57	1.17	1.63	3.68	5.12	0.39	0.00	0.64	1.44	3.64	3.09	0.37	1.83
0.12	0.29	0.24	0.18	0.78	0.78	0.86	0.49	1.21	3.69	4.37	0.10	0.19	0.53	1.37	2.93	2.61	0.39	1.87
0.09	0.21	0.31	0.24	0.90	0.00	1.89	0.60	1.51	4.09	5.26	0.20	0.19	0.63	1.55	3.21	3.21	0.21	1.89
0.05	0.28	0.23	0.21	0.84	0.00	1.75	0.64	1.77	4.23	5.51	0.22	0.00	0.56	1.53	3.35	3.25	0.13	1.89
0.18	0.23	0.26	0.22	0.34	0.55	1.88	0.80	1.62	4.01	5.47	0.26	0.12	0.60	1.59	3.38	3.20	0.17	1.79
0.04	0.31	0.25	0.21	0.88	0.00	1.78	0.87	1.67	3.64	5.01	0.32	0.03	0.54	1.49	3.14	3.05	0.11	1.68
0.07	0.27	0.27	0.20	0.85	0.00	1.97	0.75	1.92	4.13	5.75	0.29	0.00	0.57	1.59	3.37	3.32	0.12	1.86
0.06	0.31	0.30	0.20	0.46	0.41	1.93	0.79	1.95	3.82	5.52	0.32	0.02	0.53	1.55	3.39	3.29	0.14	1.77
0.07	0.33	0.22	0.22	0.81	0.00	1.73	0.86	1.71	3.68	5.43	0.33	0.05	0.54	1.45	3.18	3.04	0.18	1.79
0.06	0.28	0.32	0.17	0.87	0.00	1.97	0.74	1.85	4.06	5.90	0.39	0.00	0.37	1.79	3.39	3.23	0.10	1.84
0.04	0.31	0.28	0.23	0.23	0.68	1.86	0.88	1.80	3.85	5.46	0.12	0.22	0.53	1.55	3.20	3.12	0.11	1.74
0.06	0.25	0.21	0.19	0.80	0.00	1.71	0.76	1.71	3.41	5.26	0.14	0.02	0.48	1.52	3.06	3.06	0.17	1.83
0.06	0.33	0.22	0.28	0.88	0.00	1.72	0.89	1.60	3.92	5.57	0.36	0.00	0.56	1.58	3.24	3.33	0.21	2.00
0.08	0.29	0.26	0.20	0.86	0.38	1.30	0.83	1.72	3.59	5.23	0.11	0.25	0.56	1.51	3.10	3.16	0.23	1.98
0.06	0.28	0.29	0.18	0.89	0.00	1.81	0.91	1.63	4.05	5.33	0.26	0.11	0.52	1.53	3.29	3.10	0.11	1.76

60	61	62	63	64	65	66	67	68	69	70	71	72	73	74	75	76	77	78	79
0.00	0.21	0.51	1.15	1.09	1.96	1.10	0.82	0.16	0.53	0.00	0.74	2.98	2.69	0.34	0.44	0.18	1.74	3.00	0.66
0.20	0.14	0.33	1.43	1.07	1.97	1.14	0.83	0.29	0.42	0.24	0.78	3.05	2.64	0.40	0.57	0.27	1.93	2.91	0.81
0.15	0.10	0.55	1.08	1.04	1.88	0.98	0.79	0.06	0.52	0.00	0.70	2.96	2.60	0.33	0.50	0.70	1.20	2.95	0.63
0.00	0.15	0.36	1.24	1.04	1.86	1.11	0.74	0.13	0.55	0.00	0.74	2.90	2.76	0.29	0.48	0.15	1.73	2.93	0.62
0.19	0.14	0.33	1.28	1.17	1.88	1.16	0.80	0.31	0.41	0.17	0.81	2.98	2.62	0.40	0.58	0.23	1.90	3.03	0.74
0.12	0.14	0.40	1.12	1.10	1.90	1.00	0.68	0.13	0.49	0.00	0.70	2.89	2.70	0.40	0.39	0.80	1.08	3.03	0.67
0.00	0.20	0.42	1.33	1.10	1.97	1.09	0.84	0.19	0.53	0.00	0.71	2.90	2.79	0.28	0.43	0.20	1.77	2.93	0.66
0.26	0.07	0.56	1.23	1.23	2.10	1.28	0.97	0.29	0.28	0.36	1.01	3.45	3.39	0.45	0.60	0.74	1.76	2.92	1.42
0.10	0.08	0.61	0.84	1.50	1.98	1.09	0.88	0.23	0.64	0.00	0.83	2.91	2.79	0.42	0.62	0.56	1.50	2.87	0.83
0.00	0.26	0.28	0.99	1.24	1.96	1.11	0.81	0.16	0.34	0.00	0.77	2.89	2.78	0.31	0.33	0.06	1.75	3.03	0.59
0.26	0.12	0.43	1.12	1.23	2.01	1.08	0.77	0.17	0.26	0.21	0.74	2.94	2.84	0.32	0.45	0.14	1.75	2.89	0.76
0.14	0.06	0.56	1.16	1.03	1.88	1.01	0.71	0.16	0.45	0.00	0.61	2.82	2.67	0.29	0.44	0.60	1.32	3.13	0.72
0.00	0.13	0.47	1.02	1.15	2.06	1.17	0.80	0.14	0.43	0.00	0.68	2.93	2.81	0.35	0.29	0.29	1.46	2.93	0.76
0.16	0.12	0.47	1.18	1.14	1.95	1.15	0.78	0.16	0.22	0.22	0.75	2.99	2.87	0.34	0.32	0.65	1.09	3.05	0.57
0.11	0.13	0.59	0.98	1.17	1.88	1.15	0.71	0.14	0.56	0.00	0.73	2.99	2.52	0.34	0.43	0.72	1.15	2.76	0.82
0.00	0.31	0.16	1.20	1.11	2.02	1.12	0.75	0.16	0.41	0.00	0.76	2.62	2.82	0.26	0.20	0.06	1.72	2.89	0.62
0.16	0.21	0.45	1.15	1.11	1.99	1.15	0.78	0.16	0.23	0.21	0.77	2.98	2.81	0.30	0.34	0.69	1.24	3.16	0.61
0.16	0.16	0.40	1.07	1.02	2.00	1.15	0.81	0.21	0.47	0.00	0.73	2.81	2.80	0.40	0.36	0.73	1.03	2.88	0.65
0.00	0.26	0.54	1.04	1.07	1.99	1.19	0.87	0.16	0.52	0.00	0.73	2.86	2.82	0.39	0.49	0.55	1.17	2.88	0.75
0.07	0.11	0.46	1.07	1.10	1.87	1.27	0.78	0.18	0.23	0.27	0.76	2.95	2.75	0.42	0.39	0.18	1.12	2.95	0.75
0.15	0.06	0.57	1.06	1.13	2.02	1.06	0.69	0.11	0.45	0.00	0.68	2.89	2.76	0.34	0.39	0.68	1.13	3.00	0.67

80	81	82	83	84	85	86	87	88	89	90	91	92	93	94	95	96	97	98	99	100	101
2.74	1.03	0.82	2.28	4.86	0.58	2.91	0.06	1.42	4.70	5.63	2.46	0.49	1.32	0.00	2.83	1.53	0.18	0.13	0.52	0.56	0.10
2.87	1.14	0.81	2.39	4.87	0.67	3.10	0.15	1.59	4.42	5.66	2.71	0.54	0.98	0.40	2.71	1.58	0.19	0.11	0.44	0.54	0.09
2.71	0.98	0.75	2.27	5.06	0.57	3.03	0.05	1.46	5.10	6.46	2.91	0.50	1.59	0.00	3.26	1.73	0.22	0.18	0.58	0.65	0.16
2.86	1.02	0.85	2.14	4.95	0.63	3.03	0.10	1.43	4.74	5.81	2.65	0.56	1.41	0.00	2.85	1.63	0.19	0.14	0.54	0.62	0.14
2.82	1.07	0.79	2.28	4.99	0.70	3.07	0.12	1.39	4.55	5.69	2.51	0.51	0.88	0.34	2.70	1.54	0.16	0.12	0.39	0.59	0.13
2.72	0.92	1.30	1.73	4.82	0.55	3.01	1.44	3.76	0.54	5.73	2.49	0.39	1.10	0.00	2.72	1.55	0.22	0.15	0.49	0.60	0.09
2.74	1.00	0.79	2.23	4.80	0.56	2.95	0.19	1.36	4.63	5.53	2.60	0.52	1.36	0.00	2.76	1.61	0.18	0.13	0.49	0.59	0.12
3.59	0.93	0.31	3.38	5.35	0.61	3.44	0.13	1.43	3.99	6.17	2.63	0.45	0.94	0.22	2.53	1.62	0.14	0.11	0.42	0.58	0.11
3.06	1.09	1.49	1.63	4.88	0.62	3.10	0.08	1.54	3.80	6.20	2.63	0.52	1.27	0.00	2.78	1.51	0.15	0.08	0.54	0.54	0.09
2.89	0.92	0.99	2.04	4.86	0.55	3.00	0.03	1.38	4.64	5.78	2.65	0.40	1.22	0.00	2.82	1.74	0.22	0.14	0.50	0.61	0.11
2.94	0.74	0.22	2.94	5.05	0.58	3.12	0.13	1.31	4.45	5.74	2.64	0.47	1.11	0.14	2.59	1.57	0.15	0.11	0.38	0.54	0.08
3.05	1.00	0.99	2.32	5.55	0.59	3.33	0.01	1.39	4.80	6.21	2.70	0.45	1.32	0.00	2.75	1.57	0.14	0.11	0.44	0.53	0.10
2.97	0.89	0.96	1.91	4.88	0.64	3.00	0.09	1.22	4.32	5.68	2.57	0.47	1.21	0.00	2.71	1.60	0.18	0.10	0.42	0.53	0.10
2.93	0.87	0.93	2.00	4.86	0.55	3.16	0.12	1.24	3.75	6.26	2.57	0.46	1.02	0.22	2.54	1.52	0.14	0.10	0.37	0.46	0.07
2.81	1.00	0.92	2.08	5.06	0.52	2.98	0.07	1.26	4.52	5.79	2.51	0.46	1.24	0.00	2.53	1.51	0.18	0.11	0.45	0.55	0.10
2.78	0.88	0.95	1.84	4.50	0.71	2.77	0.03	1.26	3.89	6.06	2.20	0.54	1.22	0.00	2.63	1.52	0.20	0.16	0.46	0.56	0.06
2.94	0.91	0.91	2.09	4.97	0.57	3.05	0.10	1.28	4.36	5.64	2.49	0.43	1.03	0.16	2.70	1.61	0.15	0.11	0.44	0.52	0.11
2.91	1.18	1.10	2.24	5.76	0.69	3.53	0.07	1.45	4.75	6.18	2.46	0.39	1.12	0.00	2.45	1.44	0.12	0.10	0.44	0.53	0.13
2.99	1.05	0.84	2.19	5.00	0.57	3.03	0.14	1.39	4.44	6.07	2.60	0.46	1.23	0.00	2.90	1.60	0.17	0.10	0.46	0.57	0.12
2.99	1.04	1.02	1.98	5.29	0.63	3.30	0.08	1.40	4.60	6.39	2.93	0.50	0.96	0.29	2.89	1.72	0.22	0.13	0.53	0.63	0.11
2.87	0.92	0.93	2.15	4.95	0.58	3.08	0.04	1.32	4.71	5.70	2.58	0.40	1.19	0.00	2.73	1.62	0.18	0.13	0.48	0.55	0.11

C4:0	C5:0	C6:0	C7:0	C8:0	C9:0	C10:0	C10:1	C11:0	C12:0	C12:1n3	C12:1n2	C13:0 iso	C13:0	C14:0 iso	C14:0	C14:1n5	C15:0 iso	15:0 anteis	C15:0	C15:1	C16:0 iso	C16:0	C16:1n9	C16:1n7	C16:1n5	C17:0 iso	17:0 anteis	C17:0	C17:1a	C17:1a	C18:0 iso	C18:0
1.08	0.02	1.65	0.03	1.23	0.03	2.82	0.31	0.07	3.26	0.08	0.11	0.01	0.12	0.10	10.89	0.98	0.25	0.43	1.15	0.03	0.24	32.23	0.17	1.66	0.02	0.47	0.41	0.56	0.03	0.24	0.05	9.88
1.50	0.00	1.70	0.00	1.20	0.00	2.90	0.30	0.10	3.40	0.10	0.10	0.00	0.10	0.10	11.20	1.10	0.20	0.40	1.20	0.00	0.20	32.50	0.20	1.80	0.00	0.50	0.40	0.50	0.00	0.30	0.00	9.10
1.66	0.03	1.94	0.03	1.38	0.05	2.98	0.31	0.07	3.29	0.08	0.10	0.02	0.11	0.08	10.77	0.98	0.21	0.39	1.14	0.03	0.20	32.01	0.16	1.66	0.02	0.46	0.37	0.53	0.02	0.22	0.04	9.48
1.83	0.03	2.06	0.03	1.45	0.04	3.13	0.35	0.11	3.30	0.09	0.11	0.01	0.11	0.10	10.72	0.98	0.24	0.42	1.13	0.04	0.23	31.57	0.16	1.64	0.04	0.46	0.39	0.53	0.03	0.23	0.04	9.62
1.42	0.02	1.55	0.03	1.09	0.04	2.63	0.27	0.07	3.11	0.08	0.09	0.02	0.10	0.08	10.58	1.00	0.23	0.42	1.15	0.03	0.23	32.36	0.16	1.69	0.03	0.46	0.40	0.56	0.03	0.25	0.05	9.89
1.11	0.02	1.40	0.02	1.01	0.03	2.58	0.25	0.07	3.22	0.07	0.10	0.03	0.11	0.09	10.84	1.01	0.22	0.40	1.14	0.03	0.21	32.26	0.17	1.70	0.02	0.47	0.39	0.54	0.03	0.24	0.04	9.86
1.44	0.02	1.68	0.02	1.19	0.04	2.73	0.29	0.06	3.11	0.07	0.09	0.02	0.11	0.09	10.46	0.94	0.24	0.43	1.12	0.04	0.25	31.91	0.17	1.60	0.02	0.47	0.41	0.59	0.03	0.24	0.05	10.31
1.87	0.02	2.07	0.03	1.39	0.05	3.22	0.33	0.08	3.62	0.10	0.10	0.03	0.13	0.09	11.44	1.07	0.22	0.42	1.19	0.02	0.21	32.52	0.16	1.75	0.05	0.46	0.38	0.52	0.01	0.23	0.04	8.63
0.30	0.00	0.47	0.01	0.61	0.02	1.86	0.17	0.05	2.54	0.06	0.07	0.02	0.10	0.08	10.01	0.82	0.21	0.40	1.14	0.03	0.23	33.88	0.15	1.62	0.03	0.49	0.43	0.60	0.02	0.24	0.05	11.15
1.44	0.02	1.61	0.02	1.11	0.03	2.65	0.27	0.06	3.26	0.07	0.10	0.02	0.12	0.10	11.02	1.00	0.25	0.44	1.16	0.08	0.25	32.30	0.17	1.67	0.03	0.47	0.40	0.58	0.03	0.24	0.05	9.86
1.36	0.02	1.54	0.03	1.09	0.04	2.69	0.27	0.07	3.16	0.08	0.09	0.02	0.11	0.09	10.61	0.99	0.22	0.42	1.14	0.03	0.23	32.57	0.17	1.68	0.02	0.46	0.40	0.55	0.02	0.24	0.05	9.92
0.30	0.00	0.44	0.01	0.63	0.03	1.89	0.17	0.05	2.54	0.05	0.07	0.02	0.09	0.08	9.89	0.82	0.22	0.38	1.12	0.03	0.22	33.80	0.15	1.61	0.02	0.49	0.42	0.60	0.02	0.24	0.05	11.31
1.21	0.02	1.48	0.02	1.05	0.03	2.56	0.26	0.06	3.18	0.07	0.10	0.02	0.11	0.10	10.89	0.98	0.25	0.44	1.15	0.04	0.25	32.32	0.17	1.66	0.03	0.47	0.41	0.55	0.03	0.25	0.05	10.08
1.66	0.02	1.81	0.03	1.24	0.04	2.96	0.29	0.08	3.60	0.09	0.11	0.03	0.12	0.09	11.68	1.07	0.23	0.43	1.22	0.03	0.22	33.06	0.16	1.77	0.04	0.47	0.38	0.52	0.03	0.23	0.04	8.69
0.54	0.01	0.72	0.02	0.79	0.03	2.11	0.20	0.06	2.61	0.06	0.08	0.02	0.10	0.08	9.87	0.83	0.21	0.38	1.13	0.03	0.22	33.49	0.15	1.60	0.02	0.49	0.41	0.58	0.02	0.24	0.05	11.23
1.04	0.01	1.23	0.02	0.89	0.03	2.32	0.24	0.06	3.04	0.07	0.09	0.02	0.11	0.10	10.83	0.94	0.25	0.43	1.16	0.03	0.26	33.15	0.17	1.61	0.02	0.48	0.42	0.59	0.02	0.24	0.05	10.60
1.05	0.02	1.48	0.03	1.09	0.04	2.70	0.27	0.07	3.35	0.08	0.11	0.02	0.12	0.09	11.17	1.07	0.25	0.44	1.19	0.03	0.23	32.62	0.17	1.75	0.03	0.46	0.42	0.55	0.02	0.25	0.05	9.48
0.21	0.00	0.40	0.01	0.68	0.03	2.16	0.19	0.05	2.78	0.06	0.07	0.02	0.10	0.08	10.32	0.86	0.21	0.39	1.15	0.03	0.22	34.11	0.14	1.58	0.02	0.49	0.41	0.58	0.02	0.23	0.05	11.25
1.31	0.02	1.50	0.02	1.05	0.03	2.57	0.26	0.06	3.18	0.08	0.10	0.02	0.12	0.10	10.88	0.98	0.25	0.44	1.15	0.04	0.25	32.20	0.17	1.66	0.02	0.47	0.41	0.55	0.03	0.25	0.05	10.01
0.69	0.02	1.09	0.02	0.91	0.04	2.47	0.25	0.07	3.19	0.08	0.10	0.03	0.12	0.09	10.97	1.02	0.25	0.43	1.19	0.03	0.23	33.25	0.18	1.74	0.03	0.47	0.43	0.56	0.03	0.25	0.05	9.98
0.26	0.00	0.45	0.01	0.67	0.03	2.05	0.19	0.06	2.69	0.06	0.07	0.02	0.09	0.07	10.14	0.87	0.22	0.39	1.14	0.03	0.22	33.79	0.16	1.63	0.02	0.49	0.43	0.58	0.02	0.25	0.05	11.08

C18:1n12	C18:1n9	C18:1n7a	C18:1a	C18:1a	C18:1a	C18:1a	C18:1a	C18:2a	C18:2n6a	C18:2a	C18:2a	C18:2a	C18:2a	C19:0	C19:1	C18:2a	C18:3n3	C18:2n7	C18:2a	C18:2a	C20:0	C20:1n11	C20:1n9	C20:2n6	C20:3n6	C20:4n6	C20:5n3	C22:0
0.08	20.77	1.77	0.29	1.02	0.09	0.29	0.06	0.51	2.51	0.04	0.03	0.17	0.04	0.03	0.08	0.03	0.41	0.53	0.01	0.01	0.13	0.09	0.03	0.04	0.09	0.14	0.04	0.05
0.10	20.20	1.70	0.30	1.00	0.10	0.30	0.10	0.50	2.70	0.00	0.00	0.20	0.00	0.00	0.10	0.00	0.40	0.50	0.00	0.00	0.10	0.10	0.00	0.00	0.10	0.10	0.10	0.00
0.10	20.26	1.80	0.34	1.13	0.11	0.32	0.09	0.54	2.69	0.03	0.03	0.14	0.03	0.03	0.07	0.02	0.35	0.48	0.01	0.03	0.12	0.09	0.03	0.07	0.10	0.14	0.06	0.05
0.09	20.21	1.81	0.29	1.04	0.09	0.30	0.08	0.55	2.44	0.02	0.04	0.16	0.03	0.03	0.07	0.03	0.40	0.51	0.01	0.03	0.13	0.09	0.02	0.06	0.08	0.14	0.03	0.04
0.08	21.21	1.70	0.30	1.06	0.07	0.30	0.06	0.54	2.68	0.03	0.03	0.14	0.03	0.04	0.08	0.03	0.36	0.50	0.01	0.01	0.13	0.09	0.03	0.04	0.12	0.13	0.07	0.04
0.09	21.24	1.79	0.34	1.17	0.11	0.33	0.08	0.53	2.76	0.03	0.04	0.14	0.03	0.03	0.08	0.02	0.35	0.51	0.01	0.01	0.13	0.11	0.03	0.07	0.11	0.14	0.05	0.04
0.08	21.03	1.87	0.32	1.06	0.09	0.32	0.07	0.51	2.48	0.03	0.03	0.15	0.03	0.04	0.09	0.03	0.39	0.53	0.01	0.01	0.16	0.10	0.02	0.04	0.09	0.13	0.03	0.05
0.07	19.41	1.57	0.27	0.98	0.07	0.31	0.06	0.52	2.62	0.03	0.02	0.14	0.02	0.04	0.06	0.03	0.38	0.44	0.01	0.02	0.10	0.06	0.03	0.05	0.12	0.13	0.08	0.04
0.10	22.70	1.90	0.36	1.23	0.10	0.34	0.07	0.56	2.80	0.03	0.04	0.15	0.04	0.04	0.09	0.03	0.34	0.52	0.01	0.02	0.15	0.11	0.03	0.06	0.11	0.14	0.05	0.05
0.07	20.68	1.74	0.28	1.02	0.09	0.29	0.06	0.49	2.50	0.03	0.04	0.16	0.03	0.03	0.08	0.02	0.40	0.53	0.01	0.01	0.14	0.09	0.02	0.04	0.09	0.13	0.03	0.03
0.08	21.02	1.69	0.30	1.08	0.08	0.29	0.05	0.52	2.65	0.03	0.03	0.12	0.03	0.05	0.08	0.04	0.35	0.47	0.01	0.01	0.12	0.10	0.04	0.05	0.11	0.13	0.06	0.04
0.09	22.69	1.96	0.37	1.24	0.11	0.37	0.08	0.57	2.80	0.04	0.04	0.15	0.03	0.05	0.09	0.03	0.34	0.49	0.01	0.01	0.15	0.11	0.03	0.07	0.11	0.13	0.05	0.05
0.08	21.05	1.78	0.29	1.05	0.09	0.31	0.06	0.51	2.51	0.03	0.04	0.16	0.03	0.04	0.09	0.02	0.40	0.54	0.01	0.01	0.15	0.10	0.03	0.04	0.08	0.13	0.04	0.04
0.07	19.47	1.58	0.28	0.99	0.07	0.27	0.04	0.49	2.64	0.02	0.03	0.12	0.02	0.03	0.06	0.02	0.36	0.44	0.01	0.01	0.08	0.06	0.02	0.04	0.10	0.13	0.07	0.03
0.09	22.33	1.93	0.36	1.24	0.10	0.35	0.07	0.55	2.76	0.03	0.04	0.14	0.03	0.05	0.09	0.03	0.33	0.49	0.01	0.01	0.15	0.10	0.03	0.06	0.10	0.12	0.04	0.04
0.08	20.80	1.83	0.30	1.06	0.09	0.31	0.06	0.51	2.48	0.03	0.04	0.16	0.04	0.04	0.09	0.02	0.38	0.51	0.01	0.00	0.16	0.11	0.03	0.05	0.09	0.13	0.03	0.05
0.07	20.82	1.51	0.31	1.05	0.08	0.28	0.05	0.50	2.66	0.03	0.04	0.14	0.03	0.04	0.07	0.03	0.38	0.49	0.01	0.01	0.12	0.10	0.04	0.04	0.12	0.15	0.06	0.04
0.09	21.86	1.89	0.36	1.23	0.10	0.35	0.06	0.56	2.72	0.04	0.04	0.14	0.04	0.04	0.08	0.03	0.32	0.47	0.01	0.01	0.14	0.11	0.03	0.06	0.10	0.12	0.04	0.05
0.08	21.11	1.78	0.29	1.03	0.09	0.30	0.06	0.51	2.53	0.03	0.04	0.16	0.03	0.04	0.08	0.02	0.40	0.55	0.01	0.01	0.15	0.11	0.03	0.05	0.09	0.13	0.04	0.04
0.07	21.22	1.59	0.28	1.07	0.09	0.29	0.05	0.52	2.68	0.03	0.04	0.13	0.04	0.04	0.08	0.03	0.37	0.43	0.01	0.01	0.11	0.12	0.03	0.05	0.11	0.15	0.07	0.04
0.08	22.54	1.86	0.36	1.23	0.10	0.33	0.06	0.54	2.80	0.03	0.04	0.15	0.04	0.05	0.08	0.02	0.33	0.48	0.01	0.01	0.14	0.10	0.03	0.04	0.11	0.12	0.04	0.04

2.2. Chemical characterisation of old cabbage (*Brassica oleracea L. var. acephala*) seed oil by liquid chromatography and different spectroscopic detection systems

Analysis of the fatty acid content

GC-MS analyses for identification purposes were carried out on a GCMS-QP2010 system (Shimadzu, Milan, Italy) equipped with a split-splitless injector, an AOC-20i autosampler, and a Shimadzu GCMS-2010 mass spectrometer (Shimadzu, Milan, Italy). MS parameters in all applications were as follows: mass range 40-400 amu, scan speed: 2000 amu/s, ion source temperature: 200°C, interface temperature: 250°C. The *GCMSsolution* software (Ver. 2.71 Shimadzu, Milan, Italy) was used for data collection and handling; identification was further achieved through library using the ”FAMEs Fatty Acid Methyl Esters: Mass Spectral Database” (Wiley) with the simultaneous use of Linear Retention Indices calculated by the injection of a FAMEs solution. GC-FID analyses for quantification purposes were carried out on a GC-2010 system (Shimadzu, Milan, Italy) equipped with a split-splitless injector (280 °C), an AOC-20i autosampler, and a FID detector. A Supelcowax-10 column was employed (30 m × 0.25 mm I.D., 0.25 μm *d.p.*, Sigma-Aldrich/Supelco, Bellefonte, USA) and operated under the following programmed temperature: 50 °C to 280 °C at 3.0 °C/min. The injection volume was 0.2 μL with a split ratio of 10:1. Helium was used as the carrier at a constant linear velocity of 30 cm/s.

Individual fatty acid methyl esters are reported as percentage of total FAMEs. Area correction was performed to correct the FID response by means of theoretical relative response factors (TRF) (Ackman, 2007). Reliability of TRF was previously checked by means of standard mixtures analysis.

Analysis of the triacylglycerol content

NARP-HPLC-APCI-MS analyses were performed on a Shimadzu Prominence LC-20A system (Shimadzu, Milan, Italy), consisting of a CBM-20A controller, two LC-20AD dual-plunger parallel-flow pumps, a DGU-20A5 degasser, a SIL-20A autosampler and a Shimadzu LCMS-2010 mass spectrometer (Shimadzu, Milan, Italy) equipped with an APCI source operated in the positive ionization mode. The Shimadzu LCMSsolution software (Ver. 3.60.361) was used for data collection and handling. Chromatographic separation was achieved on an Ascentis Express C18 column (150 × 4.6 mm I.D., 2.7 μm *d.p.*, Sigma-Aldrich/Supelco, Bellefonte, USA); 5 μL of the sample were injected. A linear gradient of increasing IPA (B) percentages in ACN (A) was run, at a mobile phase flow rate of 1 mL/min: 0 min, 0% B; 50 min, 70% B (hold for 4 min); 54 min, 0% B. MS parameters for full scan analysis were as follows: 250-1100 *m/z* mass range, scan speed: 4000 amu/s, nebulizing gas (N_2) flow rate: 2.0 L/min; event time: 0.25 s; detector voltage: 1.5 kV; interface temperature: 450 °C; CDL temperature: 250 °C; heat block temperature: 200 °C.

Analysis of the tocopherol content

Tocopherol quantification was carried out by using five different concentrations of each component, in the range between 5 and 0.005 mg/L, prepared by diluting a stock solution of about 100 mg/L, using Hex as a solvent (α-tocopherol, y=337097x-15482; R^2=0.9988; γ-tocopherol, y=481282x-4784.3; R^2 = 0.9997; δ-tocopherol, y=264858x+62755, R^2=0.9983). The analyses were carried out by using a Shimadzu HPLC system (Kyoto, Japan) equipped with a LC-10AD Vp high pressure isocratic pump, an SCL-10A Vp controller, and an RF-10 AXL fluorescence detector (programmed for excitation at 290 nm and emission at 330 nm). Data acquisition was performed using the LCsolution

software (Ver. 1.12). The analyses were performed in triplicate, at room temperature (25 °C) using two serially coupled Ascentis silica columns (100 × 1.0 mm I.D., 3.0 μm *d.p.*, Sigma-Aldrich/Supelco, Bellefonte, USA). The mobile phase consisted of a of Hex and IPA (99:1 *v/v*) with a flow-rate of 50 μL/min, and the injection volume was 2 μL.

Analysis of the carotenoid content

Carotenoids were extracted from the seed oil sample by liquid-phase distribution (LPD) between DMF and Hex, according to the methodology reported by Minguez-Mosquera et al. (1992), with some modifications. Briefly, 25 g of oil were dissolved in 150 mL of DMF and treated with 5 successive 50 mL portions of Hex in a decanting funnel. The polar components and the xanthophylls were retained in the DMF phase. The hexane phase contained lipids and carotenes. The DMF phase was treated with a 2% Na_2SO_4 solution at 0 °C and extracted two times with a 100 mL mixture of Hex/ethyl ether (1:1 *v/v*). The aqueous phase was discarded, eliminating the more polar components. The organic phase was evaporated to dryness using a rotary evaporator at 30°C. The dry residue was dissolved in 2 mL of MeOH/MTBE (1:1, *v/v*) and analyzed by RP-HPLC-PDA-MS. The hexane phases were combined, concentrated, filtered through a 0.45 μm syringe filter, and reconstituted in 1.0 mL of Hex for spectrophotometric measurement. The obtained solution only contained *trans* β-carotene pigment together with a minor content of a *cis* isomer, as it was also previously determined by HPLC analysis of the hexane phase.

- ✓ *Spectrophotometric analysis*

The total carotenes were analysed by a Shimadzu UV-2600 UV-Vis spectrophotometer (Shimadzu, Milan, Italy). The absorbance (A_λ) of hexane

phase containing carotenes was measured at the absorbance maximum, at 450 nm. Quantification was carried out using the following equation:

$$c = \frac{A_\lambda}{\varepsilon \cdot l} \cdot \frac{V \cdot D_F}{m}$$

where c is the concentration, ε is the mass absorption coefficient ($g \cdot cm^{-2}$), l is the light path-length (1 cm), V is the sample volume (mL), D_F is the dilution factor, m is the sample weight (g).

- ✓ *RP-HPLC-PDA-MS analysis*

The HPLC analysis of carotenoids were performed on a Shimadzu Prominence LC-20A (Shimadzu, Milan, Italy), consisting of a CBM-20A controller, two LC-20AD dual-plunger parallel-flow pumps, a DGU-20 A_5 degasser and an SPD-M20A photodiode array detector (2.5 ⌈L detector flow cell volume). The data were processed with the software LCMSsolution (Ver. 1.12). The LC system was coupled to an LCMS-2010 mass spectrometer through an APCI source (Shimadzu, Kyoto, Japan) operated in positive and negative ionization mode. Separations were performed on a YMC C30 column (250 × 4.6 mm I.D., 3.0 μm *d.p.*, YMC Europe GmbH, Dinslaken, Germany); the mobile phase was a gradient of MeOH/MTBE/H_20 (90:7:3, *v/v/v*; eluent A) and MeOH/MTBE/H_20, (8:90:2, *v/v/v*; eluent B), as follows: 0 min 0% B; 60 min 60% B, 70 min 100% B. The flow rate was 1 mL/min and the injection volume was 20 μL. The UV–Vis spectra were acquired in the range of 250–700 nm, while the chromatograms for quantification were extracted at 450 nm (sampling frequency: 1.5625 Hz; time constant: 0.64 s). The MS was set as follows: Scan, both APCI positive (+) and negative (-), detector Voltage: 1.60 kV in negative mode, 1.35 kV; interface temperature: 450 °C; CDL temperature: 300 °C; Block heater temperature: 300 °C; Nebulizing gas flow (N_2): 2.5 L/min; full

scan range: 350-1200 m/z; event time: 600 ms. Samples were analysed in triplicate.

Carotenoid quantification was carried out from the calibration curve attained using lutein reference material at six concentration levels in the range between 1 and 200 mg/L ($y=2233x-42.22$; $R^2=0.9962$).

Analysis of the polyphenolic content

Roughly 3.01 g of the seed oil were weighed in a centrifuge tube, treated with 6 mL of a MeOH/H_2O (8:2, *v/v*) mixture, stirred and centrifugated for 10 minutes at 3000 rpm. After the first separation in two phases, the aqueous-phase (the lower one), containing polyphenols, was collected in a flask, while the remaining oil was subsequently re-treated with further four portions of 6 mL of MeOH/H_2O (8:2, *v/v*) mixture. The five obtained aqueous portions, containing polyphenols, were combined and evaporated to dryness at 30 °C. The extract was reconstituted in 1 mL of ACN and re-extracted 3 times with 1 mL of Hex, and then centrifugated for 10 minutes at 3000 rpm. The lower phase (ACN) was analyzed by HPLC analysis. The obtained extract (3.2 mg) was solubilised in 100 μL of an ACN/H_2O (1:1, *v/v*) for the three analyses.

The analyses were carried out on a Shimadzu Prominence LC-20A (Shimadzu, Milan, Italy), equipped of a binary LC-20AB pump, a CBM-20A controller, a SPD-M20A diode array detector, a DGU-20A5 degasser and a manual injector with a loop of 2 μL. For data collection and handling an LCMSsolution (Ver. 5.53) was used. The LC system was coupled to a Shimadzu LCMS-2020 Shimadzu, Kyoto, Japan), mass spectrometer through an ESI source operated in the negative ionization mode. The Shimadzu LabSsolution software (version 5.53 SP2, Milan, Italy) was used for data collection and handling.

Chromatographic separation was achieved on an Ascentis Express C18 column (150 × 4.6 mm I.D., 2.7 μm *d.p.*, Sigma-Aldrich/Supelco, Bellefonte, USA)

using as mobile phase a gradient of H_2O (0.1% of HCOOH) and ACN as follows: 0 min, 0% B; 5 min, 0% B; 30 min, 20% B; 60 min, 100% B; 65 min, 100% B; 70 min, 0% B. The flow rate of 1 mL/min (splitted to 0.2 mL/min prior to ESI-MS analysis), and the injection volume was 2 μL. Data were acquired using a PDA in the range of wavelength from 190 to 400 nm while the chromatograms were extracted at 280 nm (sampling frequency: 1.5625 Hz; time constant: 0.64 s). MS parameters for full scan analysis using ESI in negative mode were: mass range from 100 to 800 *m/z*; nebulizing gas (N_2) flow rate: 1.5 L/min; event time: 1 s; desolvation line (DL) temperature: 250°C; heat block temperature: 300°C.

Figure 1S (II-2.2.). Picture of the old cabbage (*Brassica oleracea* L. var. acephala).

Table 1S (II-2.2.). FAs identified by GC-MS analysis along with their peak area ratio percentage.

CN:DB[a]	Area%±SD
C16:0	3.11±0.024
C16:1n9	0.03±0.003
C16:1n7	0.10±0.006
C16:1n5	0.01±0.001
C16:2n4	0.01±0.001
C17:0	0.02±0.001
C16:3n3	0.06±0.001
C18:0	0.89±0.003
C18:1n9	10.46±0.047
C18:1n7	0.83±0.025
C18:2n6	11.36±0.072
C18:3n3	10.16±0.119
C20:0	0.62±0.003
C20:1n11	6.08±0.015
C20:1n9	1.57±0.012
C20:2n6	0.57±0.003
C22:0	0.61±0.004
C22:1n9	50.57±0.241
C22:2n6	0.81±0.004
C21:3n3	0.26±0.030
C24:0	0.36±0.015
C24:1n9	1.50±0.009

[a] CN, carbon number; DB, double bond.

Table 2S (II-2.2.). Identified TAGs by NARP-HPLC/APCI-MS analysis.

#	NDB	t_R	TAGs	PN	Area % (n=3)	S.D.	CV%
1	6	32.06	LLL	42	0.16	0.03	18.01
2	5	32.79	PLLn	42	0.33	0.04	13.32
3	5	34.83	OLL	44	0.26	0.03	12.53
4	7	34.97	ErLnLn	44	0.57	0.09	15.06
5	5	35.13	OOLn	44	0.37	0.03	8.76
6	4	35.32	PLL	44	0.45	0.04	8.79
7	3	36.18	PPLn	44	0.51	0.08	16.45
8	6	37.34	ErLLn	46	1.35	0.14	10.50
9	4	37.54	OOL	46	1.47	0.11	7.64
10	4	38.09	GPLn	46	1.32	0.03	2.05
11	4	38.09	SOLn	46	*	*	*
12	2	38.68	PPL	46	0.92	0.10	10.80
13	5	39.59	LL	48	1.12	0.08	6.86
14	5	39.92	ErOLn	48	3.96	0.14	3.48
15	3	40.33	OOO	48	0.55	0.08	13.85
16	4	40.47	ErPLn	48	5.24	0.34	6.58
17	2	40.78	OPO	48	0.54	0.05	9.57
18	5	41.72	ErEsL	50	1.17	0.08	7.01
19	5	42.14	ErGLn	50	7.53	0.23	3.11
20	4	42.14	ErOL	50	*	*	*
21	4	42.14	GGL	50	*	*	*
22	3	42.36	GOO	50	0.99	0.14	13.70
23	3	42.73	ErPL	50	6.99	0.16	2.31
24	2	43.00	GPO	50	0.88	0.05	5.63
25	3	43.85	ErSL	52	0.72	0.08	10.96
26	4	44.24	ErGL	52	14.21	0.69	4.86
27	5	44.24	NrGLn	52	*	*	*
28	3	44.60	ErOO	52	3.97	0.17	4.40
29	3	44.60	GGO	52	*	*	*
30	3	45.06	ErSL	52	1.30	0.16	12.40
31	2	45.18	ErPO	52	5.24	0.02	0.43
32	2	45.36	GSO	52	0.24	0.03	10.75
33	4	46.33	ErErL	54	13.20	0.31	2.35
34	3	46.63	ErGO	54	5.33	0.08	1.53
35	2	47.16	ErAL	54	0.64	0.02	3.68
36	2	47.33	ErSO	54	1.46	0.09	5.99
37	2	47.62	BOO	54	0.11	0.01	9.38
38	4	48.37	NrErL	56	0.75	0.07	9.06
39	3	48.59	ErErO	56	13.06	0.10	0.78
40	3	49.16	BErL	56	0.75	0.01	1.98
41	2	49.35	ErAO	56	0.59	0.03	5.76
42	3	50.49	NrErO	58	0.88	0.07	8.50
43	3	51.13	LiErL	58	0.34	0.01	2.16
44	2	51.29	NrAO	58	0.53	0.06	11.74
45	2	51.29	ErBO	58	*	*	*

Abbreviations:

P: Palmitic acid (C16:0); **S**: Stearic acid (C18:0); **O**: Oleic acid (C18:1); **L**: Linoleic acid (C18:2); **Ln**: Linolenic acid (C18:3); **A**: Arachidic acid (C20:0); **G**: Gadoleic acid (C20:1); **B**: Behenic acid (C22:0); **Es**: Eicosadienoic acid (C20:2); **Er:** Erucic acid (C22:1); **Li**: Lignoceric acid (C24:0); **Nr**: Nervonic acid (C24:1).

*** :** TAGs coeluting with the previous one

2.3. Analysis of lipid profile in lipid storage myopathy

Table 1S (II-2.3). PCA data elaboration.

Area %	Me. C12:0	Me. C13:0	Me. C14:0	Me. C14:1n	Me. C15:0 is	C15:0 ant	Me. C15:0	Me. C16:0 is	Me. C16:0	Me. C16:1n	Me. C16:1n	Me. C16:1n	Me. C16:2	Me. C17:0 is	C17:0 ant	Me. C17:0	Me. C17:1n
CPTII-1	0.22	0.00	1.56	0.11	0.01	0.03	0.12	0.02	23.71	0.35	2.28	0.02	0.00	0.04	0.06	0.22	0.17
CPTII-2	0.11	0.00	1.47	0.19	0.02	0.04	0.11	0.03	20.79	0.43	4.87	0.04	0.00	0.08	0.08	0.17	0.20
CPTII-3	0.00	0.27	1.03	0.06	0.00	0.06	0.21	0.00	20.17	0.29	1.48	0.00	0.00	0.08	0.00	0.27	0.00
CPTII-4	0.02	0.22	1.27	0.05	0.09	0.05	0.18	0.03	18.88	0.29	1.10	0.00	0.00	0.11	0.00	0.25	0.07
MADD-1	0.67	0.04	3.79	0.16	0.00	0.00	0.17	0.04	14.64	7.04	1.78	0.00	0.56	0.00	0.08	0.22	0.13
MADD-2	0.32	0.00	2.16	0.15	0.00	0.00	0.11	0.00	13.21	5.70	2.02	0.04	0.49	0.00	0.07	0.14	0.12
MADD-3	0.22	0.00	1.17	0.07	0.00	0.00	0.14	0.03	19.63	0.58	1.82	0.07	0.00	0.05	0.06	0.21	0.10
NLSDM-1	0.16	0.01	1.49	0.28	0.01	0.01	0.10	0.04	17.95	2.24	7.09	0.06	0.12	0.00	0.09	0.09	0.23
NLSDM-2	0.11	1.78	4.30	1.41	0.41	0.06	0.21	0.05	18.70	3.56	1.74	0.00	0.66	0.00	0.00	0.29	0.11
Control-1	0.02	0.22	1.59	0.29	0.00	0.04	0.20	0.03	20.46	0.48	4.75	0.09	0.10	0.07	0.00	0.21	0.21
Control-2	0.03	0.32	1.64	0.28	0.00	0.04	0.21	0.04	19.79	0.50	4.45	0.08	0.00	0.09	0.00	0.21	0.21

Me. C18:0 is	Me. C18:0	Me. C18:1n9	Me. C18:1n7	Me. C18:2n6	Me. C18:3n6	Me. C18:3n3	Me. C18:2n7	Me. C20:0	Me. C20:1n9	Me. C20:2n6	Me. C20:3n6	Me. C20:4n6	Me. C20:5n3	Me. C22:4n6	Me. C22:5n6	Me. C22:5n3	Me. C22:6n3
0.00	6.00	47.20	2.62	10.61	0.06	0.27	0.09	0.04	0.43	0.28	0.42	1.93	0.05	0.21	0.16	0.18	0.53
0.02	6.86	38.24	3.65	14.53	0.00	0.27	0.21	0.00	0.37	0.40	0.42	4.26	0.13	0.60	0.34	0.47	0.62
0.00	15.22	20.33	2.35	23.18	0.00	0.13	0.00	0.21	0.26	0.22	1.18	10.12	0.00	1.04	0.42	0.58	0.83
0.00	14.41	19.28	2.48	27.61	0.00	0.19	0.10	0.11	0.29	0.20	0.97	9.15	0.24	0.68	0.23	0.63	0.81
0.04	9.31	35.73	2.67	14.58	0.00	0.26	0.13	0.10	0.30	0.34	0.75	4.23	0.11	0.78	0.32	0.56	0.46
0.00	8.11	40.35	3.18	18.39	0.00	0.24	0.09	0.17	0.37	0.28	0.31	2.69	0.11	0.45	0.00	0.36	0.38
0.00	4.92	48.94	4.56	13.52	0.00	0.43	0.09	0.14	0.58	0.37	0.30	1.09	0.04	0.40	0.00	0.30	0.18
0.01	1.40	51.86	3.56	9.90	0.05	0.16	0.09	0.03	0.39	0.29	0.32	1.01	0.02	0.42	0.13	0.19	0.21
0.00	10.63	30.19	2.33	15.16	0.00	0.35	0.10	0.10	0.36	0.24	0.65	3.71	0.42	0.57	0.18	0.46	1.17
0.00	9.03	25.92	2.97	19.31	0.15	0.37	0.16	0.00	0.27	0.19	1.32	7.54	0.72	0.56	0.24	0.39	2.10
0.00	9.80	24.88	2.31	24.48	0.14	0.36	0.15	0.00	0.19	0.20	1.11	6.54	0.24	0.67	0.27	0.00	0.77

1	2	3	4	5	6	7	8	9	10	11	12	13	14	15	16	17	18	19	20
0.00	0.00	0.00	0.00	0.00	0.00	0.00	0.00	0.00	0.00	0.00	0.00	0.00	0.41	0.66	0.20	0.64	0.00	0.17	0.27
0.00	0.00	0.00	0.00	0.00	0.00	0.00	0.00	0.00	0.00	0.00	0.00	0.00	0.44	0.42	0.37	0.69	0.18	0.19	0.24
0.12	0.09	0.00	0.09	0.08	0.08	0.00	0.00	0.10	0.00	0.08	0.05	0.04	0.07	0.05	0.00	0.14	0.10	0.00	0.36
1.71	1.53	0.00	0.65	0.50	0.63	0.00	0.00	0.49	0.00	0.25	0.18	0.14	0.19	0.53	0.00	0.74	0.48	0.00	0.75
2.65	1.59	0.00	0.88	0.59	1.23	0.00	0.00	0.68	0.00	0.69	0.50	0.11	0.26	0.60	0.00	0.78	0.89	0.00	2.70
0.27	0.10	0.00	0.16	0.11	0.24	0.00	0.00	0.19	0.00	0.17	0.11	0.10	0.12	0.68	0.00	0.74	0.36	0.00	0.72
0.77	0.48	0.00	0.44	0.29	0.35	0.00	0.00	0.00	0.00	0.00	0.00	0.03	0.19	0.11	0.00	0.32	0.19	0.00	0.24
0.00	0.00	0.27	0.00	0.75	0.00	0.16	0.65	0.57	0.73	0.61	0.16	0.40	0.02	0.19	0.00	0.34	0.17	0.00	1.06
0.55	0.34	0.00	0.15	0.26	0.45	0.00	0.00	0.16	0.00	0.15	0.11	0.04	0.09	0.11	0.00	0.43	0.53	0.00	0.54
0.00	0.00	0.00	0.00	0.00	0.00	0.00	0.00	0.00	0.00	0.00	0.00	0.00	0.77	0.15	0.00	0.18	0.17	0.00	0.59
0.00	0.00	0.00	0.00	0.00	0.00	0.00	0.00	0.00	0.00	0.00	0.00	0.00	0.27	0.23	0.00	0.67	0.57	0.40	0.46

21	22	23	24	25	26	27	28	29	30	31	32	33	34	35	36	37	38	39	
	0.00	0.29	0.61	0.00	0.13	0.24	1.90	1.23	0.80	2.64	1.85	1.25	0.36	0.79	0.85	0.49	0.42	0.13	8.13
	0.00	0.35	0.63	0.00	0.22	0.15	2.14	0.82	0.41	2.06	1.11	0.98	0.65	0.62	1.03	0.62	0.20	0.51	7.30
	0.26	0.32	0.20	0.18	0.10	0.21	0.59	0.49	0.53	1.63	1.49	1.60	0.54	0.72	1.22	0.47	0.27	0.07	4.00
	0.87	0.29	0.26	0.37	0.22	0.43	0.97	1.80	1.44	1.55	2.42	1.74	0.79	0.29	0.82	0.58	0.23	0.22	5.42
	1.60	1.86	0.84	0.37	0.47	0.09	0.72	2.75	1.66	0.92	1.74	1.96	3.81	2.28	1.84	0.00	0.72	0.40	3.77
	1.25	0.80	0.88	0.34	0.22	0.10	1.78	4.84	1.03	1.06	1.38	3.49	2.93	1.48	0.86	0.00	0.25	0.16	7.53
	0.25	0.20	0.16	0.13	0.16	0.16	1.43	0.45	0.67	1.47	0.91	0.87	0.42	0.24	0.60	0.24	0.25	0.16	7.42
	2.08	0.38	2.09	0.00	0.77	0.42	0.75	1.27	1.64	1.09	0.98	2.16	1.74	1.74	2.54	1.90	0.60	0.33	4.17
	0.71	0.64	0.47	0.32	0.19	0.18	0.94	1.60	2.07	2.28	2.22	1.86	1.08	0.82	0.94	0.86	0.24	0.11	5.65
	0.00	1.14	0.45	0.00	0.84	0.53	0.92	1.71	1.47	1.80	2.73	1.99	1.54	0.32	1.22	0.81	0.27	0.26	4.58
	0.00	0.32	0.50	0.00	0.21	0.33	1.89	2.23	1.27	3.05	3.34	1.63	1.00	0.50	0.88	0.64	0.19	0.21	7.03

40	41	42	43	44	45	46	47	48	49	50	51	52	53	54	55	56	57	58	59	
	2.95	13.58	5.67	0.33	2.39	2.83	0.29	0.82	0.15	8.81	2.11	17.88	0.00	1.04	5.75	1.25	0.32	0.29	2.66	0.00
	1.52	11.67	2.99	0.35	2.06	3.17	0.05	1.02	0.22	8.18	4.27	17.21	0.00	1.61	9.08	1.89	0.21	0.28	3.45	0.00
	1.74	12.86	6.39	0.00	2.18	3.70	1.02	1.29	0.19	8.25	0.00	25.43	0.00	1.28	8.47	1.36	0.28	0.19	4.02	0.29
	4.48	10.18	7.78	0.00	1.45	2.47	0.65	1.19	0.33	8.37	0.00	20.08	0.00	1.29	5.25	0.83	0.28	0.24	2.20	0.11
	6.47	3.01	4.75	0.00	4.59	3.75	1.15	1.28	0.56	6.74	0.00	10.06	1.61	0.94	3.29	1.31	0.60	0.37	2.89	0.26
	8.80	5.74	4.01	0.00	4.94	2.68	0.80	0.64	0.45	9.50	0.00	12.52	1.55	0.97	3.24	0.91	0.57	0.29	3.46	0.27
	1.21	10.93	2.69	0.00	1.40	1.66	0.33	0.54	0.41	14.03	0.00	23.59	0.00	1.22	5.11	0.97	0.65	0.21	5.82	0.20
	0.97	12.12	4.29	1.64	2.13	4.48	0.49	1.29	0.13	5.76	2.33	15.03	0.00	1.36	7.07	1.27	0.09	0.18	2.67	0.00
	4.26	11.36	9.05	0.00	2.36	3.42	0.63	0.79	0.23	8.81	0.00	20.88	0.00	0.86	5.23	0.71	0.17	0.22	2.08	0.06
	4.40	12.29	9.15	0.75	1.85	3.72	0.07	1.01	0.07	8.33	1.17	20.54	0.00	1.27	5.58	0.91	0.15	0.12	1.84	0.00
	3.88	14.27	7.22	0.65	1.84	3.18	0.17	0.82	0.05	7.39	0.24	19.85	0.00	0.80	5.40	0.81	0.13	0.12	2.01	0.00

60	61	62	63	64	65	66	67
3.02	0.00	1.24	0.00	0.00	0.77	0.71	0.68
4.71	0.00	1.37	0.00	0.00	0.93	0.75	0.68
3.60	0.00	0.47	0.05	0.10	0.03	0.43	0.16
2.08	0.05	0.60	0.10	0.18	0.08	0.27	0.13
2.20	0.22	0.80	0.21	0.22	0.16	0.51	0.25
2.00	0.00	0.86	0.08	0.61	0.18	0.48	0.15
4.45	0.00	2.47	0.25	0.95	0.24	0.81	0.39
2.59	0.00	0.52	0.00	0.00	0.28	0.38	0.20
1.30	0.00	0.21	0.03	0.12	0.06	0.18	0.06
1.45	0.00	0.41	0.00	0.00	0.14	0.20	0.14
1.76	0.00	0.58	0.00	0.00	0.38	0.39	0.24

2.4. Determination of amines and phenolic acids in wine with benzoylchloride derivatization and liquid chromatography–massspectrometry

Table 1S (II-2.4.). Individual stock concentrations prepared in HPLC water. Stocks were stored at -80 °C prior to use. * Prepared in ethanol.

Compound	Stock (mM)	Compound	Stock (mM)
ACh	10	Hist	10
Ado	5	HVA	10
Agm	10	Leu	10
Ala	10	Lys	10
Arg	10	Met	10
Asn	10	MOPEG	10
Asp	10	NAP	10
βAla	10	Orn	10
Cad	10	PCA*	10
Caf*	10	Phe	10
Ch	1000	PhEt	10
Cit	10	Pro	50
Cou*	10	Put	10
Cys	10	Ser	10
DA	10	Sin*	10
DOMA	10	Spd	10
DOPA	10	Spm	10
DOPAC	10	Tau	10
DOPEG	10	Thr	10
ETA	10	TOH*	10
Fer*	10	Trp	5
GABA	10	TrpA	0.25
Gal*	10	Tyr	2
Glc	2000	TyrA	10
Gln	10	VA*	10
Glu	10	Val	10
Gly	10	VMA	10
His	10	VN*	10

Table 2S (II-2.4.). Preparation of low concentration standard mix. Listed volumes of each standard were mixed to create the "LOW" stock.

Compound	Stock (mM)	Vol (µL)
DA	10	5
DOMA	10	5
DOPA	10	5
DOPAC	10	5
DOPEG	10	5
MOPEG	10	5
Spm	10	5
VMA	10	5
Ado	5	10
Agm	10	10
Cys	10	10
Gln	10	10
His	10	10
Sin	10	10
ACh	10	50
Ch	1000	50
NAP	10	50
Spd	10	50
Tau	10	50
VN	10	50
TrpA	0.25	80
Cit	10	100
HVA	10	100
H_2O		1320
	Total	2000

Table 3S (II-2.4.). Preparation of calibration standards. Listed volumes of each standard were mixed to create the "5X calibration standards." Single use aliquots were prepared and stored at -80 °C until use.

Compound	Stock (mM)	Vol (µL)
Cad	10	1
PhEt	10	1
Trp	5	2
Caf	10	5
Cou	10	5
Glc	2000	5
Met	10	5
Orn	10	5
PCA	10	5
Thr	10	5
TyrA	10	5
VA	10	5
βAla	10	5
Asn	10	10
Hist	10	10
Phe	10	10
Put	10	10
Ser	10	10
Val	10	10
"LOW"		20
Arg	10	20
Asp	10	20
ETA	10	20
GABA	10	20
Lys	10	20
Tyr	2	25
Ala	10	50
Fer	10	50
Gal	10	50
Glu	10	50
Gly	10	50
Leu	10	50
TOH	10	50
Pro	50	400
H_2O		991
	Total	2000

Table 4S (II-2.4.). Preparation of internal standards. Listed volumes of each standard were mixed to create the "Internal standard stock.".

Compound	Stock (mM)	Volume (µL)	Compound	Stock (mM)	Volume (µL)
Put	10	0.25	Met	10	5
TyrA	10	0.25	MOPEG	10	5
Cad	10	0.5	Val	10	5
DA	10	0.5	VMA	10	5
DOPEG	10	0.5	Ado	5	10
PhEt	10	0.5	Cit	10	10
Spd	10	0.5	Cou	10	10
Spm	10	0.5	Gln	10	10
DOMA	10	1	Glu	10	10
DOPAC	10	1	His	10	10
Lys	10	1.25	Phe	10	10
GABA	10	2	Sin	10	10
Hist	10	2	Tau	10	10
Pro	50	2	VN	10	10
Cys	10	2.5	Fer	10	20
NAP	10	2.5	Trp	5	20
Orn	10	2.5	TrpA	0.25	20
Caf	10	4	VA	10	20
Gal	10	4	Ala	10	25
PCA	10	4	Asn	10	25
TOH	10	4	Thr	10	25
Tyr	2	4	Asp	10	50
Agm	10	5	DOPA	10	50
Arg	10	5	Glc	2000	50
βAla	10	5	Ser	10	50
ETA	10	5	Gly	10	100
HVA	10	5	H_2O		1354.75
Leu	10	5		Total	2000

Table 5S (II-2.4.). Calibration ranges for each metabolite.

Compound	Calibration Range (µM)	Compound	Calibration Range (µM)
ACh	0.0025 - 0.5	Hist	0.05 - 10
Ado	0.00025 - 0.05	HVA	0.005 - 1
Agm	0.0005 - 0.1	Leu	0.25 - 50
Ala	0.25 - 50	Lys	0.1 - 20
Arg	0.1 - 20	Met	0.025 - 5
Asn	0.05 - 10	MOPEG	0.00025 - 0.05
Asp	0.1 - 20	NAP	0.0025 - 0.5
βAla	0.025 - 5	Orn	0.025 - 5
Cad	0.005 - 1	PCA	0.025 - 5
Caf	0.025 - 5	Phe	0.05 - 10
Ch	0.25 - 50	PhEt	0.005 - 1
Cit	0.005 - 1	Pro	10 - 2000
Cou	0.025 - 5	Put	0.05 - 10
Cys	0.0005 - 0.1	Ser	0.05 - 10
DA	0.00025 - 0.05	Sin	0.0005 - 0.1
DOMA	0.00025 - 0.05	Spd	0.0025 - 0.5
DOPA	0.00025 - 0.05	Spm	0.00025 - 0.05
DOPAC	0.00025 - 0.05	Tau	0.0025 - 0.5
DOPEG	0.00025 - 0.05	Thr	0.025 - 5
ETA	0.1 - 20	TOH	0.25 - 50
Fer	0.25 - 50	Trp	0.005 - 1
GABA	0.1 - 20	TrpA	0.0001 - 0.02
Gal	0.25 - 50	Tyr	0.025 - 5
Glc	5 - 1000	TyrA	0.025 - 5
Gln	0.0005 - 0.1	VA	0.025 - 5
Glu	0.25 - 50	Val	0.05 - 10
Gly	0.25 - 50	VMA	0.00025 - 0.05
His	0.0005 - 0.1	VN	0.0025 - 0.5

Preparation of Calibration Standards and Internal Standards

Prepare individual stocks (Table 1S (II-2.4.))

- Prepare stock solution of individual standards at specified concentration
    - Water as solvent, ethanol for those with *
- Store at -80 °C if not using immediately

Prepare calibration standards

- Prepare "Low" calibration mix (Table 2S (II-2.4.))
    - Mix individual stocks with specified volumes
    - Water as solvent
- Prepare 5X standards (Table 3S (II-2.4.)
    - Mix individual stocks + "Low" mix using specified volumes
    - Water as solvent
- Prepare 20 µL aliquots of 5X standards and store at -80 °C
- On day of use:
    - Thaw aliquot and dilute 5x in calibration solvent (i.e. water)
    - Perform serial dilution to prepare calibration standards for given range (Table 5S (II-2.4.)

Prepare internal standards

- Prepare "Internal standard stock" (Table 4S (II-2.4.)
    - Mix individual stocks at specified volumes
    - Water as solvent
- Prepare BzCl reagents

  - 100 mM sodium carbonate in water
  - 2% (v/v) $^{13}C_6$BzCl in ACN (294 µL ACN, 6 µL $^{13}C_6$BzCl)
- Derivatize Internal standard stock with $^{13}C_6$BzCl
  - 500 µL mix
  - 250 µL carbonate
  - 250 µL $^{13}C_6$BzCl
  - 1-2 µL formic acid (start with 1 µL, add more if precipitate remains)
- Prepare 20 µL aliquots for one-time use
- On day of use:
  - Thaw aliquot
  - Prepare internal standard solution to use in derivatization
    - 488 µL 80% (v/v) acetonitrile
    - 5 µL Internal standard stock
    - 5 µL H_2SO_4
    - 1 µL 10 µM d4-Ach
    - 1 µL 10 µM d4-Ch

Compound	Precursor (m/z)	Product (m/z)	Fragmentor (V)	Collision Energy (V)	Cell Accelerator (V)	Retention Time (min)
Ch	104	60	120	20	4	1.25
	108	60	120	20	4	1.25
ACh	146	87	120	15	4	1.37
	150	91	120	15	4	1.37
Bz-His	260	110	130	20	4	2.44
	266	110	130	20	4	2.44
Bz-Tau	230	105	120	10	4	2.57
	236	111	120	10	4	2.57
Bz-Arg	279	105	135	30	4	2.61
	285	111	135	30	4	2.61
Bz-Hist	216	105	120	20	4	2.65
	222	111	120	20	4	2.65
Bz-Asn	237	105	120	20	4	2.66
	243	111	120	20	4	2.66
Bz-Gln	251	105	120	20	4	2.76
	257	111	120	20	4	2.76
Bz-Ser	210	105	120	20	4	2.78
	216	111	120	20	4	2.78
Bz-Cit	280	105	120	20	4	2.89
	286	111	120	20	4	2.89
Bz-Agm	235	176	110	30	4	2.96
	241	182	110	30	4	2.96
Bz-Asp	238	105	120	10	4	2.97
	244	111	120	10	4	2.97
Bz-ETA	166	105	120	20	4	2.97
	172	111	120	20	4	2.97
Bz-Glc	307	185	130	20	4	3.07
	313	185	130	20	4	3.07
Bz-Gly	180	105	120	10	4	3.1
	186	111	120	10	4	3.1
Bz-Glu	252	105	120	20	4	3.22
	258	111	120	20	4	3.22
Bz-BAla	194	105	120	20	4	3.5
	200	111	120	20	4	3.5
Bz-NAP	235	176	135	20	4	3.6
	241	182	135	20	4	3.6
Bz-Ala	194	105	120	20	4	3.7
	200	111	120	20	4	3.7
Bz-GABA	208	105	120	10	4	3.79
	214	111	120	10	4	3.79
Bz-Pro	220	105	120	20	4	4.05
	226	111	120	20	4	4.05
Bz-Ado	372	136	120	30	4	5.35
	378	136	120	30	4	5.35
Bz-Val	222	105	120	30	4	5.94
	228	111	120	30	4	5.94
Bz-Met	254	105	120	15	4	6
	260	111	120	15	4	6
Bz-Orn	341	174	120	15	4	6.4
	353	180	120	15	4	6.4
Bz-Lys	355	188	120	20	4	7.11
	367	194	120	20	4	7.11
Bz-Put	297	105	120	30	4	7.53
	309	111	120	30	4	7.53
Bz-Xle	236	105	120	30	4	8.12
	242	111	120	30	4	8.12
Bz-Phe	270	120	120	10	4	8.37
	276	120	120	10	4	8.37

Compound	Precursor (m/z)	Product (m/z)	Fragmentor (V)	Collision Energy (V)	Cell Accelerator (V)	Retention Time (min)
Bz-Thr	224	105	140	20	4	8.39
	230	111	140	20	4	8.39
Bz-VMA	320	105	120	10	4	8.4
	326	111	120	10	4	8.4
Bz-Trp	309	159	120	10	4	8.5
	315	159	120	10	4	8.5
Bz-MOPEG	306	105	120	20	4	8.55
	312	111	120	20	4	8.55
Bz-Cad	311	105	130	30	4	8.56
	323	111	130	30	4	8.56
Bz-Cys	330	105	120	20	4	10.1
	342	111	120	20	4	10.1
Bz-Spd	458	162	120	30	4	10.43
	476	168	120	30	4	10.43
Bz-PhEt	226	105	120	15	4	10.94
	232	111	120	15	4	10.94
Bz-TrpA	265	144	130	30	4	10.99
	271	144	130	30	4	10.99
Bz-HVA	304	105	120	15	4	11.75
	310	111	120	15	4	11.75
Bz-TOH	243	105	120	20	4	11.77
	249	111	120	20	4	11.77
Bz-DOMA	410	105	130	20	4	11.95
	422	111	130	20	4	11.95
Bz-VA	273	105	120	20	4	12
	279	111	120	20	4	12
Bz-Spm	619.6	497	135	25	4	12.1
	643.6	515.6	135	25	4	12.1
Bz-DOPEG	396	105	120	20	4	12.2
	408	111	120	20	4	12.2
Bz-Tyr	390	105	120	30	4	12.78
	402	111	120	30	4	12.78
Bz-Cou	269	105	120	20	4	12.89
	275	111	120	20	4	12.89
Bz-Fer	299	105	120	20	4	13
	305	111	120	20	4	13
Bz-Sin	329	105	130	20	4	13.03
	335	111	130	20	4	13.03
Bz-VN	257	105	120	20	4	13.8
	263	111	120	20	4	13.8
Bz-DOPAC	394	105	140	20	4	14.22
	406	111	140	20	4	14.22
Bz-PCA	380	105	120	20	4	14.4
	392	111	120	20	4	14.4
Bz-DOPA	510	360	120	30	4	14.53
	528	372	120	30	4	14.53
Bz-TyrA	346	105	135	25	4	14.67
	358	111	135	25	4	14.67
Bz-Caf	406	105	120	20	4	14.9
	418	111	120	20	4	14.9
Bz-Gal	500	105	140	30	4	16
	518	111	140	30	4	16
Bz-DA	466	105	140	20	4	16.02
	484	111	140	20	4	16.02

Chapter III - Building of a Linear Retention Index System in Liquid Chromatography

3.1. Proposal of a linear retention index system for improving identification reliability of triacylglycerol profiles in lipid samples by liquid chromatography methods

Supporting Information Table of Contents:

Table 1S (III-3.1.). List of identified TGs, along with their PN, LRI and ΔLRI value.

Table 2S (III-3.1.). LRI values obtained for 54 TGs on 6 different column set-ups, along with their average and ΔLRI.

Table 3S (III-3.1.). LRI values, total average and ΔLRI, obtained for 54 TGs on an Ascentis Express 100 mm L × 2.1 mm ID, 2 µm *d.p.*, in gradient mode (0-52.5 min, 0-50% B (hold 10 min)), at 3 different flow rates, at 35° C.

Table 4S (III-3.1.). LRI values, total average and ΔLRI, obtained for 54 TGs on an Ascentis Express 100 mm L × 2.1 mm ID, 2 µm *d.p.*, at 35° C and a flow rate of 400 µL/min, at 3 different gradient steepness (%B/min).

Table 5S (III-3.1.). LRI values, averages and ΔLRIs, obtained for 54 TGs on an Ascentis Express 100 mm L × 2.1 mm ID, 2 µm *d.p.*, at 400 µL/min, in gradient mode (0-52.5 min, 0-50% B (hold 10 min)), at 4 different oven temperatures.

Figure 1S (III-3.1.). histogram reporting the average LRI values between UHPLC-ELSD and HPLC-ESI-MS analyses (values are reported in Table 2); error bar corresponds to ΔLRI value.

Table 1S (III-3.1.). List of identified TGs, along with their PN, LRI and ΔLRI value.

PN	Compound Name	LRI*	ΔLRI	PN	Compound Name	LRI*	ΔLRI	PN	Compound Name	LRI*	ΔLRI
26	CaCC (p=2)	2691±6[a]	4	36	EpEpO (p=2)	3836±6	1	44	OOLn (p=14)	4360±6	11
26	CaCaCp (p=2)	2691±6[a]	4	38	OPCp (p=10)	3842±3	8	44	PPoM (p=2)	4361±2	3
26	LaCCp (p=2)	2691±6[a]	4	38	PPCp (p=8)	3843±4	7	44	OOγLn (p=2)	4364±6	3
28	LaCaCp (p=2)	2800±6	4	36	EpEpP (p=2)	3850±6	1	44	OOLa (p=10)	4364±3	8
28	MCCp (p=2)	2800±6	4	36	DhEpO (p=2)	3850±6	1	44	OPoPo (p=8)	4367±3	11
28	OCBu (p=6)	2816±4	10	36	DhEpP (p=2)	3850±6	1	44	SLLn (p=2)	4378±6	3
28	PCBu (p=6)	2816±4	10	38	γLnLγLn (p=2)	3867±6	1	44	EpSO (p=2)	4380±6	3
30	MCaCp (p=10)	2969±3	13	38	PoHtM (p=2)	3893±6	1	44	POLn (p=4)	4383±4	8
30	PCCp (p=10)	3003±3	13	38	EpPoPo (p=2)	3893±6	1	44	SPCa (p=10)	4386±3	9
30	OCaBu (p=10)	3003±3	13	36	DhDhP (p=2)	3893±6	1	44	PPLa (p=10)	4386±3	9
30	PCaBu (p=10)	3003±3	13	38	PoγLnγLn(p=2)	3915±6	3	44	SMLa (p=10)	4386±3	9
30	MLaBu (p=10)	3003±3	13	38	DhPoPo (p=2)	3937±6	2	44	PMM (p=10)	4386±3	9
30	OCpC (p=2)	3014±6	2	38	EpPoM (p=2)	3937±6	2	44	SOCa (p=8)	4387±4	9
32	LaCaCa (p=6)	3209±4	5	38	DhMM (p=2)	3937±6	2	44	POγLn (p=2)	4389±6	3
32	MCaC (p=4)	3223±4	11	40	OMCa (p=8)	3987±3	10	44	ALnLn (p=2)	4395±6	3
32	PLaBu (p=8)	3241±3	10	38	EpLnP (p=2)	3987±6	2	44	PLnP (p=2)	4395±6	3
32	MLaCp (p=4)	3241±4	10	40	OOC (p=8)	3989±4	8	44	DhSO (p=2)	4399±6	3
32	PCaCp (p=10)	3243±3	11	40	OPC (p=10)	3991±3	7	44	EpSP (p=2)	4416±6	3
32	PCC (p=2)	3249±6	1	40	MMLa (p=6)	3992±4	7	44	PγLnP (p=2)	4431±6	3
32	LLBu (p=2)	3292±6	0	40	OOCo (p=6)	3992±4	6	44	DhSP (p=2)	4433±6	3
32	PoPoBu (p=2)	3292±6	0	40	LLLn (p=10)	3993±3	6	46	OOPo (p=2)	4485±6	3
34	PCaC (p=8)	3414±3	6	40	SOCp (p=6)	3993±4	6	46	C22:1γLn (p=2)	4501±6	1
34	MCaCa (p=10)	3416±3	10	40	LLγLn (p=2)	3999±6	2	46	GLL (p=2)	4502±6	10
34	OCaC (p=2)	3426±6	0	38	DhLnP (p=2)	4004±6	2	46	OOL (p=42)	4516±1	12
34	OLBu (p=6)	3441±4	4	40	SMC (p=10)	4009±3	11	46	OOM (p=10)	4526±3	8
34	LaLaCa (p=2)	3443±6	0	40	PPC (p=10)	4009±3	11	46	PLO (p=46)	4539±1	13
34	MLaC (p=2)	3443±6	0	40	LnLnO (p=6)	4011±4	5	46	SLL (p=8)	4548±3	9
34	OMBu (p=10)	3454±4	10	40	SSBu (p=10)	4019±4	6	46	SOLa (p=8)	4551±3	15
34	PMBu (p=10)	3454±4	10	40	LnPLn (p=6)	4023±4	5	46	PoPP (p=2)	4552±6	4
30	EpEpEp (p=2)	3463±6	0	38	DpDhP (p=2)	4037±6	2	46	SOLn (p=6)	4563±4	7
30	DhDhDh (p=2)	3500±6	0	38	DhEpS (p=2)	4052±6	2	46	PLP (p=24)	4571±2	14
36	OCaCa (p=10)	3596±4	8	40	γLnγLnO (p=2)	4052±6	2	46	DhSS (p=2)	4577±6	4
36	OLaC (p=6)	3597±3	7	40	γLnPγLn (p=2)	4064±6	2	46	SMM (p=10)	4580±3	15
34	StStPo (p=2)	3600±6	1	40	LnMM (p=2)	4094±6	2	46	PPM (p=10)	4580±3	15
34	EpPoHt (p=2)	3600±6	1	40	EpOPo (p=2)	4094±6	2	46	SLnP (p=2)	4587±6	4
36	PPoCp (p=8)	3604±3	9	40	EpLP (p=2)	4112±6	2	46	SOγLn (p=2)	4599±6	4
36	PCaCa (p=10)	3604±3	9	40	DhOPo (p=2)	4135±6	2	46	SγLnP (p=2)	4631±6	4
36	OLCp (p=2)	3615±6	1	40	DhOM (p=2)	4148±6	2	47	OOPd (p=2)	4690±6	4
36	OOBu (p=8)	3620±3	10	40	DhPPo (p=2)	4148±6	2	47	OPPd (p=2)	4690±6	4
36	OMCp (p=6)	3622±4	8	42	LLL (p=24)	4160±6	10	48	$C_{22:1}$LL (p=2)	4690±6	4
34	EpStPo (p=2)	3624±6	1	42	OOCa (p=10)	4164±2	8	48	OLG (p=2)	4703±6	4
36	MMC (p=2)	3625±6	1	42	OPCa (p=8)	4164±3	8	48	$C_{24:1}$LγLn (p=2)	4723±6	9
36	MLaCa (p=2)	3625±6	1	42	PoPoPo (p=2)	4167±4	2	48	OOO (p=44)	4729±1	14
36	LaLaLa (p=2)	3625±6	1	42	PoPoM (p=2)	4167±6	2	48	GLP (p=2)	4740±6	4
36	OPBu (p=10)	3630±3	10	42	PMLa (p=2)	4175±6	2	48	SLO (p=16)	4746±2	8
36	PPBu (p=10)	3630±3	10	42	PPCa (p=10)	4176±3	9	48	SLP (p=2)	4750±6	4
34	EpHtM (p=2)	3649±6	1	42	SMCa (p=8)	4178±4	9	48	SOM (p=10)	4754±3	13
34	EpStM (p=2)	3649±6	1	42	γLnLO (p=2)	4181±6	2	48	POO (p=44)	4756±2	13
36	PMCp (p=2)	3655±6	1	42	LnPPo (p=2)	4186±6	2	48	POP (p=26)	4776±2	14
36	LnLnLn (p=6)	3668±4	5	42	LPoPo	4186±6	2	48	SMP (p=10)	4780±3	15
34	EpEpPo (p=2)	3669±6	1	42	MMM (p=2)	4190±6	2	48	PPP (p=10)	4784±3	11
34	DhStPo (p=2)	3669±6	1	42	LnLO (p=8)	4192±3	11	48	SPPo (p=2)	4785±6	4
34	DhStM (p=2)	3712±6	1	42	SPC (p=10)	4196±3	10	50	$C_{24:1}$LL (p=2)	4881±6	10
34	EpEpM (p=2)	3712±6	1	42	SSCp (p=10)	4196±3	10	50	$C_{22:1}$LO (p=2)	4890±6	4
36	γLnγLnγLn (p=2)	3747±6	1	42	OOHt (p=2)	4213±4	3	50	GOO(p=2)	4905±6	7
34	DhEpPo (p=2)	3755±6	1	42	SLnLn (p=6)	4216±4	4	50	GOP(p=2)	4921±6	8
34	DhEpM (p=2)	3755±6	1	42	LnLP (p=6)	4217±6	3	50	SLS (p=2)	4940±6	4
38	OOCp (p=10)	3785±3	8	42	γLnLP (p=2)	4221±6	2	50	SOO (p=34)	4948±2	14
38	OLaCa (p=10)	3785±3	8	42	SγLnγLn (p=2)	4221±6	2	50	SOP (p=28)	4961±3	15
38	OMC (p=8)	3796±3	8	42	EpOO (p=2)	4234±6	3	50	SPP (p=12)	4978±3	8
36	EpLnPo (p=2)	3799±6	1	42	DhOP (p=2)	4246±6	3	52	$C_{22:1}$γLn$C_{22:1}$ (p=2)	5069±6	4
36	DhPHt (p=2)	3807±6	1	42	DhPP (p=2)	4261±6	3	52	$C_{24:1}$OL (p=2)	5084±6	12
36	EpPHt (p=2)	3807±6	1	44	OLPo (p=2)	4286±6	3	52	$C_{22:1}$OP (p=2)	5084±6	4

36	EpStP (p=2)	3807±6	1	44	OPoM (p=2)	4303±6	3	52	$C_{22:1}$OO (p=2)	5091±6	4
38	PLaCa (p=8)	3809±3	8	44	PPoPo (p=2)	4338±6	3	52	SOS (p=20)	5103±2	15
38	MMCa (p=6)	3810±4	8	44	LPM (p=2)	4338±6	3	52	SSP (p=10)	5156±3	15
38	PoPoCa (p=2)	3820±6	1	44	GLγLn (p=2)	4340±6	3	54	$C_{22:1}$OG (p=2)	5238±6	5
38	PPoCo (p=2)	3820±6	1	44	LLO (p=50)	4342±1	10	54	$C_{22:1}$OS (p=2)	5271±6	5
38	PMC (p=10)	3829±3	7	44	OLM (p=10)	4349±3	5	54	SSS (p=2)	5324±6	5
38	LnLLn (p=8)	3830±3	3	44	LLP (p=24)	4358±2	7				

* Intersample average; [a] extrapolated values; p: population; fatty acid abbreviations: Bu = butyric acid, Cp = caproic acid, C = caprylic acid, Co = decenoic acid, Ca = capric acid, La = lauric acid, M = myristic acid, Pd = pentadecanoic acid; Ht = hexadecatrienoic acid, Po = palmitoleic acid; P = palmitic acid, Ed = heptadecanoic acid, St = stearidonic acid, Ln = linolenic acid, L = linoleic acid, O = oleic acid, S = stearic acid, Ep = eicosapentaenoic acid, Dh = docosahexaenoic acid, G = gadoleic acid, A = arachidic acid, $C_{22:1}$ = erucic acid, $C_{24:1}$ = nervonic acid.

Table 2S (III-3.1.). LRI values obtained for 54 TGs on 6 different column set-ups, along with their average and ΔLRI.

		LRI							LRI
PN	**Compound Name**	**2 Titan 100 mm × 2.1 mm ID, 1.9 µm *dp*(monodisperse)[a]**	**1 Titan 100 mm × 2.1 mm ID, 1.9 µm *dp*(monodisperse)[b]**	**1 Ascentis Express 100 mm × 2.1 mm ID, 2.7 µm *dp*(partially porous)[b]**	**1 Ascentis Express 100 mm × 4.6 mm ID, 2.7 µm *dp*(partially porous)[c]**	**1 Ascentis Express 100 mm × 2.1 mm ID, 2 µm *dp*(partially porous)[b]**	**TOTAL AVERAGE**	**ΔLRI**	**1 Ascentis 100 mm × 2.1 mm ID, 3 µm *dp*(totally porous)[b]**
36	LnLnLn	3668	3673	3667	3669	3654	3665	11	3606
36	γLnγLnγLn	3747	3738	3740	3732	3733	3738	9	3715
38	LnLLn	3830	3840	3842	3842	3823	3835	13	3773
38	γLnLγLn	3867	3886	3893	3889	3874	3882	14	3826
38	PoγLnγLn	3915	3914	3917	-	3913	3915	3	3875
40	LLLn	3993	4002	4006	4005	3989	3999	10	3944
40	LLγLn	3999	4022	4022	4022	4009	4015	15	3966
40	LnLnO	4011	4012	4019	4015	4002	4012	10	3956
40	LnPLn	4023	-	4042	4040	4031	4034	11	3998
40	γLnγLnO	4052	4071	4078	4072	4063	4067	15	4013
40	γLnPγLn	4086	4084	4094	4088	4081	4086	7	4049
42	LLL	4160	4165	4170	4160	4151	4161	10	4107
42	γLnLO	4181	4204	4205	4201	4189	4196	14	4151
42	LnLO	4192	4188	4193	4186	4175	4187	11	4126
42	SLnLn	4216	4206	4212	-	4198	4208	10	4162
42	LnLP	4217	4227	4236	4229	4223	4226	10	4184
42	γLnLP	4221	4223	4226	4221	4215	4221	6	4184
42	SγLnγLn	4221	4223	4226	4221	4215	4221	6	4184
44	LLO	4342	4348	4348	4339	4331	4341	10	4289
44	LLP	4358	4364	4365	4360	4352	4360	8	4321
44	OOLn	4360	4367	4370	4365	4356	4364	8	4317
44	OOγLn	4364	4382	4386	4379	4367	4375	12	4331
44	POLn	4383	4387	4393	4389	4382	4387	6	4347
44	POγLn	4389	4408	4413	4407	4402	4403	15	4370
44	PγLnP	4431	4428	4435	4431	4430	4431	4	4406

46	GLL	4502	4511	4517	4511	4498	4508	10	4454
46	OOL	4516	4525	4531	4522	4515	4522	9	4470
46	PLO	4539	4551	4557	4548	4546	4548	9	4506
46	SLL	4548	-	4575	4575	4550	4562	14	-
46	SOLn	4563	4574	4588	-	4577	4575	13	4540
46	PLP	4571	4574	4594	4584	4579	4580	14	4538
46	SOγLn	4599	4588	4610	4602	4598	4599	11	4557
46	SγLnP	4631	4625	4638	4629	4634	4631	6	4607
48	$C_{22:1}$LL	4690	4701	4706	4699	4692	4698	8	4638
48	OLG	4703	4711	4711	4710	4703	4708	5	4653
48	$C_{24:1}$LγLn	4723	4732	4717	4723	4719	4723	9	4675
48	OOO	4729	4734	4740	4732	4727	4732	7	4688
48	GLP	4740	-	4732	4740	4735	4737	5	4690
48	POO	4756	4762	4769	4763	4761	4762	7	4728
48	POP	4776	4781	4787	4779	4783	4781	6	4749
50	$C_{24:1}$LL	4881	4880	4891	4882	4873	4881	10	4814
50	$C_{22:1}$LO	4890	4893	4896	4891	4883	4890	8	4820
50	GOO	4905	4908	4910	4904	4898	4905	7	4831
50	GOP	4921	4923	4930	4919	4914	4921	8	4848
50	SLS	4940	-	-	-	4940	4940	0	4887
50	SOO	4948	4949	4947	4938	4938	4944	6	4895
50	SOP	4961	-	4945	4943	4951	4950	11	4910
50	SPP	4978	-	4978	4972	4975	4976	4	4953
52	$C_{22:1}$γLn$C_{22:1}$	5069	5065	5071	-	5052	5064	12	5013
52	$C_{24:1}$OL	5084	5081	5080	5078	5065	5077	12	5021
52	$C_{22:1}$OO	5091	5095	5097	5088	5085	5091	7	5047
52	SOS	5103	5103	5106	5106	5099	5103	4	5060
54	$C_{22:1}$OG	5238	5251	5243	5228	5230	5238	13	5180
54	$C_{22:1}$OS	5271	5282	5271	5267	5265	5271	11	5234

[a]flow rate 400 μL/min, gradient: 0-105 min, 0-50% B (hold 20 min); [b]flow rate 400 μL/min, gradient: 0-52.5 min, 0-50% B (hold 10 min); [c]flow rate 1.8 mL/min, gradient: 0-52.5 min, 0-50% B (hold 10 min). Oven temperature was 35° C in all the analyses. For fatty acid legend see Table 1S (III-3.1.).

Table 3S (III-3.1.). LRI values, total average and ΔLRI, obtained for 54 TGs on an Ascentis Express 100 mm L × 2.1 mm ID, 2 µm *d.p.*, in gradient mode (0-52.5 min, 0-50% B (hold 10 min)),at 3 different flow rates, at 35° C.

PN	Compound Name	LRI			TOTAL AVERAGE	ΔLRI
		300 µL/min	400 µL/min	500 µL/min		
36	LnLnLn	3651	3647	3643	3647	4
36	γLnγLnγLn	3733	3733	3732	3732	1
38	LnLLn	3820	3823	3826	3823	3
38	γLnLγLn	3869	3874	3880	3874	6
38	PoγLnγLn	3901	3913	3918	3910	10
40	LLLn	3982	3989	3995	3989	7
40	LnLnO	3994	4002	4007	4001	7
40	LLγLn	4003	4009	4013	4008	5
40	LnPLn	4025	4031	4036	4030	6
40	γLnγLnO	4054	4063	4067	4061	7
40	γLnPγLn	4075	4081	4084	4080	5
42	LLL	4144	4151	4157	4150	7
42	LnLO	4167	4175	4181	4175	8
42	γLnLO	4182	4189	4193	4188	6
42	SLnLn	4190	4198	4203	4197	7
42	γLnLP	4208	4215	4217	4213	5
42	SγLnγLn	4208	4215	4217	4213	5
42	LnLP	4215	4223	4229	4222	7
44	LLO	4323	4331	4337	4330	7
44	LLP	4345	4352	4357	4351	7
44	OOLn	4348	4356	4362	4355	8
44	OOγLn	4357	4367	4373	4366	9
44	POLn	4375	4382	4388	4382	7
44	POγLn	4393	4402	4406	4400	7
44	PγLnP	4424	4430	4434	4429	5
46	GLL	4492	4498	4505	4498	6
46	OOL	4510	4515	4521	4515	6
46	PLO	4541	4546	4549	4545	5
46	SLL	4546	4550	-	4548	2
46	SOLn	4571	4577	4580	4576	5
46	PLP	4577	4579	4585	4580	5
46	SOγLn	4591	4598	4603	4597	6
46	SγLnP	4625	4634	4634	4631	6
48	$C_{22:1}$LL	4682	4692	4695	4690	8
48	OLG	4695	4703	4706	4701	7
48	$C_{24:1}$LγLn	4713	4719	4721	4718	5
48	OOO	4720	4727	4729	4726	6
48	GLP	4725	4735	4738	4733	8
48	POO	4755	4761	4762	4759	4
48	POP	4778	4783	4784	4781	4
50	$C_{24:1}$LL	4864	4873	4877	4871	7
50	$C_{22:1}$LO	4874	4883	4885	4880	7
50	GOO	4890	4898	4899	4895	6
50	GOP	4909	4914	4917	4913	5

50	SOO	4933	4938	4938	4936	4
50	SLS	4936	4940	4941	4939	3
50	SOP	4944	4951	4954	4949	6
50	SPP	4968	4975	4973	4972	4
52	$C_{22:1}\gamma LnC_{22:1}$	5044	5052	5053	5050	6
52	$C_{24:1}OL$	5054	5065	5068	5062	8
52	$C_{22:1}OO$	5079	5085	5085	5083	4
52	SOS	5099	5099	5097	5098	1
54	$C_{22:1}OG$	5222	5230	5229	5227	5
54	$C_{22:1}OS$	5257	5265	5264	5262	5

For fatty acid legend see Table 1S (III-3.1.).

Table 4S (III-3.1.). LRI values, total average and ΔLRI, obtained for 54 TGs on an Ascentis Express 100 mm L × 2.1 mm ID, 2 µm *d.p.*, at 35° C and a flow rate of 400 µL/min, at 3 different gradient steepness (%B/min).

PN	Compound Name	LRI				
		0.95% B/min	1.4% B/min	0.70% B/min	TOTAL AVERAGE	ΔLRI
36	LnLnLn	3647	3647	3653	3649	4
36	γLnγLnγLn	3733	3730	3737	3733	4
38	LnLLn	3823	3815	3836	3825	12
38	γLnLγLn	3874	3865	3891	3877	15
38	PoγLnγLn	3913	3899	-	3906	7
40	LLLn	3989	3978	4002	3989	12
40	LnLnO	4002	3991	4012	4002	11
40	LLγLn	4009	3998	4020	4009	11
40	LnPLn	4031	4021	4040	4030	10
40	γLnγLnO	4063	4051	4073	4062	11
40	γLnPγLn	4081	4071	4091	4081	10
42	LLL	4151	4139	4159	4150	11
42	LnLO	4175	4163	4185	4174	12
42	γLnLO	4189	4177	4198	4188	11
42	SLnLn	4198	4186	4207	4197	11
42	γLnLP	4215	4204	4223	4214	10
42	SγLnγLn	4215	4204	4223	4214	10
42	LnLP	4223	4210	4234	4222	12
44	LLO	4331	4317	4342	4330	13
44	OOLn	4356	4343	4367	4355	13
44	LLP	4352	4340	4362	4351	12
44	OOγLn	4367	4353	4379	4366	13
44	POLn	4382	4369	4394	4381	13
44	POγLn	4402	4389	4411	4400	12
44	PγLnP	4430	4422	4435	4429	7
46	GLL	4498	4486	4512	4499	13
46	OOL	4515	4504	4527	4515	12
46	PLO	4546	4535	4554	4545	10
46	SLL	4550	4569	4579	4566	16
46	SOLn	4577	4564	4583	4575	11
46	PLP	4579	4576	4598	4584	14
46	SOγLn	4598	4618	4604	4607	11
46	SγLnP	4634	-	4636	4635	1
48	$C_{22:1}$LL	4692	4687	4700	4693	7
48	OLG	4703	4711	4710	4708	5
48	$C_{24:1}$LγLn	4719	4720	4726	4722	4
48	OOO	4727	4727	4733	4729	4
48	GLP	4735	4735	4744	4738	6
48	POO	4761	4779	4766	4769	11
48	POP	4783	4776	-	4779	4
50	$C_{24:1}$LL	4873	4866	-	4869	4
50	$C_{22:1}$LO	4883	4885	-	4884	1

50	GOO	4898	4903	-	4900	3
50	GOP	4914	4916	-	4915	1
50	SOO	4938	4932	4947	4939	8
50	SLS	4940	4944	-	4942	2
50	SOP	4951	4966	-	4959	8
50	SPP	4975	-	-	4975	0
52	$C_{22:1}\gamma LnC_{22:1}$	5052	5054	-	5053	1
52	$C_{24:1}OL$	5065	5074	-	5069	4
52	$C_{22:1}OO$	5085	5087	-	5086	1
52	SOS	5099	-	-	5099	0
54	$C_{22:1}OG$	5230	-	-	5230	0
54	$C_{22:1}OS$	5265	-	-	5265	0

For fatty acid legend see Table 1S (III-3.1.).

Table 5S (III-3.1.). LRI values, averages and ΔLRIs, obtained for 54 TGs on anAscentis Express 100 mm L × 2.1 mm ID, 2 μm *d.p.*, at 400 μL/min, in gradient mode (0-52.5 min, 0-50% B (hold 10 min)), at 4 different oven temperatures.

PN	Compound Name	LRI				TOTAL AVERAGE	ΔLRI	AVERAGE (35°C/40°C)	ΔLRI (35°C/40°C)	AVERAGE (30°C/35°C)	ΔLRI (30°C/35°C)
		30°C	35°C	40°C	50°C						
36	LnLnLn	3651	3647	3651	3664	3653	11	3649	2	3649	2
36	γLnγLnγLn	3755	3733	3724	3701	3728	27	3728	5	3744	0
38	LnLLn	3819	3823	3835	3864	3835	29	3829	6	3821	2
38	γLnLγLn	3866	3874	3891	3918	3887	31	3882	9	3870	4
38	PoγLnγLn	3897	3913	3927	3948	3921	27	3920	7	3905	8
40	LLLn	3982	3989	4001	4021	3998	23	3995	6	3986	4
40	LnLnO	3993	4002	4013	4032	4010	22	4007	5	3998	5
40	LLγLn	3998	4009	4020	4041	4017	24	4014	6	4003	5
40	LnPLn	4028	4031	4035	-	4031	4	4033	2	4030	2
40	γLnγLnO	4053	4063	4073	4092	4070	22	4068	5	4058	5
40	γLnPγLn	4075	4081	4088	4100	4086	14	4084	3	4078	3
42	LLL	4140	4151	4162	4179	4158	21	4156	5	4146	5
42	LnLO	4165	4175	4186	4204	4182	22	4180	5	4170	5
42	γLnLO	4178	4189	4198	4217	4195	22	4193	5	4183	5
42	SLnLn	4192	4198	4205	4213	4202	11	4201	4	4195	3
42	γLnLP	4206	4215	4220	4229	4217	11	4217	2	4211	5
42	SγLnγLn	4206	4215	4220	4229	4217	11	4217	2	4211	5
42	LnLP	4216	4223	4231	4246	4229	17	4227	4	4219	4
44	LLO	4320	4331	4342	4366	4340	26	4337	5	4325	6
44	OOLn	4349	4356	4366	4387	4364	22	4361	5	4352	4
44	LLP	4346	4352	4360	4376	4358	18	4356	4	4349	3
44	OOγLn	4365	4367	4382	4410	4381	29	4374	7	4366	1
44	POLn	4378	4382	4391	4405	4389	16	4386	4	4380	2

44	POγLn	4395	4402	4410	4430	4409	21	4406	4	4398	3
44	PγLnP	4429	4430	4432	-	4430	2	4431	1	4429	0
46	GLL	4485	4498	4516	-	4500	16	4507	9	4492	7
46	OOL	4502	4515	4528	4561	4526	34	4521	7	4508	7
46	PLO	4535	4546	4554	4579	4553	25	4550	4	4541	6
46	SLL	4550	4550	4575	-	4562	13	4562	13	4550	0
46	SOLn	4563	4577	4584	4611	4584	28	4580	3	4570	7
46	PLP	4573	4579	4588	4596	4584	12	4583	4	4576	3
46	SOγLn	4586	4598	4607	-	4597	11	4602	4	4592	6
46	SγLnP	4624	4634	4633	4652	4635	17	4633	1	4629	5
48	$C_{22:1}$LL	4670	4692	4700	4740	4700	40	4696	4	4681	11
48	OLG	4684	4703	4707	4743	4709	34	4705	2	4693	10
48	$C_{24:1}$LγLn	4704	4719	4722	-	4715	11	4720	1	4711	8
48	OOO	4712	4727	4730	4756	4731	25	4728	1	4720	8
48	GLP	4717	4735	4739	4765	4739	26	4737	2	4726	9
48	POO	4749	4761	4760	4776	4761	15	4760	0	4755	6
48	POP	4774	4783	4779	4785	4780	6	4781	2	4778	4
50	$C_{24:1}$LL	4849	4873	4889	4922	4883	39	4881	8	4861	0
50	$C_{22:1}$LO	4860	4883	4893	4508	4786	278	4888	5	4871	11
50	GOO	4878	4898	4907	-	4894	16	4902	5	4888	10
50	GOP	4897	4914	4923	4949	4921	28	4919	5	4906	9
50	SLS	4915	4940	4945	-	4933	18	4942	3	4927	13
50	SOO	4913	4938	4944	4964	4940	27	4941	3	4926	6
50	SOP	4927	4951	4972	4986	4959	32	4962	11	4939	0
50	SPP	4968	4975	4973	-	4972	4	4974	1	4971	4
52	$C_{22:1}$γLn$C_{22:1}$	5034	5052	5067	5105	5064	40	5060	8	5043	9
52	$C_{24:1}$OL	5049	5065	5077	5119	5077	42	5071	6	5057	8
52	$C_{22:1}$OO	5069	5085	5095	5125	5093	31	5090	5	5077	8
52	SOS	5086	5099	5103	5134	5105	28	5101	2	5092	7
54	$C_{22:1}$OG	5212	5230	5239	5269	5237	32	5234	5	5221	9
54	$C_{22:1}$OS	5248	5265	5269	5276	5264	16	5267	2	5256	8

For fatty acid legend see Table 1S (III-3.1.).

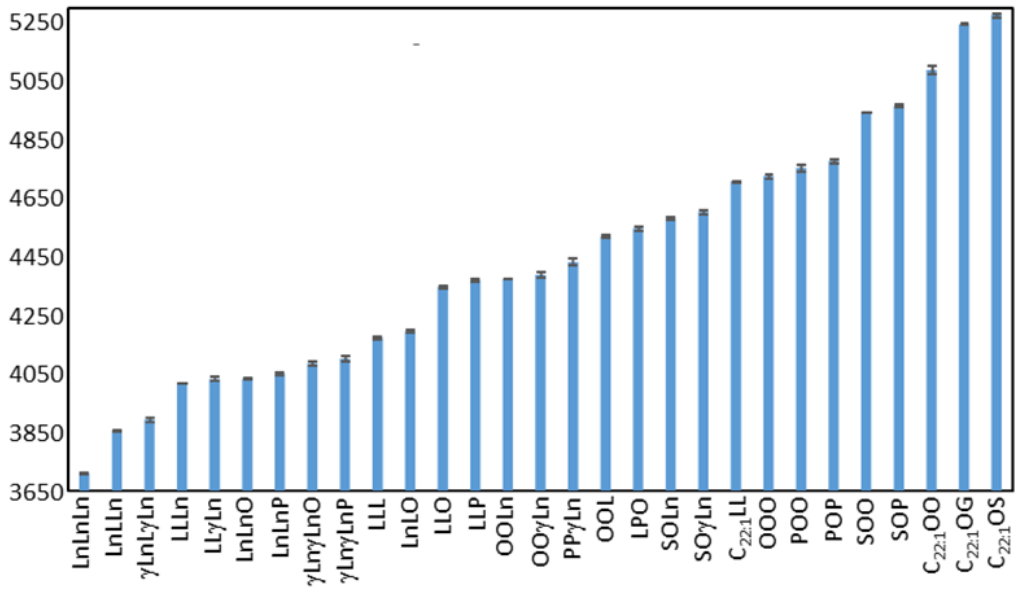

Figure 1S (III-3.1.). Histogram reporting the average LRI values between UHPLC-ELSD and HPLC-ESI-MS analyses (values are reported in Table 2 (III-3.1.)); error bar corresponds to ΔLRI value. For fatty acid legend see Table 1S (III-3.1.)).

Chapter IV - Multidimensional Liquid Chromatography

4.1. Comprehensive lipid profiling in the Mediterranean mussel (Mytilus galloprovincialis) using hyphenated and multidimensional chromatography techniques coupled to mass spectrometry detection

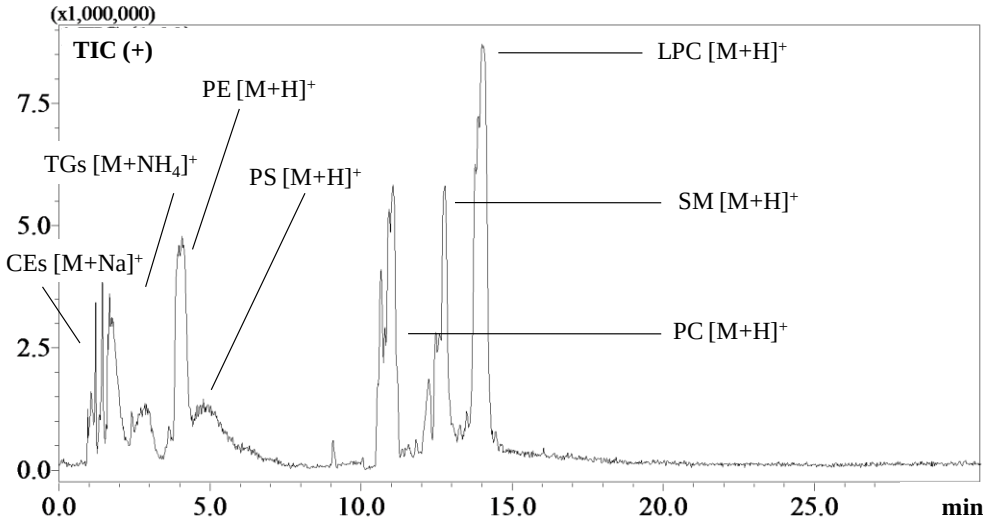

Figure 1S (III-4.1.). HILIC-ESI-MS (positive polarity) chromatogram of standard lipid material (CE, cholesteryl ester; TG, triacylglycerol; PE, phosphatydylethanolamine; PS, phosphatydylserine; PC, phosphatydylcholine; SM, sphyngomielin; LPC, lysophosphatydylcholine.

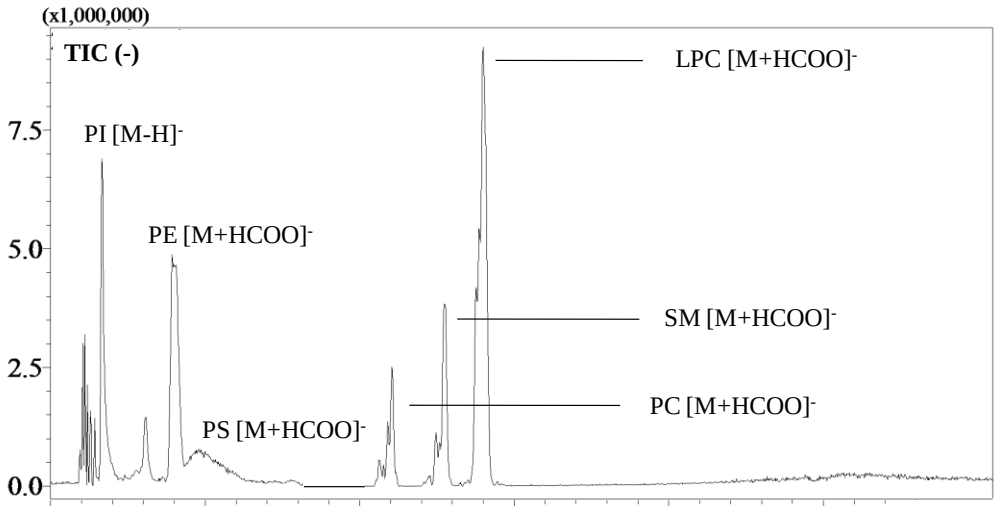

Figure 2S (III-4.1.). HILIC-ESI-MS (negative polarity) chromatogram of standard lipid material (PI, phosphatydylinositol; PE, phosphatydylethanolamine; PS, phosphatydylserine; PC, phosphatydylcholine; SM, sphyngomielin; LPC, lysophosphatydylcholine.

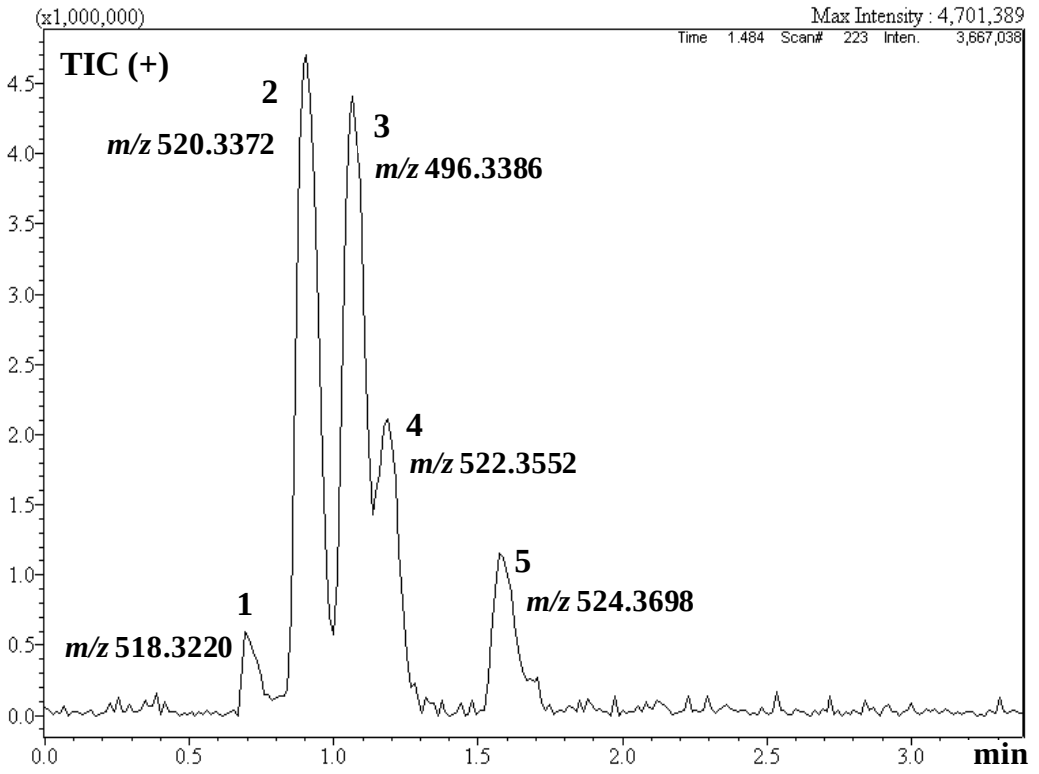

Figure 3S (III-4.1.). Two-min RP-LC separation of phosphatydylcholine standard species, detected by ESI-MS (positive polarity).

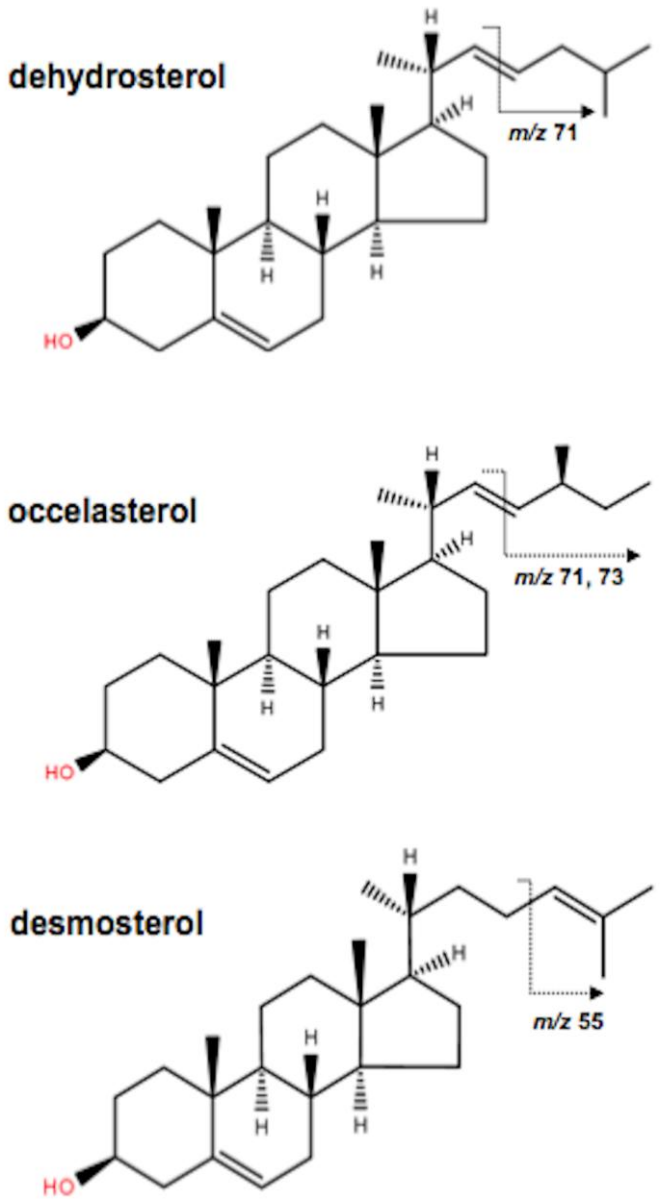

Figure 4S (III-4.1.). ESI($^{+}$) MS/MS fragmentation pattern of free sterols from the lipidome mussel.

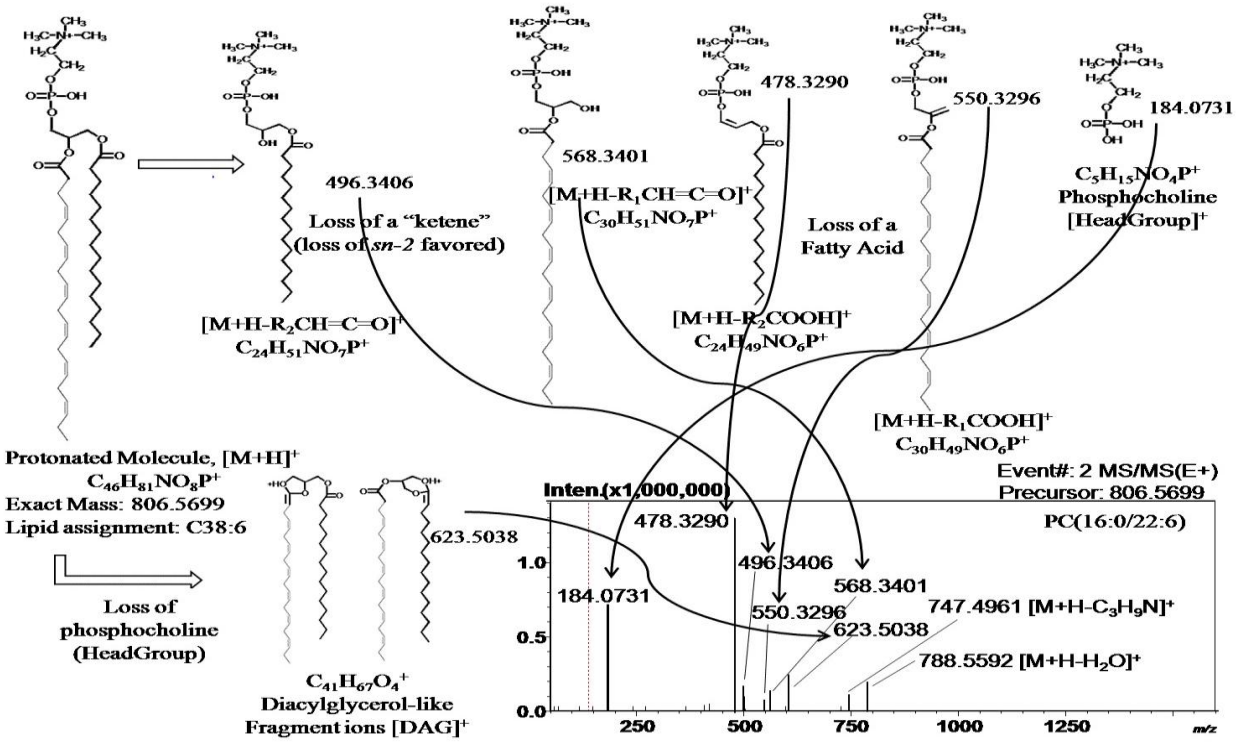

Figure 5S (III-4.1.). ESI($^{+}$) MS/MS analysis of PC(16:0/22:6) from the lipidome mussel.

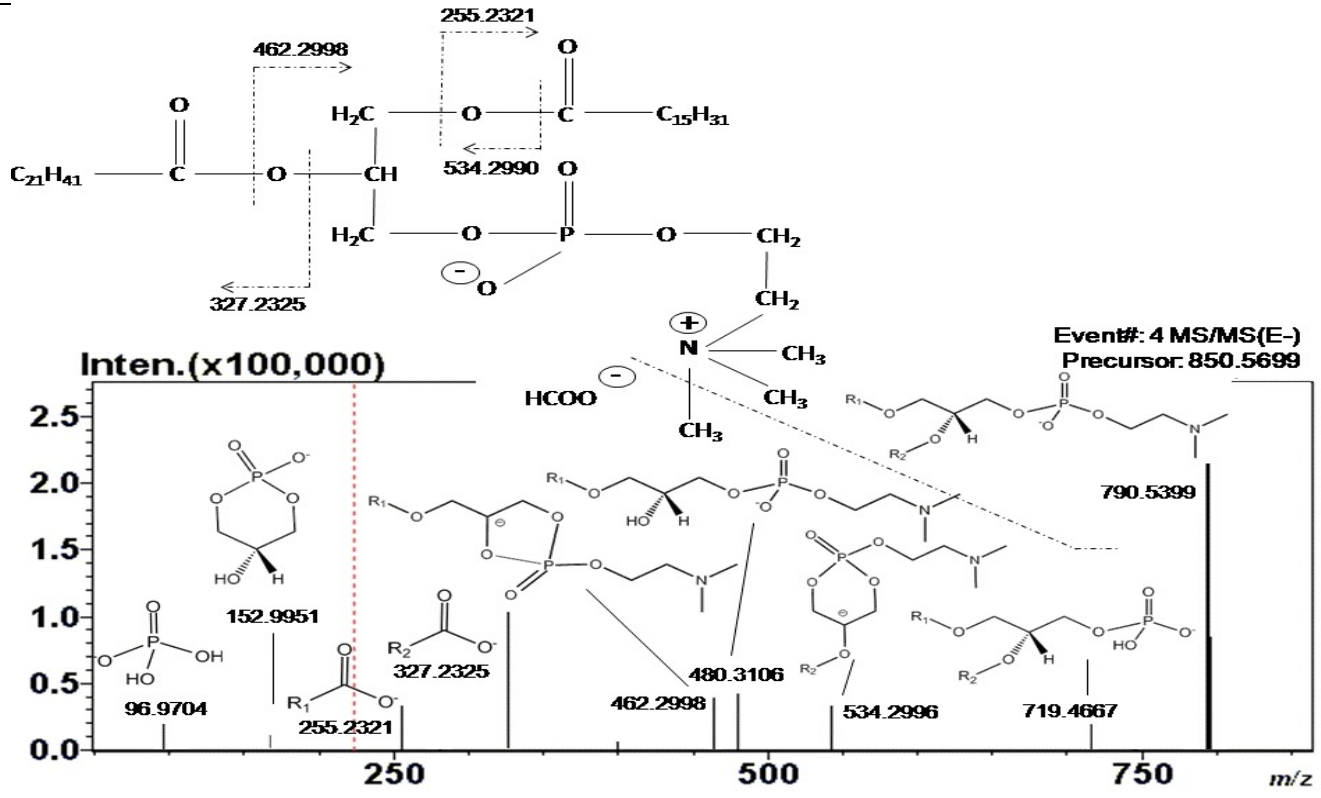

Figure 6S (III-4.1.). ESI(-) MS/MS analysis of PC(16:0/22:6) from the lipidome mussel.

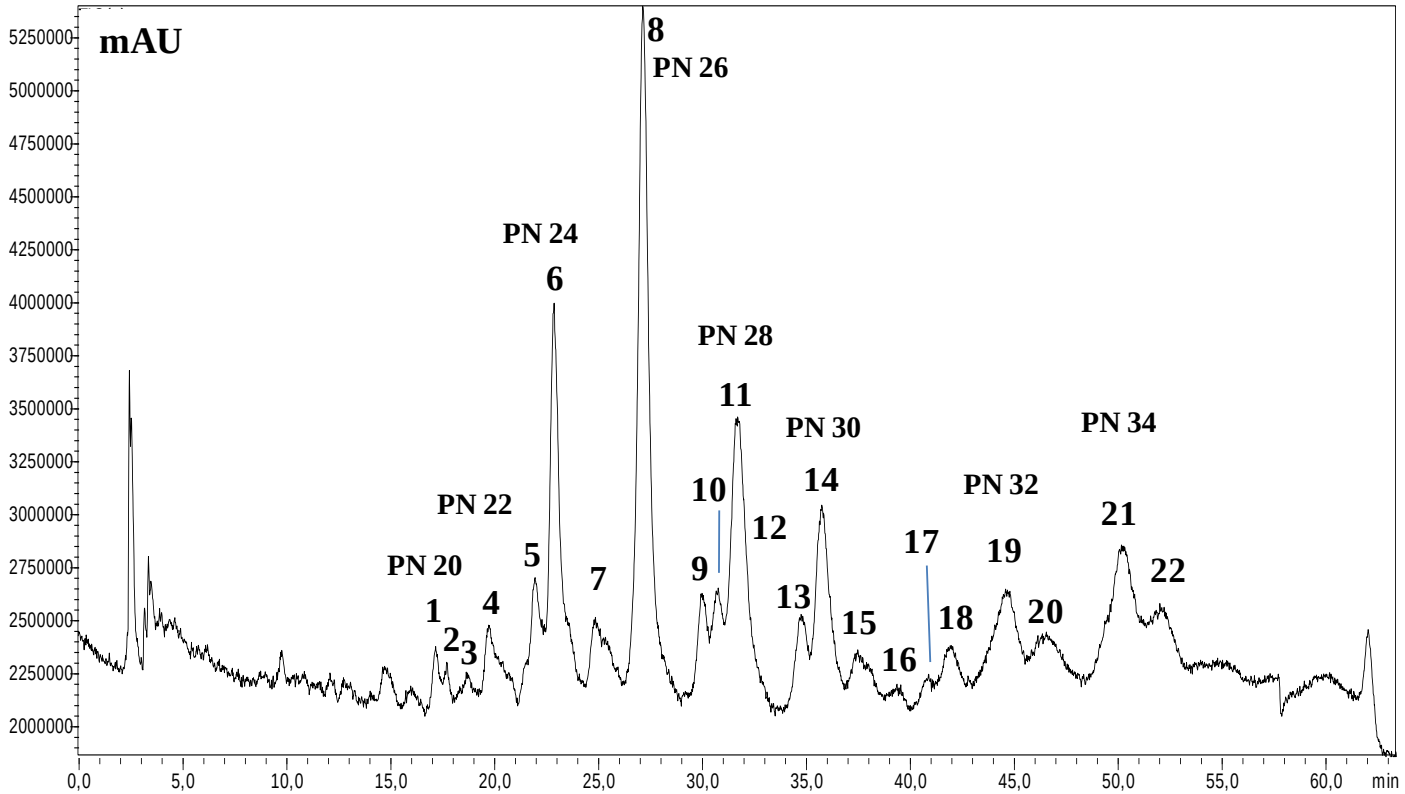

Figure 7S (III-4.1.). RP-LC separation of the offline collected fractions, showing the PC species, as eluted according to their increasing partition number (PN).

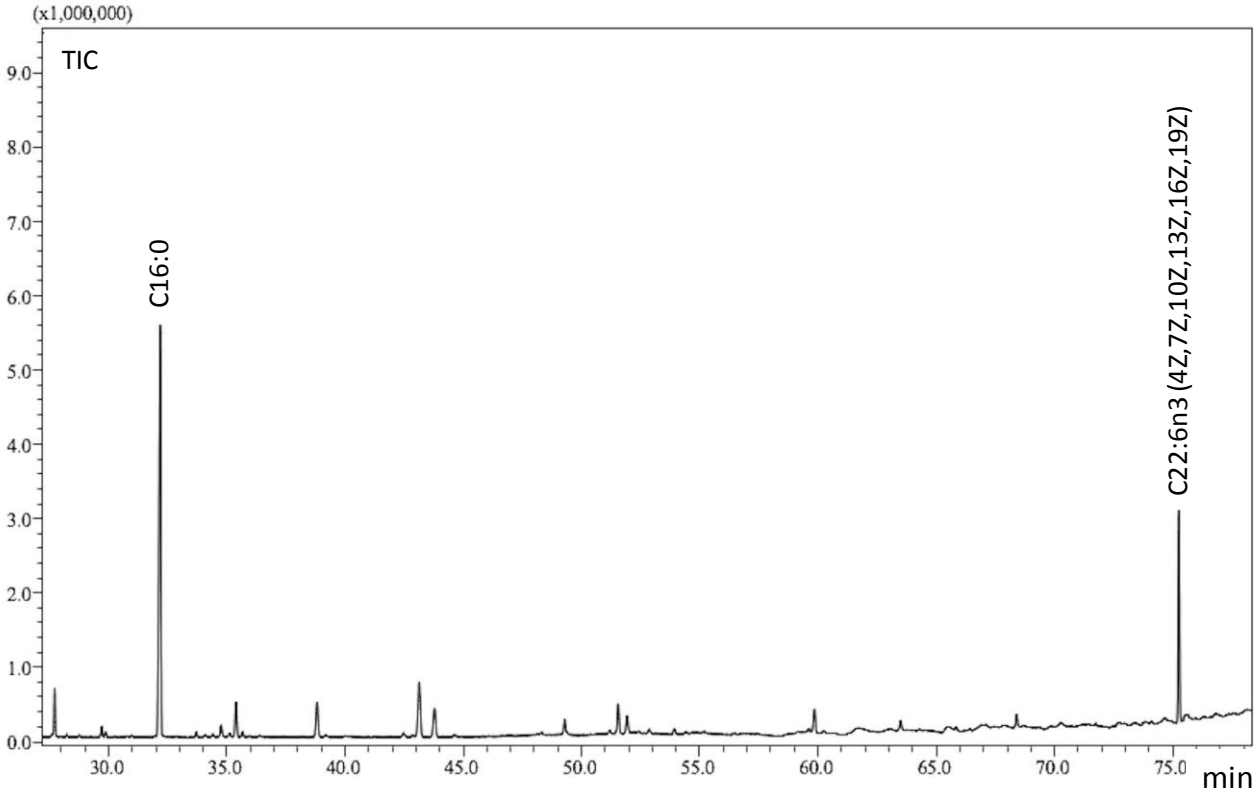

Figure 8S (III-4.1.). GC-MS separation and identification of PC species eluting according to a PN value of 26 (peak 8 in Figure 7S), showing evidence of the presence of Me.C16:0 and Me.C22:6n3.

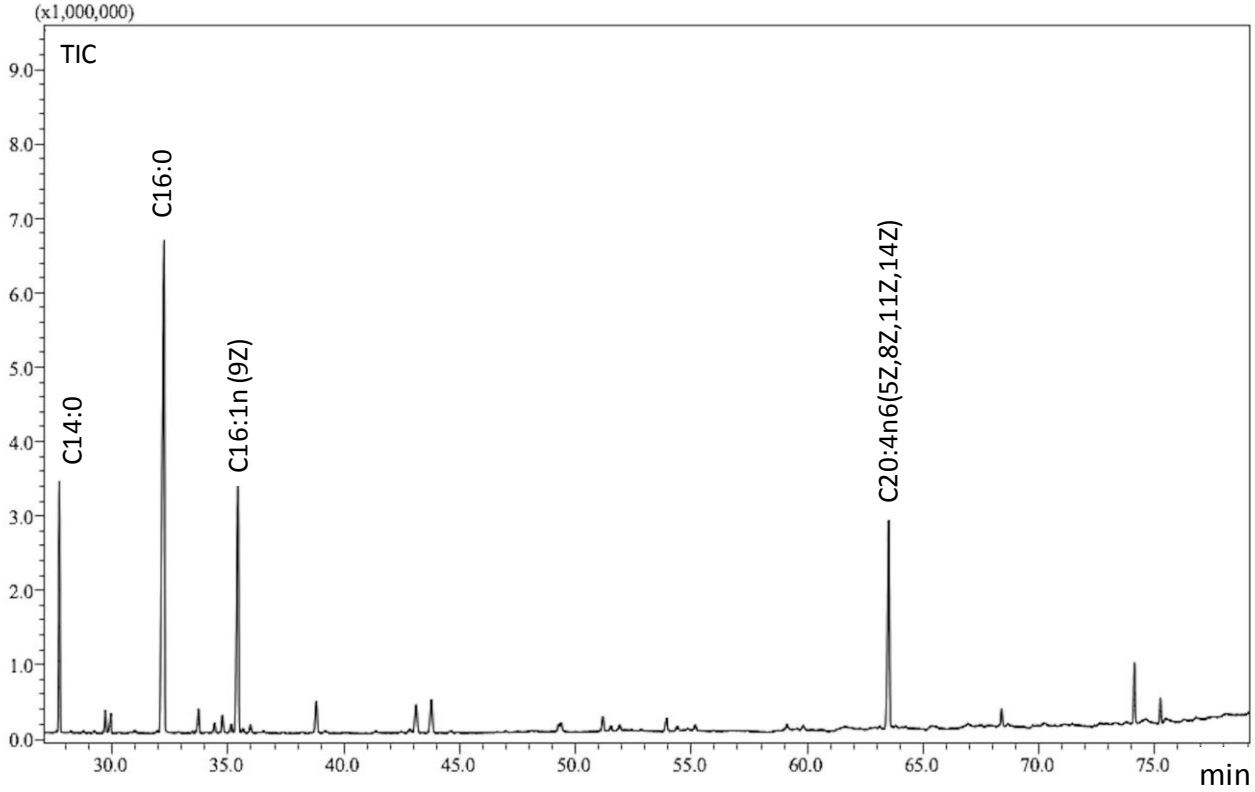

Figure 9S (III-4.1.). GC-MS separation and identification of PC species eluting according to a PN value of 28 (peak 11 in Figure 7S), showing evidence of the presence of Me.C14:0,Me.C16:0, Me.C16:1n7 and Me.C20:4n6.

APPENDIX II
List of publications

- Marco Beccaria, Marianna Oteri, Giuseppe Micalizzi, Ivana Lidia Bonaccorsi, Giorgia Purcaro, Paola Dugo, Luigi Mondello. Reuse of Dairy Product: Evaluation of the Lipid Profile Evolution During and After Their Shelf-Life. Food Anal Meth 9 (2016) 3143; DOI 10.1007/s12161-016-0466-x.
- Francesco Cacciola, Marco Beccaria, Marianna Oteri, Margita Utczas, Daniele Giuffrida, Nicola Cicero, Giacomo Dugo, Paola Dugo, Luigi Mondello. Chemical characterisation of old cabbage (Brassica oleracea L. var. acephala) seed oil by liquid chromatography and different spectroscopic detection systems. Nat Prod Res 30 (2016) 1646. doi: 10.1080/14786419.2015.1131982.
- M'hammed Aguennouza, Marco Beccaria, Giorgia Purcaro, Marianna Oteri, Giuseppe Micalizzi, Olimpia Musumesci, Annmaria Ciranni, Rosa Maria Di Giorgio, Antonio Toscano, Paola Dugo, Luigi Mondello. Analysis of lipid profile in lipid storage myopathy J Chromatogr B, 1029–1030 (2016) 157. http://dx.doi.org/10.1016/j.jchromb.2016.06.039.
- Paige A. Malec, Marianna Oteri, Veronica Inferrera, Francesco Cacciola,Luigi Mondello, Robert T. Kennedy. Determination of amines and phenolic acids in wine with benzoylchloride derivatization and liquid chromatography–mass spectrometry. J Chromatogr A, 1523 (2017) 248. http://dx.doi.org/10.1016/j.chroma.2017.07.061.
- Francesca Rigano, Marianna Oteri, Marina Russo, Paola Dugo, and Luigi Mondello. Proposal of a linear retention index system for improving identification reliability of triacylglycerol profiles in lipid samples by liquid chromatography methods. Anal Chem 90 (2018) 3313. DOI: 10.1021/acs.analchem.7b04837.

- Paola Donato, Giuseppe Micalizzi, Marianna Oteri, Francesca Rigano, Danilo Sciarrone, Paola Dugo, Luigi Mondello. Comprehensive lipid profiling in the Mediterranean mussel (*Mytilus galloprovincialis*) using hyphenated and multidimensional chromatography techniques coupled to mass spectrometry detection. Anal Bioanal Chem 410 (2018) 3297. doi: 10.1007/s00216-018-1045-3.
- Paola Donato, Daniele Giuffrida, Marianna Oteri, Veronica Inferrera, Paola Dugo, Luigi Mondello. Supercritical Fluid Chromatography × Ultra-High Pressure Liquid Chromatography for Red Chilli Pepper Fingerprinting by Photodiode Array, Quadrupole-Time-of-Flight and Ion Mobility Mass Spectrometry (SFC × RP-UHPLC-PDA-Q-ToF MS-IMS). Food Anal Meth 1-11. doi:10.1007/s12161-018-1307-x.

ACKNOWLEDGMENTS

Alla fine di questo percorso di Dottorato, vorrei ringraziare ed esprimere la mia gratitudine nei confronti di tutte le persone che, in modi diversi, mi hanno incoraggiato e permesso la realizzazione di questa tesi di dottorato.

Mio Padre...la prima persona a cui dico Grazie! Mi ha accompagnato dalla nascita all'ultimo giorno della stesura di questa tesi. Con amore ed orgoglio era pronto, anche in silenzio, a starmi sempre vicino.

Un doveroso e sentito ringraziamento va al Prof. Luigi Mondello e alla Prof.ssa Paola Dugo per avermi dato l'opportunità di svolgere il mio Dottorato di Ricerca in un laboratorio all'avanguardia, dell'Università di Messina, gestito da loro, con dedizione e professionalità; per me è stata una vera esperienza di crescita.

Grazie alla mia Tutor, la Prof.ssa Paola Donato, che mi ha seguito in questi anni, trasmettendomi tanta precisione, le sue conoscenze e la sua passione per questo lavoro di ricerca, inoltre, grazie per la costante disponibilità dimostratami.

Prof. Peter Q. Tranchida, sempre pronto ad incoraggiarmi nel credere nelle mie capacità.

Grazie al Prof. Francesco Cacciola per aver reso possibile un' esperienza di vita, per me molto importante, ovvero l'esperienza all' Università del Michigan. A tale riguardo, vorrei ringraziare il Prof. Robert Kennedy, Dott. Paige A. Malec e tutti i miei colleghi americani per l'ospitalità e la collaborazione; inoltre, grazie all' Università di Messina per il supporto attraverso il Progetto “Research and Mobility”, il Michigan Regional Comprehensive Metabolomics Resource Core (MRC2) ed il National Institute of Health of Michigan.

Mi piacerebbe ringraziare la mia collega, la Dott.ssa Francesca Rigano, con la quale di solito mi confronto e collaboro; lei ha sempre creduto in me.

Grazie a tutti i miei colleghi del Laboratorio gestito dal Prof. Mondello per i momenti trascorsi insieme. Non è possibile menzionare tutti, ma per me è importante ricordare il mio primo "maestro", il Dott. Marco Beccaria, che mi ha dedicato molto del suo tempo all' inizio di questo percorso.

Un ringraziamento riconoscente a Shimadzu, MilliporeSigma/Supelco Corporations e Waters per il loro continuo supporto.

Grazie al Progetto PON04a2_F "BE & SAVE", finanziato dal "Ministero italiano per l' Università e la Ricerca (MIUR)" ed al Dott. Paolo Oliveri per il supporto chemiometrico.

Un pensiero speciale va alla mia famiglia che mi ha sempre sostenuto ed incoraggiato in questa esperienza.

Per ultimo, ma non meno importante, un grazie alla Prof.ssa Mariella Toscano, mia insegnante di vita, sempre presente durante tutti i miei momenti di difficoltà e soddisfazione; grazie per l'incoraggiamento ed i consigli che mi ha offerto durante l'intero corso dei miei studi.